PB90-110123

Symposium on Fugitive Emissions: Measurement and Control (Fifth) Held in Charleston, South Carolina on May 3-5, 1982

(U.S.) Environmental Protection Agency, Research Triangle Park, NC

Sep 89

U.S. Department of Commerce
National Technical Information Service
NTIS

TECHNICAL REPORT DATA

(Please read Instructions on the reverse before completing)

1. REPORT NO. EPA/600/9-89/085	2.	3. RECIPIENT'S ACCESSION NO. PB90 110123/AS
4. TITLE AND SUBTITLE Fifth Symposium on Fugitive Emissions: Measurement and Control (May 3-5, 1982, Charleston, South Carolina)		5. REPORT DATE September 1989
		6. PERFORMING ORGANIZATION CODE
7. AUTHOR(S) D. Bruce Harris and William B. Kuykendal, General Chairmen		8. PERFORMING ORGANIZATION REPORT NO.
9. PERFORMING ORGANIZATION NAME AND ADDRESS See Block 12		10. PROGRAM ELEMENT NO.
		11. CONTRACT/GRANT NO. NA (Inhouse)
12. SPONSORING AGENCY NAME AND ADDRESS **EPA, Office of Research and Development** Air and Energy Engineering Research Laboratory **Research Triangle Park, NC 27711**		13. TYPE OF REPORT AND PERIOD COVERED Proceedings; May 1982
		14. SPONSORING AGENCY CODE **EPA/600/13**

15. SUPPLEMENTARY NOTES AEERL project officer was D. Bruce Harris, Mail Drop 54, 919/541-7807. Symposium was held May 3-5, 1982, in Charleston, SC.

16. ABSTRACT
The proceedings document presentations at the Fifth Symposium on Fugitive Emissions: Measurement and Control, May 3-5, 1982, in Charleston, SC. The Symposium was sponsored by the U.S. EPA's Air and Energy Engineering Research Laboratory (known then as the Industrial Environmental Research Laboratory) in Research Triangle Park, NC, as part of the Agency's continuing effort to develop methods for measuring and controlling airborne and waterborne fugitive emissions from energy and industrial processes. The objective of the symposium was to bring together people from industrial, academic, research, and government organizations with experience or interest in fugitive emissions problems to exchange information of mutual potential benefit. The program included presentations by individuals from a variety of organizations describing their experience and viewpoints regarding the impact, measurement, and control of fugitive emissions. An international flavor was provided by presentations by authors from Belgium, Canada, and Sweden.

17. KEY WORDS AND DOCUMENT ANALYSIS

a. DESCRIPTORS		b. IDENTIFIERS/OPEN ENDED TERMS	c. COSATI Field/Group	
Pollution	Coal Storage	Pollution Control	13B	08I
Measurement	Coal Dust	Stationary Sources	14G	21D
Emission	Roads	Fugitive Emissions		
Processing	Dust Control	Particulate	13H	05E
Leakage	Aerosols	Dust Suppressants		07D
Hydrocarbons	Particles	Street Sweepers	07C	

18. DISTRIBUTION STATEMENT **Release to Public**	19. SECURITY CLASS *(This Report)* **Unclassified**	21. NO. OF PAGES 288
	20. SECURITY CLASS *(This page)* **Unclassified**	22. PRICE

EPA Form 2220-1 (9-73)

PB90-110123

EPA/600/9-89/085
September 1989

FIFTH SYMPOSIUM ON

FUGITIVE EMISSIONS: MEASUREMENT AND CONTROL

(May 3-5, 1982, Charleston, South Carolina)

EPA General Chairmen:
D. Bruce Harris and William B. Kuykendal
Air and Energy Engineering Research Laboratory
(Industrial Environmental Research Laboratory)
Research Triangle Park, North Carolina 27711

AIR AND ENERGY ENGINEERING RESEARCH LABORATORY
OFFICE OF RESEARCH AND DEVELOPMENT
U.S. ENVIRONMENTAL PROTECTION AGENCY
RESEARCH TRIANGLE PARK, NC 27711

REPRODUCED BY
U.S. DEPARTMENT OF COMMERCE
NATIONAL TECHNICAL INFORMATION SERVICE
SPRINGFIELD, VA. 22161

ABSTRACT

These proceedings document presentations at the Fifth Symposium on Fugitive Emissions, held May 3-5, 1982, in Charleston, South Carolina. The symposium was sponsored by the U. S. Environmental Protection Agency's Industrial Environmental Research Laboratory (now known as the Air and Energy Engineering Research Laboratory) in Research Triangle Park, North Carolina, as part of the Agency's continuing effort to develop methods for the measurement and control of airborne and waterborne fugitive emissions from energy and industrial processes.

The objective of the symposium was to bring together people from industrial, academic, research, and government organizations with experience or interest in fugitive emissions problems to exchange information of mutual potential benefit.

The program included presentations by individuals from a variety of organizations describing their experience and viewpoints regarding the impact, measurement, and control of fugitive emissions. An international flavor was provided by presentations by authors from Belgium, Canada, and Sweden.

EPA REVIEW NOTICE

This report has been reviewed by the U.S. Environmental Protection Agency, and approved for publication. Approval does not signify that the contents necessarily reflect the views and policy of the Agency, nor does mention of trade names or commercial products constitute endorsement or recommendation for use.

This document is available to the public through the National Technical Information Service, Springfield, Virginia 22161.

CONTENTS

Page

SESSION I--Session Chairman Alfred B. Craig (EPA/IERL-RTP)

Results of Measurement Programs for Fugitive Hydrocarbons Using a Downwind Crossectional Flux Analysis Method--P.R. Harrison (Envirosol) 1-1

Test Protocol for Evaluating Fugitive Emissions from Active Coal Storage Piles--D. Carnes, P. Catizone, T. Kincaid (TRC Environmental Consultants); D. B. Harris (IERL-RTP) 2-1

Characterization of Fine Particulate Emission Factors for Paved Roads--C. Cowherd, P. Englehart (Midwest Research Institute) 3-1

SESSION II--Session Chairman William Hague (Julius Koch, USA, Inc.)

Micron Droplet Dust Suppression Proves Out in Variety of Fugitive Dust Applications--W. Hartshorn (Sonic Development), L. Strand (Andeze AB, Sweden) 4-1

The Optimization of Wind Screens for Fugitive Emission Control Using Wind Tunnel Tests--C. J. Williams (MHTR)* 5-1

Evaluation of Field Test Results on Wind Screen Efficiency--A. Larson (TRC Environmental Consultants)* 6-1

Effects of Street Sweeping of Fugitive Emissions from Urban Roadways--D. F. Gatz (Illinois State Water Survey) 7-1

Evaluation of Road Carpets and Chemical Road Dust Suppressants--A. Larson (TRC Environmental Consultants)* 8-1

Evaluation of Weathering Characteristics of Dust Suppressant Chemical Additives--W. B. Kuykendal, D. C. Drehmel, B. E. Daniel (IERL-RTP) 9-1

SESSION III--Session Chairman John E. Yocom (TRC Environmental Consultants)

On the Use of SF_6 Tracer Releases for the Determination of Fugitive Emissions--B. Vanderborght, J. G. Kretzschmar, T. Rymen (SCK/CEN, Belgium); F. Candreva, R. Dams (INW-RUG, Belgium) 10-1

(*) Alternate paper provided.

Contents (cont.)

Page

An Atmospheric Tracer Investigation of Fugitive Emissions Transport in the Colorado Oil Shale Region--G. A. Sehmel (Pacific Northwest Laboratory) 11-1

Laboratory Testing to Improve Rail Car Sealant Spray and Loading Techniques for the Abatement of Fugitive Coal Dust--C. J. Williams, W. F. Waechter (MHTR)** 12-1

Studies of Nontraditional Fugitive Particulate Control Techniques--B. M. Nicholson (EPA/OAQPS), M. Borcherding (City of Portland), G. Ekhardt (State of Minnesota), R. Mohr (State of Colorado)** 13-1

Evaluation of the Efficiency of a Charged Fog Generator in Controlling Inhalable Particles at a Steel Plant (C. V. Mathai, B. M. Muller (AeroVironment); W. B. Kuykendal (EPA/IERL-RTP)* 14-1

SESSION IV--Session Chairman James A. Dorsey (EPA/IERL-RTP)

Estimation of Ambient TSP Impacts of Coal Storage and Handling Facilities--R. C. Wells, D. C. Doll (Enviroplan), J. Hattrup (Baltimore Gas and Electric) 15-1

A Determination of the Impact of Fugitive VOC Emissions from a Municipal Hazardous Waste Incinerator on the Surrounding Community--G. A. Holton (Oak Ridge National Laboratory), L. J. Staley (EPA/IERL-Cin)* 16-1

Impact of Fugitive Emissions on PM-10 Concentrations--T. G. Pace (EPA/OAQPS)** 17-1

Application of Dispersion Dictated Mass Balance for Calculating Fugitive Dust Emissions--C. F. Cole (TRC Environmental Consultants), J. G. Moldovan (Anaconda Minerals), P. B. Kunasz (Consultant) 18-1

Modeling the Emission of Aerosols in and Around a Metallurgical Plant--B. Vanderborght, I. Mertens, J. G. Kretzschmar (SCK/CEN, Belgium); F. Adams (UIA, Belgium); R. Dams (INW, Belgium)** 19-1

SESSION V--Dennis J. Martin (TRC Environmental Consultants)

New York State Industrial Coal Pile Drainage Regulations and Guidelines--C. Hornibrook (NYSERDA) 20-1

(*) Alternate paper provided.
(**) Abstract only.

Contents (cont.)

Page

Calibration and Verification of a Coal Pile Drainage Model--J. A. Ripp, G. T. Brookman, P. B. Katz (TRC Environmental Consultants); J. G. Holsapple (New York Power Pool) 21-1

Coal Pile Simulation Study--A. Schumacher, E. G. Hanson (Environmental Science and Engineering) 22-1

Control of Acid Problems in Drainage from Coal Storage Piles--H. Olem, T. L. Bell, J. J. Longaker (TVA) 23-1

ATTENDEES A-1

RESULTS OF MEASUREMENT PROGRAMS FOR FUGITIVE HYDROCARBONS USING A DOWNWIND CROSSECTIONAL FLUX ANALYSIS METHOD

PAUL R. HARRISON

Envirosol
Environmental Solutions
1700 N. Fiske Avenue
Pasadena, California 91104

The work described in this paper was not funded by the U.S. Environmental Protection Agency. The contents do not necessarily reflect the views of the Agency and no official endorsement should be inferred.

ABSTRACT

A method to quantify fugitive volatiles organic compounds (hydrocarbons) has been in the developmental process for the last seven years. Recent activities have significantly improved the method and have quantified the precisions and accuracies under both controlled and field conditions. This paper is a summary of various applications and their results. Special attention is given to the precision (repeatability) of the data in field conditions. Facilities, components, and other area sources have been selected to demonstrate the flexibility of the method. Actual data are given.

The major conclusions are that the technique is operational to most applications with precisions of less than 30%, with 8% nominal. Ultimate accuracies are not yet determined due to lack of an acceptable standard. The method is the most flexible available and is providing emission rates hitherto unavailable. The application to the "bubble rule" is encouraging.

I. INTRODUCTION

This paper is a summary of a developmental program to further develop a method to quantify fugitive emission rates of VOC's under all reasonable meteorological and physical condition. The initial impetus for the work was a problem with applying the U.S.EPA emission rates (AP-42) for refineries to non-refinery operation, i.e. a small crude oil gas treatment plant. In this initial program the measured leak rate for individual components differed from the published factors by orders of magnitude. By use of a downwind plume mapping technique in conjunction with the first reported "Direct maintenance program", an understanding of the differences was achieved.[1] Since this initial program, performed in 1976, the technique has been further perfected and applied to total refineries and petrochemical facilities as well as their sub-units and individual components. In addition, Natural Seeps, Impoundments, wastewater treatment facilities, tankers and storage tank emission rates have been quantified, usually to much better precision than achieved by more passive measurements. Due to the response characteristics of the continuous VOC monitor preferred for these measurements, and due to the question of quantitative determinations of precisions and accuracies the method had not, until now, been advertised as operational. Since very few data existed for fugitive emissions and due to the unusually high variability of most fugitive sources, the task of objective evaluation of the method was not at all trivial.

This paper will briefly describe the technique, summarize the past applications and present data for some emission rates found. It will also present the results of precision and accuracy tests performed on recent data.

Results will be offered to show that the technique is quite flexible and will provide adequate, defensible emission factors at a relatively inexpensive cost (the more precision required, the more work required). At this point the method is operational. Although it can be performed by semi-technical personnel, tests should conducted under the direction of an experienced person, especially if one desires a cost effective program and a data set with optimum accuracy.

II. THE TECHNIQUE

The method makes very few assumptions. The most critical is that the downwind signature has a Bionominal or "Gaussian" distribution, especially in the horizontal. Since we know that on the average, the turbulence structure will distribute itself to the Gaussian condition in the micro and mesoscale meteorological volumes, the assumption is relatively sound. The key is to choose the distance from the source and the wind conditions so as to map the plume at the most likely isotropic turbulent condition. As a matter of practicability this condition must be compromised, but one can recognize the condition and compensate if necessary by early data reduction and a presurvey measurement.

The formula used is straight out of Turner's handbook[2] (or any other pertinent resource for that matter) and is for a centerline concentration of a ground level source.

From diffusion theory and measurements, the following equation applies for ground-level sources:[2]

$$Q = \pi \sigma_y \sigma_z \Delta\chi_{max} \bar{u} C K$$

where

Q = Emission rate of hydrocarbons (gm/sec)

$\Delta\chi$ max = Peak, net concentration of hydrocarbons in Gaussian fit curve (ppm)

K = Conversion constant from ppm to $\mu g/m^3$; 665×10^{-6} gm/m^3 for methane at 20°C

σ_y = Lateral extent of Gaussian plume (m)

σ_z = Vertical extent of Gaussian plume (m)

C = Correction factor from methane equivalent to actual mass emission rate due to instrument response

π = 3.141....

$\bar{u}$ = Mean wind speed (m/sec)

All parameters are usually obtained from field measurements. (In some instances, σ_z is obtained theoretically from σ_y.[2] Care must be taken to prevent over or underestimation of this value in areas severely affected by local, mechanically-induced turbulence.)

The transect method of sampling is used to actually map the dimensions and concentrations of a plume. From this mapping, a reasonably accurate emission rate can be calculated.

Two types of plume mapping have been used: single level transect at an optimum distance and conditions from source, and a complete plume crossectional mapping. The former method is less work (expense) but may not be as accurate due to the necessity of calculating the vertical extent of the plume (σ_z) from theory. If the conditions are classical, a classical theory will give good results. Please see Figure 1.

The second and preferred method when ideal conditions are not present (or possible) is the multilevel and complete plume mapping technique as shown in Figures 2, 3, and 4. In this latter case no assumptions are made except reasonable isotropic turbulence. For close-in measurements of area sources this method is necessary since σ_z calculated from σ_y may overestimate the emission rate. Please see Figure 3.

The actual physical measurement techniques will not be discussed at this time since, although they are not particularly unique, they do require specific protocols that must be followed in order to achieve optimal accuracies.

III. EXAMPLES OF APPLICATIONS

This section will present a selection of the actual applications to the quantification of fugitive VOC from various facilities and devices. Please note that fugitive VOC emission rates vary greatly within and from facility to facility. The following data will demonstrate the typical precisions found in steady-state conditions as well as those in highly varying conditions.

° REFINERIES, TOTAL FACILITIES

REFINERY I

In this case the wind conditions were unusually ideal. A single level set of transects were used in the calculations, but the vertical extent of the plumes were verified by use of a slow aircraft. Five data sets were obtained over a three month period. Each "signature" was unique but the data agreed very well, i.e.:

Test	Q (tons/day)
1	29.0
2	24.3
3	27.1
4	24.3
5	28.1
AVERAGE	26.6 ± 2.2, (8%)

° REFINERY II

In this case the conditions were such that the transect line was very close to the edge of the complex. Both vertical and a single level mapping were taken. Figure 2 is a typical signature of the close-in facility fugitive VOC emissions. Note that the single level transect would miss part of the plumes. Comparison of the two types of data resulted in an emission rate of 3.2 tons/day but with a precision of twenty three percent. These data demonstrate the loss of precision due to the unfavorable transect or mapping conditions as well as the possible effect of a non-uniform emission rate (a turn-around was underway at Refinery II).

- PETROCHEMICAL (A sub-unit and components)

Most petrochemical data are proprietary; however, we can use one case to demonstrate how a single unit can be isolated from the total complex.

In one case a sub-unit was quantified both upwind and downwind. At the same time each individual emission point (component) or area was quantified.

The sum of the most significant of the 19 leaking components was 706 ± lbs per day. The downwind minus the upwind value was 824 lb per day, thus there was an agreement within fifteen percent between the two methods. (Both single and multilevel transects were made but the multilevel results were used preferentially in these calculations.) It is interesting to note that the precision of these single day comparisons were better than the comparison in results taken on separate days, i.e. the variance of four separate emission rates using the plume mapping technique was 21%. This, of course, was a result of process variations as well as the data sets themselves.

Finally, the small components were bagged and timed to find their emission rates. A tail gas compressor was two large to bag, thus both a single level and multilevel transect was used to gain results of 88 and 81 lbs/day respectively. As one can see, the agreement is quite good under these conditions. Other individual areas quantified were loading racks, a flare pipe leak, and a spill; each was identifiable within the upwind transects. An intermittent process such as "Trap Blowing" was also quantified (148 lb/hr of operation). Please see Figure 4.

- CRUDE OIL GAS TREATMENT PLANT

In this instance the fugitive VOC emission rate for the total facility was initially 74 lb/day. After the directed maintenance program the rate was measured downwind as 7 lb/day.

- PROCESSED CRUDE OIL STORAGE TANK

This double seal storage tank contained warm crude that had undergone dewatering and used a heater/treater process to remove volitiles. The emission rate during draw-down was 25 lb/day. This measurement used a single level transect and a plume centerline vertical profile for determining the plume dimensions.

- NATURAL OCEAN SEEPS

Over the last several years a large natural ocean seep has been quantified by use of both the single and multilevel methods. The source strength is known to vary from visual observations; thus precisions also include natural variations:[3]

NATURAL SEEP EMISSION RATES

Year		Emission Rate T/day
1977		8.7
1978		10.7
1979		21.0
1980		16
		25
		20
		24
		22
	AVERAGE 1980	21 ± 3.2 (15%)

Since 32% was non-methane, it was determined to be equal to one-half the county hydrocarbon inventory and that it was commercially feasible to trap the gas for sale as product. Finally, a bonus was realized from some of these measurements in that we were able to document revised dispersion coefficients over the cold California oceans.

° REFINERY WASTEWATER TREATMENT

Currently, under a U.S. EPA contract, an evaluation of the emission rates of refinery wastewater treatment facilities is taking place. Subunits and components are also being quantified. These data will be presented later after review. They will include preliminary information such as effect of covers, operating characteristics, age and configuration. Detailed comparisons of of purely statistical treatment of the data versus the graphical treatment used are also being determined. Since these devices are so dynamic in the material received it represents a severe test for the method. For example, not only are the locations of components usually not ideal, the input to them is highly variable and represents a large mix of VOC constituents. Also, the liquid surface conditions vary greatly and can control the fugitive emission rates as much as the potential VOC in the bulk water. This study will also discuss the accuracy of the methods in greater detail.

IV. ACCURACIES AND/OR PRECISIONS OF THE METHOD

Although the "plume mapping" or "downwind crossectional analysis" method of quantifying fugitive emissions has been used in even a more primitive form for particulates as well as for other gases and tracer studies, there has been some resistance to its acceptance. The primary reason may be that, although it uses off-the-shelf equipment and is relatively simple in theory, it is tedious and requires judgement as to the best measurement location to optimize the turbulence conditions so to approach the classical normal distributed plume. It marries the real world with turbulence and statistical theory in a rather unique way that crosses disciplines, thus making it suspect; i.e. it's a unique combination of established procedures.

A recent obstacle that has been removed is the calibration of the continuous monitor to the unique hydrocarbon mix encountered in most areas (if only one VOC is present there is no problem). By using in-field analyses for total, NMHC, and MHC, we can determine the calibration factor C in equation (1) for each condition. Since the VOC are all converted to methane, we can eliminate the necessity of calibration to each constituent. Since the procedure is a step-wise progression of operations to the data, the variations are easily exposed and not lost in the intervening calculations. Said another way, the process must not only result in a reasonable final data point, each step or parameter must also make physical sense.

As part of all these studies we have attempted to focus part of our efforts toward objective determination of precisions and accuracies (few of the data sets are complete).

Table I is a summary of the precision of much data available to date. Please note most of these cases are dynamic and contain process variations as well as variations due to methodologies.

Recent data taken over several days verify these results but also contain standard deviations varying as high as 69% and as low as 18%. (For data taken at different times during the same day, the precisions improve to 15%.) Naturally we observe that the quality of the data sets goes down as the variation among the data goes up. However, the realistic test in these data is to compare data taken in close time sequence on the same device. These comparisons are those shown in Table I. These are a great improvement over the thousand percentage deviations obtained in other studies on wastewater facilities.

Accuracy tests were also conducted by comparison of the results of the downwind method to metered releases and to a temporarily ducted source. The ducted sources were less accurate and more variable than the transect method due to leaks and the effects of wind direction orientation to the ducts. Local turbulence was also a major factor in the poor showing of the ducted method. Standard deviations ranged from 220% to 7%, much larger than the transects. Ratios of transect to ducted resulted in an accuracy of 150% ± 68%. Since we lost much of the VOC from the ducts we are not surprised the ratios are usually in greater than 100%. A similar test using a metered rate of release of propane resulted in a ratio of transect to metered rate of 1.6 ± 19%. Although the precision was in the range seen before, the accuracy is not as good. We have since discovered that as the propane was released, some of it was nearly liquid at the rotometer. Thus, the reported metered release rate is too low, especially since the metering apparatus is cooled by the gas phase change. The resultant ratios confirm this finding. In conclusion, we know the precision for these tests is within 30% and the average accuracy is better than 60%. A definite test of the system's ultimate accuracy has not yet been made due to these difficulties in the accuracy of the calibration methodologies themselves. It is probably equal or better than the precisions.

TABLE I

PRECISION OF DATA SETS AVAILABLE TO DATE

Test	σ, Precision, %	Number of Tests
Refinery I	8	5 days
Refinery II	NA	-
Petrochemical	15	2 methods
Tail gas compressor	9	2 methods
Petrochemical	21	4 days
Ocean Seeps, 1980	15	5, same day
Refinery II Wastewater Treatment		
° Test in succession, 1	21	3
° Test in succession, 2	31	3
° Test in succession, 3	7	3
° Test in succession, 4	28	3
° All tests, same device	69*	13

*Conducted over several days and includes process variations.

Finally, by using purely statistical manipulations on the raw data sets, the agreements are also acceptable. Variations within the various statistical methods themselves vary between a standard deviation (σ) of 7% to 13%. The purely statistical analysis and graphical methods agree within a range of 60% to 120% (± 40% to 20%) of each other with one of three comparisons within 3%.

CONCLUSIONS

From the data presented we can make the following conclusions:

- A method exists to quantify fugitive VOC with precisions typically within 30% and to 8% for well behaved plumes.
- Ultimate accuracies are not yet determined but are known to be better than ± 60%.
- The method uses a combination of classical theories in a unique way.
- The method has great utility and can be used on most sources accessable downwind (one can also forecast wind shifts).
- This method is providing data never before quantified with acceptable precisions or accuracy.
- The method has application to the bubble rule and can verify the effectiveness of the directed maintenance program.

REFERENCES

1. Harrison, P. R., "Comparison of Component Emission Rates to AP-42 for a Gas Treatment Plant at Ellwood, CA," ARCO Production Co., Envirosol Report No. 1461, 1976.
2. Turner, D. B., "Workbook of Atmospheric Dispersion Estimates," U.S. EPA (PHS) Publication 999-AP-26, 1970. (NTIS PB191482.)
3. Harrison, P. R. and Mass, S. T., "Dispersion Over Water: A Case Study of a Non-Bouyant Plume in the Santa Barbara Channel, California," AMS Joint Conference, November 29, 1977.

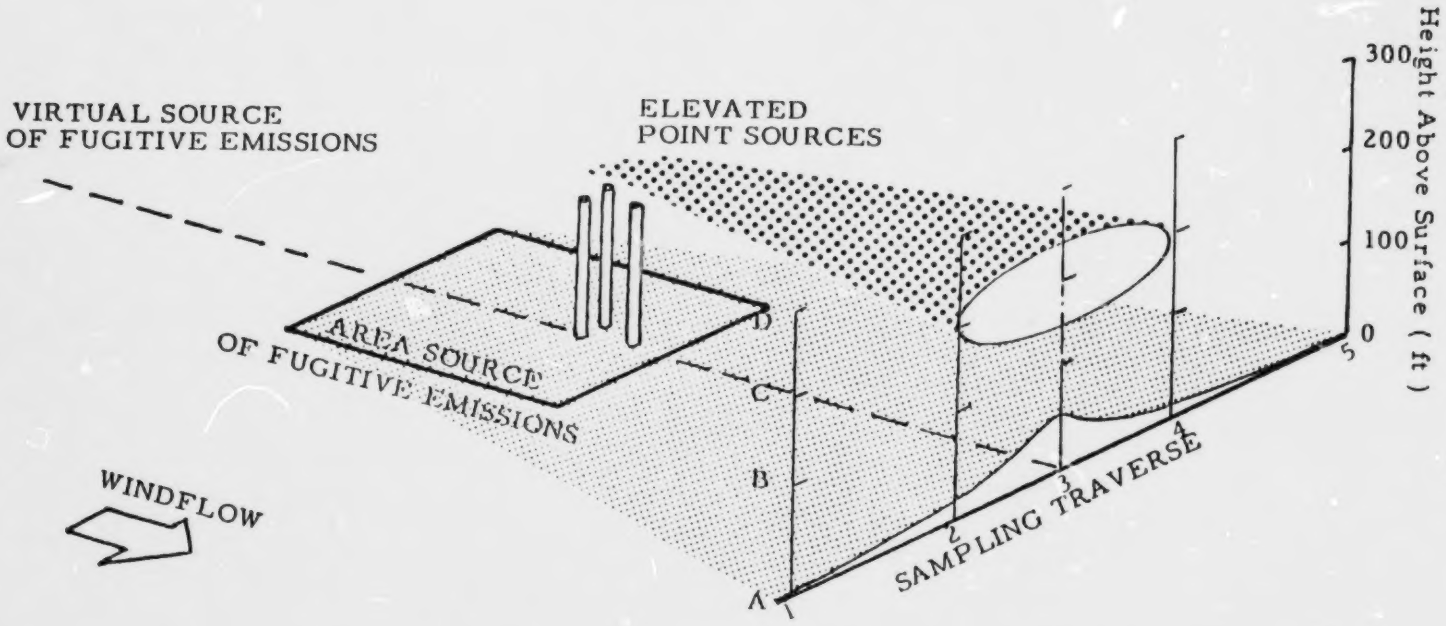
VIRTUAL SOURCE
OF FUGITIVE EMISSIONS
ELEVATED
POINT SOURCES
Height Above Surface (ft)
300
200
100
0
AREA SOURCE
OF FUGITIVE EMISSIONS
WINDFLOW
A
B
C
D
1
2
3
4
5
SAMPLING TRAVERSE

Figure 3: **Schematic representation of vertical point profiles (1, 2, 3, 4, 5) and elevated horizontal transect lines (A, B, C, D).**

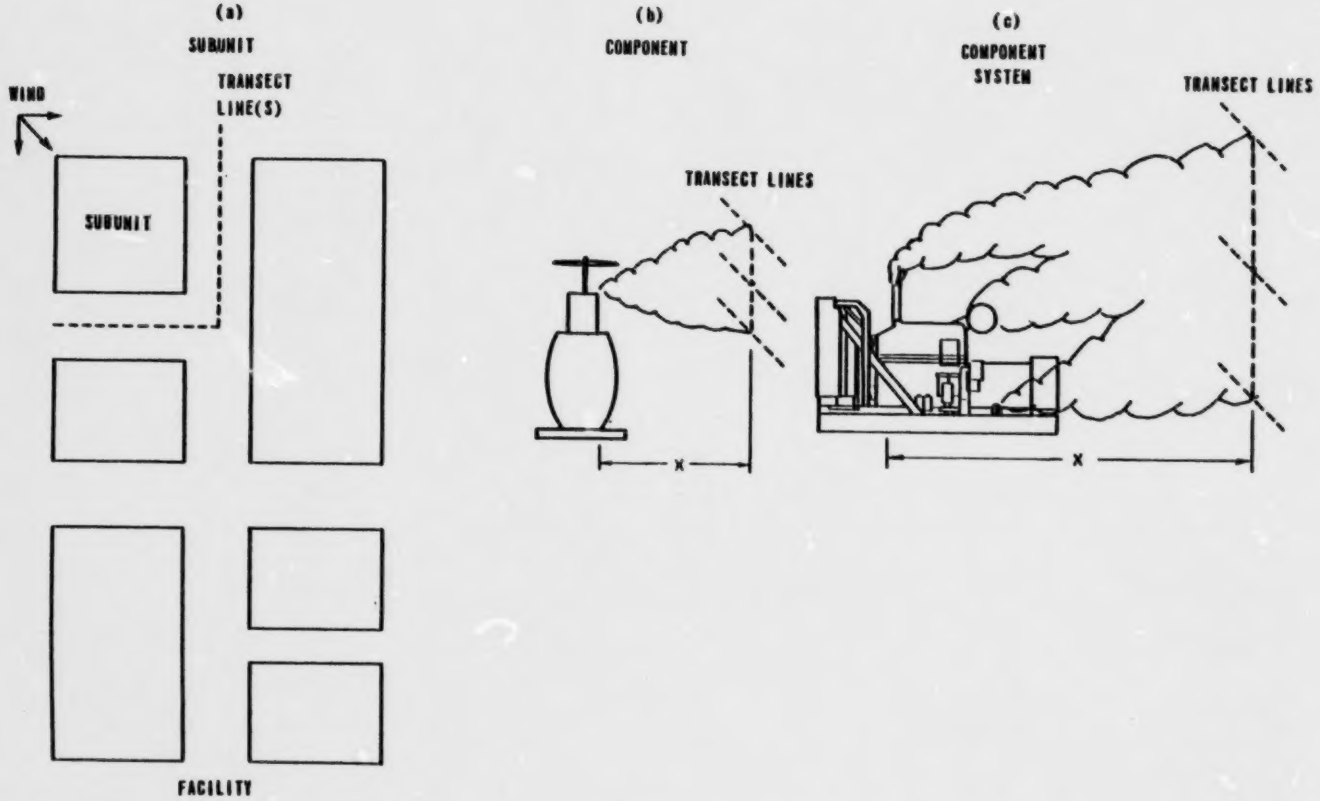
(a)
SUBUNIT
WIND
TRANSECT
LINE(S)
SUBUNIT
FACILITY
(b)
COMPONENT
TRANSECT LINES
x
(c)
COMPONENT
SYSTEM
TRANSECT LINES
x

Figure 4: Schematic of cross-sectional measurement for subunits, components, or component system.

Questions

Greg Holt, Oak Ridge National Lab:

Q: How far downwind were you measuring for API unit?

A: Well, you know, when you are in structures, you have to be careful because you have to go far downwind to try to get your turbulence distributed; sometimes that is not practical. In this particular case, we are approximately 5 meters downwind.

Q: What was your time frame for your measurements? For each transect or total? Well, your averaging time, considering your air movement. I'm thinking your Gaussian assumption is awfully close. I would think perhaps a box model would be just as good.

A: Well, one of the things I can't argue with is when you take the data you plotted up, it sure looks Gaussian and it also satisfied the Gaussian tests within reason, there is no such thing as a perfect Gaussian. The averaging times, typically, it takes a half hour to get a data set, which is good enough. Sometimes you get wind shifts, that is why we've altered the technique, rather than take several at one level, and then several at the next level, etc., to work your way up, we take a couple at each level and move up and down - we keep going that way as opposed to doing all the averaging at one level, because a shear will come along sometimes and your plume will get bent over. It's no real problem because you see that happening and you just measure directly up rather than slantwise, so we've altered that. We get kind of a data set within 15 minutes or so and just repeat it.

George Sehmel, Pacific Northwest Laboratory

Q: What is downwind distance and how long is that wind effective? Do you feel plume is contained in lower 2 meters? Not sure what you did there.

A: Well, these are more theoretical questions than practical questions. The practical answer to that is that you take sufficient height until you look at your signature and you take sufficient points until you actually see this coming out, so you see the data at its real time and you map the plume, and you don't care what the tail up there looks like that much becasue the real important part of it is the center line of the plume and you take sufficient height and you clearly define that at least 70% of the plume and the only problem you get into is that you have to make sure you take enough data points discrimination to get close to the maxima. If you don't do enough of them within the maxima, then you have a problem with what is the maxima. You can get fairly large error that way. Now, in some of these techniques you notice that we talk about selected interperlated data you are actually searching and interperlating a maximum concentration at the center line. And you will find that it helps a little bit but it doesn't change it that much. The real question is that I don't assume anything, I actually measure it. There are no assumptions here at all, except that it's Gaussian distributed and then if you are really concerned about that (it being Gaussian) you can actually test it for its Gaussian fit, which we do. The statistical techniques are purely statistical techniques, using a logrithmic Gaussian fit and those are your results and you compare that to the graphical, which just assumes a straightforward Gaussian. It is not a box model really, it certainly looks like it doesn't have sharp wedges at all; if anything, it is a Gaussian.

Q: You were taking measurements at a horizontal, were you also taking measurements at vertical as well?

A: We took several measurements at various levels. You will find it is easier to take the horizontal at various levels than try to go up and down it at various horizontal positions.

Q: Then you were at more than one plane?

A: Absolutely, you map both the vertical. I showed one example of a single plane which again was more or less a ground level source which assumed certain vertical dispersion characteristics, but we progressed from that a couple of years ago and by various means, either by long poles or actually a tethered sonde balloon system where we actually record the height and tow the balloon back and forth if it is a very high type plume. Yes, we get both vertical and horizontal disperson parameters.

Q: In one of your examples, you mentioned you were as close as 5 meters to a unit source. What was your regular distance when doing entire refineries?

A: One-quarter of a mile.

Q: And how high did you go?

A: In a total refinery, remember we're looking for fugitives only, you'd have to go maybe 500 feet. At this particular refinery, I don't have that data here and it's somewhat proprietary, but we use an aircraft as well as simultaneous surface measurements. The problem with the total refineries is that you have cooling towers, you have flares, you have stacks, etc., so the assumption was that if you took your transects close enough in, and this happened to be the case, and flares were on the downwind side, so you get close enough so that the flares were not touching down in your transect line and took about one transect line, you can use your assumption of vertical dispersion characteristics and come up with a good number, using only one transect line of about 3 meters. On that particular refinery, that was what we did and it worked very well. We were looking only for fugitives, that was the purpose of that particular task; although we did measure the total refinery. But to separate the fugitives from the flares and other materials, we could not go too high.

Q: In a tethered balloon, what do you do, bring your sample down a small diameter tube or how do you do that?

A: Well, it depends on the height. We can get up to about 500-600 feet with tethered lines and bring the sample down. There's no real problem with that, it's just a matter of lift and some of the other work we've done on total chemistry of the detached plumes, we've been able to lift quite a bit up into the plume and get easily a few hundred feet of line up there. If you get much higher than that, you just can't lift that much line and then we go into remote control samplers, but you don't get a continuous sample, you get a point source sample. It's hard to map a plume from one point or point data taken in sequence over a period of time. We've towed the balloon several hundred feet high.

Q: What are your remote control samplers?

A: I've built these myself. I own the balloons, the telemetry and the sampler.

Q: The best method?

A: It depends on what you're looking for. Most of the time, we've been after sulfates, sulfur, etc., but you can either use absorbents, you can use a bubbler, whatever you want, it doesn't matter. It's just a matter of turning the pump on and off at precise times, recording the meteorological phenomena, time, location, depending on what your position is, but it's nothing really sexy about it, you just turn it on and off, apply it to whatever level you want in the plume, but once you get above, if you want a continuous sample, say 500 feet, you almost have to use a slow flying aircraft. But, for large facilities, that is not so bad. It is that point source plume that is the problem with an aircraft.

TEST PROTOCOL FOR EVALUATING FUGITIVE EMISSIONS FROM ACTIVE COAL STORAGE PILES

David Carnes
Pietro Catizone
Thomas Kincaid

TRC Environmental Consultants, Inc.
800 Connecticut Boulevard
East Hartford, Connecticut 06108

and

D. Bruce Harris

Industrial Environmental Research Laboratory
Research Triangle Park, North Carolina 27711

This paper has been reviewed in accordance with the U.S. Environmental Protection Agency's peer and administrative review policies and approved for presentation and publication.

Introduction

A sampling program was developed to collect fugitive particulate matter emissions data from an active coal storage pile servicing an electric utility. The data were used to determine the relationship between program costs and relative accuracy for variously sized monitoring networks.

The upwind-downwind sampling method was selected for the study because it is the most appropriate method for assessing the source strength of relatively large sources that cannot be sampled by traditional techniques. This method entails measuring downwind concentrations, correcting this value for ambient background concentrations (upwind contribution), and using diffusion equations to calculate apparent source strength. These equations assume that pollutant diffusion has a normal distribution about the plume centerline in both the horizontal and vertical dimensions. The equations also assume a uniform emission rate of pollutant and that total reflection of the plume takes place at the Earth's surface. The area source is represented as a virtual point source using the techniques of Turner.[1] Because the position of the virtual point source varies with stability, the downwind distance of the samplers changes slightly between tests.

Since emissions from fugitive dust sources are normally estimated from measurements made at remote distances from the source, loss of material from the plume between the source and the measurement point will affect the source strength estimate. If the source being measured generates a signficant number of large particles, many of the particles may be deposited before the plume reaches the measurement point. To take the effect of plume depletion into account, correction factors were developed to adjust the apparent source strength. By collecting dustfall samples at downwind distances where suspended particle concentration is also being sampled, deposition velocity may be calculated by taking the ratio of the deposition rate to the immediate ground level air concentration. Chamberlain and others describe a method for computing a source depletion relationship by modifying the equations published by Sutton.[2] The depletion fraction using this method is a function of downwind distance, Pasquill-Gifford atmospheric stability class, source elevation and particle deposition velocity. The estimates of source strength, corrected for dry deposition, were statistically analyzed to determine the cost effectiveness of variously sized monitoring networks for similar area sources.

Monitoring Program

Design of the sampling array to monitor source emissions is illustrated in Figure 1. The active area of the coal pile, which constitutes the major source of fugitive coal dust, measured approximately 177 meters (580 feet) long, 116 meters (380 feet) wide, and was oriented with the long axis in the east-west direction. Activities within this area included loading onto the active pile through a telescopic chute and spreading and reclaiming coal by bulldozers and scrapers. The level of activity within the source area varied from test to test and therefore the generation rate of the fugitive emissions also varied.

The orientation of the sampling array with respect to the source was based on 5-year average seasonal wind rose data collected at a nearby

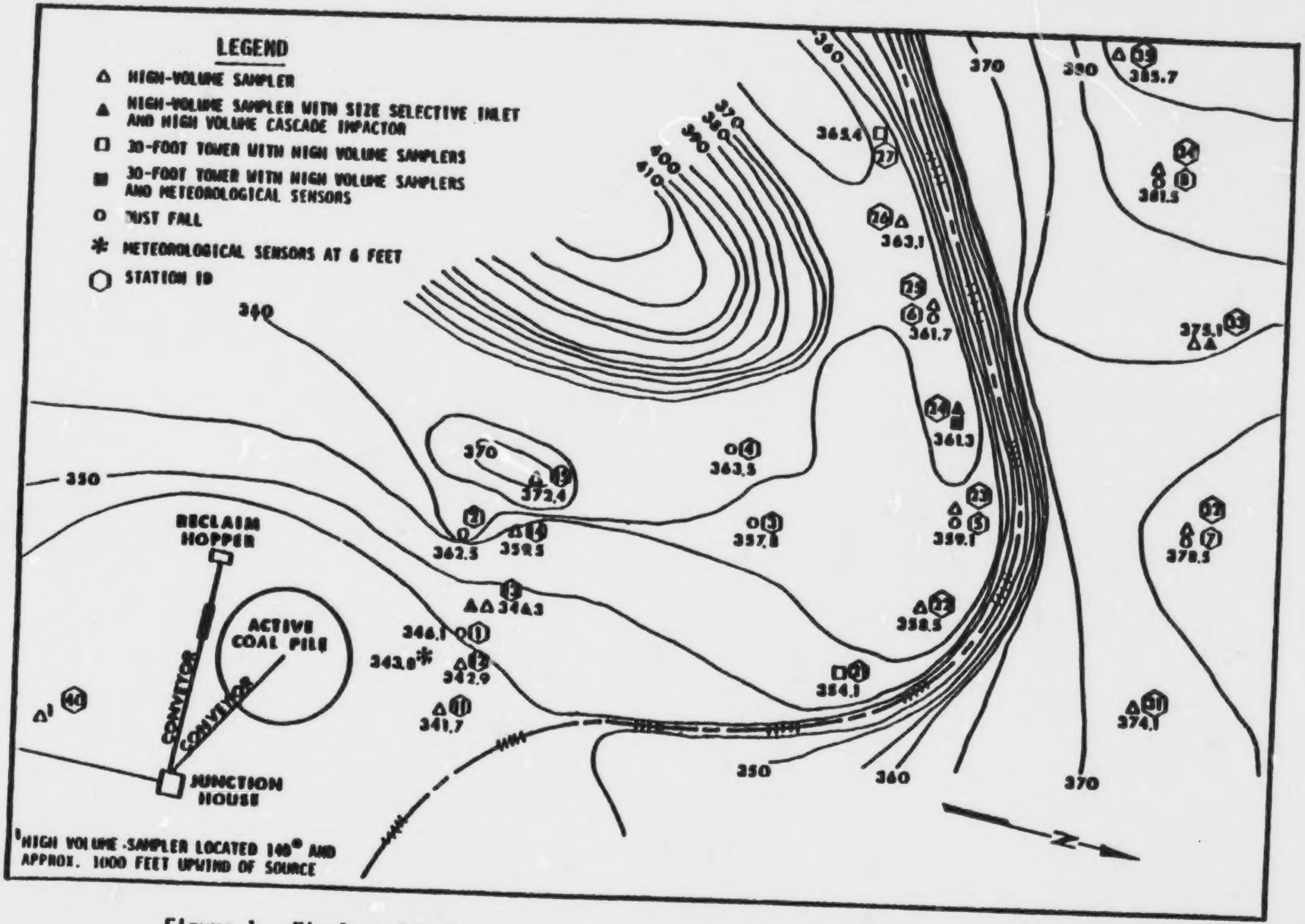
LEGEND
△ HIGH-VOLUME SAMPLER
▲ HIGH-VOLUME SAMPLER WITH SIZE SELECTIVE INLET AND HIGH VOLUME CASCADE IMPACTOR
□ 30-FOOT TOWER WITH HIGH VOLUME SAMPLERS
■ 30-FOOT TOWER WITH HIGH VOLUME SAMPLERS AND METEOROLOGICAL SENSORS
○ DUST FALL
* METEOROLOGICAL SENSORS AT 6 FEET
⬡ STATION ID
RECLAIM HOPPER
CONVEYOR
CONVEYOR
ACTIVE COAL PILE
JUNCTION HOUSE
340
350
360
370
380
390
400
410
370
380
390
363.4
27
26
363.1
25
6
361.7
24
361.3
23
5
359.1
22
358.5
21
354.1
385.7
8
381.5
375.1
7
378.5
374.1
4
363.5
3
357.8
2
362.5
359.5
372.4
344.3
346.1
1
343.8
342.9
341.7
11
350
360
370
N

¹HIGH VOLUME SAMPLER LOCATED 140° AND APPROX. 1000 FEET UPWIND OF SOURCE

Figure 1. Final monitoring network layout and site topography (elevations in feet).

National Weather Service station. The upwind station was located approximately 1,000 feet south of the source area. Three downwind sampling locations were established at approximately 150 feet, 1,000 feet and 1,400 feet, based on estimates and preliminary analyses of source strength and deposition characterization. The crosswind dimension of the array spanned approximately a 45° sector.

Initiation of a test occurred only when wind flow was at speeds greater than 1 mps (2.2 mph). The length of each test was determined by the activity level within the source area and the time required to collect a measurable sample at all stations within the dust plume. Experience showed that when filters became visibly dark in color, sufficient particulate matter had been accumulated for accurate weighing. Site characteristics during the test periods are described in Table I.

TABLE I. Site characteristics during test periods

Test Number	Wind Speed (m/s)	Wind Direction††	Temp. (°C)	Pasquill-Gifford Stability Category	Coal Pile Activity
1*					2 bulldozers 2 scraper(s)
2*					2 bulldozers 2 scraper(s)
3	2.3	146	23.9	B	1 bulldozer 1 scraper(s)
4†	3.6	220	23.9		1 bulldozer 2 scraper(s)
5†	1.5	60	27.8		
6	3.6	147	24.4	B	1 bulldozer 1 scraper(s)
7	3.1	146	24.4	B	2 bulldozers
8	3.6	145	21.1	B	2 bulldozers 2 scraper(s)
9	2.9	143	23.3	B	2 bulldozers 2 scraper(s)

* Preliminary tests to determine lateral and downwind configuration of sampling array.

† Tests that were terminated because of shifting wind flow out of the desired sector.

†† Readings are in degrees relative to true north.

Monitoring Equipment

The high-volume samplers used to collect total suspended particulate matter (TSP) data were Misco Model 680 samplers. These samplers are equipped with constant flow controllers to maintain the airflow through the filter medium at a relatively constant volume rate of 40 cfm.* At the colinear stations 13, 24 and 33, an additional high-volume sampler equipped with a Sierra size selective inlet (SSI) and a Sierra five-stage cascade impactor (CI) was run simultaneously at approximately 20 cfm. This lower flow rate was used to reduce particle bounce within the impactor head. The design cut-point of 15 μm at 40 cfm for the SSI was altered to about 16 μm by the change in flow rate. Sierra glass-fiber filters, Models C-230-GF and C-305-GF, were used as collection substrates for the cascade impactor and standard high-volume measurements, respectively.

In addition to the high-volume data, particle deposition measurements were made using 20.3 centimeter (8-inch) diameter dustfall buckets. The buckets were mounted on 1.8-meter tripods to prevent contamination by saltating particles near the ground. Grab samples of coal were collected from the source area during each test and sealed in glass jars. These samples were used to determine moisture content and grain size distribution of the source material.

Meteorological data were collected routinely during each test at station 24 and included sky cover, temperature, wind speed and wind direction. Wind speed and wind direction were also monitored near the source area. A Climatronics Mark III Wind System was placed at the 10-meter level on a telephone pole located at station 24. A similar wind system, Climatronics Electronic Weather Station, was mounted on a tripod 1.8 meters (6 feet) high and placed near station 12. Wind speed and direction data were recorded on analog charts at both locations. A standard mercury thermometer and a Bendix aspirated psychrometer system were used to obtain ambient temperature, dew-point temperature and relative humidity data.

Analytical Methods

Glass-fiber filters were inspected for defects, numbered and stored for 24 hours in a desiccator. Filters were weighed before and after testing in a controlled atmosphere where the temperature was between 20°C and 25°C, and the relative humidity below 50 percent. Results were verified for 10 percent of the filters, randomly selected, according to the criteria presented in the EPA Quality Assurance Handbook.[3]

Each dustfall sample was filtered to determine the total settleable particulate matter. The total water soluble content of the samples was determined by the evaporation of an aliquot of the sample. Both values were corrected by using a control sample for the fluid used (water). The sum of the total suspended solid matter and total water soluble matter was defined as the total dry settleable particulate matter.

The moisture content of the bulk samples of coal was determined following the American Society for Testing and Materials (ASTM) procedure D3173-73, "Moisture in the Analysis Sample of Coal and Coke." Grain size distribution was determined following ASTM procedure D410-38, "Sieve Analysis of Coal."

(*) 1 cfm = 0.0005 m^3/s.

Hourly average meteorological data were determined from the data collected during each test. Average wind speed and wind direction values were obtained by reducing the analog charts and were converted to appropriate engineering units. Atmospheric stability conditions were characterized as Pasquill-Gifford stability categories and estimated as suggested by Turner.[1]

Results and Discussion

The calculated emission rates varied among samplers because of a combination of random and systematic errors. Random error in the data results from factors influencing data collection, data reduction procedures and from the contamination of samplers by downwind sources within the sampling array. These factors were present in all five tests, and theoretically are manifest as the deviation among individual estimates of the source emission rate. Systematic error, introduced through the use of the Gaussian equation, was not quantifiable in this study because actual source emission rates were not known. The accuracy of the predictive equations was considered to be a factor of 2.

Surface Sediments

Surface sediments within the source area were characterized in terms of moisture content and grain size distribution. Both of these parameters are important because of their influence on the emission rate. As the moisture content increases, particles bind together and the erodability of the surface material decreases. The grain size distribution provides an indication of the availability of particles in the finer fractions and also the surface roughness which influences wind flow in the vicinity of individual grains. The moisture content on test days was between 3 percent and 4 percent by weight. The surface sediment ranged from clay to pebble size fractions. About 50 percent of the surface material was larger than 4 millimeters and the quantity of material finer than 62.5 μm ranged between 0.5 percent and 5 percent.

Suspended Sediment Characteristics

Within the source area, surface sediment is mechanically broken into smaller size fractions by the activity of bulldozers and scrapers. This activity occurs routinely and prevents the development of a surface crust by cementing agents or an ablative surface where fines are selectively winnowed and coarser materials stabilize the surface. The finer fractions may be eroded solely by winds, or by a combination of winds and vehicles perturbing the surface and ejecting particles upward into regions of higher wind velocity. Airborne particles will remain in suspension if wind turbulence can overcome gravity effects. The modes of transport include surface creep, saltation and suspension.

TRC's study focused only on material leaving the source area in the suspension mode. This material was analyzed to determine the distribution of grain sizes. (Histogram plots of samplers located at downwind distances of 219 meters, 481 meters and 612 meters are presented in Figure 2.) The data indicated that there was a paucity of material in the 1.3-μm to 4.2-μm size range. Also, a slight decrease was observed in the greater-than-10-μm size range with increasing downwind distance. This trend,

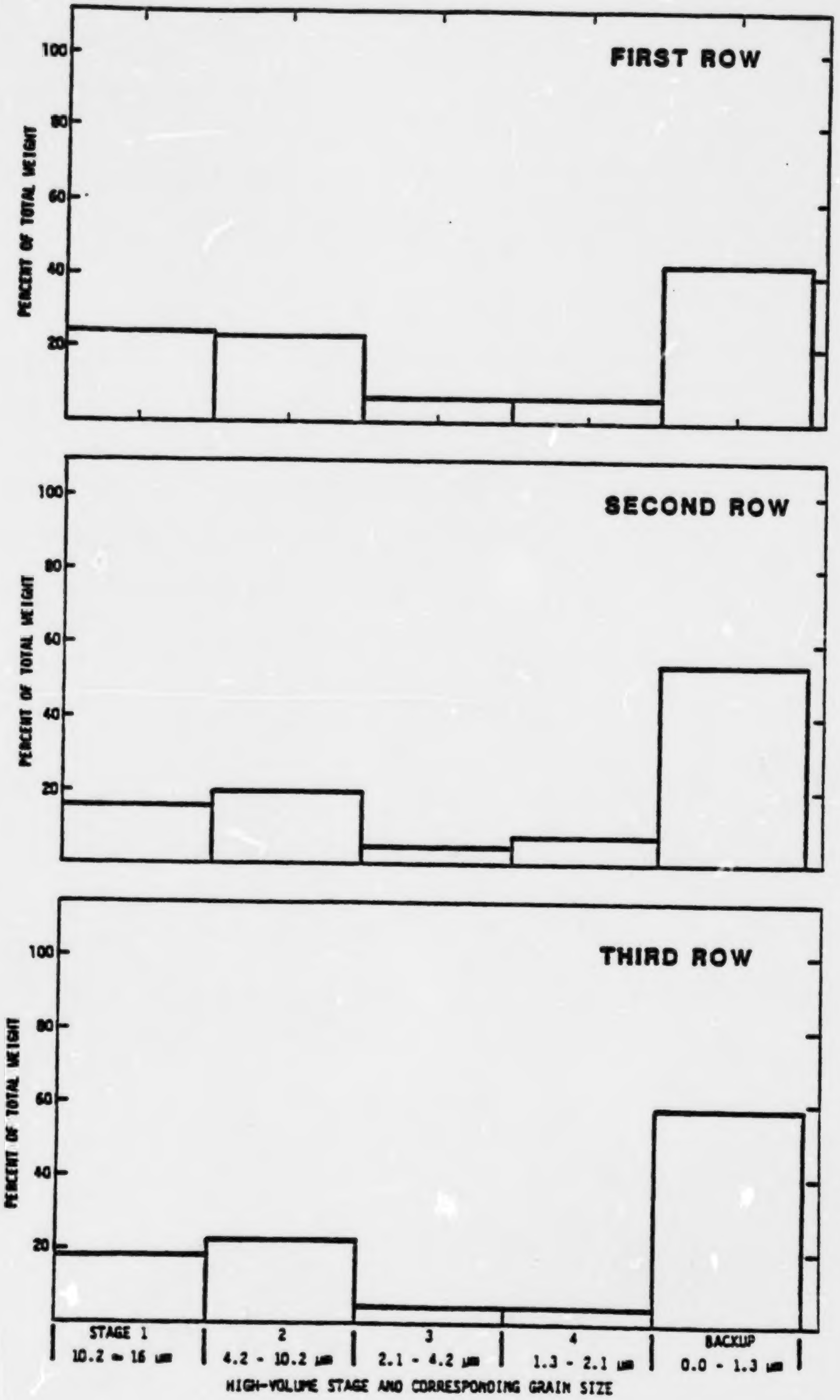

Figure 2. Grain size distribution for centerline samplers.

coupled with a slight increase in the finer fractions with downwind distance, is believed to reflect deposition of coarser materials.

Observed dustfall with downwind distance is illustrated in Figure 3. The bulk of the material was deposited within 50 meters of the source where the average deposition rate was 11 grams/m^2/min. The deposition rate decreased to 1.7 grams/m^2/min and 1.0 grams/m^2/min at downwind distances of 160 meters and 380 meters, respectively.

Source Emission Strength

Each TSP measurement was used to back-calculate source emission strength using Gaussian diffusion equations. To solve these equations for the source strength term, the source area was represented by a virtual point source which was located using Turner's techniques. The results for the complete tests (nos. 3, 6, 7, 8 and 9) are presented in Table II. TSP concentrations were corrected for background contamination by subtracting the upwind sample concentration value from the value observed downwind. Background concentrations were low (approximately 30 μg/m^3) and did not change significantly during the test period. The downwind TSP concentration decreased dramatically between samplers located at line 1 and line 2. The apparent source strength values were also corrected to account for the depletion of the dust cloud as a result of the dry deposition of airborne particulate matter. The calculated correction factors for the three downwind distances are 1.24, 1.37, and 1.46 for lines 1, 2 and 3, respectively.

Estimation of Program Cost

Program costs were estimated by grouping those tasks required to attain a specific objective and by developing man-hour and other direct costs for each group. Table III illustrates how tasks were grouped to estimate the costs associated with using the upwind-downwind test method. The relative importance of each component identified in Table III varies among programs. For example, the proximity of the monitoring site to the organization completing the tests affects travel expenses. However, basic assumptions may be made and costs developed for variously sized programs. Figure 4 compares the total program cost with the number of high-volume samplers used to monitor the fugitive emission source. The increase in cost is a step function owing mainly to the addition of field personnel to handle the increased work load.

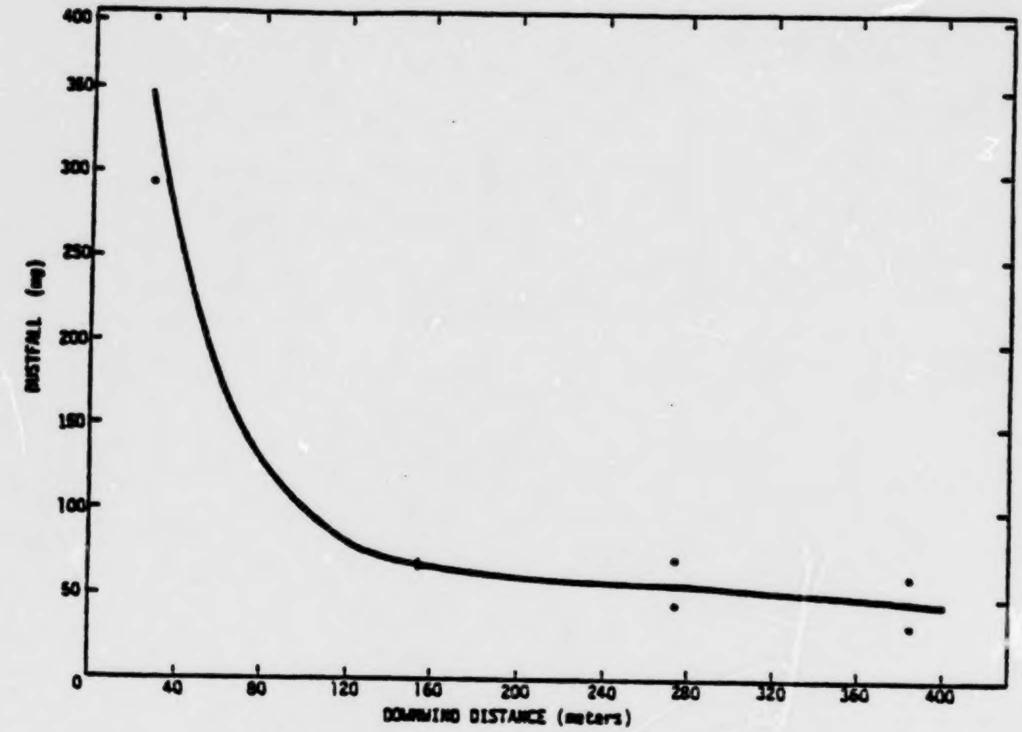

Figure 3. Comparsion of total dustfall collected by sampler with downwind distance from source.

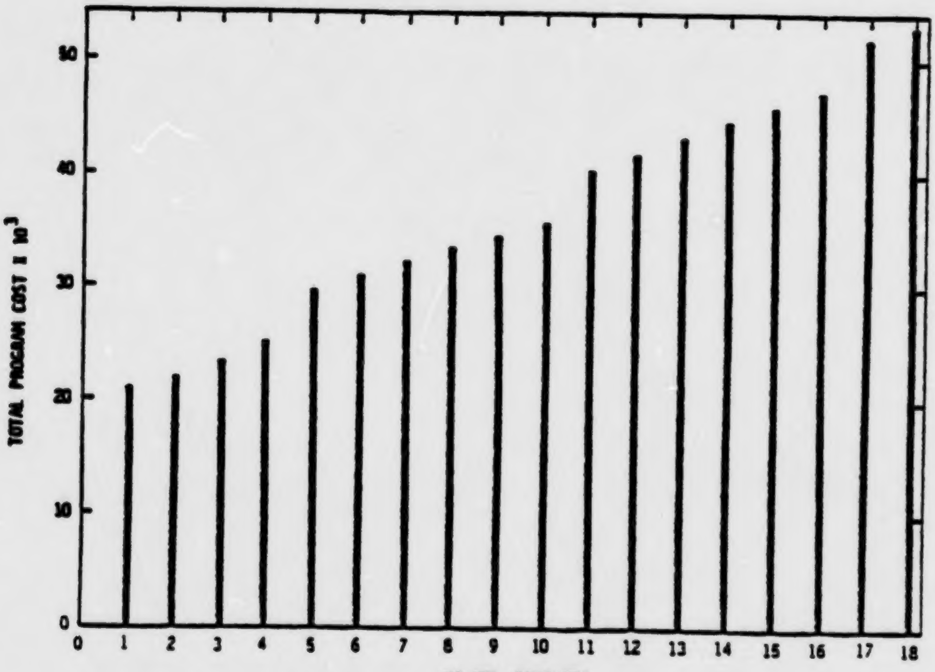

Figure 4. Comparison of total program cost and the number of high-volume samplers using the upwind-downwind method to determine fugitive source emissions.

TABLE II. Estimated Emission Rates for the Area Source

	Test #3		Test #6		Test #7		Test #8		Test #9	
Station	Distance From Source* (m)	Estimated Emission Rate (g/s)	Distance From Source* (m)	Estimated Emission Rate (g/s)	Distance From Source* (m)	Estimated Emission Rate (g/s)	Distance From Source* (m)	Estimated Emission Rate (g/s)	Distance From Source* (m)	Estimated Emission Rate (g/s)
11	173.2	17.2	177.4	50.0	184.1	59.5	183.6	138.4	187.6	99.9
12	190.9	7.1	194.8	34.9	201.8	37.8	201.6	79.1	206.3	71.8
13	208.2	7.8	211.8	32.1	219.1	24.5	219.2	57.6	224.6	48.1
14	235.5	18.8	238.6	45.9	246.4	48.2	247.2	94.6	253.7	83.1
15	256.4	19.8	259.1	53.7	267.3	66.8	268.4	162.1	275.6	84.3
21	372.2	27.6	--	--	383.1	53.1	381.7	105.8	383.6	46.3
22	421.9	19.3	426.7	56.8	432.8	56.5	431.6	67.1	434.2	48.5
23	451.7	18.9	455.9	47.9	462.6	56.6	462.1	56.7	465.8	33.4
24	--	--	473.7	33.2	481.1	42.8	481.4	39.8	486.8	36.4
25	470.3	24.8	472.7	34.9	481.2	53.9	482.4	57.3	489.7	37.9
26	476.4	32.5	477.9	55.8	--	--	489.4	86.1	490.5	50.2
27	--	--	--	--	--	--	495.7	105.7	506.3	91.8
31	507.6	38.4	--	--	--	--	--	--	--	--
33	600.8	19.7	604.3	39.8	611.7	75.4	611.9	56.4	--	--
34	607.6	18.8	609.7	44.1	618.5	43.2	620.8	63.3	627.6	35.5
35	606.1	34.2	606.9	29.5	--	--	619.9	104.4	630.3	59.8

* "Distance from source" is the distance in meters between the samplers and the virtual point source. This distance varies between tests because the position of the virtual point source is a function of atmospheric stability.

TABLE III. Components of program cost

- Management and program administration
- Development of test plan
- Calibration and preparation of equipment
- Travel to/from the monitoring site; shipment of equipment
- Data collection
- Checking and cleaning equipment
- Data reduction
- Data analysis
- Report preparation

Determination of Optimum Sampling Protocol

To determine the optimum sampling protocol, estimates of source emission rates were analyzed using standard statistical techniques. A summary of the results for each test is contained in Table IV. The values for skewness range from a low of 0.066 for test 7 to a high of 0.662 for test 8, which indicates a slight to moderate bunching of the smaller values about the mean. The values for kurtosis range from a low of -1.244 for test 6 to a high of 1.485 for test 7. None of the values for kurtosis are indicative of a significant departure from normality.

TABLE IV. Statistical analysis of emission rate estimates

Test Number	Number of Observations	Mean (g/s)	Standard Deviation (g/s)	Coefficient of Variation	Skewness	Kurtosis
3	14	29.9	13.6	45.6	0.382	-0.096
6	13	57.4	12.6	21.9	0.102	-1.244
7	12	68.8	19.8	28.7	0.066	1.485
8	15	113.0	41.8	37.0	0.662	-0.321
9	14	77.1	28.1	36.4	0.639	-1.047

The wide range of values exhibited by the coefficient of variation indicates that the mean and standard deviation do not change together, and for that reason the data from the five tests could not be combined to obtain the desired solution. Instead each test was analyzed independently and the results were compared to determine the variability of relative accuracy for sampling arrays of different size. The data values from the five tests were combined, however, to determine whether the sample population exhibited a normal distribution and whether any significant differences exist among the data values because of the techniques employed in estimating the source emission rate.

Test for normality. Because the mean of the emission rate values were different for each test, the values were standardized separately for each test using the following expression:

$$z_i = \frac{Q_{ij} - \bar{Q}_j}{s_j/\sqrt{n_j}} \qquad i = 1, 2, 3, \ldots n_j \tag{1}$$

where:

Q_{ij} represents the emission rate values
$\bar{Q}_j$ is the sample mean for the Q values for test j
s_j is the sample standard deviation of Q values in test j
n_j was the number of Q values in test j

The standardized values for the five tests were combined and grouped in nine categories. A chi-square "goodness-of-fit" test indicated that the z_i's were values from a normal distribution.

Analysis of variance. A univariate analysis of variance was also performed on the data values obtained for each test. The array of high-volume samplers was divided into three lines and the samplers in each line grouped into five positions. This division resulted in the layout shown in Table V.

TABLE V. Layout of samplers by sampler ID number

	Position				
Line	1	2	3	4	5
1	11	12	13	14	15
2	21	22	23,24,25	26	27
3	31	32	33	34	35

For each test, the following model for the Q values was employed:

$$Q_{ijk} = \gamma + \alpha_i + \beta_j + (\alpha\beta)_{ij} + e_{ijk} \qquad \begin{array}{l} i = 1, 2, 3 \\ j = 1, 2, 3, 4, 5 \\ k = 1, \ldots\ldots, n_{ij} \end{array} \tag{2}$$

where:

γ is the general mean

α_i is the effect due to line i

β_j is the effect due to position j

$(\alpha\beta)_{ij}$ is the effect due to the interaction of line i with position j

e_{ijk} is the error term

n_{ij} is the number of observations in line i and position j

The e_{ijk} values are assumed to be independent random variables normally distributed with a mean of zero and a variance of σ^2. Also, all three effects are assumed to be fixed effects.

An analysis of variance was performed for the five tests (3, 6, 7, 8 and 9). For all tests except test 9, there was no significant effect because of the interaction of line and position. An analysis of variance was also performed on the data for all five tests combined. For this case there was not a significant effect because of the interaction of line and position. There was also no difference among the lines, but there was a significant difference among the positions. Duncan's multiple range test was performed on the position means using an alpha level of 0.05 (see Table VI).[4] This test showed that position 5 was significantly different from positions 2 and 3. For all tests combined, the ranking of the position means from largest to smallest was 5, 1, 4, 2 and 3. This ranking indicates a trend for the outer positions in the rows to have a higher mean than the inner positions.

TABLE VI. Duncan's multiple range test for estimated emission rates

Sampler Grouping	Mean Value of Estimated Emission Rates (g/s)					All Tests Combined
	Test 3	Test 6	Test 7	Test 8	Test 9	
All samplers	29.9	57.4	68.8	113.0	77.1	70.1
Line 1	17.5	53.7	58.7	131.9	95.8	71.5
Line 2	33.7	62.4	71.8	101.2	65.9	69.3
Line 3	40.6	55.2	86.6	109.0	69.6	69.1
Position 1	38.4	62.0	73.3	157.8	93.7	82.7
Position 2	17.6	60.0	62.2	95.0	71.8	61.3
Position 3	24.6	51.4	69.8	72.7	51.8	55.4
Position 4	31.7	65.9	61.5	109.2	74.5	69.1
Position 5	37.3	54.9	82.8	166.1	105.9	98.4

The difference between the positions within the sampling array suggests that representing the area of fugitive emissions by a virtual point source does introduce a bias into the estimates of emission strength. Samplers located farthest from the plume centerline estimate higher source emission rates than does the population mean. Conceivably, the source area might be better represented by a line source with segments weighted differently to reflect the variability in emissions within the source area. An iterative process may be used to determine the proper weighting factors for each line segment to eliminate the bias in the data set. However, this technique would require a different description for each test of each source with the result that determining the emission characteristics of the line source would be difficult for programs that attempt to use a reduced number of samplers.

Relative Accuracy Using Reduced Number of Samplers. It was desired to determine the number of samplers that would be required to estimate the mean within plus or minus (100 x r) %, where r is a number between 0 and 1. The coefficient of variation was employed to obtain the desired estimates. The coefficient of variation from each test was treated as a datum point. The mean of five values was 0.339 and the standard error of this mean was 0.112. A 95 percent confidence interval for the mean coefficient of variation may be obtained by the following expression:

$$x \pm t_{\alpha/2,\, v}(s/\sqrt{n}), \tag{3}$$

where:

x is the mean coefficient of variation

$t_{/2,\, v}$ is the value of Students' t-distribution with a probability level of $\alpha/2$ and degrees of freedom, v

$s/\sqrt{n}$ is the standard error of the mean

For this case $\alpha = 0.05$

$v = n-1 = 4$, and the value of t is 2.776.

The lower bound of the 95 percent confidence interval on the mean is 0.228 and the upper bound is 0.451.

For any number of samplers (n) the following equation may be solved for a value of r:

$$r = \frac{t_{\alpha/2,\, n-1}\,(c.v.)}{\sqrt{n}} \tag{4}$$

where:

c.v. is a value of the coefficient of variation

Using successive values of n from 4 to 25 inclusively, values of r were obtained for the mean coefficient of variation in addition to the upper and lower confidence bounds for the coefficient of variation. To illustrate the results in terms of relative accuracy, the number of high-volume samplers (n) were tabulated with values of 1-r (see Table VII). The total program cost for incremental increases in program size were compared with relative accuracy using the mean coefficient of variation. These results are presented in Figure 5 and show that the most cost-effective program would use 10 downwind samplers.

Conclusions

A study was conducted to determine the effect of varying sampling network size on the cost and relative accuracy of the information obtained. The results of the study indicate that the most cost-effective program would use 10 downwind samplers and would provide, when deployed in accordance with the guidelines of Kolnsberg, an estimate of emission strength accurate to within approximately 25 percent of the value possible using 30 or more samplers. These results, however, should only be assumed valid for similar fugitive emission sources. Additional work is necessary to determine the minimum size sampling network for more complicated source areas or prevailing meteorological conditions.

TABLE VII. Values of 1-r for α of 0.05

		1-r Values		
n	$t_{\alpha/2,n-1}$	Lower Limit C.V. = 0.228	Mean C.V. = 0.339	Upper Limit C.V. = 0.451
4	3.182	.637	.461	.282
5	2.776	.717	.579	.440
6	2.571	.761	.644	.527
7	2.447	.789	.689	.583
8	2.365	.809	.717	.623
9	2.306	.825	.739	.653
10	2.262	.837	.758	.677
11	2.228	.847	.772	.697
12	2.201	.855	.785	.713
13	2.179	.862	.795	.727
14	2.160	.868	.804	.740
15	2.145	.874	.812	.750
16	2.131	.879	.819	.760
17	2.120	.883	.826	.768
18	2.110	.887	.831	.776
19	2.101	.890	.837	.783
20	2.093	.893	.841	.789
21	2.086	.896	.846	.794
22	2.080	.899	.850	.800
23	2.074	.901	.853	.805
24	2.064	.904	.857	.810
25	2.056	.906	.861	.815

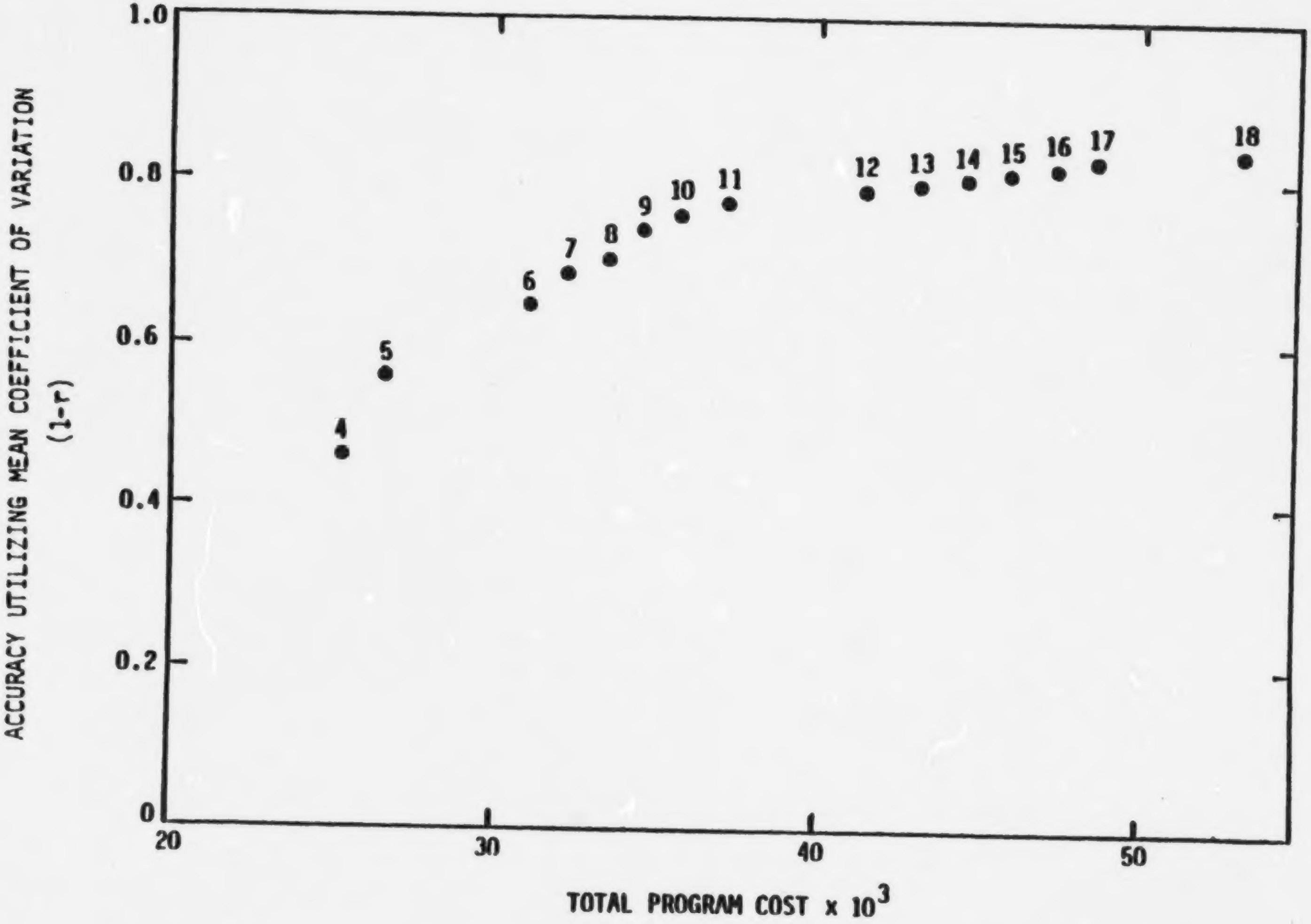

Figure 5. Comparison of relative accuracy (utilizing mean coefficient of variation) to total program cost. Numbers denote the quantity of downwind samplers.

References

1. D.B. Turner, Workbook of Atmospheric Dispersion Estimates. U.S. Environmental Protection Agency AP-26. 1970. (NTIS PB191482.)

2. D.H. Slade, Ed., Meteorology and Atomic Energy. U.S. Atomic Energy Commission, July 1968. 445 pp.

3. Environmental Protection Agency, Quality Assurance Handbook for Air Pollution Measurement Systems. EPA-600/4-77-027A. 1977. (NTIS PB273518.)

4. D.B. Duncan, "t-tests and intervals for comparisons suggested by the data." Biometrics 31: 339-59 (1975).

CHARACTERIZATION OF FINE PARTICULATE EMISSION FACTORS FOR PAVED ROADS

by

Chatten Cowherd, Jr.
Phillip J. Englehart

Midwest Research Institute
425 Volker Boulevard
Kansas City, Missouri 64110

This paper has been reviewed in accordance with the U.S. Environmental Protection Agency's peer and administrative review policies and approved for presentation and publication.

ABSTRACT

This paper presents the results of an expanded measurement program to develop emission factors for particulate emissions generated by traffic entrainment of paved road surface particulate matter. The emission sampling procedure used in this program provided emission factors for the following particle size ranges: < 15 μm, < 10 μm, and < 2.5 μm aerodynamic diameter. Testing was performed at sites in the Kansas City and St. Louis areas. These sites were representative of significant urban paved road emission sources within the following land use categories: commercial/industrial, commercial/residential, expressway, and rural town.

The measured inhalable particulate emission factors ranged from 0.06 to 8.8 g/VKT. Lowest emissions were measured for the "expressway" road category; highest emissions were measured for the "rural town" road category. Approximately 90% of the IP emissions (< 15 μm aerodynamic diameter) consisted of particles smaller than 10 μm in aerodynamic diameter, and approximately 50% of the IP emissions consisted of particles smaller than 2.5 μm in aerodynamic diameter.

Correlation analysis of particulate emissions with parameters characterizing the source conditions showed the existence of a relatively strong positive relationship between intensity of emissions and roadway surface silt loading. This relationship was used as the basis for derivation of predictive emission factors for each particle size range. The equation for IP emissions was found to represent measured IP emissions more accurately over a much larger range of values than does the AP-42 single-valued factor.

To facilitate the use of these particle size specific equations in the development of emission inventories, a classification system of mean or typical silt loadings as a function of roadway category was derived. These mean silt loadings were then inserted into the respective emission factor equations to derive a matrix of emission factors for specific roadway categories and particle size fractions.

INTRODUCTION

Traffic-entrained particulate from paved roads has been identified as a major cause of nonattainment of air quality standards for total suspended particulates (TSP) in urban areas.[1] Therefore, the quantification of this source is necessary to the development of effective strategies for the attainment and maintenance of the TSP standards, as well as the anticipated standard for particles smaller than 10 micrometers (μm) in aerodynamic diameter.

Few data on directly measured dust emissions from paved streets are available in the literature. An isolated study of dust emissions from a paved road in the Seattle area yielded an emission factor of 0.83 lb/vehicle-mile at 20 mph.[2,3] The test road was noticeably dusty and had no curbs or street cleaning program; it was located adjacent to gravel roads and unpaved parking lots from which dirt was tracked. Dust emissions generated by vehicular traffic with average daily traffic exceeding 200 vehicles were estimated to equal the amount removed by sweeping every 2 weeks.[3]

A single-valued emission factor of 3.7 g/vehicle-kilometer for dust entrainment from paved roads was developed from another field study.[4] Emission measurements were obtained using the upwind-downwind technique with high-volume samplers. Thirty-five successful tests were completed. It was determined through microscopy that 78% (by weight) of the emissions consisted of particulate less than 30 μm in size. Also through optical microscopy, it was found that 59% of the particulate collected was mineral matter, while 40% consisted of combustion products. It was also concluded in this study that particulate emissions from a street are proportional to traffic volume but independent of street surface dust loading.

In a third field study, quantitative emission factors for dust entrainment from paved urban roads were developed using exposure profiling.[5] Field testing was conducted at three representative sites in the Kansas City area. At one location, controlled amounts of pulverized top soil and gravel fines were applied to the road surface. Eight tests were performed at the artificially loaded site, and five tests were made at a different site under actual traffic conditions. Emissions were found to vary directly with traffic volume and surface loading of silt (fines). The dust emission factor for normally loaded urban streets ranged from 1 to 15 g/vehicle-kilometer, depending upon land use. Approximately 90% of the emissions (by weight) were found to be less than 30 μm in Stokes diameter and 50% less than 5 μm in Stokes diameter, based on a particle density of 2.5 g/cm^3. Measured emission factors for street particulate reentrainment added to vehicle exhaust were found to be an order of magnitude larger than the factors for vehicle exhaust alone.[6]

This document presents the results of an expanded measurement program to develop particulate emission factors for paved roads. The emission sampling procedure used in this program provided emission factors for the following particle size ranges.

IP = Inhalable particulate matter consisting of particles smaller than 15 μm in aerodynamic diameter

PM-10 = Particulate matter consisting of particles smaller than 10 μm in aerodynamic diameter

FP = Fine particulate matter consisting of particles smaller than 2.5 μm in aerodynamic diameter

Results are presented for winter testing in the Kansas City, Missouri, area and spring testing in areas of St. Louis, Missouri, and Granite City, Illinois. These results are used as a basis for the derivation of a matrix of emission factors for specific road categories and particle size ranges.

SAMPLING SITE SELECTION

Eight candidate sampling areas in Kansas, Missouri, and Illinois were designated by the Environmental Protection Agency (EPA) as representative sites for the field study. These areas represented a range of typical road, traffic, geographical, and environmental conditions within residential, commercial, and industrial land uses. Each sampling area contained a TSP monitoring site providing historical air quality data.

A wide variety of road and traffic characteristics was found in the presurveys of these areas. Equivalent hourly traffic volume ranged from 36 vehicles to 2,944 vehicles. Road width varied from 22 to 216 ft. Both asphalt and concrete street surfaces, curbed and uncurbed, were included. Street surface conditions ranged from smooth to rough, and surface particulate loadings varied from light to heavy in comparison with typically observed loadings.

Three major criteria were used to determine the suitability of each candidate site for sampling of road dust emissions by the exposure profiling technique.[7]

1. Adequate space for sampling equipment.

2. Sufficient traffic and/or surface dust loading so that adequate mass would be captured on the lightest loaded collection substrate during a reasonable sampling time period.

3. A wide range of acceptable wind directions, taking into account (a) the street orientation relative to the predominant wind directions for the locality, and (b) upwind obstacles (houses, buildings, or trees) to free wind flow.

Although roads with light traffic were excluded from consideration, such roads probably do not contribute substantially to total emissions of traffic entrained dust in urban areas.

Based on the above criteria, nine sites were selected for this testing program:

Kansas City Area - three sites

7th Street in Kansas City, Kansas (commercial/industrial)
Volker Boulevard/Rockhill Road in Kansas City, Missouri (commercial/residential)
4th Street in Tonganoxie, Kansas (rural town)

St. Louis, Missouri - two sites

I-44 (expressway)
Kingshighway (commercial/residential)

Granite City, Illinois - two sites

Madison Street (commercial/residential)
Benton Road (commercial/residential)

SAMPLING EQUIPMENT

A variety of sampling equipment was utilized in this study to measure particulate emissions, roadway surface particulate loadings, and traffic characteristics.

The primary tool for quantification of emissions was the MRI exposure profiler, which was developed under EPA Contract No. 68-02-0619.[7] The profiler consisted of a portable tower (4 m height) supporting an array of four sampling heads. Each sampling head was operated as an isokinetic total particulate matter exposure sampler directing passage of the flow stream through a settling chamber (trapping particles larger than about 50 μm in diameter) and then upward through a standard 8- by 10-in. glass fiber filter positioned horizontally. Sampling intakes were pointed into the wind, and sampling velocity of each intake was adjusted to match the local mean wind speed, as determined prior to each test. Throughout each test, wind speed was monitored by recording anemometers at two heights, and the vertical profile of wind speed was determined by assuming a logarithmic distribution. Normally, the exposure profiler was positioned at a distance of 5 m from the downwind edge of the road.

The recently developed EPA version of the size selective inlet (SSI) for the high volume air sampler was used to determine the IP concentrations. To obtain the particle size distribution of IP, a high-volume parallel-slot cascade impactor (CI) with greased substrates was positioned beneath the SSI. This five stage cascade impactor has, at a flow rate of 40 SCFM, 50% efficiency cutpoints at 7.2, 3.0, 1.5, 0.95, and 0.49 μm aerodynamic diameter. SSIs fitted with high-volume cascade impactors were placed at 1- and 3-m heights to determine the respective IP and FP mass fractions of the total particulate emissions.

Standard high-volume air samplers were used to measure TSP matter consisting of particles smaller than about 30 μm in aerodynamic diameter. These samplers were operated at a height of 2 m.

The basic upwind equipment included SSIs and a standard high-volume air sampler. In the Kansas City testing, two SSIs at heights of 2 and 4 m were used to obtain the IP concentration of upwind particulate matter. In the St. Louis testing, the primary upwind equipment included a high-volume air sampler and an SSI/CI with greased substrates. For the secondary deployment array, two SSIs were used to obtain the vertical distribution of IP.

Samples of the dust found on the roadway surface were collected during the source tests. In order to collect this surface dust, it was necessary to close each traffic lane for a period of approximately 15 min. Normally, an area that was 3 m by the width of a lane was sampled. For each test, collection of material from all travel lanes and curb areas (extending to about 25 to 30 cm from the curbing) was attempted. A hand-held portable vacuum cleaner was used to collect the roadway dust. The attached brush on the collection inlet was used to abrade surface compacted dust and to remove dust from the crevices of the road surface. Vacuuming was preceded by broom sweeping if large aggregate was present.

The characteristics of the vehicular traffic during the source testing were determined by both automatic and manual means. The vehicular characteristics included: (a) total traffic count, (b) mean traffic speed, and (c) vehicle mix.

Total vehicle count was determined by using pneumatic-tube counters. In order to convert the axle counts to total vehicles, visual 1-min vehicle mix summaries were tabulated every 15 min during the source testing. The vehicle mix summaries recorded vehicle type, number of vehicle axles, and number of vehicle wheels. From this information, the total axle counts were corrected to the total number of vehicles by type.

The speed of the traveling vehicles was determined by noting the posted speed limits of the roadway test section. As a check against this determination method, speeds of the vehicles were determined through the occasional use of a hand-held radar gun. The weights of the vehicle types were estimated by consulting automobile literature and distributors of medium-duty and semi-trailer type trucks.

SAMPLING AND ANALYSIS PROCEDURES

The sampling and analysis procedures employed in this study were subject to the Quality Control guidelines which met or exceeded the requirements specified by EPA.[8,9] As part of the QC program for this study, routine audits of sampling and analysis procedures were performed. The purpose of the audits was to demonstrate that measurements were made within acceptable control conditions for particulate source sampling and to assess the source testing data for precision and accuracy. Examples of items audited include gravimetric analysis, flow rate calibration, data processing, and emission factor calculation.

Particulate samples were collected on type A slotted glass fiber impactor substrates and on type AE (8- by 10-in.) glass fiber filters. To minimize the problem of particle bounce, the glass fiber cascade impactor substrates were greased. The grease solution was prepared by dissolving 140 g of stopcock grease in one liter of reagent grade toluene. No grease was applied to the borders and backs of the substrates. The substrates were handled, transported, and stored in specially designed frames which protected the greased surfaces.

Prior to the initial weighing, the greased substrates and filters were equilibrated for 24 hr at constant temperature and humidity in a special weighing room. During weighing, the balance was checked at frequent intervals with standard weights to assure accuracy. The substrates and filters remained in the same controlled environment for another 24 hr, after which a second analyst reweighed them as a precision check. Substrates or filters that could not pass audit limits were discarded. Ten percent of the substrates and filters taken to the field were used as blanks. Paper bags for the vacuum cleaner were conditioned and tared in a similar manner.

Prior to equipment deployment, a number of decisions were made as to the potential for acceptable source testing conditions. These decisions were based on forecast information obtained from the local U.S. Weather Service office. A specific sampling location was identified based on the anticipated wind direction. Sampling would be initiated only if the wind speed was forecast between 4 and 20 mph. Sampling was not planned if there was a high probability of measurable precipitation (normally > 20%) or if the road surface was damp.

Sampling usually lasted 4 to 6 hr. Occasionally, sampling was interrupted due to occurrence of unacceptable meteorological conditions and then restarted when suitable conditions returned. The unacceptable meteorological conditions most frequently encountered consisted of light winds (below 4 mph) and insufficient angle (< 45 degrees) between mean (15-min average) wind direction and road direction.

To prevent particulate losses, the exposed media were carefully transferred at the end of each run to protective containers within the MRI instrument van. Exposed filters and substrates were placed in individual glassine envelopes and numbered file folders and then returned to the MRI laboratory. Particulate that collected on the interior surfaces of each exposure probe was rinsed with distilled water into separate glass jars.

When exposed substrates and filters (and the associated blanks) were returned from the field, they were equilibrated under the same conditions as the initial weighing. After reweighing, 10% were audited to check precision.

The vacuum bags were weighed to determine total net mass collected. Then the dust was removed from the bags and was dry sieved. The screen sizes used for the dry sieving process were the following: 3/8 in., 4, 10, 20, 40, 100, 140, and 200 mesh. The material passing a 200 mesh screen is referred to as silt content.

The vertical distributions of the product of plume concentration and mean wind speed were numerically integrated to calculate emission factors. The size selective inlet/cascade impactor sampler combinations provided reliable point concentrations for IP and finer particle size fractions. Plume height was determined by extrapolation of the vertical profile of total particulate concentration as measured by the MRI exposure profiler.

TEST RESULTS

The winter testing was conducted during the months of February and March 1980 at three sites in the Kansas City area. The spring testing was conducted during the month of May 1980, at two sites in St. Louis and at two closely spaced sites in Granite City, Illinois.

The source tests were evaluated according to established QA criteria. Seven of the nine Kansas City tests met all of the QA criteria, while only three of the ten tests conducted in the St. Louis, Granite City area met the QA criteria. The spring testing, in particular, was hampered by unseasonably light wind conditions. Wind speed for four of the ten spring tests did not meet the minimum wind speed criterion of 4 mph.

The results of the 10 runs which met the QA criteria were used as input to Multiple Linear Regression (MLR) analysis (see below). These runs are subsequently referred to as the "MLR" data set.

During each emissions sampling run and at other times when emissions sampling was not being conducted, samples of street surface particulate were collected to determine total particulate loadings and silt percentages. Silt loadings on active travel lanes ranged from about 0.022 g/m^2 on a freeway (I-44) to more than 2.5 g/m^2 on a lightly traveled rural road in Tonganoxie. As expected, loadings in curb areas substantially exceeded loadings in travel lanes. The range of day-to-day variations in loadings at a given site was generally within a factor of 2. Higher loadings tended to occur after a precipitation event.

The upwind and downwind particulate mass concentrations for the various particle size fractions measured during the field program were analyzed to determine representative mass fraction ratios. The IP concentration measured downwind of the test road segment was found to decrease with height. At a sampling height of 2 m, the mean ratio of downwind IP to TSP concentration was 0.45 (σ = 0.14), and the corresponding mean upwind ratio was 0.54 (σ = 0.18). This indicates that background TSP, although lower in concentration, contains a higher percentage of IP. Similar differences are also evident in the mean upwind versus downwind PM-10 to TSP ratios and FP to TSP ratios.

The mean downwind ratio of FP to IP was 0.52 (σ = 0.098) while the mean upwind ratio was 0.53 (σ = 0.085). This finding implies that there is no significant enrichment of fine particles attributable to the paved road source.

Table 1 summarizes, by land use category and test series quality, the emission factor data. As can be seen, the smallest emission factors were measured in the freeway category which also had the lowest surface silt loadings. The highest emission factor was measured in the rural town category which showed a correspondingly high surface silt loading.

Intercomparison of emission factors by land-use category indicates that relative to the mean expressway IP emissions: (a) mean commercial/residential IP emissions were approximately 10 times larger; (b) commercial/industrial emissions were approximately 20 times larger; and (c) the rural town roadway produced IP emissions that were roughly 60 times larger. Relative to mean expressway silt loading: (a) the silt loading for commercial/residential roadways was approximately 25 times higher; (b) the silt loading for commercial/industrial roadways was roughly 15 times higher; and (c) silt loading on the rural town roadway was approximately 115 times higher.

MULTIPLE REGRESSION ANALYSIS

Stepwise MLR was the method used to evaluate independent variables for possible use as correction factors in a predictive emission factor equation. MLR is a statistical technique available in the Statistical Package for the Social Sciences (SPSS).[10] Because it was desirable to have multiplicative rather than additive correction factors in the emission factor equations, all independent and dependent variable data were transformed to natural logarithms before being entered in the MLR program.

The independent variables evaluated initially as possible correction factors were silt loading (g/m^2), total loading (g/m^2), average vehicle speed (Kph), and average vehicle weight (tonnes). The rationale for including measures of roadway particulate loading stems from findings of an earlier MRI program[5] which indicated that the magnitude of roadway emissions was directly related to variations in surface loadings. The vehicle parameters--mean weight and speed--were included largely by analogy to MRI's unpaved road equation,[11] although it was recognized that the dust generation mechanism for paved roads may differ from that for unpaved roads. The moisture content of the road surface particulate was not included as a correction parameter because of the difficulty of collecting a sample without altering its moisture content.

Preliminary MLR analysis of the entire data set indicated that all the independent variables except vehicle weight were highly intercorrelated. Although the stepwise algorithm would include vehicle speed first in a predictive equation, silt loading and total loading showed essentially the same correlation with IP emissions ($r \approx 0.60$). In other words, the variables represent a common set of source conditions--either low vehicle speed, high surface loading and emissions; or high vehicle speed, low loading and emissions.

TABLE 1. SUMMARY OF PAVED ROAD EMISSION FACTORS

Land use category	Test series quality	IP emission factor			PM-10 emission factor			FP emission factor		
		$\bar{x}$ (g/VKT)	σ (g/VKT)	RSD/RD[a]	$\bar{x}$ (g/VKT)	σ (g/VKT)	RSD/RD[a]	$\bar{x}$ (g/VKT)	σ (g/VKT)	RSD/RD[a]
Commercial/ industrial	All tests	2.43	1.06	0.44	2.07	0.88	0.42	1.31	0.40	0.30
	MLR tests	2.43	1.06	0.44	2.07	0.99	0.42	1.31	0.40	0.30
Commercial/ residential	All tests	0.94	0.99	1.05	0.80	0.80	1.01	0.46	0.36	0.79
	MLR tests	1.75	1.35	0.77	1.46	1.00	0.68	0.75	0.25	0.34
Expressway	All tests	0.14	0.069	0.50	0.13	0.062	0.48	0.66	0.029	0.44
	MLR tests	0.14	0.12	1.16	0.12	0.10	1.16	0.068	0.041	0.85
Rural town	All tests	8.77	-	-	6.96	-	-	1.42	-	-
	MLR tests	8.77	-	-	6.96	-	-	1.42	-	-

[a] RSD (relative standard deviation) calculated when more than two data points are present.

$$\text{RD (relative deviation)} = \frac{\Sigma\left[\bar{x} - x_i\right]}{\bar{x}}$$ calculated when two data points are present.

The decision was made to use silt loading rather than total loading or vehicle speed in the development of the emission factor equation from the "MLR" data set. This decision was based on the perception that (a) silt loading is the most physically plausible indicator of the magnitude of IP emissions, and (b) it will yield more reproducible results in independent applications than total loading, a parameter which can be biased by the presence of large particles (i.e., gravel).

Including silt loading as the primary predictor effectively precluded total loading or vehicle speed from entering the equation for the "MLR" data set. This follows from the high intercorrelations (multicollinearity) mentioned above. Examination of the regression statistics indicated that inclusion of vehicle weight as a second correction parameter could not be justified.

The raw MLR equation for the "MLR" data set was as follows:

$$e_{IP} = 4.37\ (sL)^{0.8} \qquad (1)$$

where:

e_{IP} = IP emission factor expressed in grams per vehicle kilometer traveled (g/VKT)

sL = Silt loading of road surface particulate matter expressed in grams per square meter (g/m²)

This equation explained 73% of the variation in the emission factors. As noted earlier, the "MLR" data set did contain data from all the land use categories sampled during the field program.

The comparable predictive IP emission factor equation normalized to a typical value for silt loading was as follows:

$$e_{IP} = 2.54\ \left(\frac{sL}{0.5}\right)^{0.8} \qquad (2)$$

The emission factor equation was found to predict the "MLR" series test data with a precision factor of 2.0. The precision factor (f) for an emission factor is defined such that the 68% confidence interval for a predicted value (P) extends from P/f to Pf. The precision factor is determined by exponentiating the standard deviation of the differences (standard error of the estimate) between the natural logarithms of the predicted and observed emission factors.

The precision factor may be interpreted as a measure of "average" error in predicting IP emissions from the regression equation. Assuming that the actual IP emission factors are normally distributed about the regression line, it can be stated that approximately 68% of the predictions are within a factor of 2. The effective outer bounds of predictability are determined by exponentiating twice the standard error of the estimate. The resultant estimate of predictive accuracy, in this case 4.0, then encompasses approximately 95% of the predictions.

To put the precision factor of the IP predictive emission factor equation emission factor into perspective, two comparisons were undertaken utilizing the single-valued emission factor found in the current AP-42 manual.[6] However, before valid comparisons could be made, it was necessary to convert the AP-42 single-valued factor, which represents TSP emissions, to an approximate IP emission factor. This was accomplished by multiplying the AP-42 value by 0.4 which is the mean ratio of net IP (downwind minus upwind) to net TSP concentrations as determined from the data collected in this study.

The first comparison involved the calculation of a precision factor for the AP-42 data set. The resulting value of 2.1 is a measure of the ability of the single-valued factor to represent the 40 pieces of data which were averaged originally to produce the AP-42 factor. The second comparison involved the calculation of a precision factor using the single-valued AP-42 factor to represent the "MLR" data set, as collected in this study. This comparison yielded a precision factor of 4.4.

The precision factors and the range of the data values (emission factors) upon which they are based are presented graphically in Figure 1. The ideal model has a precision factor of 1.0, implying that each predicted value is identical to the corresponding observed value, over an infinite range of emission factors. The most important conclusion that can be drawn from Figure 1 is that the emission factor equation, though far from ideal, does predict IP emissions more accurately over a much greater range of values than does the AP-42 single-valued factor over a considerably smaller range of data values corresponding to the AP-42 data set. Furthermore, application of the single-valued AP-42 factor to represent the wide range of IP emissions from paved roads, as measured during this program, yields a precision factor which is more than double (4.4 versus 2.0) that associated with the predictive equation. This ability of the predictive equation to more accurately represent variations in IP emissions is directly attributable to the relatively strong relationship between roadway surface silt loading and IP emissions.

Though not the primary focus of the program, it was possible to develop predictive emission factor equations for the PM-10 and FP particle size fractions using the same procedure as that applied in developing the equation for IP. Derivation of TSP emission factors for use in developing a predictive equation required different initial calculations, since only two TSP samplers (one upwind, one downwind) were operated during the measurement phase of the program. In essence, the initial calculation involved multiplication of the IP emission factor for each run in the "MLR" series data set by the corresponding net ratio of TSP to IP concentration as measured by appropriate samplers. This procedure assumes that the TSP/IP ratio is constant over the vertical extent of the plume.

The general form of the emission equation factors, applicable to all particle size fractions, is as follows:

$$e = k \left(\frac{sL}{0.5}\right)^{P} \quad \text{(metric)} \qquad (3)$$

$$e = K \left(\frac{sL}{0.7}\right)^{P} \quad \text{(nonmetric)} \qquad (4)$$

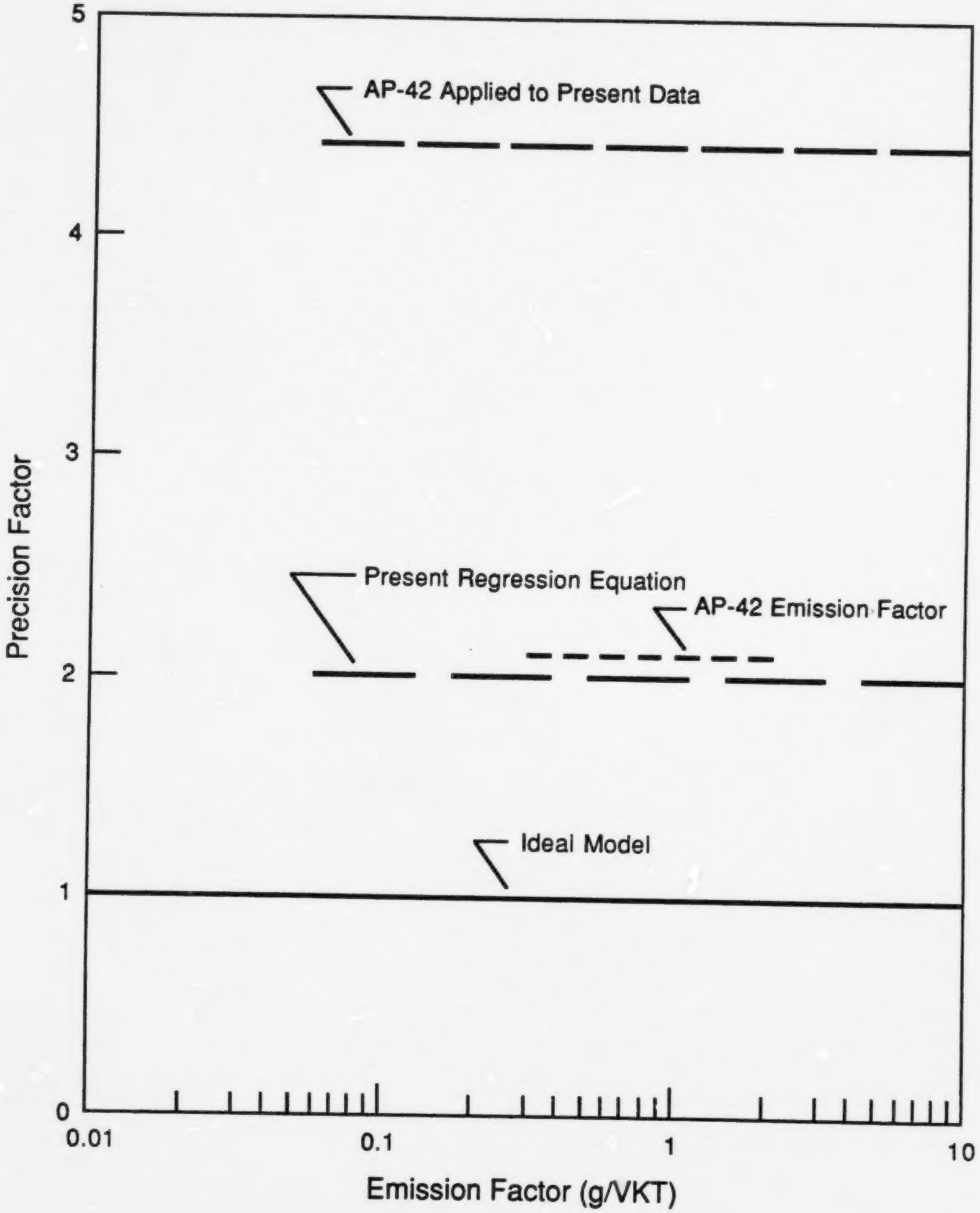

Figure 1. Comparison of emission factor precision

The base emission factor coefficients (k, K), exponent (P), and precision factor for each size fraction are listed in Table 2. For the metric equation, silt loading is expressed as grams per square meter; for the nonmetric equation, silt loading is expressed as grains per square foot.

TABLE 2. PAVED ROAD EMISSION FACTOR EQUATION PARAMETERS
(by particle size fraction)

Particle size fraction	k (g/VKT)	K (lb/VMT)	P	Precision factor[a]
TSP	5.87	0.0208	0.9	2.4
IP	2.54	0.0090	0.8	2.0
< 10 µm	2.28	0.0081	0.8	2.2
FP	1.02	0.0036	0.6	2.2

[a] Represents the interval encompassing 68% of the predicted values.

It should be noted that the tendency for the power term in the equation to increase with larger particle size fraction is generally consistent with MRI's previous paved road equation in which silt loading to the 1.0 power was employed to account for variations in TSP emissions.

EMISSIONS INVENTORY APPLICATIONS

For the majority of emissions inventory applications involving urban paved roads, actual measurements of silt loading will probably not be made. Therefore, in order to facilitate the use of the previously described equations, it is necessary to characterize silt loadings according to a parameter(s) more readily available to persons developing emissions inventories. After examination and analysis of silt loading and traffic data collected during relevant MRI sampling programs, as well as surface loading data gathered in connection with an extensive study of urban water pollution, the decision was made to characterize variations in silt loading based upon a roadway classification system. This roadway classification system is presented in Table 3. This system generally corresponds to the functional classification systems employed by transportation agency personnel; and thus the data necessary for an emissions inventory--number of road miles per road category and traffic counts--should be easily obtainable.

TABLE 3. PAVED ROADWAY CLASSIFICATION

Roadway type	Average daily traffic (ADT)	No. of lanes
Freeways/expressways	> 10,000	≥ 4
Major streets/highways	> 10,000	≥ 4
Collector streets	500-10,000	2[a]
Local streets	< 500	2[b]

[a] Total roadway width ≥ 32 ft.
[b] Total roadway width < 32 ft.

It should be recalled that traffic volume is not the only factor affecting roadway silt loadings. For all roadways that provide access to immediately adjacent areas, land use, particularly as it relates to the potential for mud and dirt "tracking," is important. Silt loadings may also be affected by street surface type and condition, the presence or absence of curb, as well as public works practices and season of the year. However, given the present data base, it is not possible to incorporate relationships between these factors and silt loadings in a manner applicable to the majority of emissions inventories.

The data base, made up of 44 samples collected and analyzed according to the procedures outlined above, may be used to characterize the silt loadings for each roadway category. These samples, obtained during MRI field sampling programs over the past 3 years, represent a broad range of urban land use and roadway conditions. Geometric means for this data set are broken out by sampling location (i.e., city) and roadway category in Table 4.

The sampling locations can be considered representative of most large urban areas in the United States with the possible exception of those located in the Southwest. Except for the collector roadway category, the overall mean silt loadings do not vary greatly from city to city, though the St. Louis mean for major roads is somewhat lower than the other four cities. The substantial variation within the collector roadway category is probably attributable to the deposition effects of land use associated with the specific sample locations. It should also be noted that an examination of data collected at three cites in Montana during early spring indicates that winter road sanding may produce loadings five to six times higher than the means of the loadings given in Table 4 for the respective road categories.

TABLE 4. SUMMARY OF SILT LOADINGS (g/m^2) FOR URBAN PAVED ROADWAYS[a] BY CITY

City	Roadway category							
	Local		Collector		Major		Overall	
	$\bar{X}g$[b]	n	$\bar{X}g$	n	$\bar{X}g$	n	$\bar{X}g$	n
Baltimore[c]	1.42	2	0.72	4	0.39	3	0.68	9
Buffalo[d]	1.41	5	0.29	2	0.24	4	0.56	11
Granite City (Ill.)[e]	-	-	-	-	0.82	3	0.82	3
Kansas City[e]	-	-	2.11	4	0.41	13	0.60	17
St. Louis	-	-	-	-	0.16	3	0.16	3
Overall	1.41	7	0.92	10	0.36	26	-	-

[a] Freeway/expressway data not included; only one value (0.022 g/m^2) obtained.
[b] $\bar{X}g$'s are geometric means based on the corresponding n sample size.
[c] Reference 12.
[d] Reference 13.
[e] From this study.

Table 5 presents the emission factors broken out by roadway category and particle size. These were obtained by inserting the above mean silt loadings into the emission factor equations with parameters defined in Table 2. These emission factors can be utilized directly for emission inventory purposes. It is important to note that the current AP-42 paved road emission factors[6] for TSP agree quite well with those developed in this study. For example, those cited in connection with MRI's previous testing[5] were conducted at two roadway sites in the major street and highway category. Those tests yielded a mean TSP emission factor of 4.3 g/VKT versus 4.4 g/VKT as determined from the data presented here.

SUMMARY AND CONCLUSIONS

The purpose of this study was to quantify inhalable particulate emissions generated by traffic entrainment of paved road surface particulate matter. Paved road source testing was performed at sites representative of significant emission sources within a broad range of urban land-use categories.

The measured inhalable particulate emission factors ranged from 0.06 to 8.77 g/VKT. Lowest mean emissions were measured for the "expressway" road category; highest mean emissions were measured for the "rural town" category. Approximately 90% of the IP emissions consisted of particles smaller than 10 μm in aerodynamic diameter, and approximately 50% of the IP emissions consisted of particles smaller than 2.5 μm in aerodynamic diameter.

TABLE 5. RECOMMENDED EMISSION FACTORS FOR SPECIFIC ROADWAY CATEGORIES AND PARTICLE SIZE FRACTIONS

Roadway category	Emission factor by particle size fraction							
	TSP		< 15 µm		< 10 µm		< 2.5 µ	
	g/VKT	lb/VMT	g/VKT	lb/VMT	g/VKT	lb/VMT	g/VKT	lb/VMT
Local	15	0.053	5.8	0.021	5.2	0.018	1.9	0.0067
Collector	10	0.035	4.1	0.015	3.7	0.013	1.5	0.0053
Major street and highway	4.4	0.016	2.0	0.0071	1.8	0.0064	0.84	0.0030
Expressway	0.35	0.0012	0.21	0.00074	0.19	0.00067	0.16	0.00057

Correlation analysis of IP emissions with parameters characterizing the source conditions showed the existence of a relatively strong positive relationship between intensity of emissions and roadway surface silt loading. This confirms the findings of earlier testing.[5] Based on regression analysis of a subset of acceptable ("MLR") test runs, the following predictive IP emission factor equation was developed:

$$e_{IP} = 2.54 \left(\frac{sL}{0.5}\right)^{0.8} \qquad (5)$$

where: e_{IP} = Inhalable particulate emission factor (g/VKT)

sL = Road surface silt loading (g/m^2)

This predictive equation has an associated precision factor of 2.0 in relation to the "MLR" data set. By way of comparison, the AP-42 single-valued factor (corrected to represent IP emissions) has a precision factor of 2.1 for its data set and a precision factor of 4.4 for the "MLR" data set, which spans a much larger range of values than the AP-42 data set. Therefore, the predictive equation, though far from ideal, does represent IP emissions more accurately over a much larger range of values than does the AP-42 single-valued factor. This fact is directly attributable to the relationship of IP emissions to silt loading.

Extension of the regression analysis to include emission factor equations for other particle size fractions--FP, PM-10, and TSP--yielded a set of equations in which the power term for silt loading increased with larger particle size fraction. This result is generally consistent with MRI's previous paved road equation in which silt loading to the 1.0 power was employed to account for variations in TSP emissions.

To facilitate the use of these particle size specific equations in the development of emission inventories, a classification system of mean or typical silt loadings as a function of roadway category was derived. These mean silt loadings were then inserted into the respective emission factor equations. The resultant emission factors for specific roadway category and particle size fractions can be utilized directly for emissions inventory purposes. By accounting for variations in silt loading, these emission factors are significantly more reliable than an overall average emission factor in developing components of an urban paved road emission inventory.

ACKNOWLEDGMENT

The work upon which this paper is based was performed pursuant to EPA Contract No. 68-02-2814, Assignment No. 32, and EPA Contract No. 68-02-3158, Technical Directive No. 19. Dennis Drehmel and William Kuykendal served as EPA project officer for the study.

REFERENCES

1. Lynn, D. L., G. Deane, R. Galkiewicz, R. M. Bradway, and F. Record. National Assessment of Urban Particulate Problem. Volume I - Summary of National Assessment. U.S. Environmental Protection Agency, Publication No. EPA 450/3-76-024, NTIS PB263665, July 1976.
2. Roberts, J. W., A. T. Rossano, P. T. Bosserman, G. C. Hofer, and H. A. Watters. The Measurement, Cost and Control of Traffic Dust and Gravel Roads in Seattle's Duwamish Valley. Paper No. AP-72-5, Presented at the Annual Meeting of the Pacific Northwest International Section of the Air Pollution Control Association, Eugene, Oregon, November 1972.
3. Roberts, J. W., H. A. Watters, C. A. Margold, and A. T. Rossano. Cost and Benefits of Road Dust Control in Seattle's Industrial Valley. Paper No. 74-83, Presented at the 67th Annual Meeting of the Air Pollution Control Association, Denver, Colorado, June 9 to 13, 1974.
4. Axetell, K., and J. Zell. Control of Reentrained Dust from Paved Streets. EPA Publication No. EPA-907/9-77-007, NTIS PB288325, August 1977.
5. Cowherd, C., Jr., C. M. Maxwell, and D. W. Nelson. Quantification of Dust Entrainment from Paved Roadways. U.S. Environmental Protection Agency, Publication No. EPA-450/3-77-027, NTIS PB272613, July 1977.
6. Compilation of Air Pollutant Emission Factors, Third Edition, U.S. EPA, Publication No. AP-42, NTIS PB275525. August 1977.
7. Cowherd, C., Jr., K. Axetell, Jr., C. M. Guenther, and G. Jutze. Development of Emission Factors for Fugitive Dust Sources. Final Report, Midwest Research Institute for U.S. Environmental Protection Agency, Publication No. EPA-450/3-74-037, NTIS PB238262, June 1974.

8. Quality Assurance Handbook for Air Pollution Measurement Systems. Volume II - Ambient Air Specific Methods. U.S. Environmental Protection Agency, Publication No. EPA 600/4-77-027a, NTIS PB273518, May 1977.

9. Ambient Monitoring Guidelines for Prevention of Significant Deterioration. U.S. Environmental Protection Agency, Publication No. EPA 450/2-78-019, NTIS PB283696, May 1978.

10. Nie, N. H., et al. Statistical Package for the Social Sciences, Second Edition. McGraw-Hill, Inc., New York, 1975.

11. Cowherd, C., Jr., R. Bohn, and T. Cuscino, Jr. Iron and Steel Plant Open Source Fugitive Emission Evaluation. Final Report, Midwest Research Institute for U.S. Environmental Protection Agency, Publication No. EPA-600/2-79-103, NTIS PB299385, May 1979.

12. Cuscino, T., Jr. Total Suspended Particulate Matter Analysis in Baltimore, Maryland. State of Maryland, Baltimore, Maryland, October 1981.

13. Bohn, R. Evaluation of Open Dust Sources in the Vicinity of Buffalo, New York. EPA Contract No. 68-02-2545, Assignment 1, Environmental Protection Agency, New York, New York, March 1979.

MICRON DROPLET DUST SUPPRESSION PROVES OUT IN VARIETY OF FUGITIVE DUST APPLICATIONS

The work described in this paper was not funded by the U.S. Environmental Protection Agency. The contents do not necessarily reflect the views of the Agency and no official endorsement should be inferred.

By: Wayne Hartshorn
Executive Vice President
Sonic Development Corporation
Mahwah, New Jersey 07430*

Lennart Strand
President
Andeze AB
Helsinborg, Sweden

---

* 305 Island Road

ABSTRACT

In recent years, a little known dust suppression technology called Dry Fog™* has proven successful in troublesome applications. Normally a baghouse or conventional wet-spray system is assigned these problem applications. This paper will detail this new technology and examine four individual applications. Specifically, applications where it is successfully controlling fugitive dust emissions in-situ -- at 40 percent lower cost vs baghouses.

Initially, the technology was applied almost exclusively to rock product plants, which pose a dusting problem characterized by multiple, widely dispersed dust generation points. The individual points are located throughout the entire materials handling system. More recently many quarries, chemical plants and coal handling operations have also reported success. These will be discussed in specific terms.

In light of recent interest in coal conversions in many industries, operating experience in coal handling operations at Dayton Power & Light and Westvaco Pulp & Paper will be detailed fully.

Since Dry Fog Dust Suppression is a relative newcomer, the paper will examine and discuss its basic principle of operation. Essentially, small, micron-size water droplets -- the size of airborne dust particles themselves -- are generated to blanket the dust and trigger in-situ agglomeration. It is accomplished without discernible wetting and with no chemical additives. It is the tiny droplet size that differentiates this technology from any other.

The paper will also discuss the technological and economic factors pertaining to matching the Dry Fog technology to other applications. Included will be the pros and cons of Dry Fog vs other technologies commonly considered for fugitive dust control. Feasibility, capital costs, operating costs, space and ease of installation, additives and wetting will be explored.

---

*Dry Fog™ is a registered trademark of Sonic Development Corporation,
305 Island Road, Mahwah, NJ 07430

INTRODUCTION

As you know, wet spray dust suppression has been around for decades. The Dry Fog concept itself is similar to the scrubbing process where a spray of water droplets remove dust particles out of an air or gas stream. However, in dust suppression, rather than pumping the mixture from a scrubbing vessel, liquid drops agglomerate with dust particles and knock them down in-situ.

Many of these wet spray dust suppression systems -- commonly termed chemical or conventional type systems -- are saddled with a major problem. While they do an adequate job of treating the material being handled, often times the droplets sprayed do not evaporate quickly or completely, thus contaminating the product. Without quick and complete evaporation, product wetting is inevitable. In many materials handling operations, such as cement, aggregate crushing, and coal preparation operations, it is essential to keep the product dry. In coal handling, for example, moisture directly impairs the heating value of the coal. With wet coal, too much heat is dissipated in evaporating that moisture. Therefore, less BTU's of heat per ton of coal are available to generate steam.

DROPLET SIZE HINDERS EVAPORATION

The reason why these water droplets produced by conventional wet-spray systems cannot evaporate quickly or completely is their size. They are too large. The second problem with large droplets is that when droplet size greatly exceeds that of the dust particles, there is very little chance of particle-to-droplet contact to trigger the desired agglomerating action. Instead, very little particle-to-droplet contact actually occurs so the dust particles simply move around the water droplets (Figure 1).[1]

At Sonic, however, we have engineered a system that is capable of producing a superfine atomization of water droplets that greatly enhances particle-to-droplet contact. And it evaporates before wetting anything but the dust. These atomized water droplets are best described as fog. Since it doesn't wet product, call it Dry Fog.

The system operates on one underlying principle: By producing water droplets of approximately the same size as the dust particles,

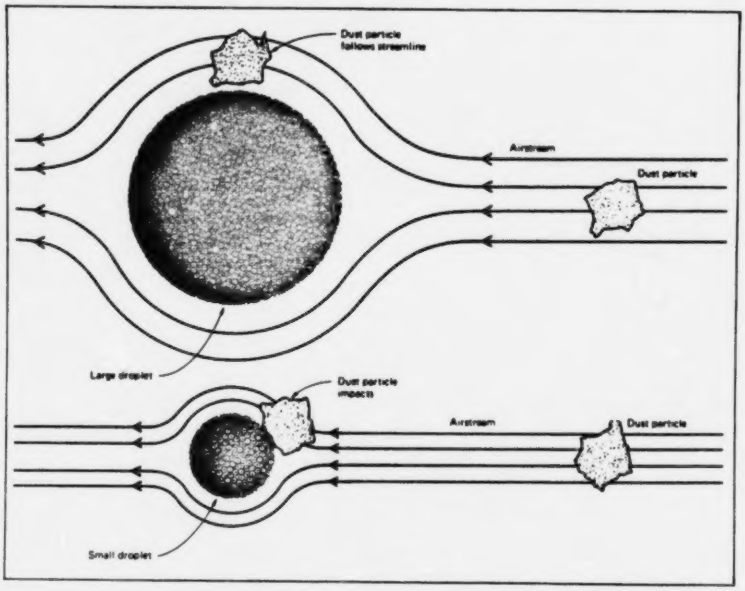
Dust particle follows streamline
Airstream
Dust particle
Large droplet
Dust particle impacts
Airstream
Dust particle
Small droplet

Figure 1. Airflow around large water droplet (top) prevents coal dust particles from contacting the droplet. The dust particle, however, easily impacts a smaller droplet (bottom).

the probability of collision between the two will be extremely high. The superfine spray of water droplets rapidly agglomerates with the individual dust particles and immediately knocks them out of the atmosphere, causing them to fall down in-situ. Also, the droplets equal the diameters of the dusts over a wide range of operating conditions and particle sizes.

As mentioned, the tiny droplet size differentiates this technology from any other wet-spray dust suppression system. The superfine fog rapidly agglomerates with airborne particulate and immediately knocks it down, in place. Knockdown is quick and it is accomplished without product wetting.

The Dry Fog system is capable of consistently producing the uniformly small droplets over all operating conditions. This is attributable to the manner in which they are created. The Sonicore® spray nozzle is the key to the Dry Fog system (Figure 2). It's actually an air-driven acoustic oscillator that creates a sonic shock wave which shatters the liquid, producing very fine droplets.

In addition to suppressing dust while insuring minimal moisture addition to the product, the Dry Fog system has other advantages over conventional methods of dust suppression -- including baghouses. For example, a Dry Fog system can be installed for as little as 40 percent of the capital cost of installing a baghouse and in less than 20 percent of the time. Since particle knockdown is achieved in-situ, there's no need for long duct runs to convey the dust to a central collection point. In most cases, it can also be installed while the plant operates at 100 percent capacity. A typical baghouse installation can last up to 3-6 weeks, and sometimes forces production to come to a standstill.

The system also offers these advantages over conventional wet-spray dust suppression alternatives:

- -- Low water consumption averaging only one to three gallons per hour (per nozzle). Conventional hydraulic systems consume anywhere from five to 15 gallons per hour to perform the same task.

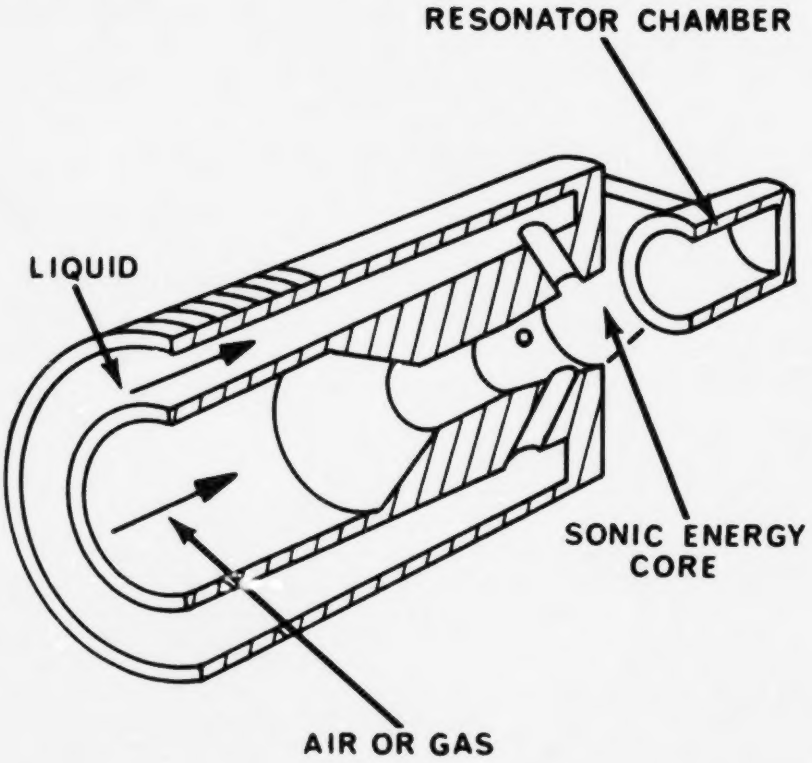
RESONATOR CHAMBER
LIQUID
SONIC ENERGY CORE
AIR OR GAS

Figure 2. Schematic of the Sonicore® spray nozzle.

-- Low water pressure eliminates the need for costly pumping systems. Usually 30-50 psi supply pressures are adequate. The Sonicore nozzle will typically operate at 20 psi.

-- Air consumption is only seven scfm per nozzle at 65 psi. Most plants have sufficient air available. Larger systems will require supplemental air.

-- Almost no water is added to the process -- less than 0.1 percent; this percentage runs as high as 1-10 percent with wet spray systems.

-- Costly wetting agents and their associated controls are eliminated with Dry Fog.

-- Dry Fog will not freeze. Independent research has proven that water droplets less than 30 microns will not freeze above minus (-) 40°F below zero.

-- Self-cleaning nozzles. The Sonicore nozzle has no internal screens or filters to plug. The liquid ports are large enough to pass large particles and the sonic action of the nozzle keeps it clean.

-- Lowered maintenance costs. The system requires no handling of chemicals and/or surface active agents.

-- No major plant modifications required for installing the system. Enclosures, skirting, and shrouds, similar to baghouse requirements, are all that are necessary.

In addition, many engineers overlook additional factors -- such as cost control, space management, and maintenance and operating costs -- when they search for a fugitive dust control system. The Dry Fog system cuts capital costs over a baghouse and some conventional spray systems by as much as 20-60 percent. It also takes up less space and can be installed in many applications where there isn't room for a baghouse. For example, the entire system's space requirement is less than 50 percent of conventional hydraulic systems, and less than 95 percent of the space of a baghouse. Only electricity and water constitute annual operating costs. Also, because there are fewer parts, equipment, and no chemical handling, maintenance is minimal.

CONTROL STANDARDS

The principle objective of the Dry Fog dust suppression system is to meet fugitive emission control regulations. Systems are designed to control practically all types of dusts that measure one to 10 microns in diameter, as well as larger fugitive dusts that measure up to 600 microns. Figure 3 shows average emission concentrations at a typical aggregate crushing plant located in Sweden, with and without the system in service.

IN-SITU, ON-SITE

As mentioned earlier, the main feature of this new technology involves its ability to ensure that almost no moisture is added to the product. Coal handling operations for example, require dry coal at all times for maximum heating efficiency. Two very recent applications, one a midwestern utility plant, the other a southern pulp and paper mill, both solved major dust problems in their coal prep operations. The systems have been successfully controlling fugitive dust for close to two years and without a trace of wet or frozen coal.

Dayton Power & Light Company's Longworth Station needed to comply with tight EPA regulations. They had a problem suppressing fugitive dust in their coal prep operation. Each time they ran the conveyor that leads to its coal bunkers dust was generated.

Conventional wet-spray type dust suppression systems controlled the dust, but left a residual moisture on the coal. This left them with the dual problem of excessive energy costs for coal heating and frozen coal during the winter months. With the wet-coal problem, some of the heat generated inside the boiler was dissipated in

Figure 3

AVERAGE RESULTS AT SWEDISH STONE CRUSHING PLANT

Points Treated	Dust Level (mg/m^3)	
	System Off	System On
Reclaim Tunnel	6.0	1.2
Crusher Discharge	190.0	16.0
Crusher Feed	73.0	2.6
Screen #1	2.7	0.4
Transfer Point	15.0	1.0
Screen #2	11.0	0.9

evaporating that moisture. Consequently, less BTU's of heat per ton of coal were available to generate steam.

Dry Fog eliminated both problems at half the capital investment compared to another alternate method -- a baghouse.

The Dry Fog system was installed at several points in DP&L's coal handling gallery. These points include a screen, a crusher, three transfer points, and a 20' x 40' open bunker area. The installation time required for the Dry Fog system was minimal and no major modifications of the existing plant facilities were necessary. Also, Dry Fog virtually eliminated maintenance costs.

For each gallon of water used in the process, Dry Fog yields a much greater distribution of micron-sized droplets. This, of course, means greater knockdown power since the size of the droplets is equal or close to the size of the airborne dust particles.

The resulting dust suppression satisfied the regulations and brought a cleaner air environment for plant workers.

For DP&L's essentially intermittent operation, the Dry Fog system functions only once or twice a day. The application of Dry Fog has been so successful that they are considering applying it to other facilities.

Westvaco Corporation of Charleston, SC holds the distinction of being the first full scale coal prep installation of a Dry Fog system.

During its conversion from oil to coal, plant engineers found a great amount of dust being generated over the crusher and transfer towers. To control this problem, several wet-spray dust suppression systems were examined. Finally Westvaco installed Dry Fog spray bars at the inlets and outlets of its coal crusher and transfer points.

The system proved superior to a baghouse -- a baghouse would have required duct runs ranging from 150-200 feet between its coal crusher and transfer tower. Also, lack of adequate space in its coal prep room, and the high cost that accompanies a baghouse installation, steered them toward Dry Fog.

Dry Fog's tiny droplets triggered agglomeration so that the coal dust was knocked down in-situ. This eliminated the need for long duct runs to carry the dust to a central pickup point. And, since Dry Fog's droplets evaporated quickly, Westvaco experienced no moisture addition to the coal.

SCIENTIFICALLY PROVEN

The emission concentrations at the stone crushing plant located in Vilhelmina, referenced earlier, are fully supported by a series of tests conducted by the Swedish National Board of Occupational Safety and Health.

The test site was a fluidized stone crushing plant that operates only six months out of the year due to harsh winter months. Figure 4 gives a plot plan of the crushing operation showing the location of the primary crusher, screens and hoppers.

In this particular crushing plant, raw materials are crushed in two stages -- primary crushing and secondary crushing. These two crushers are also the main dust generation points. After the raw materials are crushed they are assorted into two fractional sizes -- 0-8 mm and 8-16 mm. Daily output is about 200 to 250 cubic meters. Crushing rate is close to 50 percent.

The Dry Fog system was tested over a three day period to determine its efficiency as a dust control method. Samples were taken from the test site with Dry Fog equipment in service for two days. The third day of testing was conducted without the Dry Fog system in operation. Temperature and wind velocity varied over the three days. Temperatures ranged from 8°C to 13°C and the wind velocity varied between slight westerly to northwesterly winds. Production output each day was approximately 25-30m^3/hr. Water usage was about 120 liters per hour. The system consisted of a total of nine Sonicore nozzles.

Samples were taken at several points. The stone crushing operation's dust levels were measured at the following points: the reclaim tunnel, where coarse sand is loaded onto a conveyor; at the jaw crusher; the main bell crusher; the primary and secondary screens; and a transfer point.

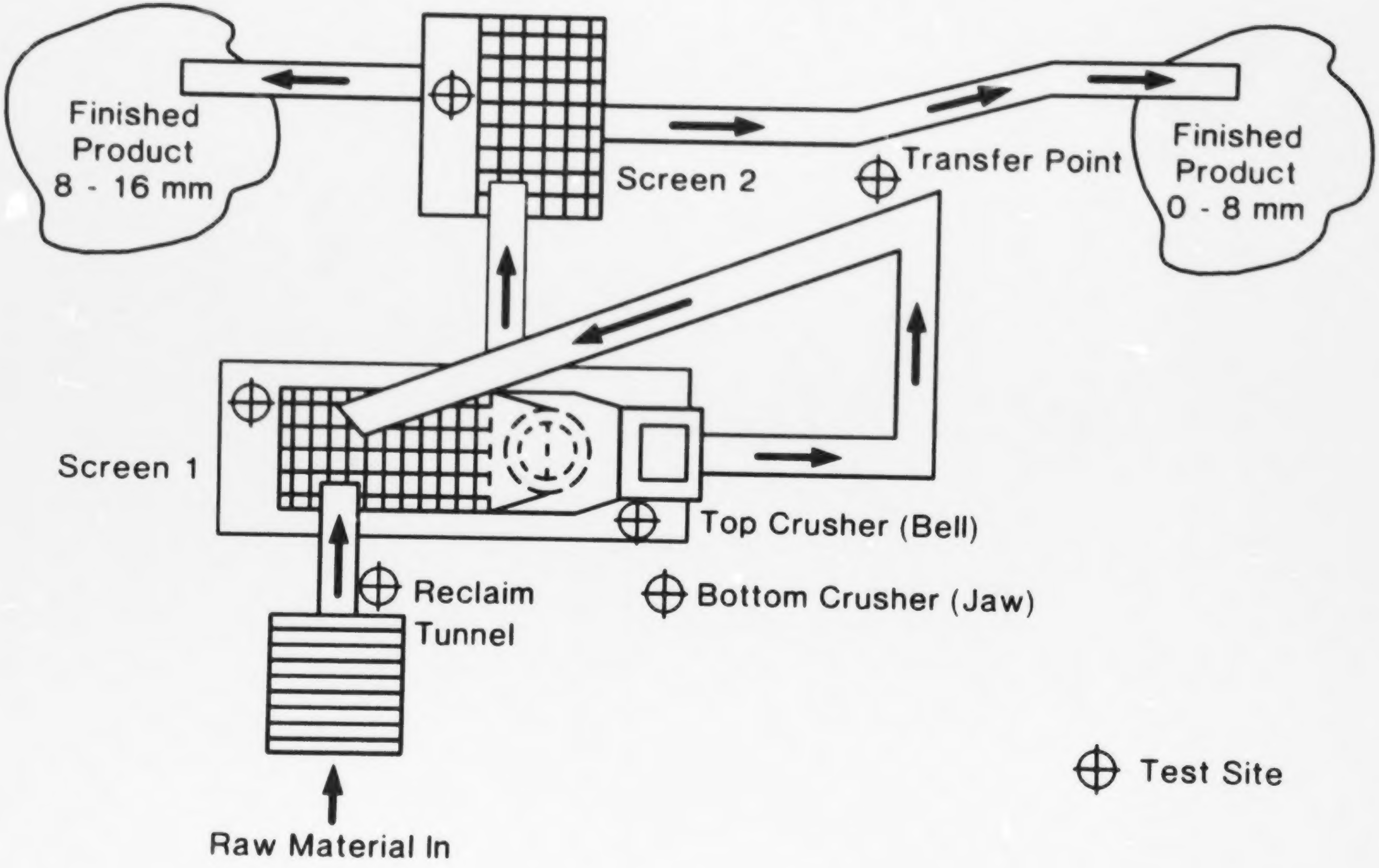
Finished Product 8 - 16 mm
Screen 2
Transfer Point
Finished Product 0 - 8 mm
Screen 1
Top Crusher (Bell)
Reclaim Tunnel
Bottom Crusher (Jaw)
Test Site
Raw Material In

Figure 4. Schematic of Swedish stone crushing plant.

Figure 5 is an overall summary of test results with the Dry Fog Dust Suppression system in service and without the system in service. Dust concentrations were measured in mg/m^3.

These government sponsored tests show that airborne particulate levels are significantly reduced by the Dry Fog system. At the same time, they also show that it accomplished the necessary reduction without any discernible product wetting.

FURTHER TESTING

A second, more detailed experiment on the Dry Fog system was performed at another Swedish crushing site in early 1981. This was conducted at an underground mining operation. Figure 6 is a plot plan of the mining operation. Over a four-day testing period, the system's performance was measured for its ability to suppress fugitive dusts on a section of this underground mine. During normal mining operations, the Dry Fog system was activated. At the same time, six sampling units measured atmospheric particulate levels. Figure 7 is an overall summary of test results with the Dry Fog system in service.

Three tests were run during a four-day period. On the first day, this particular section of the mine was shut down. However, the fugitive dust samplers recorded atmospheric readings for particulate content for comparison purposes vs particulate levels during normal operation. The significance of the overall findings is uncovered in the three days the mine was in actual operation vs the one day it was not in service. The comparison shows that there was no appreciable difference in airborne particulate levels when the section was operating with the Dry Fog System in service and the day the entire mining section along with the Dry Fog system was shut down.

In the final report, test engineers stated that "there was no excess of applicable limit values for the total dust volume detected during the testing period." This means they didn't exceed the total dust volume limit allowable according to Swedish local and federal regulations for the area. The allowable limit is 10 mg/m^3.

REFERENCE

[1] Schowengerdt, F.D., Brown, J.T., "Colorado School of Mines Tackles Control of Respirable Coal Dust," COAL AGE, April 1976, Copyright 1976 McGraw Hill, Inc.

Figure 5

INDIVIDUAL RESULTS AT SWEDISH STONE CRUSHING PLANT

with Dry Fog

	Reclaim Tunnel	Crusher Discharge (jaw)	Crusher Feed (bell)	Screen (#1)	Transfer Point	Screen #2
Test: 1	1.3	9.3	1.5	0.6	1.4	1.3
2	1.0	16.1	3.0	0.3	1.0	0.6
3	1.3	22.9	3.2	0.4	0.4	0.7
Average	1.2	16.0	2.6	0.4	1.0	0.9

without Dry Fog

	Reclaim Tunnel	Crusher Discharge (jaw)	Crusher Feed (bell)	Screen (#1)	Transfer Point	Screen #2
Test: 1	5.6	210	84	3.7	23	19
2	3.2	190	68	1.9	12	6.4
3	9.1	170	61	1.9	6.8	2.3
Average	6.0	190	73	2.7	15	11

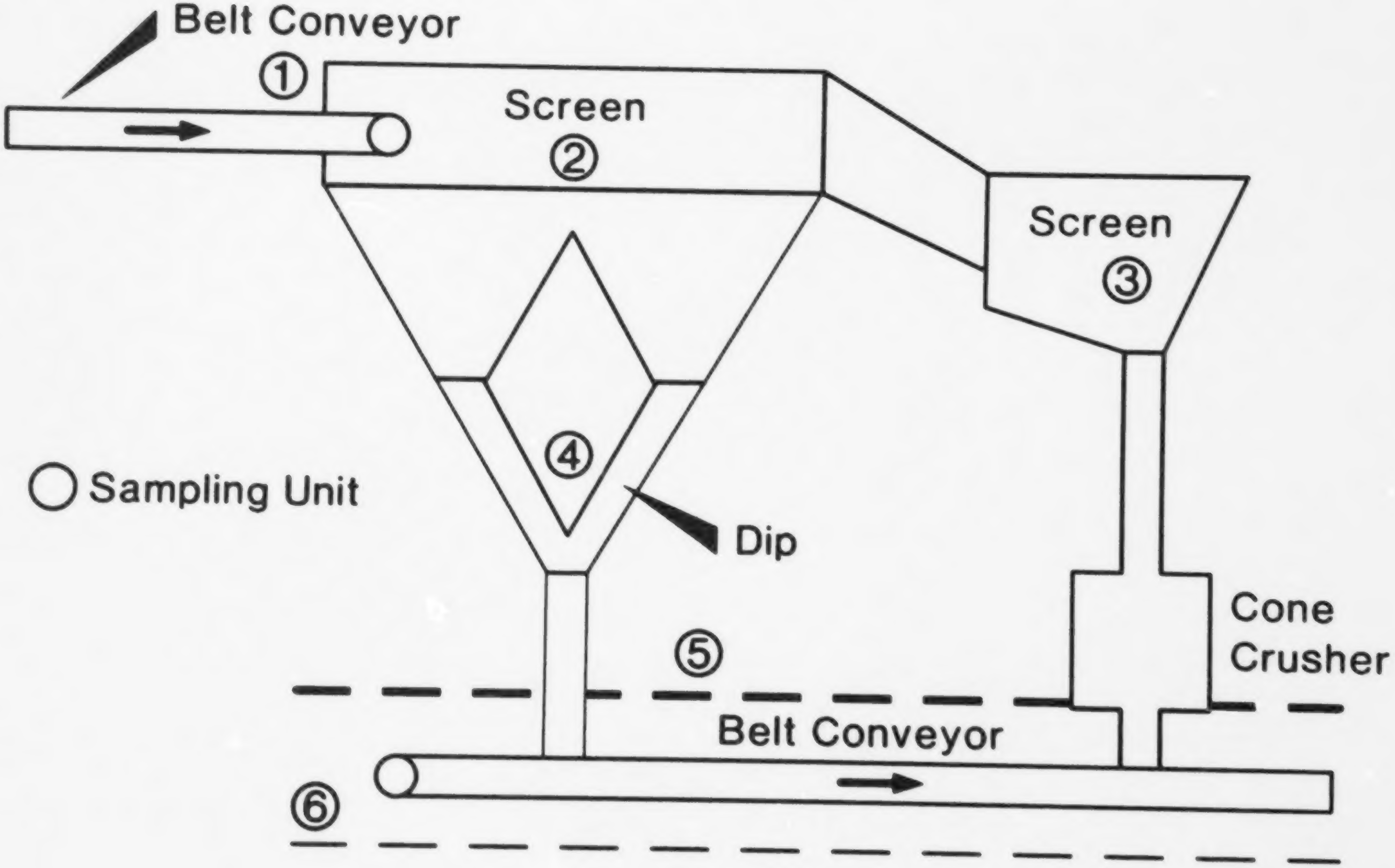
Belt Conveyor
①
Screen
②
Screen
③
④
Sampling Unit
Dip
Cone
Crusher
⑤
Belt Conveyor
⑥

Figure 6. Schematic of Swedish underground mine.

Figure 7

TEST AT SWEDISH UNDERGROUND MINE

Points Treated		Total Dust Measured mg/m^3			Average Per Day	Total Average
Belt Conveyor	System Off	0.57	1.10	1.02	0.90	
	System On	1.51	1.29	0.66	1.15	1.13
		0.70	1.06	1.01	0.92	
		1.39	1.01	1.52	1.31	
Screen #1		0.65	0.78	0.78	0.74	0.58
		1.44	0.84	0.30	0.86	
		0.53	0.34	0.52	0.46	
		0.59	0.35	0.29	0.41	
Screen #2		1.26	1.67	1.66	1.53	1.30
		1.11	0.97	0.68	1.48	
		1.03	0.55	0.88	0.82	
		2.03	1.41	1.33	1.59	
Transfer Point #1		1.18	1.70	1.62	1.50	1.32
		0.76	0.72	0.69	0.72	
		1.00	0.46	0.81	0.76	
		2.49	2.63	2.29	2.47	
Transfer Point #2		0.68	0.75	0.89	0.77	0.89
		0.77	0.66	0.46	0.63	
		1.67	0.32	0.60	0.86	
		0.91	1.39	1.22	1.17	
Transfer Point #3		2.68	4.74	4.68	4.03	4.78
		3.54	3.98	2.70	3.41	
		5.13	3.38	4.18	4.23	
		6.71	8.16	5.21	6.69	

The work described in this paper was not funded by the U.S. Environmental Protection Agency. The contents do not necessarily reflect the views of the Agency and no official endorsement should be inferred.

FUGITIVE DUST CONTROL STUDIES USING SCALE MODELS AND MASS LOSS ESTIMATES*

by: Michael F. Lepage, Anton E. Davies
Colin J. Williams

ROWAN WILLIAMS DAVIES & IRWIN Inc.
650 Woodlawn Road West
Guelph, Ontario, Canada
N1K 1B8

(*) Although this is not the actual presentation made at the May 1982 meeting, it closely resembles that presentation, which was entitled, "The Optimization of Wind Screens for Fugitive Emission Control Using Wind Tunnel Tests," C. J. Williams (then of MHTR, Ltd.).

INTRODUCTION

Fluid model studies of bulk storage facilities provide an inexpensive means of testing dust control strategies before implementing them in the field. The potentially high cost of implementing a successful dust control program requires careful planning to ensure that the best result is obtained.

There has been growing pressure in recent years to improve air quality around bulk storage sites (e.g. coal stockpiles, sawdust piles and fly ash lagoons) by reducing dust emissions (see Figure 1). Improved air quality, however, is only one of the benefits of a dust control program, since dust losses often represent losses of valuable inventory. In many cases, the cost of implementing dust controls is more than offset in the long run by the reduction in lost inventory.

There are two principal approaches to dust control at bulk storage facilities. The first is to clean up the site, compact loose surfaces and encrust exposed dust which would be available for emission. The second approach is to reorganize the stockpiles and erect wind breaks in order to reduce local wind speeds below the threshold of dust emissions. The most efficient dust control program is typically a combination of both approaches.

Fluid model studies provide a means of optimizing dust control while avoiding costly trial and error in the field. By examining local wind conditions on a scale model in a wind tunnel or water flume, one can identify the windiest and hence most sensitive areas of the site and can evaluate the relative merits of different schemes for localized wind speed reduction. To give further meaning to the results, actual samples of material from the site are tested in the wind tunnel to determine the relationship between wind speed and the level of dust emission (which can vary significantly from one site to another). By feeding this information together with data from the scale model tests into a computer simulation of dust emission, wind reduction schemes can then be evaluated in terms of their impact on overall emissions at the site.

The present paper describes the fluid modelling techniques currently being practiced at Rowan Williams Davies & Irwin Inc.'s fluid dynamics laboratory at Guelph, Ontario. The techniques have undergone a number of refinements since they were first presented[1]. The objective, which has remained unchanged, is to determine the most effective configuration windbreaks and stockpile geometry for minimizing local wind speeds. The techniques in question have been applied to numerous sites, such as: the coal handling facilities of Kerr McGee Inc. at Trona, California; the Pennsylvania Electric Company at Homer City, Pennsylvania; the Dofasco steel mill at Hamilton, Ontario; and Ontario Hydro's thermal generating stations at Nanticoke and Atikokan, Ontario, Canada.

EXPERIMENTAL METHODS

Scale Model Tests

The fluid modelling techniques for dust control studies at Rowan Williams Davies & Irwin Inc. include testing a scale model of the study site in the simulated wind flow of both the boundary layer wind tunnel and the open channel water flume. Photographs of both pieces of equipment are shown in Figure 2.

The boundary layer wind tunnel is an open circulation type, 27m long, 2.4m wide and 1.8m high. The test section, located near the downwind end of the tunnel, has a 2.4m diameter automatic turntable built into the floor. Spires and roughness elements can be placed on the floor upwind of the test section to simulate the characteristics of the mean wind and turbulence approaching the study site[2]. Wind speed is controlled automatically and can achieve values in excess of 25 m/s.

The open channel water flume is a 12m long, 1.2m wide and 0.5m deep apparatus that operates on the same principles as the wind tunnel but uses flowing water to simulate wind. Flow patterns on a scale model are visualized by injecting coloured dye into the stream. Drifting of relatively large particles, such as snow grains, is simulated using silica sand.

Scale models of bulk storage facilities are typically constructed at scales between 1:400 and 1:600. The principal modelling material is plexiglas, with stockpiles modelled in clay to facilitate reshaping. The models are mounted on a 2.4m diameter base that fits on the turntable of the wind tunnel test section. Various wind directions are simulated by rotating the turntable. The base of the model is divided into two sections: an inner disk and an outer annulus. The 1.2m diameter inner disk fits into the test section of the water flume.

Local wind speeds on the scale model are measured using an array of surface-mounted omnidirectional sensors[3] as shown in

Figure 3. Speeds are measured at the equivalent height of 2.0m above grade full scale and are sampled at a rate of 300 Hz. The data are low-pass filtered at 200 Hz which is well above the dominant frequency of atmospheric turbulence. The local speeds are normalized by the free stream (gradient) speed, U_g, measured above the model using a pitot-static tube. The results are recorded in the form U/U_g and s/U_g where U is the one-hour mean speed and s is the RMS (standard deviation) of the wind at each sensor location. Using previously measured profiles, the ratios are then converted to the form U/U_o and s/U_o where U_o is the mean speed at 2.0m above grade in an unobstructed area. The resulting ratios can be thought of as local wind speed magnification or reduction factors due to the presence of terrain features, buildings or windbreaks.

Dust Sample Tests

A schematic of the apparatus for testing dust samples in the wind tunnel is shown in Figure 4. The quantity of dust lifted into the atmosphere is evaluated by weighing portions of the samples before and after exposure to the wind. The apparatus is designed to distinguish between dust particles that are sufficiently small to remain suspended in the atmosphere and undergo turbulent diffusion (airborne particulates), and heavier particulates that are subjected to the saltation process (saltating particulates).

Three adjacent trays embedded in the floor of the wind tunnel test section are filled with samples of the dust. The middle tray is fixed to the floor while the upwind and downwind trays are removable for the purpose of weighing. When the wind is turned on, the saltation process quickly reaches equilibrium. The middle tray is sufficiently long that the downwind tray experiences a flux of saltating particles leaving the tray equal to the flux entering from upwind. Hence, any measured weight loss after a time t is attributable to airborne particulates. The upwind tray, on the other hand, experiences no flux of saltating material from upwind so that the measured weight loss is a combination of both saltating and airborne particulates. The difference in weight loss between the upwind and downwind trays, therefore, gives the estimate of the outward flux of saltating particulates.

In summary, if W_1 is the upwind weight loss and W_2 is the downwind weight loss after a time t, and if A_1 and A_2 are the surface areas of the upwind and downwind trays, then:

W_2/A_2 = emission of airborne particulates per unit area
$W_1/A_1 - W_2/A_2$ = outward flux of saltating particulates

Wind speed is monitored using a pitot-static tube, which can be set at any desired height above the samples, and the tests are repeated for a range of wind speeds. Spires and roughness elements are used to generate turbulence. Although full scale turbulence cannot be generated in the wind tunnel due to the limitation of having walls and a ceiling, the turbulence produced is thought to be sufficiently close to full scale for the purpose of the dust sample tests. The impact of turbulence intensity on these tests is the subject of ongoing investigations.

Computer Simulation

The computer simulation combines the results of the dust sample tests and the wind speed ratios described in the previous sections with wind measurements from a meteorological station near the study site in order to predict dust emissions for individual wind events. Dust losses are calculated for the area around each model sensor location and summed to obtain a global dust loss for the entire site. The simulation has the capacity of integrating the results for several years' worth of wind events to predict average annual dust losses.

The dust loss from the area around each sensor location is calculated hour by hour as follows. The reference hourly mean wind speed, U_o, and wind direction are obtained from the nearby meteorological station. The local mean speed at 2.0m above grade is calculated by taking the product of U_o and the local wind speed ratio, U/U_o, that was measured during the scale model tests. The results of the dust sample tests are then used to determine the local dust losses for the given hour. The local RMS ratio, s/U_o, is not currently used in the analysis but will be added in future studies as more data becomes available on the relationship between turbulence intensity and the level of dust emissions. For the present, it is assumed that the level of turbulence throughout the study site is uniformly the same as was generated in the wind tunnel during the dust sample tests.

The dust sample results allow the local dust loss to be divided into its airborne and saltating portions. When calculating the saltating portion, consideration has to be given to the fact that a partial balance exists between the flux of material away from the sensor location and the flux into the area from upwind. The net flux is determined using a two-dimensional centred-difference technique in which the difference in dust loss between surrounding sensor locations is examined.

Before the local dust losses can be calculated, initial conditions have to be established - i.e. the amount of dust available for erosion at each sensor location prior to the wind event. The initial conditions are highly site-dependent and can vary from one event to another. The calculated hourly dust losses are subtracted from the initial amount until the remaining amount reaches zero. When the remaining amount at a particular sensor location has reached zero, no further dust loss is permitted to occur at that location. If the area is continually disturbed by vehicle traffic, then the material available for erosion may be unlimited. To account for such cases the initial condition is set sufficiently high so that the remaining amount does not reach zero during the event.

Optimization and Evaluation of Dust Control Strategies

The fluid model studies are designed to evaluate the following types of dust control strategies:

(i) development of an optimum stockpile geometry to achieve maximum wind speed reductions in critical areas;

(ii) development of haul roads and operating procedures that minimize disturbance of the surface of the storage piles in critical areas;

(iii) development of an optimum arrangement of windscreens, berms and other windbreaks upwind of critical areas.

Semi-permeable windbreaks may also be used downwind of critical areas to trap saltating particles before they leave the property, but are generally ineffective at trapping airborne dust. Typically, it is not feasible to design a dust control program that works for all wind directions but the program can be designed for the directions most frequently responsible for high wind events.

The following are some of the practical limitations by which dust control programs tend to be constrained:

(a) the cost and availability of material for berms and other windbreaks;

(b) the need for efficient haul routes, unobstructed by windbreaks;

(c) the need for sufficiently large working areas uncluttered by windbreaks;

(d) temporary windscreens must be practical to assemble, disassemble or move about.

By and large, flow visualization on the scale model in the water flume is adequate for determining which set of control strategies works best[1]. A qualitative judgement, however, is less convincing than a numerical assessment, and the pros and cons of various possible strategies are best weighed by using predicted dust emissions from the computer simulation.

EXAMPLE OF RESULTS

Figure 5 shows a plan of the fly ash lagoon at Ontario Hydro's Generating Station at Nanticoke, Ontario. During the course of some thirteen years of ash storage operations the level of deposited ash exceeded the waterline in some areas. Eventually, dry ash became exposed resulting in significant dust emissions during strong winds.

In order to continue using the lagoon, Ontario Hydro drained off most of the water and compacted the ash surface sufficiently to allow the traffic of heavy vehicles. Several settling cells were created in the western half of the lagoon. At present, the ash, which is a by-product of the coal-fired boilers at the generating station, comes to the lagoon in a liquid slurry poured from pipelines into the settling cells. The ash is allowed to settle and is then removed by drag lines and transported by truck to the permanent storage area. A fluid model study was undertaken to determine the optimum method of continuing this procedure over the next twenty years while minimizing dust emissions at the site.

Since most observed incidents of high dust emissions occurred during winds from WSW, the design of dust control strategies focused on that direction. Figure 6 shows contours of wind speed ratios derived from the scale model tests in the wind tunnel. The highest values occur in the most elevated areas which are exposed to the highest wind speeds.

Ash samples were collected from the site and an example of the data from wind tunnel tests on the samples is shown in Figure 7. Weight losses of airborne particulates are plotted for wind speeds of 6.0, 8.0 and 10.0 m/s (measured at 15 cm height) and for various durations of wind exposure. Wind speeds of 2.0 and 4.0 m/s were also tested but no weight loss was observed, from which it was concluded that the threshold speed of dust emissions is between 4.0 and 6.0 m/s. For durations greater than 0.2 hours, the data shown in the figure fit to an expression of the form $W = at + b$ where W is the weight loss, t is the duration of wind exposure, and a and b are constants which vary with wind speed. The constants a and b were found to be approximately related to the square of the wind speed.

A scheme for storing ash was developed, taking into account all of the economical and practical limitations relating to the site, and is shown in Figure 8. The plan shows the entire ash lagoon as it would appear after approximately twenty years of operation. The sections at the bottom show the progression of the permanent storage area over the same period. Berms mounted with windscreens are placed west-southwest of areas where ash is being dumped. The dumping begins just east of the settling cells (see Figure 5) and eventually progresses eastward until the permanent storage area is filled to a height of 15m above the level of the surrounding dyke. A 15m high porous windscreen along the western perimeter of the lagoon protects the settling cells area where much of the vehicle traffic occurs. Solidity ratios between 0.5 and 0.8 were recommended for various windscreens in order to obtain the optimum compromise between maximum wind speed reduction and maximum extent of protection.

The scheme shown in Figure 8 was modelled and tested in the wind tunnel. To assess the impact of the scheme on dust emissions, the computer simulation was run using the wind conditions that occurred during a particular dust event, on January 13 and 14, 1985, which was chosen as a representative case. Wind speed and direction during the event were recorded at a tower located a few kilometres north of the lagoon. Wind directions were observed to range between southwest and northwest and the highest hourly mean wind speed recorded was 35 km/hr (at 10m above grade). As an initial condition for the event, it was assumed that the entire ash storage area was covered in a uniform thin layer of loose dust. Although this was an oversimplification of the true situation, it was an adequate assumption to assess the relative impact of the recommended berms and wind screens.

Figures 9 and 10 show contours of airborne dust emissions as predicted by the computer simulation for the present ash lagoon configuration (Figure 9) and for the ash lagoon after twenty years of operation. The size of the shaded area, indicating emissions of 0.2 kg/m^2 or greater, is significantly reduced in the future configuration despite the fact that the ash is piled considerably higher than in the present case. In the future configuration, the areas downwind of the protective berms and windscreens experience minimal dust emissions. The upwind slope of the westernmost berm in the permanent storage area experiences accelerated winds and consequently high values of dust emission, but in practice this area would be permanently sealed and seeded with grass.

Integration of the dust losses over the entire area indicated that the future configuration would experience about half the total dust emissions of the present configuration for the same initial conditions. If permanently sealed and grassed areas are accounted for then the emissions would be further reduced.

CONCLUSIONS

Fluid modelling studies are an excellent visual and quantitative tool in the design of dust control programs for bulk storage facilities. Areas where refinements to the physical model approach are anticipated in the future include: the establishment of more realistic initial conditions for the computer dust simulation that account for the rate of disturbance by vehicles, the moisture content of the surface material and other factors; an indepth study of dust emissions resulting directly from vehicle activity; a further study of the relationship between airborne emissions and turbulence intensity.

A further addition currently being implemented consists of applying a numerical dispersion model to predict the rate of dispersion of the dust emissions downwind of the study area, the results of the numerical model can then be compared to field measurements with high volume samplers.

REFERENCES

1. A.E. Davies, "A physical model approach to the solution of fugitive emission problems", Proceedings of the 73rd Annual Meeting and Exhibition of the Air Pollution Control Association, Montreal, June 22-27, 1980.

2. H.P.A. Irwin, "Design and use of spires for natural wind simulation", National Research Council of Canada, N.A.E. Report LTR-LA-233, 1979.

3. H.P.A. Irwin "A simple omnidirectional sensor for wind tunnel studies of pedestrian level winds", Journal of Wind Engineering and Industrial Aerodynamics, 7, pp. 219-239 (1981).

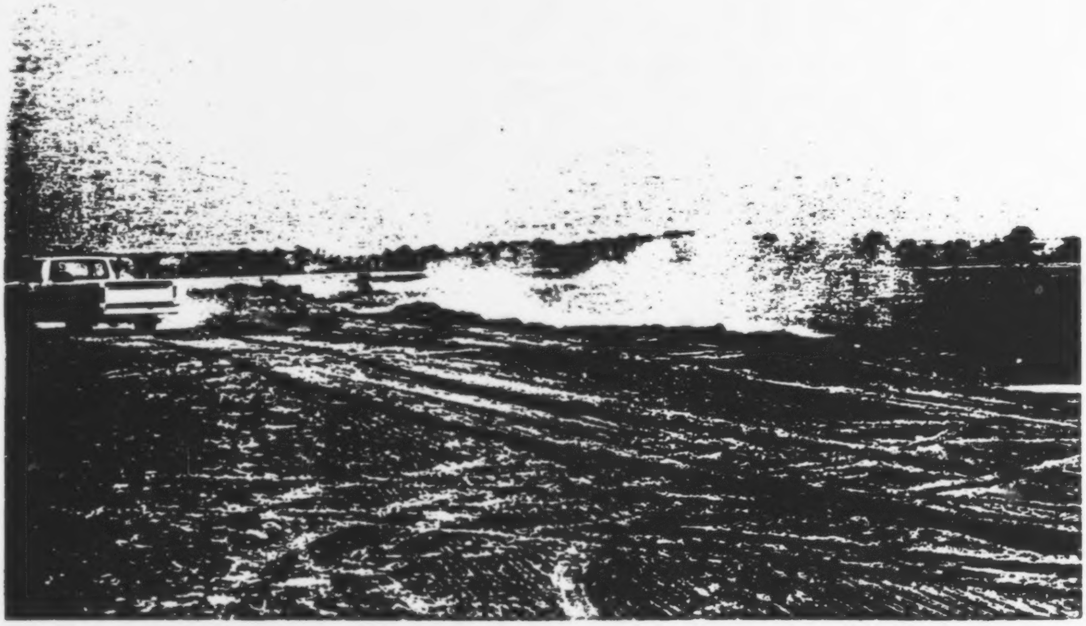

Figure 1. Dust emissions at a fly ash storage area.

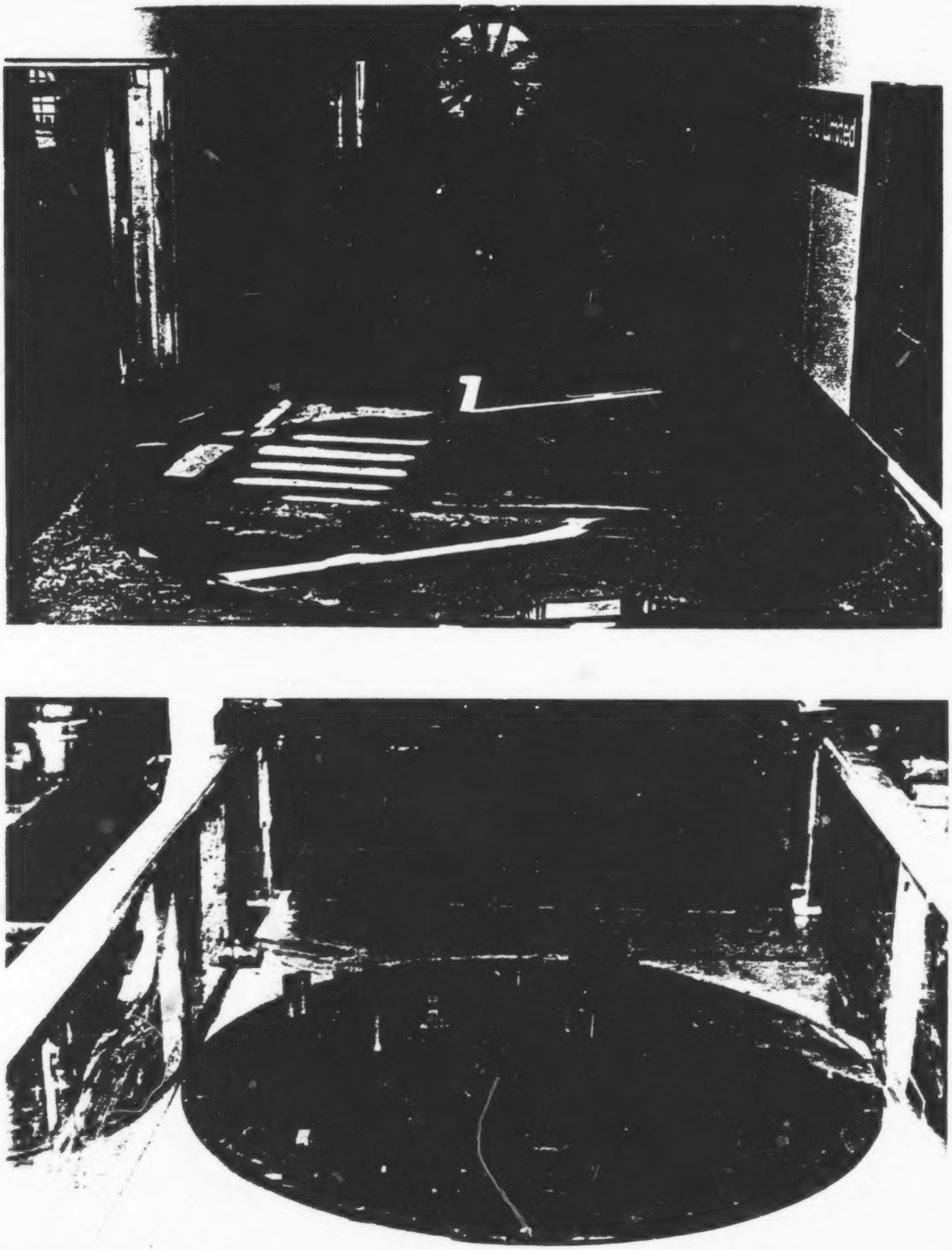

Figure 2. The boundary layer wind tunnel (top) and open channel water flume.

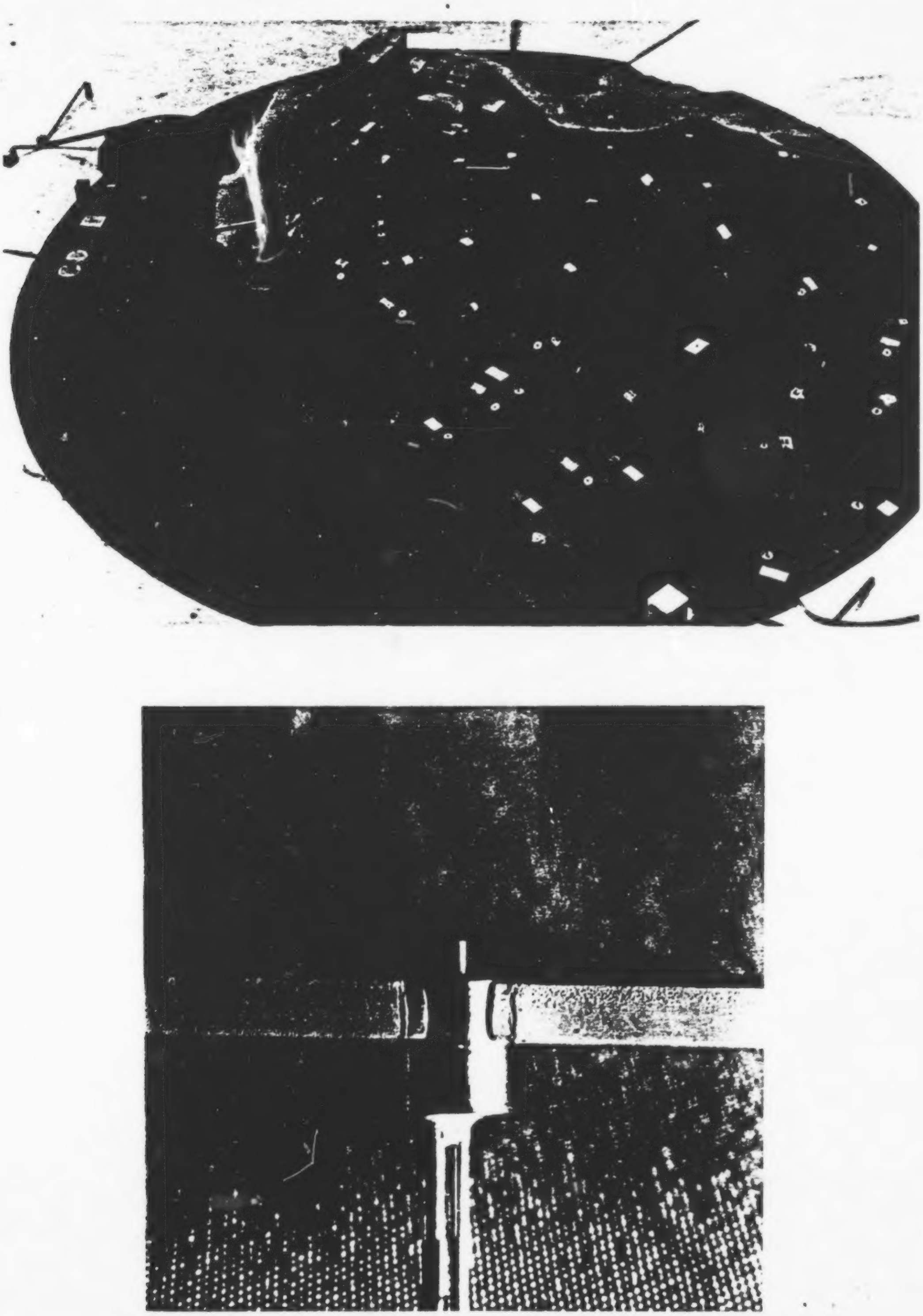

Figure 3. Omnidirectional wind sensors on a model (top) and a side view of an individual sensor.

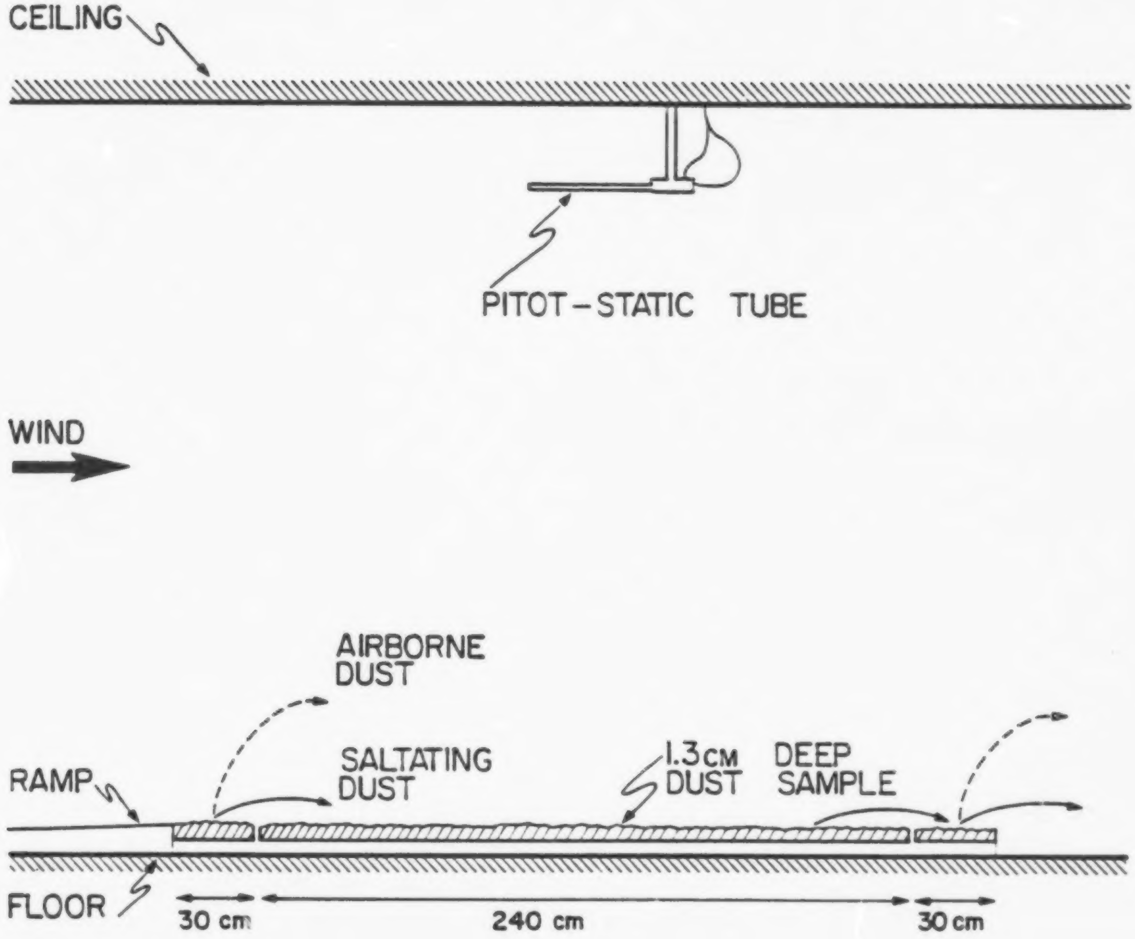
CEILING
PITOT-STATIC TUBE
WIND
AIRBORNE DUST
SALTATING DUST
1.3 CM DEEP DUST SAMPLE
RAMP
FLOOR
30 cm
240 cm
30 cm

Figure 4. Schematic of the dust sample test apparatus.

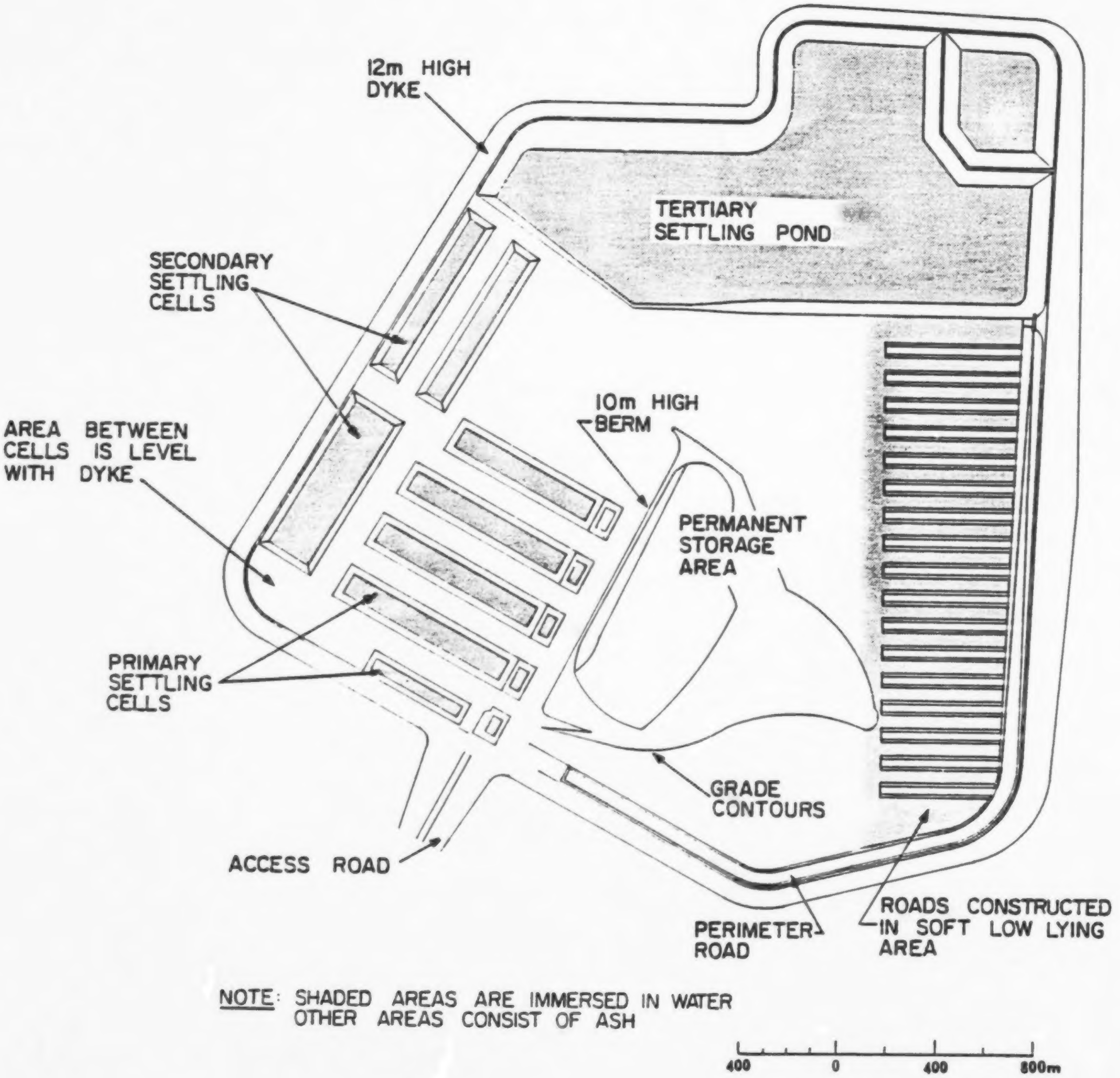
12m HIGH DYKE
TERTIARY SETTLING POND
SECONDARY SETTLING CELLS
AREA BETWEEN CELLS IS LEVEL WITH DYKE
10m HIGH BERM
PERMANENT STORAGE AREA
PRIMARY SETTLING CELLS
GRADE CONTOURS
ACCESS ROAD
PERIMETER ROAD
ROADS CONSTRUCTED IN SOFT LOW LYING AREA
NOTE: SHADED AREAS ARE IMMERSED IN WATER OTHER AREAS CONSIST OF ASH
400
0
400
800m

Figure 5. Plan of the ash lagoon at Nanticoke, Ontario, in its present state.

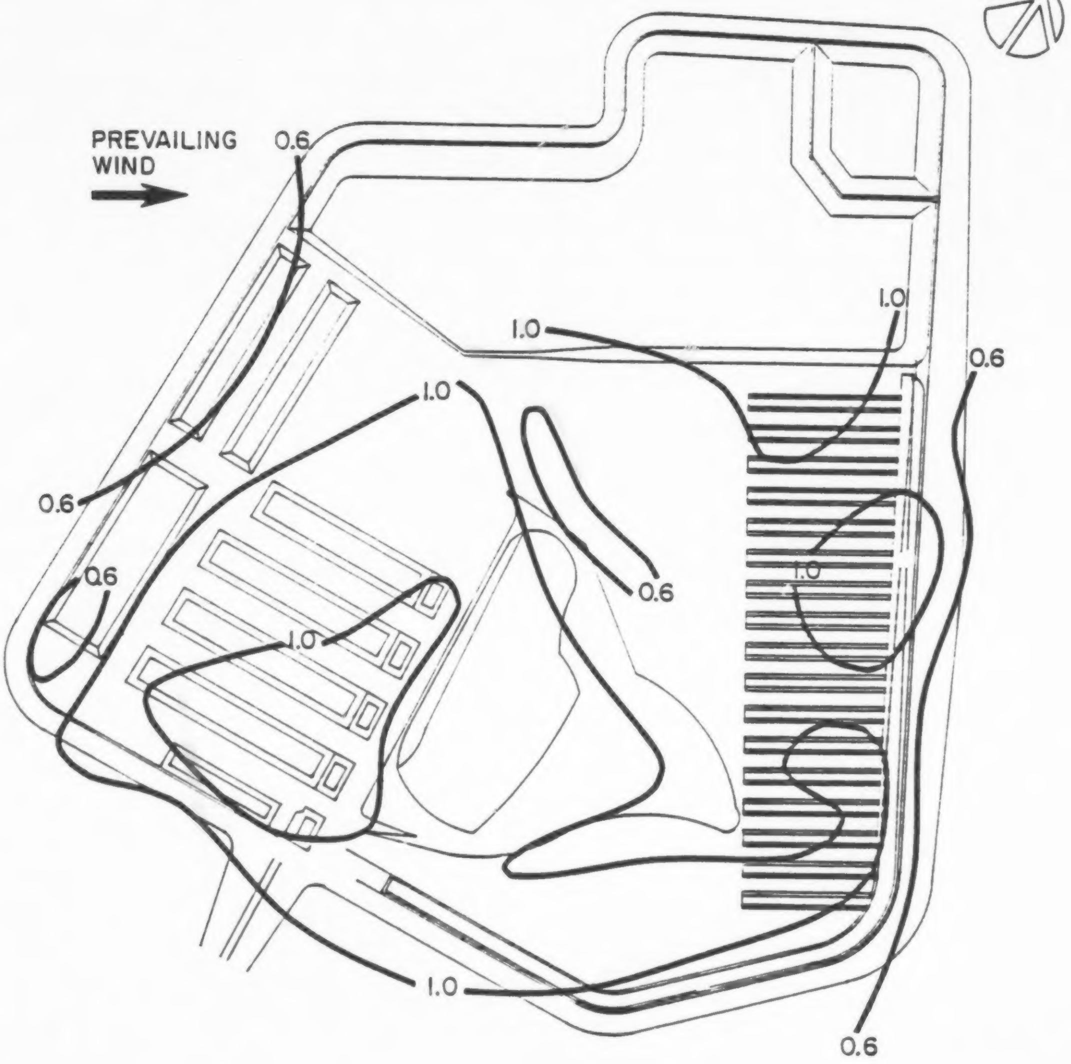
PREVAILING WIND
0.6
1.0
1.0
0.6
0.6
1.0
0.6
1.0
0.6
1.0
1.0
0.6
1.0
0.6

Figure 6. Wind speed ratios, U/U_o, as measured in the wind tunnel for winds from WSW.

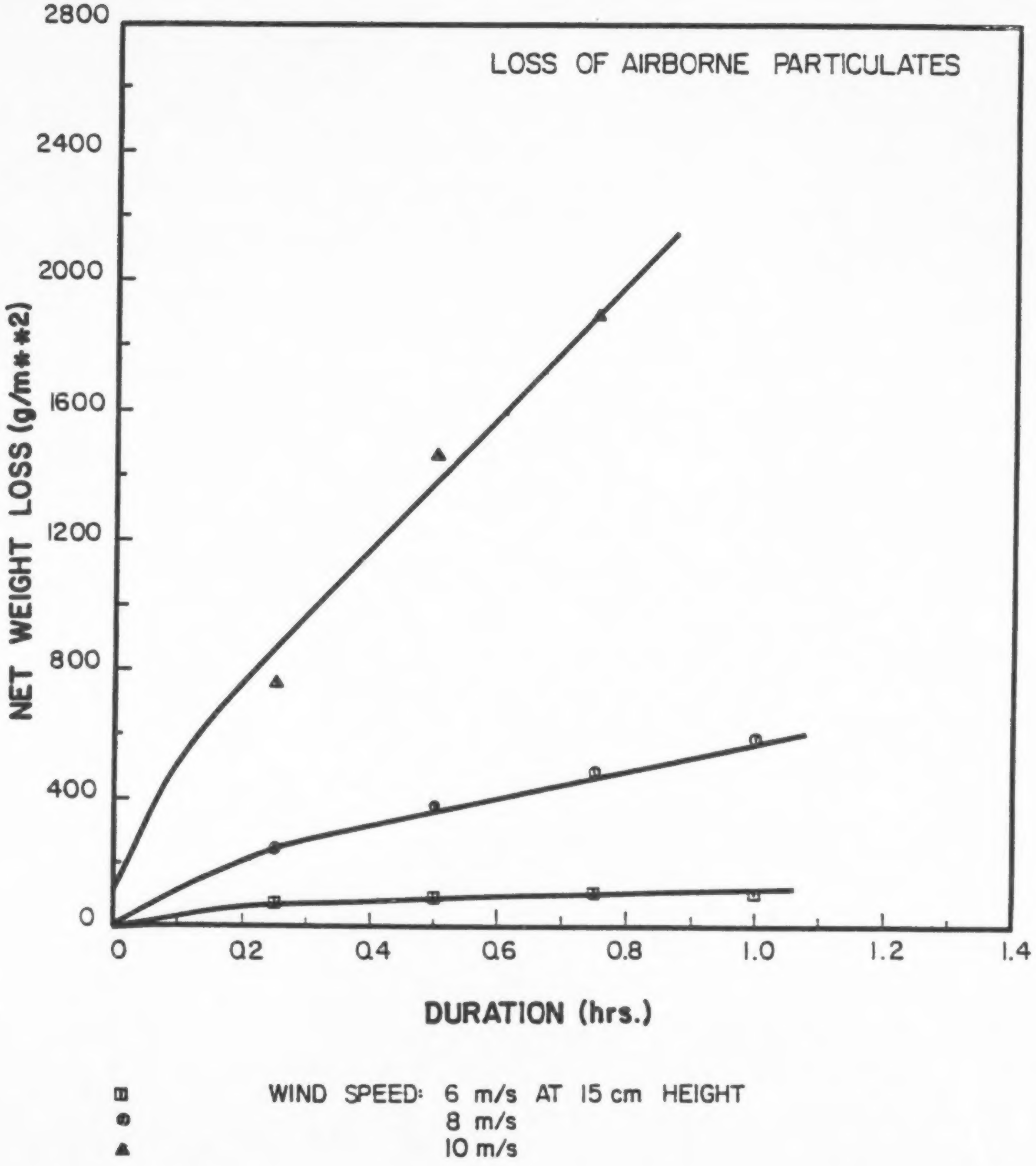

Figure 7. Example of dust sample test results showing loss of airborne material versus duration of wind exposure.

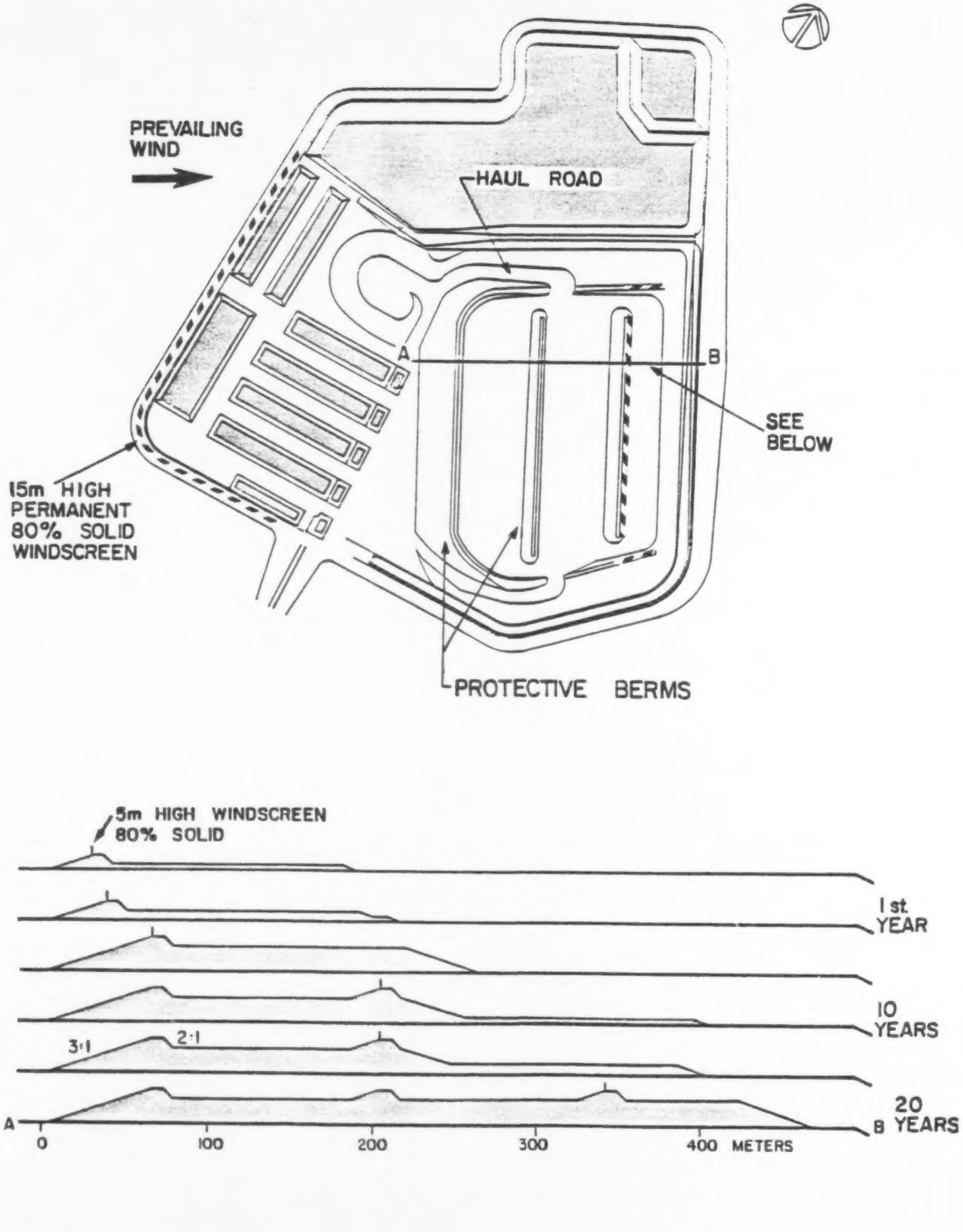
PREVAILING WIND
HAUL ROAD
A
B
SEE BELOW
15m HIGH PERMANENT 80% SOLID WINDSCREEN
PROTECTIVE BERMS
5m HIGH WINDSCREEN 80% SOLID
1 st. YEAR
10 YEARS
3:1
2:1
20 YEARS
A
B
0
100
200
300
400 METERS

Figure 8. Twenty-year storage plan.

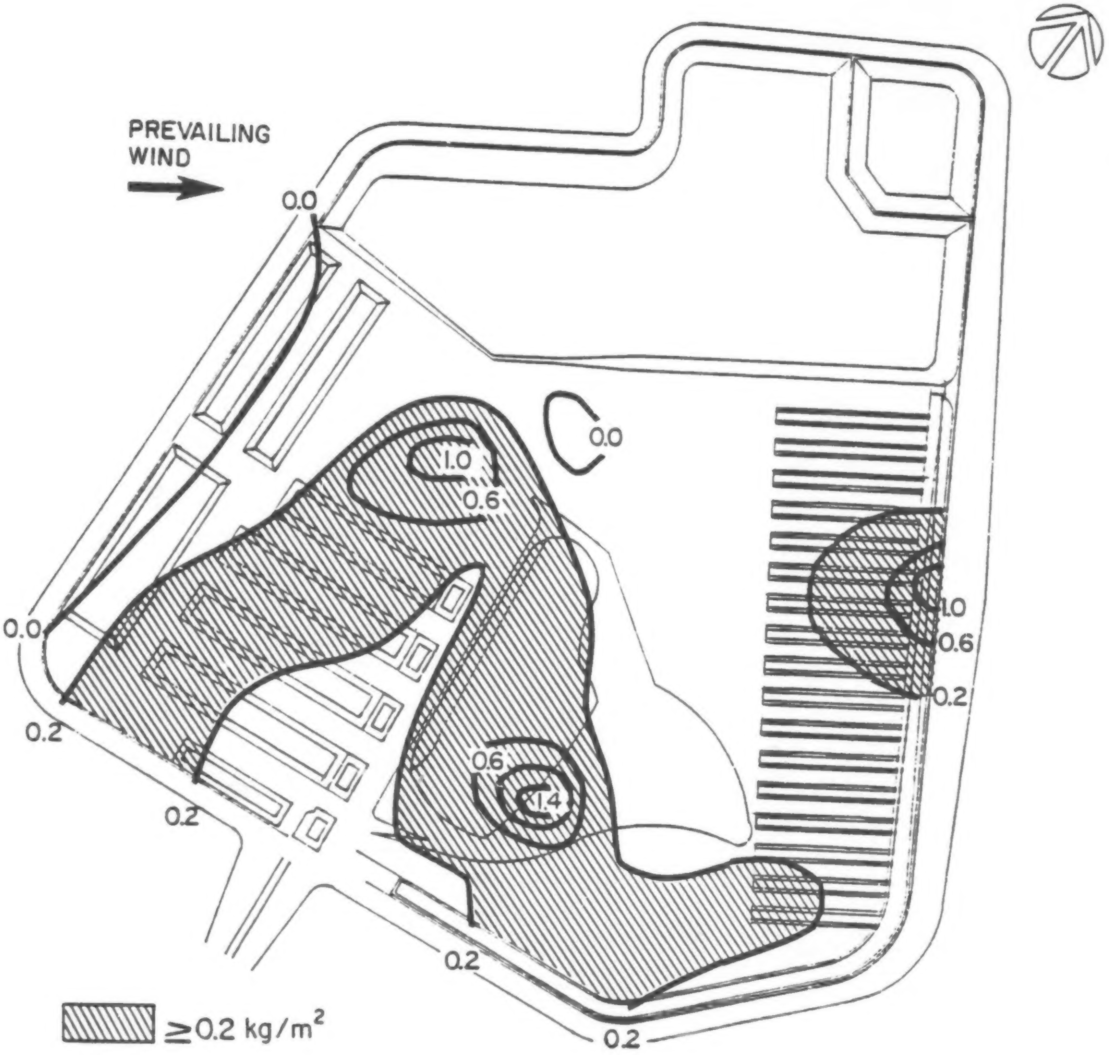
PREVAILING WIND
0.0
0.0
1.0
0.6
0.0
1.0
0.6
0.2
0.2
0.6
1.4
0.2
0.2
0.2
0.2
▨ ≥0.2 kg/m²

Figure 9. Contours of airborne dust emission (kg/m^2) during a typical dust event for the ash lagoon in its present configuration.

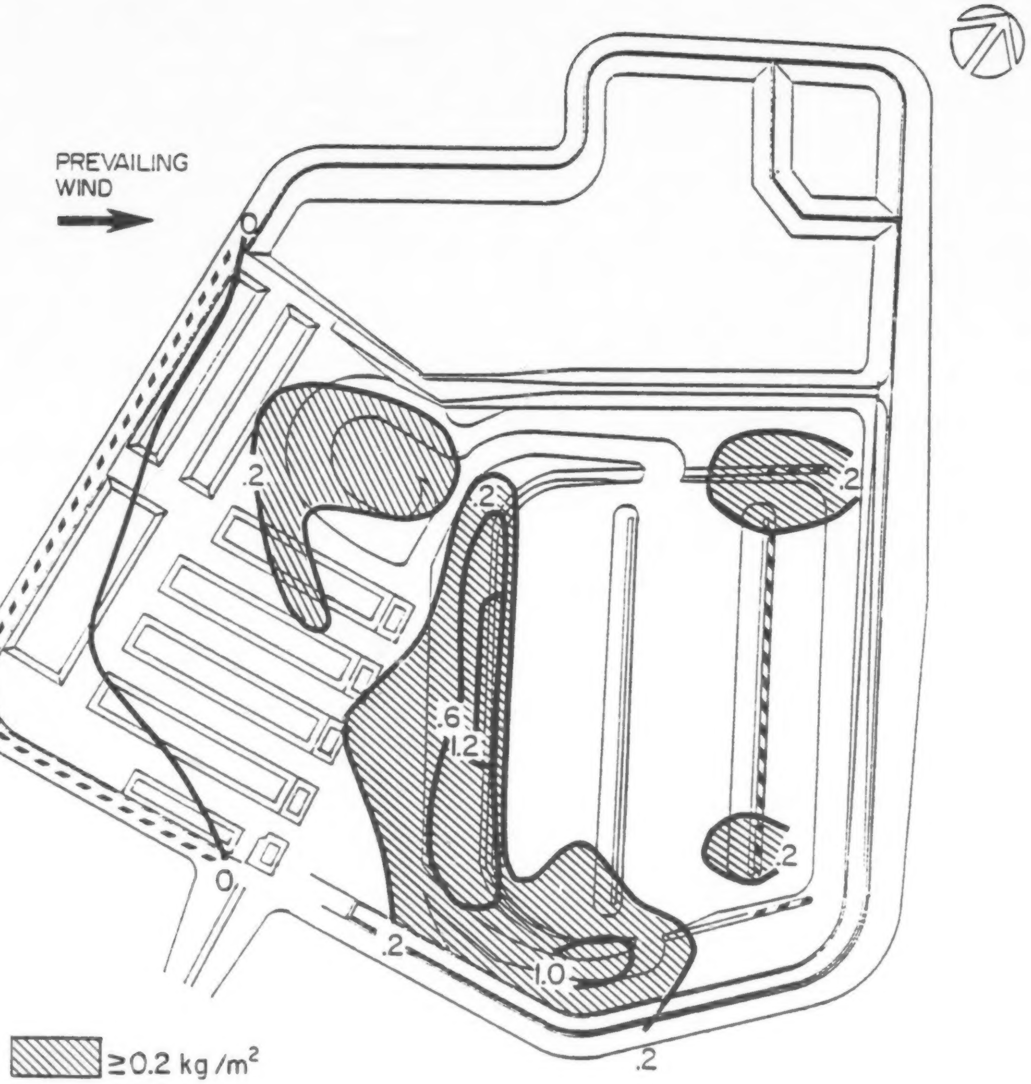
PREVAILING WIND
0
.2
.2
.2
.6
1.2
.2
0
.2
1.0
.2
.2
▨ ≥0.2 kg/m²

Figure 10. Same as Figure 9, but for the recommended scheme after 20 years.

EVALUATION OF FIELD TEST RESULTS ON WIND SCREEN EFFICIENCY*

by

Alan G. Larson**

TRC Environmental Consultants, Inc.
Englewood, Colorado

This paper has been reviewed in accordance with the U.S. Environmental Protection Agency's peer and administrative review policies and approved for presentation and publication.

(*)Although this is not the actual presentation made at the May 1982 meeting, it describes the same work and covers the same general time period. It represents work funded under EPA contract 68-02-3115, Technical Directive 117.

(**)Current address: The Kentwood Moore Co., 5690 Denver Tech Center Blvd., Englewood, CO 80111.

Abstract

A field measurement project was conducted to generate data which would lead to a preliminary determination of the effectiveness of wind screen material as an inhibitor of fugitive windblown dust emissions from a stockpile. A stockpile comprised of fly ash was used as the test material and a wind screen was erected upwind of it to comprise the test configuration. Standard hivolume samplers were used to collect samples of Total Suspended Particulates (TSP) and hivolume samplers fitted with size selective heads were used to collect samples of Inhalable Particulates (IP) (less than 15 μm). Particulate concentration measurements due to wind erosion from the stockpile both with and without the wind screen were made. Low threshold anemometery was used to document wind conditions. It was found that the wind screen did reduce the fugitive emissions of TSP but the reduced emissions of IP were insignificant.

Introduction

The emission of windblown fugitive dust from stockpiles can be a significant problem at mines, power plants, steel mills, rock-handling facilities, and many more industrial concerns which stockpile raw materials, fuel, and waste materials. Stockpiles which are inactive (not drawn upon) can be effectively treated for fugitive dust control by several methods including chemical crusting agents, coverings, etc. Active stockpiles, however, present a much more difficult dust control problem because of the need for access and because of surface disturbances caused during access. One approach which has been suggested as a means of reducing windblown fugitive emissions from both active and inactive stockpiles employs wind screen materials.

Wind screen material is comprised of a fabric-like construction of high tenacity polyester fiber, woven to varying degrees of porosity and prepared in different widths. The manufacturer holds that the material, when erected vertically like a fence, will reduce the wind speeds at levels directly adjacent to the ground surface in the lee of the wind screen. Further, the manufacturer contends, when the wind speed is reduced due to the presence of the wind screen, windblown dust in the lee of the screen will also be reduced. It is therefore expected that use of the wind screen material as a wind break will result in reduced fugitive windblown particulate matter in a limited region downwind from the wind screen. This report describes a preliminary investigation which was conceived to determine the actual effectiveness of one type of wind screen material toward control of fugitive dust emission.

TRC Environmental Consultants, Inc. (TRC), under contract to the EPA Industrial Environmental Research Lab (IERL) in Research Triangle Park, North Carolina, has performed a preliminary field study which investigated the effectiveness of wind screens to control fugitive windblown dust from stockpiles. The study was conducted around a test stockpile of fly ash material. The stockpile was located in a remote portion of property owned by Colorado Public Service Company's Valmont Power Plant in Boulder, Colorado. The site was chosen because of the high incidence of consistent wind direction (westerly) in several wind speed categories.

Fly ash material was chosen to comprise the test stockpile for this field investigation because it is a common waste material where coal is used for fuel, it is comprised of relatively small particulates, and thus is susceptible to be windblown at moderate wind speeds, and it was readily available at no cost. The fly ash being susceptible to wind erosion simplified the experimental work because measurement of material removed from the test stockpile was possible over a wide range of wind conditions. All of this was judged as being optimum to lead to the most expeditious determination of the effectiveness of the wind screen material as an inhibitor of windblown particulate matter from stockpiles.

The study was designed to determine the total suspended particulate matter (TSP) and the inhalable particulate matter (IP, less than 15 μm) due to wind action. The emissions of particulate matter were measured from a simulated active stockpile before and after installation of a wind screen. Hivolume samplers (hi-vols) and hi-vols fitted with Sierra size selective heads were installed upwind and downwind of the test stockpile to determine the TSP and IP concentrations under different wind conditions. The upwind sampler measured background concentrations and the downwind samplers measured the particulates emanating from the test stockpile along with the background concentrations. Anemometers and wind vanes were located upwind and downwind of the wind screen to record wind speeds and directions that resulted in the windblown particulate emissions.

Test Methodology

The test site was located on a native grass covered mesa. The mesa is elevated above the surrounding terrain by about 50 feet* and is oriented in an east-west direction which coincides with the direction of the most frequent and highest winds. The test site was situated on the eastern portion of the mesa in order to allow the west winds to stabilize prior to reaching the test site. The test stockpile of fly ash material was placed in a rectangular geometric shape. The fly ash material was taken from the waste dump where the Valmont Plant waste material is disposed. The elevated landform provided an isolated test site with an unobstructed fetch of about 3/4 mile* (for west winds) and was isolated from interfering particulate matter sources by about 3/4 mile to the west, about 1/2 mile to the northwest, and about 1/3 mile to the east where the Valmont waste dump is located. Tests were not conducted during easterly wind conditions, so the only interferences experienced were those located to the northwest and west. It is believed that during most conditions when interferences were experienced, those interferences were adequately documented by upwind sampling. The stockpile was shaped to a size of approximately 8 feet wide, 12 feet long (N-S), and 4 feet high. The leading edge of the stockpile was located approximately 12 feet downwind of the wind screen. The wind screen used in the study was commercially available high tenacity polyester fabric wind screen manufactured by Julius Koch USA, Inc. The screen was 6 feet tall, 165 feet long, and had approximately 50 percent porosity. The

---

(*) For nonmetric units used in this paper, please use: 1 ft = 0.3 m, and 1 mi = 1.61 km.

screen material was mounted on steel poles set in the ground. Wind screen material of 50 percent porosity was selected based on recommendations of the manufacturer which were directed to configurations most likely to result in maximum wind speed reduction at the levels adjacent to the ground surface. Material six feet tall was chosen so as to enable employment of a stockpile being a significant height above the flat mesa test surface (4 feet) and having a stockpile height to wind screen height ratio of 2 to 3--also as recommended by the wind screen manufacturer. A section of wind screen material 165 feet in length was chosen so as to avoid end effects at the test stockpile (wind eddying effects) and to allow for a reasonable wind direction variation of as much as ± 30°.

After the test stockpile was placed, it was allowed to dry before tests were conducted. Following the drying period, the stockpile was covered between tests with a tarpaulin to protect it from exposure to precipitation. Samples of fly ash material were collected during each field experimental day and were subsequently analyzed for moisture content.

The instrument array used to generate test data was comprised of three pairs of hi-vol samplers and three anemometer/wind vane sets. The upwind hi-vol pair measuring TSP and IP were located 20 feet upwind of the screen on the east-west centerline of the stockpile. Two Climatronics Mark 3 anemometer/wind vane sets were located adjacent to the upwind hi-vols at heights of 4 feet and 12 feet. Another anemometer/wind vane set was located adjacent to the stockpile at a height of 4 feet, level with the top of the stockpile. One pair of hi-vols measuring TSP and IP were located on the E-W centerline 20 feet downwind and another pair was located on the same centerline 50 feet downwind of the stockpile. Two hi-vols measuring only TSP were located 50 feet downwind of the stockpile, one 30 feet north and one 30 feet south of the east-west centerline. The wind screen was 165 feet in length with approximately half of the screen on either side of the east-west centerline. A diagram of the study site is shown in Figure 1.

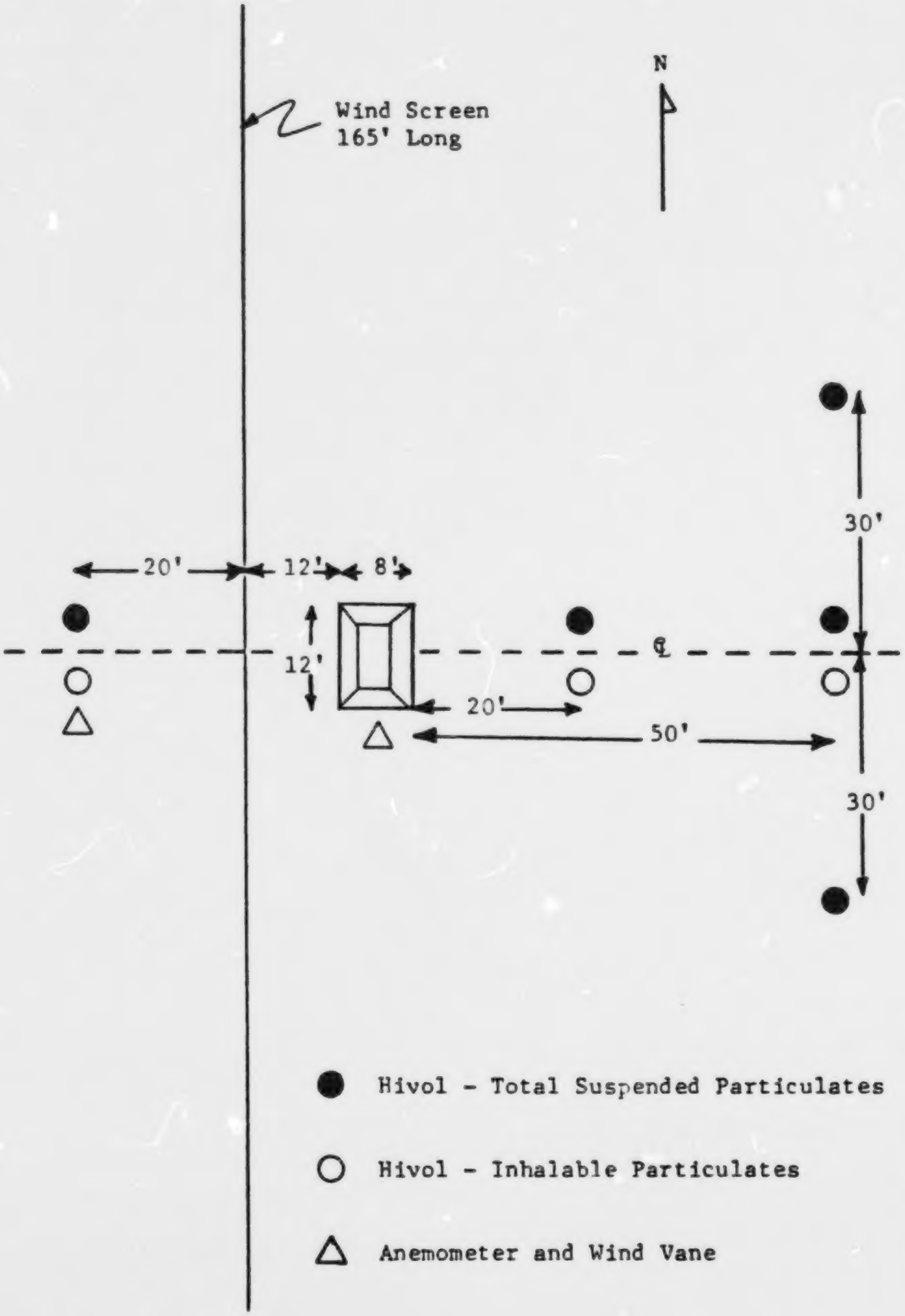
Wind Screen
165' Long
N
20'
12'
8'
12'
℄
20'
50'
30'
30'
● Hivol - Total Suspended Particulates
○ Hivol - Inhalable Particulates
△ Anemometer and Wind Vane

Figure 1. Test site layout.

The plan for each test consisted of 6 separate steps:

1. Remove tarpaulin from stockpile.
2. Set up anemometer/wind vane equipment.
3. Shift hi-vols to be on the centerline of the wind and stockpile.
4. Rake stockpile surface to loosen any packed ash.
5. Install filter paper in hi-vols.
6. Measure dust concentrations for approximately one hour total sampling time.

Steps 1 and 2 were only required at the beginning of each test day as usually two or three tests were conducted on a given day. During the testing period, the hi-vols were moved, as necessary between individual tests, to be on the centerline of the wind and the stockpile. Each test period lasted approximately 60 minutes. At the end of the test day, the equipment was removed to a storage area and the tarpaulin was replaced on the stockpile. When more than one test was conducted during a single day, Step 4 was repeated just prior to each additional test. This was done to assure that each test dealt with the same particle size distribution of fly ash as much as possible.

A total of 7 tests were run without the wind screen and 12 tests were run with the wind screen installed.

Data Analyses

Assay Methods

The data collected during each hour-long test consisted of hi-vol filters for both TSP and IP samplers, wind direction, wind speed, and moisture content of the surface fly ash material. Particle size analysis of the material on the stockpile surface was done from a single composite sample obtained from all the faces of the stockpile.

The hi-vol filters were assayed gravimetrically in accordance with 40 CFR 50 Appendix B Reference Method for Determination of Suspended Particulates in the Atmosphere (Hivolume Method).

Wind data were compiled from visual strip chart recordings to represent hourly average directions and speeds, peak gusts, and an index consisting of a gust-duration product. The compilation of averages and peak gusts is straightforward resulting in conventional values. The gust-duration product index was devised in an attempt to derive a wind representation that would directly relate to the physical processes of the wind erosion phenomena. It was reasoned that, since wind erosion is a direct function of both the wind speed and the duration of high wind speeds, an index incorporating both wind speed gusts and the duration of those gusts should relate directly to the measured sampler concentrations. In practice it is difficult to determine the level at which a wind gust becomes important. Therefore the gust-duration index was derived simply by integrating the total area under the wind speed curve for each experimental period. In this way a set of indices was developed which relate to one another but not to other field experimental work. The indices are in arbitrary units and can only be used as a measure of the relative wind erosion potential for each of the tests represented in this analysis.

Moisture content of the fly ash material was determined from samples of the material collected during each experimental day. Each sample of fly ash material consisted of about 60 grams of ash. Samples were taken from each face of the stockpile, placed in a sealed bag, then transported to the assay laboratory. Samples were placed in dried crucibles, and promptly weighed to determine the mass of fly ash and moisture prior to drying. Samples were baked at 105°C for one hour to drive off all moisture, then placed in a dessicating chamber until cooled. After cooling, the samples were weighed again to determine the moisture loss. Moisture content was represented as percent reduction (by mass) due to drying. The mean moisture content of the stockpile for an experimental day was determined as a mean of the values from all faces of the stockpile.

Particle size analysis of a composite ash sample, which was comprised of material from all the faces of the stockpile, was done manually with eight sieves from number 10 to 325. The sieves are USA Standard Testing Sieves which conform to ASTM specifications. The sieving of the composite sample was done manually in order that the mechanical action of the sieving process which might break up agglomerated particles would be held to a minimum and the resulting analysis would as nearly as possible represent the true surface particle size distribution.

Selection of Data To Be Used for Analysis

A total of 19 tests were conducted to represent wind erosion both with and without the presence of the wind screen. The data collected were assayed as described above and a series of comparisons were made to assist in selecting those tests that would best represent the effects of the wind screen as an inhibitor of fugitive windblown dust.

For several reasons not all the test data collected were used in the analysis. As a way of selecting the most representative TSP and IP concentration data, all of the concentration and wind data were plotted on scale diagrams so as to graphically illustrate the tests which exhibited consistent wind and dust erosion conditions. It was found that the wind direction variability (especially during peak gust conditions) during some tests caused a portion of the eroded dust to pass by the sampling array during some portions of some tests. In addition to this, sampler failure resulted in inadequate representation of upwind or background concentration levels on two tests. As a result, six of the nineteen tests were only partially successful leaving eleven to be used for analysis. The TSP and IP concentrations along with the supporting wind data and measurements of other test conditions are listed in Tables 1, 2, and 3.

TABLE 1: TSP & IP CONCENTRATIONS FOR TESTS WITHOUT WIND SCREEN

TEST NUMBER	TSP ($\mu g/m^3$)			IP ($\mu g/m^3$)		
	UPWIND	$\Delta\chi 20$	$\Delta\chi 50$	UPWIND	$\Delta\chi 20$	$\Delta\chi 50$
3	225	151	95	158	26	34
5	118	97	6	35	40	21
6	70	195	16	57	22	19
7	82	--	7	70	--	--
Means	124	148	31	80	29	25

$\Delta\chi 20 = \chi$ (at 20 feet) $-\chi$ Upwind

$\Delta\chi 50 = \chi$ (at 50 feet) $-\chi$ Upwind

TSP & IP CONCENTRATIONS FOR TESTS WITH WIND SCREEN

8	300	138	72	126	81	78
9	72	53	86	35	23	25
10	80	16	7	72	--	--
11	88	59	—	53	4	--
12	--	--	--	20	7	33
13	44	4	24	6	21	15
17	201	189	88	86	2	42
Means	131	76	55	57	23	39

TABLE 2: WIND DIRECTION, SPEED, PEAK GUST (mph) AND GUST DURATION INDEX

DURING TESTS WITHOUT WIND SCREEN

TEST NUMBER	U-12 DIR*	U-12 SPEED	U-12 PK GUST	U-4 DIR	U-4 SPEED	U-4 PK GUST	D-4 DIR	D-4 SPEED	D-4 PK GUST	GUST DURATION INDEX**
3	285	10.5	20.6	295	8.0	15.5	290	7.5	15.5	52
5	225	11.0	22.5	215	10.0	19.8	205	10.0	20.3	52
6	240	13.5	24.2	215	11.5	19.5	210	12.5	19.2	63
7	220	8.5	14.4	210	7.0	16.6	220	7.0	17.4	40
Means		10.9	20.4		9.1	17.8		9.2	18.1	52

WIND DIRECTION, SPEED, PEAK GUST (mph) AND GUST DURATION INDEX

DURING TESTS WITH WIND SCREEN

8	290	13.0	25.0	--	--	--	290	3.8	12.5	68
9	280	10.0	18.0	--	--	--	280	3.0	8.5	49
10	250	13.2	21.4	--	--	--	255	4.5	7.5	58
11	230	12.2	20.8	240	10.5	16.4	230	4.8	5.6	60
12	285	12.0	20.6	275	11.0	17.4	250	4.0	7.5	61
13	300	11.4	20.2	285	10.5	16.5	265	3.7	6.9	54
17	210	16.0	19.2	255	13.0	19.8	235	4.5	10.1	71
Means		12.5	20.7		11.2	17.5		4.0	8.4	60

*U-12 = Upwind, 12 feet height. Direction (DIR) = bearing (true) in degrees.

**Gust Duration Index is in arbitrary units.

MOISTURE CONTENT OF SURFACE FLY ASH MATERIAL DATA FROM FIVE FACES OF STOCKPILE ON DAYS HAVING WIDEST VARIATION OBSERVED (PERCENT BY MASS)

	NORTH FACE	EAST FACE	SOUTH FACE	WEST FACE	TOP	AVERAGE
Day 1	2.7	1.6	1.1	1.9	1.7	1.8
Day 2	1.4	1.0	1.3	2.6	0.8	1.4
				OVERALL AVERAGE MOISTURE CONTENT		1.6

TABLE 3: PARTICLE SIZE DISTRIBUTION OF SURFACE FLY ASH MATERIAL

SIEVE NUMBER	SIZE OF SIEVE OPENINGS (μm)	RANGE OF PARTICLE SIZES COLLECTED (μm)	PERCENT OF TOTAL SAMPLE
10	2,000	> 2,000	22.88
50	300	300 - 2,000	24.18
100	150	151 - 300	13.26
140	106	107 - 150	12.82
180	83	84 - 106	7.45
250	58	59 - 83	14.74
325	45	46 - 58	4.61
Pan		< 45	.07
			100.01

Results

Wind Speed Reduction

A measure of the effectiveness of the wind screen can be shown through an analysis of the reduction of wind speeds resulting from the presence of the wind screen material. The data sample that can be employed for this purpose is somewhat larger than is shown in Table 2 above since it does not matter about the success of the concentration measurements. For this efficiency, the tests are used which were conducted when the wind screen was in place and wind measurements were made at the same heights above the ground both upwind and downwind of the wind screen.

The average wind speeds and peak gust wind speeds as summarized in Table 4 show that the average downwind wind speeds are reduced to 36 percent of the upwind value and the peak gusts are reduced to 41 percent of the upwind value. These reductions should be expected to vary somewhat by location for both distance downwind of the wind screen and for height above the ground. The values presented here should be representative of the fugitive windblown dust measured in these tests because the downwind wind speed was measured adjacent to the stockpile and at the height of the stockpile.

TABLE 4: WIND SPEEDS UPWIND AND DOWNWIND OF WIND SCREEN AT 4 FEET HEIGHT (mph)

TEST NUMBER	UPWIND SPEED	DOWNWIND SPEED	UPWIND PEAK GUST	DOWNWIND PEAK GUST	% REDUCTION WIND SPEED	% REDUCTION PEAK GUST
11	10.5	4.8	16.4	5.6	54	66
12	11.0	4.0	17.4	7.5	64	57
13	10.5	3.7	16.5	6.9	65	58
14	10.0	3.5	16.0	7.0	65	56
15	12.5	4.0	19.6	7.9	68	60
16	12.7	4.0	18.4	6.2	69	66
17	13.0	4.5	19.8	10.1	65	49
18	11.5	4.0	18.8	6.5	65	65
19	10.5	4.0	16.0	7.5	62	53
				Means	64	59

Airborne Concentration Reductions

The most graphic and direct measure of the effectiveness of the wind screen as an inhibitor of windblown fugitive dust can be seen by close examination of the TSP and IP concentration values as shown in Table 1. Several relations of significance are described in the following paragraphs.

Without the wind screen, an average of 148 $\mu g/m^3$ increase in TSP concentration is seen at 20 feet downwind. By the time the windblown plume has traveled to 50 feet downwind the average increase in concentration value has dropped to 31 $\mu g/m^3$ above the upwind value. With the wind screen in place, an average of 76 $\mu g/m^3$ increase in concentration is seen at 20 feet downwind. However, an increase of 55 $\mu g/m^3$ is still seen at 50 feet downwind. These differences are of significance. Without the wind screen, the increase in TSP concentration above background levels is high, but drops off rapidly probably due to deposition. With the wind screen, the increase in TSP concentration isn't as high above background levels as in the case without the screen but the elevated concentrations remain elevated for a longer period. This latter case is probably due to increased turbulent suspension of particulates, where the increase in turbulence results from the air flowing over the wind screen.

It can be seen from the wind speed averages and the wind gust duration indices (as shown in Table 2) that the winds were higher during the tests with the wind screen than during the tests without the screen. Therefore, there was a greater potential for windblown fugitive emissions during the tests with the wind screen. Some adjustment should be made so as to allow a more direct comparison between the two sets of concentration values. Probably the best manner in which such an adjustment can be is to normalize the mean concentrations to the Gust Duration Index (I), since this index incorporates both wind speed and duration. Such a normalization results in the following:

$$\text{Normalized Concentration Without Screen} = \frac{\Delta\chi 20}{I} = \frac{148}{52} = 2.85$$

and,

$$\text{Normalized Concentration With Screen} = \frac{\Delta\chi 20}{I} = \frac{76}{60} = 1.27$$

then the ratio between concentrations with the wind screen and concentrations without the wind screen is simply,

$$\frac{1.27}{2.85} = .45$$

This says that when TSP concentration differences at 20 feet downwind are normalized to a common base (wind conditions), the wind screen reduces the windblown TSP dust concentration to approximately 45 percent of what it is without the wind screen.

It is also seen from Table 1 (as noted above) that the concentration differences stay higher with distance with the wind screen than without it. Therefore, to obtain a more representative measure of the total effectiveness of the wind screen, this difference with distance should also be incorporated. This incorporation can be made as follows.

$$\text{Normalized Mean Concentration Without Wind Screen} = \frac{\left(\frac{\Delta\chi 20 + \Delta\chi 50}{2}\right)}{I} = 1.73$$

and,

$$\text{Normalized Mean Concentration With Wind Screen} = \frac{\left(\frac{\Delta\chi 20 + \Delta\chi 50}{2}\right)}{I} = 1.10$$

The ratio between mean conditions with the wind screen and without it is simply,

$$\frac{1.10}{1.73} = .64$$

This then says that the total effectiveness of the wind screen is to reduce the downwind fugitive windblown TSP emissions to 64 percent of what they were without the wind screen.

The situation is considerably different for IP concentrations. Also from Table 1 it is seen that the mean differences in IP concentrations without the wind screen are 29 and 25 $\mu g/m^3$ at 20 feet and 50 feet, respectively. With the wind screen in place the mean differences in IP concentrations is 23 and 29 $\mu g/m^3$. Considering the accuracy and resolution of particulate sampling with the hi-vol sampler and gravametric assay, these concentration differences are for all intents and purposes the same. If, however, the same normalization exercise as was used above is carried out, it is seen that,

$$\text{Normalized IP Concentration Without Screen} = \frac{\left(\frac{\Delta\chi 20 + \Delta\chi 50}{2}\right)}{I} = .52$$

and,

$$\text{Normalized IP Concentration With Screen} = \frac{\left(\frac{\Delta\chi 20 + \Delta\chi 50}{2}\right)}{I} = .52$$

then, the ratio between conditions with the wind screen and without it is,

$$\frac{.52}{.52} = 1$$

To reiterate, the wind screen, although it reduces the wind speed in its lee area where the windblown emissions originate, appears to make no difference in the fugitive emission of windblown IP (small particle) material.

It must be said that concentration data of the type collected during this set of experiments are inherently variable. This variability is due in large part to variations among the atmospheric processes which result in the windblown activity. Also, various aspects of the sampling system used to make the concentration measurements lead to data variabilities. In this analysis, a great deal of care was taken to screen the data collected in order to assure that as many of the irregular occurrences as possible were eliminated from the data base. This was done in an attempt to remove those factors that might obscure the true behaviors. It is felt that this data screening was quite successful and the resulting data base is of comparative high quality. However, by screening the data base and eliminating those cases during which atypical conditions existed, the data base was made to be quite small. For this reason it is recommended that the results presented here be respected as preliminary.

Conclusions

Wind screen material will reduce both the wind speed and fugitive windblown dust emissions from stockpiled material. The amount of wind speed reduction was found to be 64 percent of the mean wind and 59 percent of the peak gust values. That is the mean wind was reduced to 36 percent of the upwind value and the peak gusts were reduced to 41 percent of the upwind value in the configuation tested. This configuration was with a six feet high wind screen where the downwind wind speed was measured at a point four feet above the ground and sixteen feet downwind from the wind screen.

The amount of reduction of windblown fugitive TSP is 55 percent lower at a location 20 feet downwind of the stockpile. That is, the TSP was 45 percent of what it was without the wind screen. When considering both the data from 20 feet and 50 feet downwind of the stockpile, the TSP reduction was 36 percent, or 64 percent of what it was without the wind screen.

The analysis of reduction of IP (small particulate emissions) did reveal some small differences between the case with the wind screen and without it. However, the differences are at an insignificant level. It is concluded that the presence of the wind screen makes no significant difference in the amount of windblown fugitive IP emissions.

The overall conclusion is that the wind screen both reduces the wind speed in its aerodynamic wake and also reduces the particulate emissions. There remains a question about the wind screen's effectiveness at reducing the emissions of inhalable particulate matter (< 15 μm) and additional measurements will be necessary to resolve that issue.

EFFECTS OF STREET SWEEPING ON FUGITIVE EMISSIONS FROM URBAN ROADWAYS

The work described in this paper was not funded by the U.S. Environmental Protection Agency. The contents do not necessarily reflect the views of the Agency and no official endorsement should be inferred.

Donald F. Gatz

Atmospheric Chemistry Section
Illinois State Water Survey
P.O. Box 5050, Station A
Champaign, Illinois 61820

ABSTRACT

To determine the effects of street sweeping on urban particle concentrations, three standard high volume samplers were operated near a four lane road in a commercial area, and another sampler was operated in a residential area, in Champaign, Illinois. Results show that street-related sources increased the total airborne particle mass about 20 $\mu g/m^3$ at 7 m downwind when the wind had a component perpendicular to the street. Analysis of variance, comparing periods with and without sweeping in spring and summer sampling periods, showed higher downwind-upwind concentration differences in summer than in spring for east and west winds, apparently caused by higher street dust loadings in summer, but no effect from street sweeping.

1 INTRODUCTION

Provisions of the Clean Air Act enacted in 1977 required states to revise their State Implementation Plans (SIPs) for all areas that had not attained National Ambient Air Quality Standards (NAAQS). The Illinois SIP for Total Suspended Particulates (TSP) was conditionally approved by the U.S. Environmental Protection Agency (USEPA) with certain minor deficiencies. One of the reasons for the conditional approval of the Illinois TSP SIP was inadequate documentation of the impacts and effects of various controls on non-traditional fugitive sources of TSP. These sources include paved and unpaved roads, parking lots, and agricultural lands. This and similar studies have been designed to correct those deficiencies and will be submitted to the USEPA as part of the SIP for that purpose. The results of these studies will be used by the Illinois Environmental Protection Agency (IEPA) to define further the estimated impacts of non-traditional fugitive dust sources on TSP non-attainment areas throughout the state. They will also be used to refine the control strategies which may need to be applied to various non-traditional fugitive dust sources.

The purpose of this study was to assess the effects of street sweeping on air quality in Champaign, Illinois, by comparing aerosol concentrations measured by high volume (hivol) samplers in the presence and absence of regular street sweeping.

This study was planned so as to utilize the program of regular street sweeping being conducted in Champaign by a research group from the Water Survey´s Surface Water Section and funded by USEPA as part of the Nationwide Urban Runoff Program (NURP); the Principal Investigator of that study is Michael L. Terstriep, Head of the Surface Water Section.

2 EXPERIMENTAL METHODS

2.1 AEROSOL SAMPLER LOCATIONS

A map of a portion of Champaign, showing the aerosol sampling sites within the NURP study basins, is shown in Figure 1. Three hivol samplers were operated in the commercial "Mattis South" basin along Mattis Avenue. As shown in the figure, two samplers were located on the west side of Mattis Avenue, and one on the east side. An additional hivol sampler was operated in a residential Champaign neighborhood; this is designated the John Street site in Figure 1.

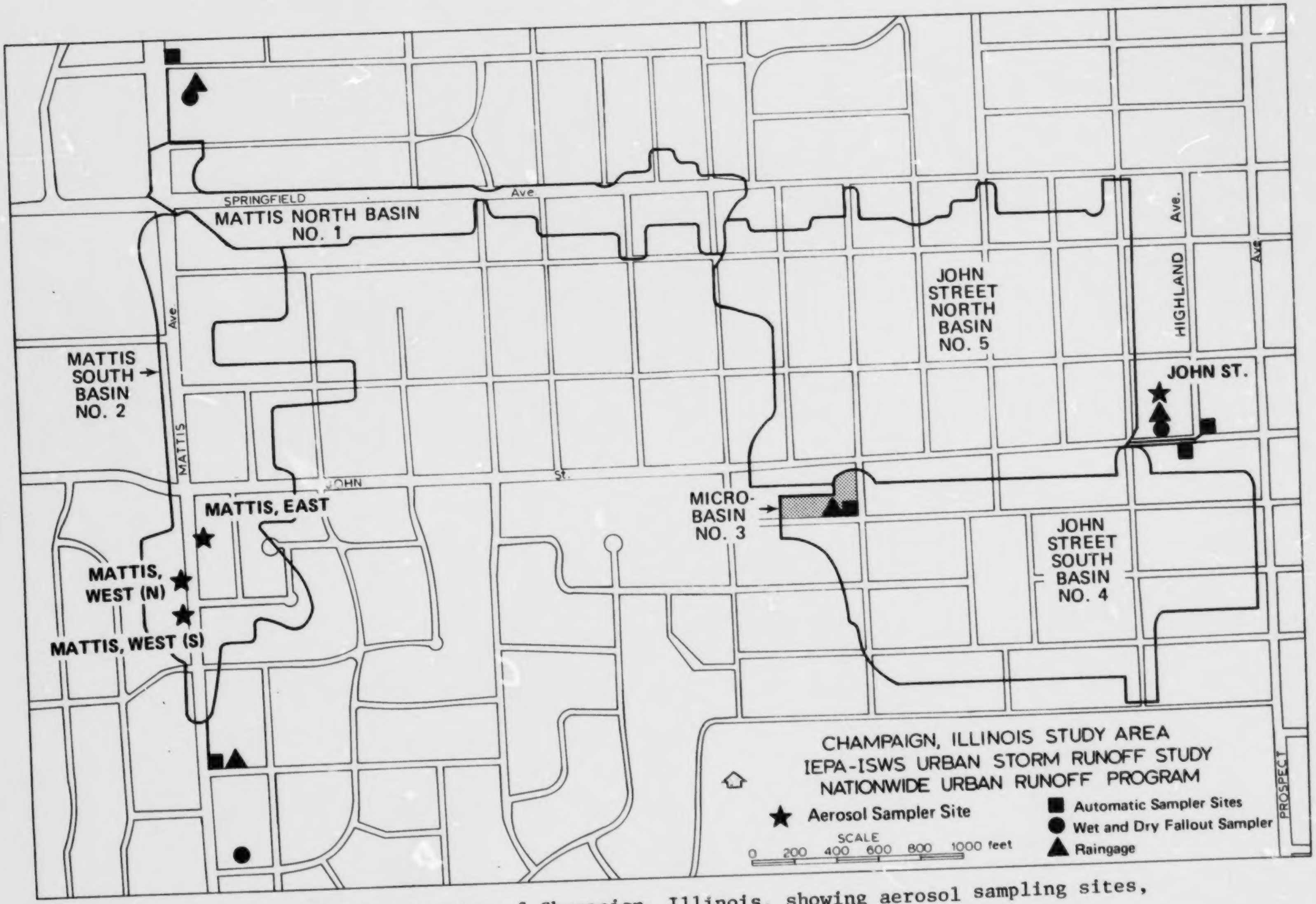
SPRINGFIELD Ave.
MATTIS NORTH BASIN NO. 1
MATTIS SOUTH BASIN NO. 2
MATTIS Ave.
JOHN St.
MATTIS, EAST
MATTIS, WEST (N)
MATTIS, WEST (S)
MICRO-BASIN NO. 3
JOHN STREET NORTH BASIN NO. 5
JOHN STREET SOUTH BASIN NO. 4
HIGHLAND Ave.
Ave.
JOHN ST.
PROSPECT
CHAMPAIGN, ILLINOIS STUDY AREA
IEPA-ISWS URBAN STORM RUNOFF STUDY
NATIONWIDE URBAN RUNOFF PROGRAM
★ Aerosol Sampler Site
■ Automatic Sampler Sites
● Wet and Dry Fallout Sampler
▲ Raingage
SCALE
0 200 400 600 800 1000 feet

Figure 1. Map of a portion of Champaign, Illinois, showing aerosol sampling sites, drainage basins, and sampling sites of the Water Survey's project in the Nationwide Urban Runoff Program (Modified from Terstriep et al, 1981).

The hivol samplers near Mattis Avenue were all located 7.0 m (± 0.4 m) from the curb to minimize any effects of distance from the street on the concentrations measured by the various samplers. At the John Street site the hivol was 17.6 m north of the curb.

2.2 AEROSOL SAMPLING METHODS

All the aerosol samplers were installed so that their inlets were 2 m above ground level. Thus, they conformed to the standard height, i.e., between 2 and 15 m, at which hivol inlets must be placed. The hivol samplers were all positioned so that their inlets faced the street. It was important to be consistent on this detail since there is evidence (Ortiz, 1978) that hivol sampling effectiveness varies with sampler orientation to the air flow, at least in strong winds.

The standard hivol samplers were provided and calibrated by the IEPA, which also provided replacement pumps when airflow fell below minimum acceptable rates. The IEPA also provided glass fiber filters for the hivol samplers, weighed the filters before and after exposure, and calculated TSP concentrations.

The hivol filters were changed at approximately 9:00 a.m. each Monday through Friday, from 16 April to 20 October, 1981. This schedule provided five 24-hr duration filters each week from each sampler. The first filter of the week began Monday morning and the last ended Saturday morning.

2.3 STREET SWEEPING OPERATIONS

The street sweeper made single passes along both east and west curbs of the Mattis South basin once per week, normally on Tuesday morning, between 15 April and 26 May 1981. The sweeper used was a 1973 Elgin, Model Pelican "S," a three-wheeled mechanical sweeper with right and left side gutter brooms and a main rotary broom. Its sweeping path using one outside broom was 2.4 m (8 ft) wide.

Measurements of collection efficiency by Bender (1982) indicated that the sweeper collected about 67% of the total dust mass on the street. This approximate efficiency was maintained for all particle sizes down to 125 μm, below which efficiency decreased markedly. Other measurements by Bender (1982) indicated that 46% of the total dust mass was in particles greater than 1000 μm in diameter.

In six sweepings of the Mattis South basin, the median mass collected was 28.8 g/curb m (102 lb/curb mi). The maximum collection was 44.5 g/curb m (158 lb/curb mi) and the minimum 13.2 g/curb m (47 lb/curb mi).

2.4 SUPPORTING DATA

Several kinds of supporting data were also collected to aid in interpretation of the air quality data. Precipitation was measured at the Mattis Avenue and John Street raingage sites, as shown in Figure 1, and provided to us, along with street sweeping data, by the Water Survey NURP project mentioned earlier. Wind measurements were made at the Water Survey Headquarters in Champaign, about 4 km east of the Mattis Avenue sites.

3 RESULTS AND DISCUSSION

An illustration of a small portion of the available data, plotted against time, is given in Figure 2. The data include TSP measurements at four sites, along with daily rainfall amount, dates of street sweeping, and winds. Wind directions are shown by direction category. The westerly wind category (W in Figure 2) includes days when the hourly mean wind direction was from the 202 to 338 degree sector for at least 75% of the hours between 6 a.m. and midnight. Wind direction was not considered relevant in the remaining hours of the sampling period because only a very small fraction of the traffic occurs then. Similarly, the easterly wind category (E) includes days when the hourly mean wind direction was from the 22 to 158 degree sector at least 75% of the hours in the same time interval. The "other" wind direction category (O) includes all other days. Mean wind speed during sample collection and daily maximum 1-minute gust speed are also shown.

Figure 2 shows that rainfall was frequent and relatively heavy during the period shown, with seven days having 1.27 cm (0.5 in.) or more. Streets were swept at approximately weekly intervals during the period. Figure 2 includes only a small fraction of the data collected, but it illustrates several relationships that occurred throughout the sampling period. One of these is the generally high correlation between TSP observations from the several samplers, including the one located in a residential area. Generally, on days when TSP concentrations were unusually high at one site, they were unusually high at all sites. There were still differences in concentration between sites, of course. A very obvious difference in Figure 2 was that the residential (John) site had consistently lower concentrations than the commercial sites. Differences between collectors on opposite sides of the commercial roadway are also apparent in Figure 2.

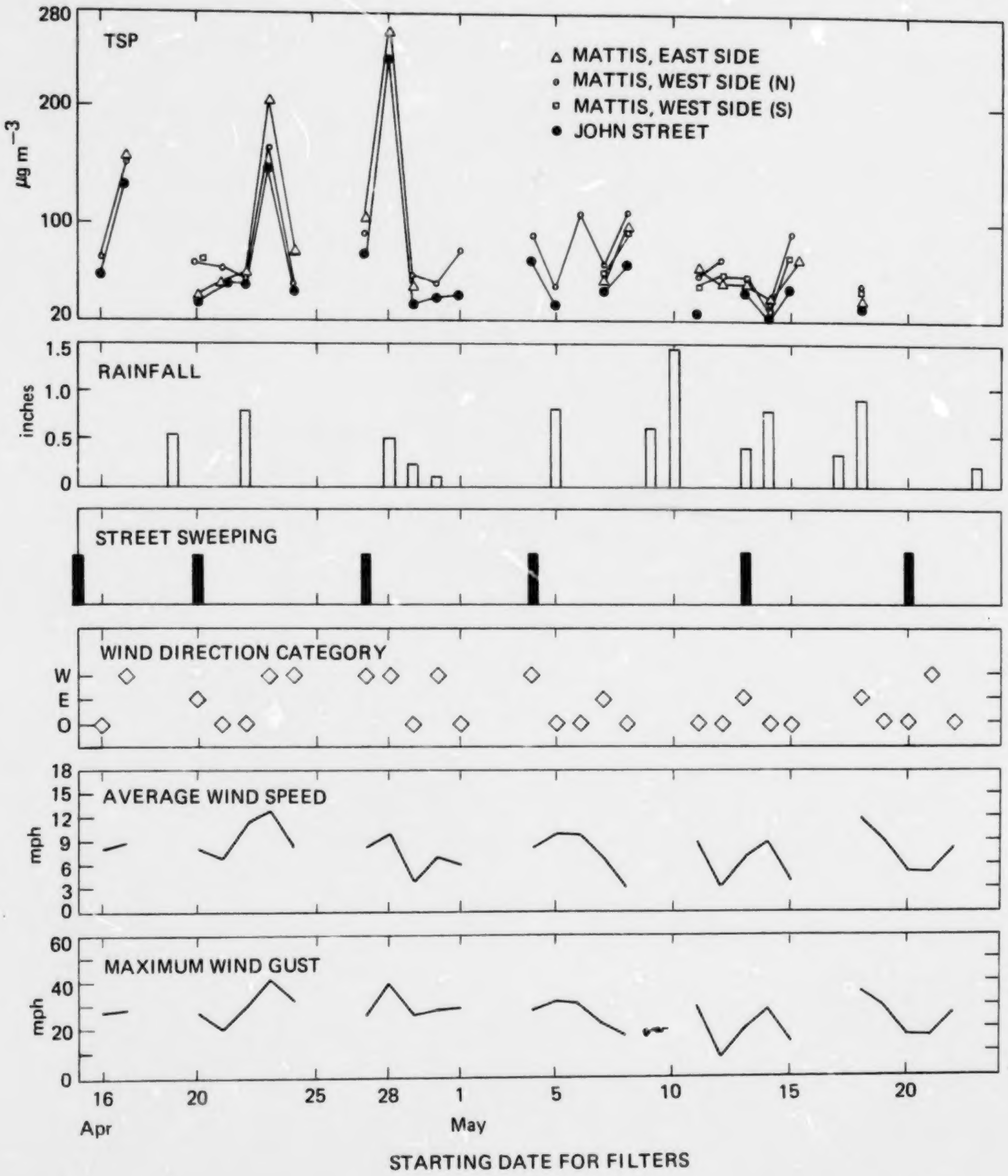

Figure 2. Illustration of data collected in 1981 for evaluation of effects of street sweeping on air quality.

In assessing possible effects of street sweeping on air quality, it was first necessary to establish whether the test roadway was indeed a source of aerosols. To examine this question, I divided the data according to the wind direction categories mentioned earlier. This was done to assess which samplers were upwind, and which downwind, when the wind direction was either easterly or westerly (i.e., having a large cross-wind component, relative to Mattis Avenue) and to identify those days when the wind (1) was from either north or south, or (2) blew from both east and west at different times during sample collection, so that it was difficult to assign upwind and downwind. Results for the east and west wind cases are shown in Figure 3, and those for the "other" winds in Figure 4.

Figure 3 includes only measurements made in easterly or westerly winds, and shows a clear tendency for the downwind samplers to have higher TSP values. The upwind samplers experienced higher TSP concentrations with westerly winds. For example, the upwind means were 71 $\mu g/m^3$ for 26 days with west winds and 60 $\mu g/m^3$ for 30 days with east winds, a difference of 18%, relative to the east wind value. For both east and west winds, however, the downwind samplers had higher TSP values, clearly showing the road to be a source of airborne particles. As before, the solid line in the figure represents perfect agreement between upwind and downwind samplers. The dashed line is the least squares regression line for estimating the downwind concentration, D, from the upwind value, U: $D = 0.94(U) + 21.7$. Since the slope of the regression line is close to 1.0, the intercept, 21.7 $\mu g/m^3$ gives a good indication of the extra airborne dust concentration that may be attributed to the roadway. The slope near 1.0 shows that the added TSP concentration caused by the roadway is approximately constant for all upwind concentrations.

To consider the possibility that the differences in mean upwind TSP concentrations were the result of differences in mean wind speed, the following wind speed data are presented. The mean value of the daily mean wind speed, for 26 west wind samples, was 6.4 m/sec (S.D. = 2.0 m/sec), while the corresponding value for 30 east wind samples was 5.0 m/sec (S.D. = 2.1 m/sec). Analogous means for the maximum gusts were 24.0 m/sec (S.D. = 8.6 m/sec) for west wind samples and 18.2 m/sec (S.D. = 5.4 m/sec) for east wind samples. Thus, the relative differences in mean wind speed (28%) and mean maximum gust speed (32%) between easterly and westerly winds were somewhat greater than the relative differences in TSP concentrations, but wind speed differences cannot be ruled out as a possible cause. Another possible cause is that the site was closer to agricultural sources with west winds, since it was located near the western edge of the Champaign-Urbana metropolitan area.

Figure 4 shows the relationship between TSP concentrations on the east and west sides of Mattis Avenue for the "other" wind category. There was no strong tendency for either side of the street to have higher values, as would be expected in the absence of a strong wind component perpendicular to the street.

The evidence presented thus far makes it clear that the street was indeed the source of airborne particles, since the downwind sampler had higher

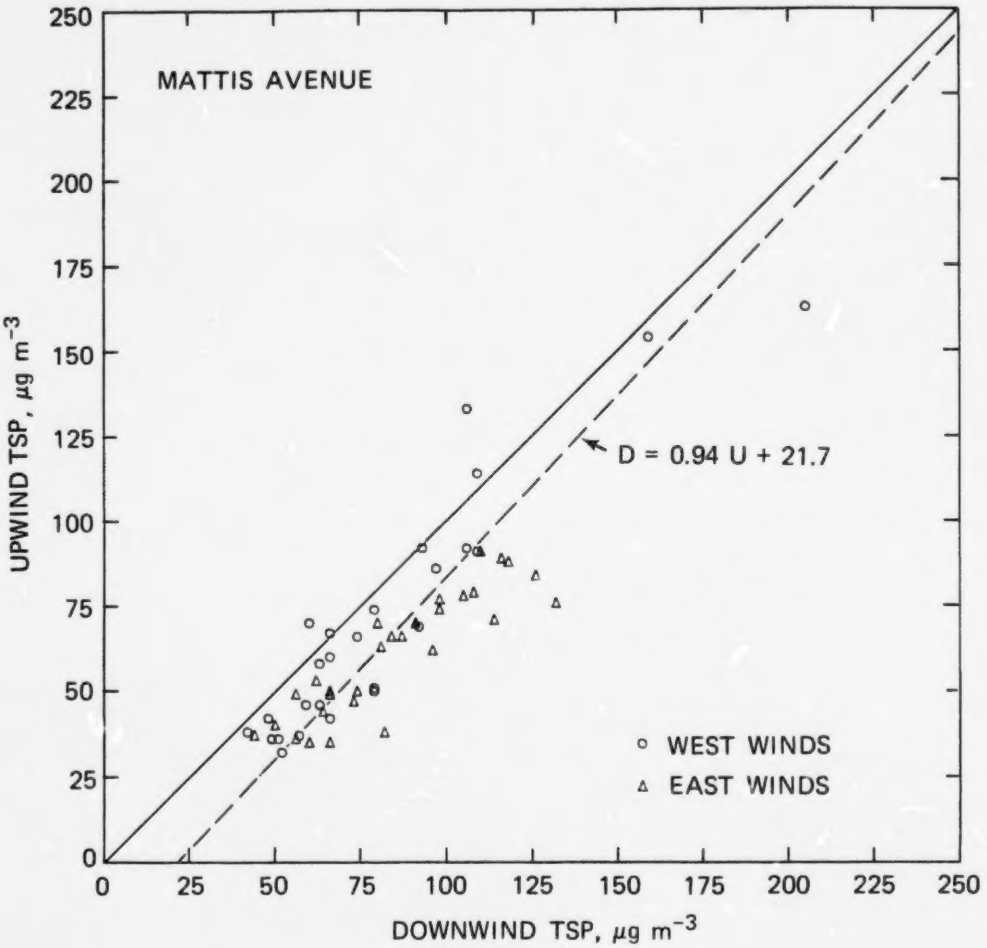

Figure 3. Comparison of TSP concentrations upwind and downwind of Mattis Avenue on days when winds were predominantly from the east or west.

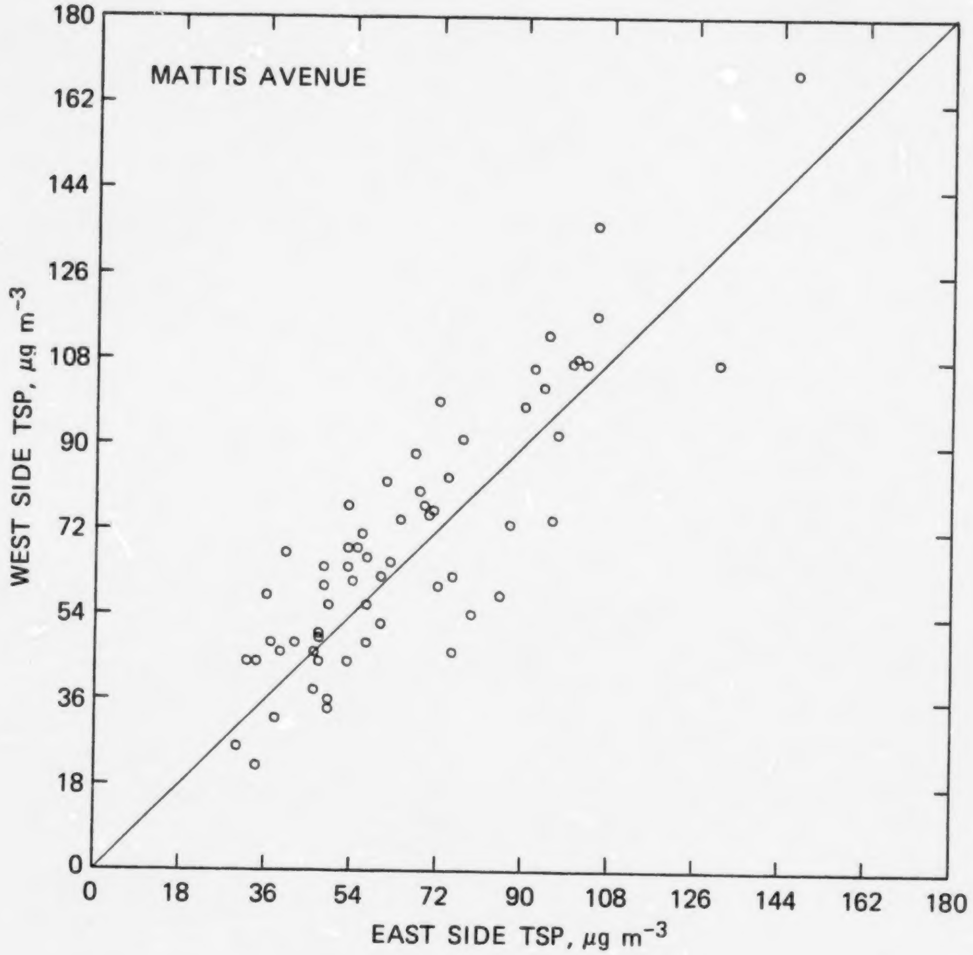

Figure 4. Comparison of TSP concentrations on the east and west sides of Mattis Avenue on days when winds were not predominantly from the east or west.

concentrations in *both* east and west winds, but neither side had predominantly higher concentrations with "other" winds. Next we address the question of whether street sweeping had any effect on reducing the strength of this source. This is done by comparing downwind-upwind differences during periods with and without regular weekly sweeping. A day was considered to be in the "swept" period if the street was swept on that day or any of the previous seven days, and in the "unswept" period otherwise. A second comparison examines commercial-residential differences with and without weekly sweeping (by the same criteria) at the commercial site. (The residential site was not in one of the experimental or control basins, and thus was swept irregularly, at intervals of 2-4 weeks, during the sampling period.)

Table 1 presents results of a two-way analysis of variance (Brown, 1977) on downwind-upwind differences (TSP1). It examines both sweeping and time as sources of variance. The upper part of the table gives mean downwind-upwind differences in TSP concentrations for swept and unswept periods in both "spring" (up to 30 June) and "summer" (after 30 June). There appear to be differences between *seasons* (with higher concentrations in summer than in spring), but not between periods of sweeping and not sweeping. The analysis of variance table in the lower part of the table confirms that there were no significant differences between periods of sweeping and no sweeping, but also indicates that the differences between seasons were significant at the 0.10 level, but not at the 0.05 level. Table 2 presents results of a similar analysis of variance on commercial-residential TSP differences (TSP2). Again, differences between seasons appear large (with concentration differences higher in *spring* than in summer in this case), but differences between swept and unswept periods look small. The analysis of variance table in the lower part of Table 2 confirms that the differences between swept and unswept periods were not significant, but also shows that seasonal differences were significant at the 0.0001 level. Interactions between sweeping and time were not significant in either comparison.

The main question addressed by this paper has now been answered. Although the test roadway was shown to be a source of TSP, no evidence was found to indicate that street sweeping had any effect, either beneficial or detrimental, on air quality at 7 m downwind.

Table 3 summarizes TSP concentrations and the two TSP differences discussed above. Mean TSP values are shown for three different data sets: (1) all samples, (2) the samples used in the downwind-upwind comparison, and (3) the samples used in the commercial-residential comparison. It is apparent that the mean TSP concentrations in the commercial (Mattis) and residential (John) sites do not vary much between sample sets. For example, the Mattis mean shows a maximum of 87 $\mu g/m^3$ and a minimum of 84 $\mu g/m^3$ in the three data sets shown. Similarly, at the John site the highest mean was 65 $\mu g/m^3$ and the lowest 62 $\mu g/m^3$ Thus, regardless of the data set, mean TSP values were higher at both sites in spring than in summer. The Mattis site had higher concentrations by about 20 $\mu g/m^3$ in the spring and about 8 $\mu g/m^3$ in the summer.

Table 1. Results of 2-way analysis of variance on upwind-downwind TSP differences ($\mu g/m^3$) across the test roadway

	Spring		Summer	
	Swept	Unswept	Swept	Unswept
No. of Cases	12	11	4	18
Mean	12.9	12.8	19.8	23.0
S.E.M.	4.2	5.2	1.8	3.1

Source of variance	Sum of squares	Degrees of freedom	Mean square	F	Tail probability
Time	603.4	1	603.4	2.96	0.0931
Sweeping	20.7	1	20.7	0.10	0.7518
Interaction	23.4	1	23.4	0.11	0.7368
Error	8369.3	41	204.1		

Table 2. Results of 2-way analysis of variance of commercial-residential TSP differences ($\mu g/m^3$)

	Spring		Summer	
	Swept	Unswept	Swept	Unswept
No. of cases	27	19	8	36
Mean	22.0	19.6	7.2	11.0
S.E.M.	3.0	2.0	3.5	1.7

Source of variance	Sum of Squares	Degrees of freedom	Mean square	F	Tail probability
Time	2251.4	1	2251.3	15.91	0.0001
Sweeping	8.1	1	8.1	0.06	0.8116
Interaction	159.1	1	159.1	1.12	0.2919
Error	12166.8	86	141.5		

Table 3. Summary of TSP concentrations and differences by season for three different sample sets

		Spring				Summer			
Sample set	Site	N	Mean	±	S.E.	N	Mean	±	S.E.
All samples	Mattis*	53	86	±	6	77	62	±	2
	John	52	65	±	5	74	54	±	2
Δ TSP1**	Mattis	23	87	±	7	33	65	±	3
	Downwind-upwind difference	23	13	±	3	22	22	±	3
Δ TSP2***	Mattis	46	84	±	5	68	63	±	2
	John	46	62	±	4	68	55	±	2
	Mattis-John difference	46	21	±	2	44	10	±	2

*Includes days with at least one sample from both sides of Mattis Ave; both sides weighted equally.

**Includes days with measurements on both sides of Mattis Ave., and east or west winds (as defined in the text).

***Includes days with measurements on both sides of Mattis Ave. and at John St., with no restriction on wind direction.

TSP concentration differences, however, display different seasonal behavior depending on the data set used. The mean commercial-residential difference (ΔTSP2) was higher in spring than summer, as were TSP concentrations at both sites. The mean downwind-upwind difference (ΔTSP1), on the other hand, was larger in the summer, when the Mattis site had lower concentrations.

The higher TSP concentrations in spring are consistent with an agricultural soil dust source, which would be expected to be stronger in the spring from tilling operations, lack of ground cover by crops, and generally stronger winds. It is reasonable for the Mattis site to have higher TSP concentrations than the John St. site because it is closer to the sources with prevailing winds, and because the John St. site is located in a somewhat older part of town, where the more mature trees may help to remove particles from the atmosphere.

The downwind-upwind differences were greatest in summer, when TSP concentrations were lower at both the John and Mattis sites. Others (e.g., Cowherd and Englehart, this Symposium) have found that roadway emissions depend on both traffic volume and roadway surface silt loading. We could find no evidence for significantly greater traffic volumes in summer than in spring, but according to data provided by Bender (1982) , the mean and standard error of 11 spring measurements of total street loadings were 108 ± 5 g/curb-m, while the same values for 10 summer measurements were 189 ±11 g/curb-m. Thus, the spring/summer ratio of loadings, 1.75, is very close to that of ΔTSP1, 1.69, and it appears that differences in street surface loadings between seasons could well have caused the observed seasonal differences in ΔTSP1.

4 SUMMARY AND CONCLUSIONS

To determine the effects of street sweeping on urban TSP concentrations, three standard hivol samplers were operated near a four lane commercial roadway, and an additional sampler was operated in a residential area of Champaign, Illinois, between April and October, 1981. When winds were blowing across the test roadway in either direction, downwind concentrations at 7 m from the curb exceeded upwind by an average of about 20 $\mu g/m^3$. In a comparison of downwind-upwind TSP concentration differences during a period of regular weekly street sweeping with those from another period when sweeping was discontinued, analysis of variance was unable to detect a significant effect of sweeping on the amount of TSP produced by the roadway. Thus, for a commercial urban roadway clearly shown to be a source of airborne particles, street sweeping could not be shown to have any effect in reducing the amount of dust produced.

5 ACKNOWLEDGEMENTS

This research was carried out under support from the Illinois Department of Energy and Natural Resources, Project 10.093. Mr. William P. Murphy was the Project Manager.

The results were achieved only through the dedicated efforts of Susan Wiley, who collected most of the samples and performed the data analysis, and Bruce Komadina, who devised a convenient means of mounting the hivols and supervised their installation. Thanks are also due Randall K. Stahlhut, for programming assistance, Eberhard Brieschke, who helped with the installations, and Mr. Kenneth Porter, Mr. Lawrence Boastick, and Dr. and Mrs. Glenn Stout, who allowed us to operate samplers on their property. The Illinois EPA, through the assistance of Mr. Arden Ahnell, Mr. Bob Hutton, and Mr. John Shrock, provided, calibrated, and maintained the standard hivols, and provided and weighed the filters. We also thank Mr. Michael Terstriep and Mr. Michael Bender for their cooperation in supplying data.

6 REFERENCES

Bender, G. M., 1982. Personal communication. Mr. Bender is associated with the Water Survey's Nationwide Urban Runoff Program.

Brown, M. B., Editor, 1977: BMDP-77 Biomedical Computer Programs, P-Series, University of California Press, Berkeley, 880 pp.

Ortiz, C. A., 1978: Aerosol collection characteristics of ambient aerosol samplers. M.S. Thesis, Texas A & M University, College Station, Texas.

Terstriep, M. L., G. M. Bender, and D. C. Noel, 1981: National Urban Runoff Project, Champaign, Illinois. Evaluation of the Effectiveness of Municipal Street Sweeping in the Control of Urban Storm Runoff Pollution. First Annual Report, Prepared for the Illinois Environmental Protection Agency and the U. S. Environmental Protection Agency, Region V. Illinois State Water Survey, Champaign.

EVALUATION OF THE EFFECTIVENESS OF CIVIL ENGINEERING FABRICS AND CHEMICAL STABILIZERS IN THE REDUCTION OF FUGITIVE EMISSIONS FROM UNPAVED ROADS*

by

Alan G. Larson**
Donald L. Shearer

TRC ENVIRONMENTAL CONSULTANTS, INC.
Englewood, CO 80111

Dennis C. Drehmel

U.S. EPA, INDUSTRIAL ENVIRONMENTAL RESEARCH LABORATORY
RESEARCH TRIANGLE PARK, NC 27711

Gary W. Schanche

U.S. ARMY CORPS OF ENGINEERS,
CONSTRUCTION ENGINEERING RESEARCH LABORATORY
CHAMPAIGN, IL 61820

This paper has been reviewed in accordance with the U.S. Environmental Protection Agency's peer and administrative review policies and approved for presentation and publication.

(*) Although this is not the actual presentation made at the May 1982 meeting, it describes the same work and covers the same general time period. It represents work funded, in part, under EPA contract 68-02-3115. The title of A.G. Larson's presentation was "Evaluation of Road Carpets and Chemical Road Dust Suppressants."

(**) Current address: The Kentwood Moore Co., 5690 Denver Tech Center Blvd., Englewood, CO 80111.

Introduction

Emissions of fugitive dust from unpaved roads constitute a significant portion of the total suspended particulate matter (TSP) emitted in the United States. These roads may be managed by local governments for the use of the public or managed privately by an industrial user (e.g., mining, lumber, oil and gas, manufacturing). Emissions of fugitive dust from unpaved roads may exacerbate an air quality problem, and possibly cause violations of the National Ambient Air Quality Standards (NAAQS). Therefore, many state and local governments have required dust control measures to be used on unpaved roads.

The U.S. EPA's Region 8, its Industrial Environmental Research Laboratory-RTP (IERL), and the U.S. Army Construction Engineering Research Laboratory agreed to conduct a field study at Ft. Carson, Colorado, to evaluate the effectiveness of two potential control techniques--civil engineering fabrics (road carpets) and chemical dust suppressants. TRC was contracted by the EPA to design and manage a short-term study program to evaluate these materials and to coordinate with the Army on a long-term study. The Army was enthusiastic about conducting the tests at Fort Carson because of the significant number of unpaved road miles on the facility. The Army wanted to find an effective, but inexpensive, control technique for fugitive road dust control. EPA Region 8 was interested in participating in the study because an effective solution to the fugitive road dust problem is of concern to Region 8. EPA-IERL was interested in evaluating the overall effectiveness of these two specific dust control techniques.

The short-term study was designed to measure the effectiveness of each fugitive dust control application at two points in time--immediately following application of the road carpet or chemical suppressants (measuring maximum control efficiency) and after a few months of road use by local vehicles (measuring average control efficiency). Also, by limiting the measurements to a short time period (in this case, approximately 1 hour), the influence of weather (i.e. precipitation) and abnormally high winds was minimized and any bias in the results due to these elements reduced. The long-term study was designed to measure the overall efficiency of each dust control application. The effects of weather, abnormal traffic patterns, and inconsistent wind patterns were measured. By reclaiming the high-volume (hi-vol) filters every 3 days, the decay in the effectiveness of the chemical test sections could also be observed. In these studies, TSP and inhalable particulate matter originating from each section of road carpet or chemical dust suppressant were measured.

Several manufacturers of the road carpets and chemical dust suppressants were contacted. It was the objective of the tests to evaluate as many of the generically different products within each control technology as possible. Space constraints limited the test to three road carpet and three chemical dust suppressant test sections. The road carpets consisted of spunbonded woven polypropylene, needlepunched woven polypropylene, and nonwoven polypropylene sections. A cross-sectional drawing of the road carpet application is presented in Figure 1. The chemical dust suppressants tested were an oil-latex emulsion, an elastomeric asphalt emulsion, and a calcium lignosulfonate. An untreated road section was also maintained as a control.

Methodology

The test road is an existing gravel road located on Ft. Carson Army Base, just south of Colorado Springs, Colorado. Traffic on the road is generally light duty trucks and automobiles. Occasionally, a heavy duty truck or troop transport uses the road. The test road was divided into six test sections and one control section. Each section was approximately 200 yards (183 meters) long and 30 feet (9 meters) wide.

The three road carpets were each installed over the gravel road, employing standard road constructon methods with special techniques applied when recommended by the manufacturers. The road carpets were covered with approximately 6 inches (15 cm) of 2-inch (5 cm) or smaller aggregate.

For application of the oil-latex emulsion and the elastomeric asphalt emulsion, the gravel road was first scarified to a depth of 4 to 6 inches. The latex emulsion was applied as 1 part emulsion to 5 parts water solution and blade-mixed by several passes with a road grader. The scarified section was then graded smooth and packed. After scarifying, the asphalt emulsion section was windrowed with a road grader and the emulsion applied over the scraped section. After several windrowing passes with the grader to mix the road base and emulsion, and further application of the emulsion, the section was smoothed and packed. The calcium lignosulfonate section was graded smooth and the chemical applied to the gravel road surface. No scarifying was recommended by the supplier.

Hi-vol samplers were installed on platforms along the test road. The platforms each supported a pair of hi-vols--one for collecting TSP and one for collecting particles in six size fractions smaller than 30 μm. The hi-vol pairs were located 14 feet (4 meters) above ground downwind of each test section at a distance of 50 yards (46 meters) from the downwind edge of the section. One pair was located approximately 75 yards (69 meters) upwind of the test road (Figure 2). The operation of the hi-vols was regulated by wind direction controllers. The hi-vols operated only when the wind was out of a direction $\pm 60^\circ$ either side of a line normal to the road. This operating mode helped reduce cross contamination from one test section to another. An additional hi-vol to measure background TSP was located in an undisturbed area of the fort several miles downwind of the experimental area.

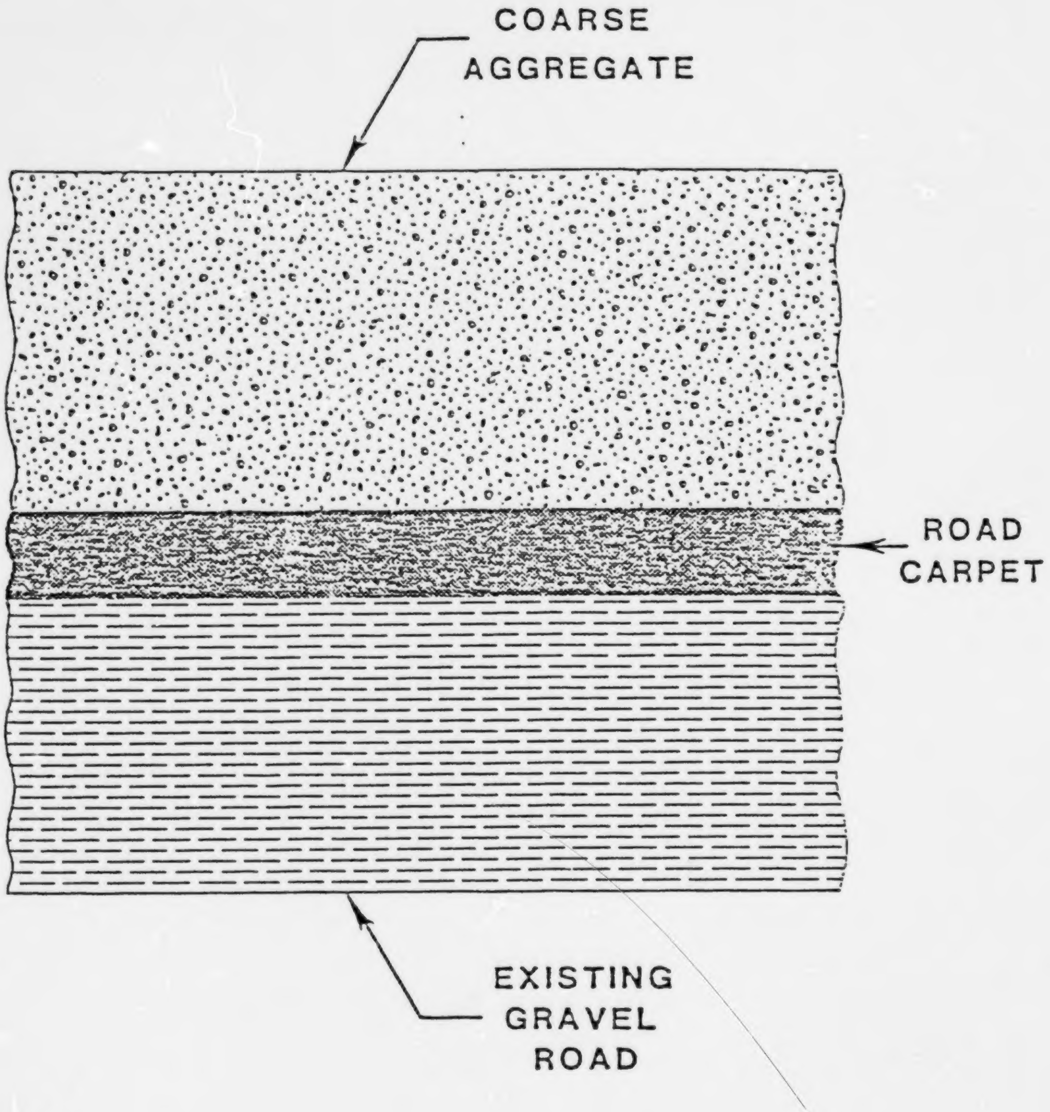
COARSE AGGREGATE
ROAD CARPET
EXISTING GRAVEL ROAD

FIGURE 1: ILLUSTRATION OF ROAD CARPET APPLICATION

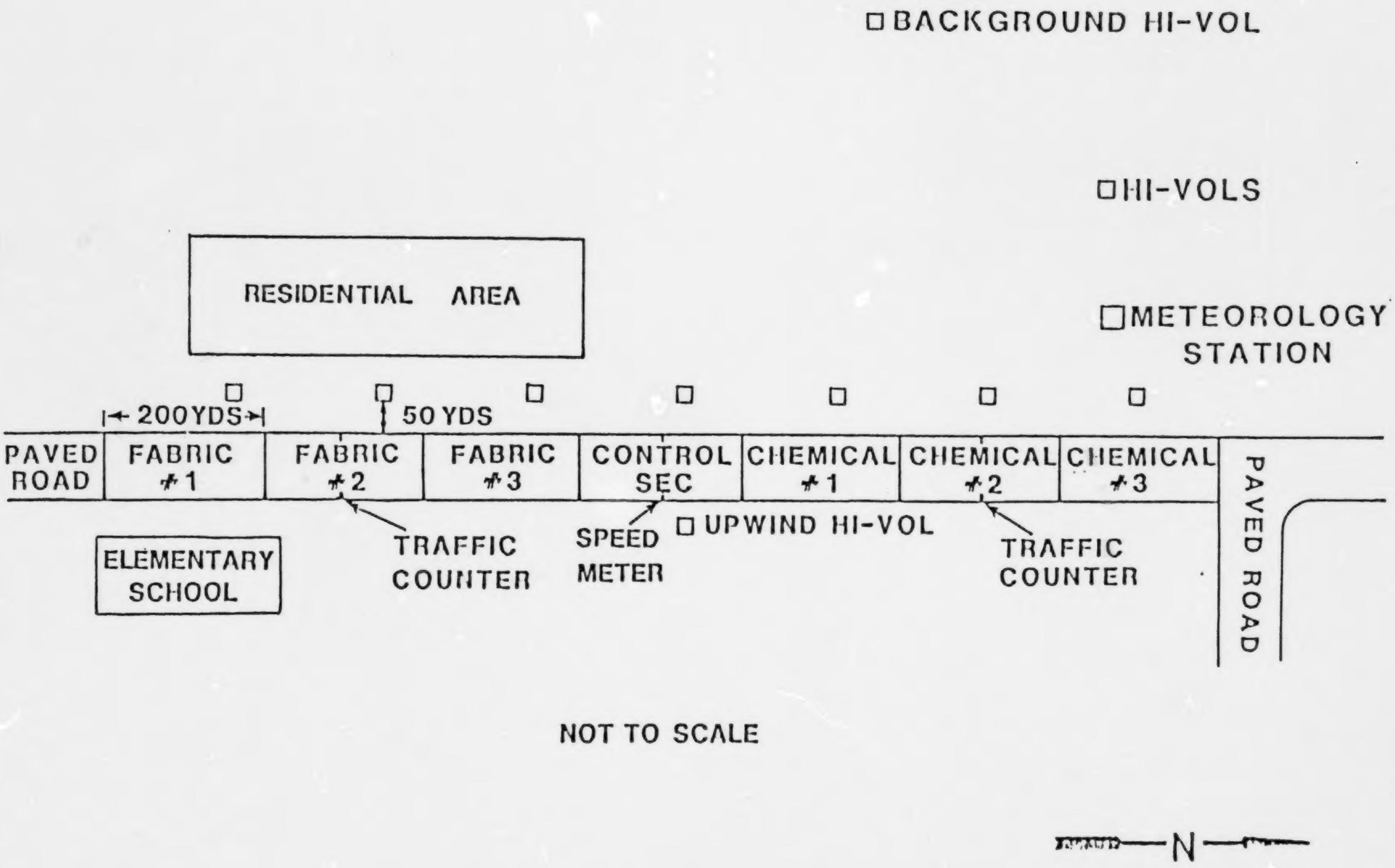
BACKGROUND HI-VOL
HI-VOLS
METEOROLOGY STATION
RESIDENTIAL AREA
200 YDS
50 YDS
PAVED ROAD
FABRIC #1
FABRIC #2
FABRIC #3
CONTROL SEC
CHEMICAL #1
CHEMICAL #2
CHEMICAL #3
PAVED ROAD
ELEMENTARY SCHOOL
TRAFFIC COUNTER
SPEED METER
UPWIND HI-VOL
TRAFFIC COUNTER
N

NOT TO SCALE

FIGURE 2: FIELD TEST DESIGN

Wind speed and direction were measured at a meteorological station located approximately 150 yards (137 meters) downwind of Chemical Section 3. The test road was equipped with traffic counters at each end to measure the traffic volume and patterns on the road and a speed meter in the control section to measure vehicle speeds along the road.

Following the long-term tests, each chemical will be evaluated for the following criteria:

- Effectiveness in reducing TSP and inhalable dust particles from the road surface.
- Frequency of chemical retreatment of test road sections.
- Cost of chemicals for each application and costs over the course of the 1-year test period.

From these criteria, the cost effectiveness of each chemical dust suppressant will be determined.

Results

At the time the road carpets were installed, only 2-inch or smaller sized aggregate was available. This aggregate had a relatively high percentage (8 percent, by weight, less than 97 μm) of fine materials. At the request of local residents, the road section was watered to reduce the dust. Consequently, a hardpan road surface developed and any dust control potential which the road carpets may have exhibited was negated. In retrospect, a washed aggregate appears essential for testing the dust control capabilities of road carpets. Plans are being made to treat the road carpet sections with chemical stabilizers and to measure the effectiveness of the chemicals in reducing fugitive road dust.

Raw data have been compiled for total suspended particulate matter and for particles less than 30 μm in diameter for the three chemical test sections, the control section, and the upwind and background stations. The sub-30 μm particles were collected in six stages, with average particles sizes of:

Stage 1	6.8 μm
Stage 2	3.3 μm
Stage 3	1.8 μm
Stage 4	0.9 μm
Stage 5	0.5 μm
Stage 6	Remainder of particles

The respirable range of particles is a combination of Stages 2-6. The total respirable particle concentration can be expressed as(1):

$$\chi = (0.19 \times S2) + (0.70 \times S3) + S4 + S5 + S6$$

Where: χ = respirable particle concentration ($\mu g/m^3$)

S2 = concentration of particulate matter on Stage 2
S3 = concentration of particulate matter on Stage 3
S4 = concentration of particulate matter on Stage 4
S5 = concentration of particulate matter on Stage 5
S6 - concentration of particulate matter on Stage 6

Particulate matter concentrations have been tabulated for the first nine long-term sampling periods. These concentrations are presented in Table I. The particulate matter concentrations measured from the calcium lignosulfonate, Chemical Section 1, are consistently higher than the concentrations measured from Chemical Sections 2 and 3 and the control section.

The manufacturers suggested application rate for the calcium lignosulfonate was too low to provide sufficient covering of the road surface or to allow for absorption of the chemical into the road and therefore did not result in measurable dust control. The manufacturer has since modified the recommended application procedures to include scarifying of the road surface prior to chemical application and increased dosage of the chemical. The manufacturer has also required ambient temperature consistently above 45-50°F before application of the chemicals can begin. Therefore, the collection of any reliable dust concentrations will have to wait until the calcium lignosulfonate is reapplied in spring 1981. One thing that appears to apply to the calcium lignosulfonate test section is that grading the road prior to chemical application loosened enough surface particles to cause particulate matter concentrations which are greater than those measured from the control section. The control section had been packed by the combined effects of precipitation and traffic.

The concentrations from the road sections treated with the oil-latex emulsion and the elastomeric asphalt emulsion are generally much lower than the control section. When compared with the control section, control efficiencies of the oil-latex emulsion range from approximately 6-70 percent for respirable particles and approximately 13-80 percent for TSP. Control efficiencies for the elastomeric asphalt emulsion range from approximately 30-96 percent for respirable particles and approximately 56-86 percent for TSP.

TABLE I

Measured concentrations* (µg/m^3) of respirable and total suspended particulate matter

SAMPLING PERIOD	CHEMICAL #3 OIL-LATEX EMULSION	CHEMICAL #2 ELASTOMERIC ASPHALT EMULSION	CHEMICAL #1 CALCIUM LIGNOSULFONATE	CONTROL SECTION	UPWIND STATION	BACKGROUND STATION
12-14-80						
Respirable	111	23	241	118	**	9
TSP.	282	64	**	326	365	24
12-17-80						
Respirable	**	**	244	207	90	**
TSP	91	64	653	454	**	21
12-20-80						
Respirable	**	1	61	24	26	1
TSP	54	19	143	44	116	12
12-23-80						
Respirable	15	35	**	51	26	4
TSP	51	**	142	102	66	14
12-26-80						
Respirable	27	8	88	62	38	11
TSP	53	20	191	105	85	12
12-29-80						
Respirable	**	**	**	26	**	**
TSP	102	51	547	269	149	15
1 - 2-81						
Respirable	24	29	94	76	34	5
TSP	82	33	253	162	39	13
1 - 5-81						
Respirable	**	10	**	**	**	**
TSP	134	58	573	274	167	24
1 - 8-81						
Respirable	**	26	**	244	**	**
TSP	144	91	909	434	102	**

* These concentrations are raw data

** At the time this report was prepared, the data for these points had been measured and weighed but had not been processed through the quality assurance programs.

Because of the impending inclusion of three more chemical test sections, the short-term tests have been postponed until all test sections are operational. Two short-term tests have been completed for the existing test sections. The limited data from these two tests show that for the oil-latex emulsion, TSP has been reduced more than 50 percent. For the elastomeric asphalt emulsion, TSP has been reduced by 90 percent. Additional short-term tests are planned immediately after application of the new chemicals and again in the summer. (Tables II and III.)

The influence of wind speed, wind direction, and vehicle use rates have not been compiled for correlation with the particulate matter concentrations. These correlations will be made in spring and summer 1981.

Conclusions

The effectiveness of road carpets as a fugitive dust control technique on unpaved roads is uncertain. The results of field tests to evaluate this effectiveness are inconclusive. In order to adequately study the emission control capability of the road carpets, a clean, washed aggregate must be used over the carpet.

The application of chemical dust suppressants to unpaved roads is an effective method of controlling fugitive dust. A wide range of control efficiencies can be realized. For an oil-latex emulsion, up to 70 percent control of respirable particles and up to 80 percent control of TSP has been measured. For an elastomeric asphalt emulsion, up to approximately 96 percent control of respirable particles and up to 86 percent of TSP has been measured. The dependence of the control efficiencies on wind speed, vehicle speed, and weathering of the chemicals is still being evaluated.

The cost:benefit ratio for each chemical application is also being evaluated. This evaluation will include the initial cost of chemical application, costs of successive reapplication, and control efficiencies achieved. From this cost:benefit ratio, chemical dust suppressants which can be tailored to the economic and dust control requirements of the user will be presented.

References

(1)V.A. Marble, "A Fundamental Study of Inertial Impactors" (Ph.D. theses, University of Minnesota, 1970).

TABLE II

LATEX EMULSION CONTROL EFFICIENCY

DATE	CONTROL SECTION*	LATEX EMULSION*	CONTROL %	
12-14-80	325.8	282.4	13.3	
12-17	400.0	146.6	63.4	
12-18	453.9	90.8	80.0	
12-20	215.1	67.8	68.5	
12-21	44.4	54.0	--	
12-23	80.4	51.8	35.6	
12-24	102.0	50.6	50.4	
12-26	103.6	52.1	49.7	
12-27	105.0	53.1	49.4	
12-29	105.0	71.6	31.8	
12-30	214.6	102.3	52.3	
12-31	269.3	102.3	62.0	**
1-02-81	206.9	88.8	57.0	
1-03	162.4	82.1	49.4	
1-05	204.1	103.6	49.2	
1-06	273.6	133.6	51.2	
1-08	333.7	137.3	58.9	
1-09	433.8	143.5	66.9	
3-24	118.7	64.9	54.7	
3-26	68.0	60.0	11.8	
3-27	37.5	54.5	--	
3-29	42.3	43.5	--	
3-30	45.7	37.9	17.1	
4-01	58.7	54.4	7.3	
4-02	68.0	64.3	5.4	

(*) $\mu g/m^3$

(**) Below this line represents respirable particles; above this line represents TSP

TABLE III

EMULSIFIED ASPHALT CONTROL EFFICIENCY

DATE	CONTROL SECTION*	EMULSIFIED ASPHALT*	REDUCTION %	
12-14-80	325.8	64.1	80.3	
12-17	400.6	64.3	83.9	
12-18	453.9	64.3	85.8	
12-20	215.1	36.1	83.2	
12-21	44.4	19.2	56.8	
12-23	80.4	25.5	68.3	
12-24	102.0	29.2	71.4	
12-26	103.6	24.5	76.4	
12-27	105.0	20.4	80.6	
12-29	105.0	31.9	69.6	
12-30	214.6	51.1	69.6	
12-31	269.3	51.1	81.0	**
1-02-81	206.9	40.1	80.6	
1-03	162.4	33.5	79.4	
1-05	204.1	42.7	79.1	
1-06	273.6	58.1	78.8	
1-08	333.7	70.3	78.9	
1-09	433.8	90.6	79.1	
3-24	118.7	30.6	74.2	
3-26	68.0	40.1	41.0	
3-27	37.5	44.8	--	
3-29	42.3	26.1	38.3	
3-30	45.7	12.8	72.0	
4-01	58.7	21.5	63.3	
4-02	68.0	26.8	60.5	

(*) $\mu g/m^3$

(**) Below this line represents respirable particles; above this line represents TSP

EVALUATION OF WEATHERING CHARACTERISTICS OF DUST SUPPRESSANT CHEMICAL ADDITIVES

by: William B. Kuykendal, Dennis C. Drehmel, Bobby E. Daniel
U. S. Environmental Protection Agency
Industrial Environmental Research Laboratory
Research Triangle Park, North Carolina 27711

ABSTRACT

This paper presents the results of an experimental program to evaluate the effect of natural weathering on selected dust suppressant chemical additives. A previous study had evaluated the performance of eight commercially available additives. Four of these were selected for evaluation of their weathering characteristics. The four additives were: Coherex, Lignosulfonate, SP 301, and Polyco 2151. Three concentrations of each additive were sprayed on a test panel of pulverized coal and then exposed to the weather for periods of 30, 60, and 90 days. The test panels were then evaluated in a wind tunnel to determine the performance of the additives after weather exposure. The results show that no significant performance degradation occurred for any of the additives tested.

This paper has been reviewed in accordance with the U.S. Environmental Protection Agency's peer and administrative review policies and approved for presentation and publication.

INTRODUCTION

The Environmental Protection Agency has sponsored an active program to develop technology to suppress fugitive particulate emissions. A facet of this program has been aimed at the reduction of fugitive particulate emissions through the application of dust suppressant chemical additives. In addition to the work described by this paper, two other projects have been conducted by EPA to evaluate the effectiveness of chemical dust suppressants. In an earlier in-house study, Drehmel and Daniel[1] evaluated the relative effectiveness of 10 different dust suppressants using a wind tunnel. Their results will be briefly reviewed in the following section. Under a contract study, Larson[2] evaluated four dust suppressants in a field study conducted over several months on an unpaved road in Colorado.

Before chemical dust suppressants can gain widespread use, they must demonstrate the ability to effectively suppress fugitive emissions in a manner that is cost effective when compared to other fugitive control options. A major factor in determining cost effectiveness is how often the dust suppressant needs to be reapplied. Two factors determine the durability of a dust suppressant: wear and weathering. In applications such as inactive storage piles where there is little or no wear, the only factor affecting durability is weathering. The purpose of this work is to evaluate the effectiveness of several dust suppressants after exposure to natural weathering.

PRIOR WORK

The initial wind tunnel evaluation on the relative effectiveness of dust suppressants by Drehmel and Daniel tested 10 commercially available products. These products were evaluated in the same wind tunnel using the same technique described in the experimental section of this paper. Of the 10 dust suppressants evaluated, 8 gave consistent results and are summarized in Table 1. Each dust suppressant was evaluated over a range of application rates to determine the effectiveness of each as the application rate varied. In order to compare the performance of each dust suppressant on a common basis, the effectiveness for each, expressed as entrainment velocity, was determined for an application rate calculated at a cost of $300 per acre. Entrainment velocity is defined later in the paper, but the higher the value, the more effective the additive. It should be emphasized that the dilution ratios determined by the above method were not necessarily the ones recommended by the manufacturer.

From these results four dust suppressants were selected for the weathering study: Coherex, Lignosulfonate, SP-301 and Polyco 2151. The selection was based on having a variety of chemical makeups and manufacturers rather than on performance alone.

A brief literature review of weathering test procedures was conducted to identify the key weather parameters that should be included in the experimental plan. Since the purpose of the study was to evaluate

TABLE 1. ADDITIVE PERFORMANCE RESULTS FROM DREHMEL AND DANIEL[1]

Additive	Chemical	Additive Supplier	Performance[a]
Coal Dyne	Unknown	Aquadyne	16.8
Coherex	Petroleum Resin in Water	Witco	13.4
CPB-12	Acrylic Latex	Wen Don	9.8
Lignosulfonate	Lignosulfonate	Wen Don	18.6
Oil & Water	Mineral Oil	Wen Don	18.3
SP-301	Synthetic Polymer	Johnson & March	6.4
Pentron DC-3	Acrylic in Water	Apollo	9.1
Polyco 2151	Synthetic Copolymer	Borden	15.2

[a] Entrainment velocity (m/sec) for an application cost of $300/acre.

weathering effects on dust suppressants, which are usually sprayed on coatings, the available literature on paint and building materials was reviewed. Three publications[3,4,5] were located along with one ASTM procedure.[6] Each reference identified the key weather related parameters as: solar radiation (particularly ultraviolet), relative humidity, rainfall, and temperature. In addition, it was decided to vary the weathering exposure time so that a degradation rate could be determined.

EXPERIMENTAL

Since an evaluation of the weathering characteristics was the primary objective of the study, the selection of the weathering method was important. Natural weathering has the advantage of being "real world" testing and requires a minimum amount of experimental apparatus. The disadvantage is, of course, that the weather related variables cannot be controlled. Simulated weathering tests conducted indoors do offer a controlled weather environment, but there are no standard accepted test procedures (see References 3 and 4). In addition, they are experimentally complex. For these reasons the natural weathering method was selected.

Having selected the dust suppressants to be evaluated and identified the key weather related parameters, it was then necessary to develop a test matrix. The variables selected were dust suppressant, concentration of the dust suppressant, and weather exposure time.

The selection of the dust suppressant concentrations required balancing several factors. It was decided to select three concentrations for each of the four dust suppressants. Furthermore, it was desirable from the standpoint of the statistical design that the concentrations for each additive be selected such that the medium concentration was half way between the high and low concentrations. Care had to be taken in the selection of the high and low concentrations to ensure that the experimental procedure would be able to detect a result. If too high a concentration were used, the maximum speed available in the wind tunnel (30 m/sec) would not erode any of the test material. Conversely, too low a concentration would show no effect when compared to an untreated test material. Based on Drehmel and Daniel's results, it was possible to select dust suppressant concentrations that would yield results within the range of the experimental capability. The values of the dust suppressant concentrations selected are given in Table 2. It should be emphasized that these concentrations are not the concentrations recommended by the manufacturer. Rather they were selected to accommodate the experimental procedure used so that weathering effects could be determined over a range of concentrations.

From a practical standpoint it was decided to limit the outside exposure time to a maximum of 90 days. It was felt that if a dust suppressant were still effective after this length of time that it would be useful as a fugitive control technique. Intermediate intervals of 30 days and 60 days were selected in addition to zero days (no explosure). This variable of exposure time posed a problem in that the weather occurring during any 30 day period would not be the same as for any other 30 day period. The test matrix accommodated this by including three replicates of the zero day tests, two replicates

TABLE 2. ADDITIVE CONCENTRATIONS TESTED

Additive	Concentration, $1/m^2$ Low	Medium	High
Coherex	0.022	0.044	0.066
Lignosulfonate	0.005	0.011	0.016
SP-301	0.005	0.022	0.038
Polyco 2151	0.0018	0.0034	0.0052

of the 30 day tests, two replicates of the 60 day test, and one set of tests for 90 days. All of the weathering tests were conducted between mid-August and mid-November 1981 at EPA's Research Triangle Park, North Carolina, facility.

These variables were developed into a partial factorial design which consisted of 96 tests. These tests are summarized in Table 3. One of the test samples was destroyed during the course of the experiment so that 95 tests were actually conducted.

The material selected for use in evaluating the dust suppressants was pulverized coal. A sieve analysis gave an average size of about 200 μm. The size distribution is shown in Figure 1. The coal was then placed in a test panel made of plexiglass which had a test volume 305 mm x 305 mm x 19 mm deep. The test panel was always loosely filled with the coal, even with the top of the panel, and any excess coal was brushed off. The dust suppressant was then applied with a spray bottle and allowed to dry overnight. After drying, the test panels were placed in outside racks and exposed to the weather.

Shortly after initiating the exposure tests a problem became apparent with the planned exposure test procedure. A severe thunderstorm occurred with the resulting large rain drops impacting on the treated coal causing the surface to be destroyed. It was decided that the best solution would be to place a cover over the test panels. The selection of the cover material became quite important. Although the test panels would no longer be exposed directly to rainfall it was necessary to maintain as many of the weather related parameters as possible, particularly solar radiation. Several candidate cover materials were selected and evaluated on an ultraviolet spectrophotometer. Ultraviolet was selected since it had been identified as a major factor in prior weathering studies. Two of the materials screened were judged to be satisfactory. These were polyethylene (0.0762 mm thickness) and styrene (0.1905 mm thickness), and the results are shown in Figure 2. Also shown in Figure 2 is a plot of the relative energy of the sun as a function of wave length. As can be seen from Figure 2 both polyethylene and styrene transmit about 70% of the incident solar radiation. Polyethylene was selected as the cover material because it was readily available. The polyethylene was fashioned into an open tent and placed over racks each of which held eight test panels as shown in Figure 3. This permitted free air circulation under the cover which allowed the test panel to "see" ambient temperature and relative humidity.

After exposure to the weather the test panels were brought inside for evaluation in a wind tunnel. The wind tunnel had a 0.61 m square cross section with an active length of 9.76 m. The first 4.88 m was used for establishing the desired velocity profile prior to the location of the test panel. The test panel was located in the wind tunnel such that the coal surface was flush with the bottom of the wind tunnel. Past the test panel, the remainder of the active section was used for disengagement. Beside the active section of the tunnel is an air return loop. In the air return section is a baghouse to clean recycled air to the active section of the tunnel. Design of the active section was intended to produce a turbulent boundary layer similar to that found for wind passing over open ground or a storage pile. Details of this design are given by Viner et al.[7]

TABLE. 3 TEST MATRIX

Additive	Concentration Levels[a]	Exposure Days	Replicates	Planned Tests	Actual Tests
Coherex	3	0	3	36	36
Lignosulfonate	3	30	2	24	24
SP-301	3	60	2	24	23
Polyco 2151	3	90	1	12	12
			TOTAL	96	95[b]

[a] A total of 12 tests.

[b] One test sample was destroyed during the experiment.

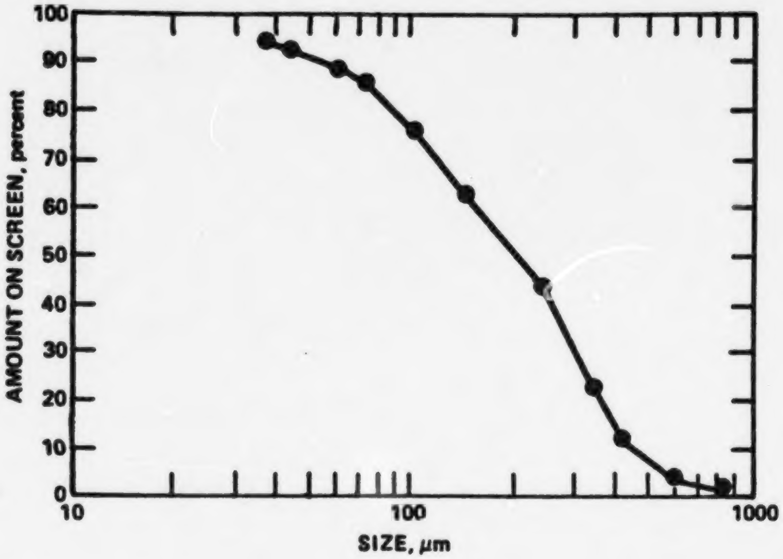

Figure 1. Sieve analysis of pulverized coal.

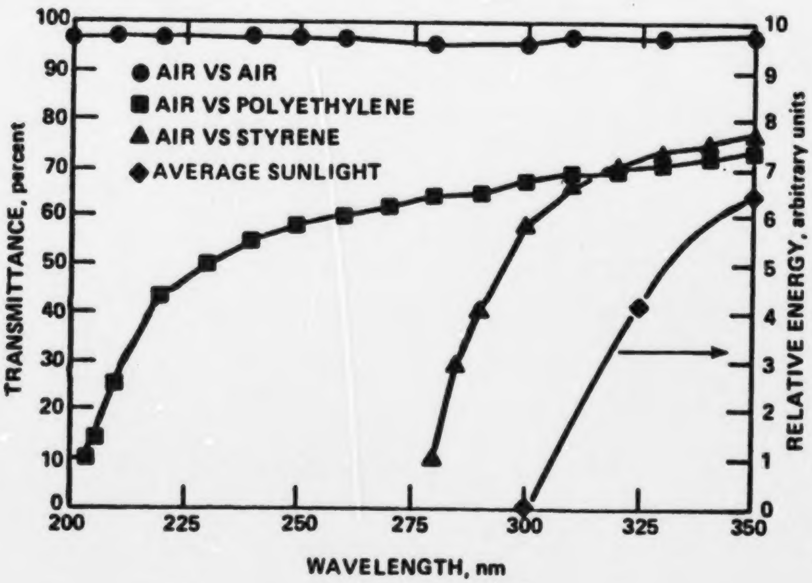

Figure 2. Optical transmittance of candidate cover materials.

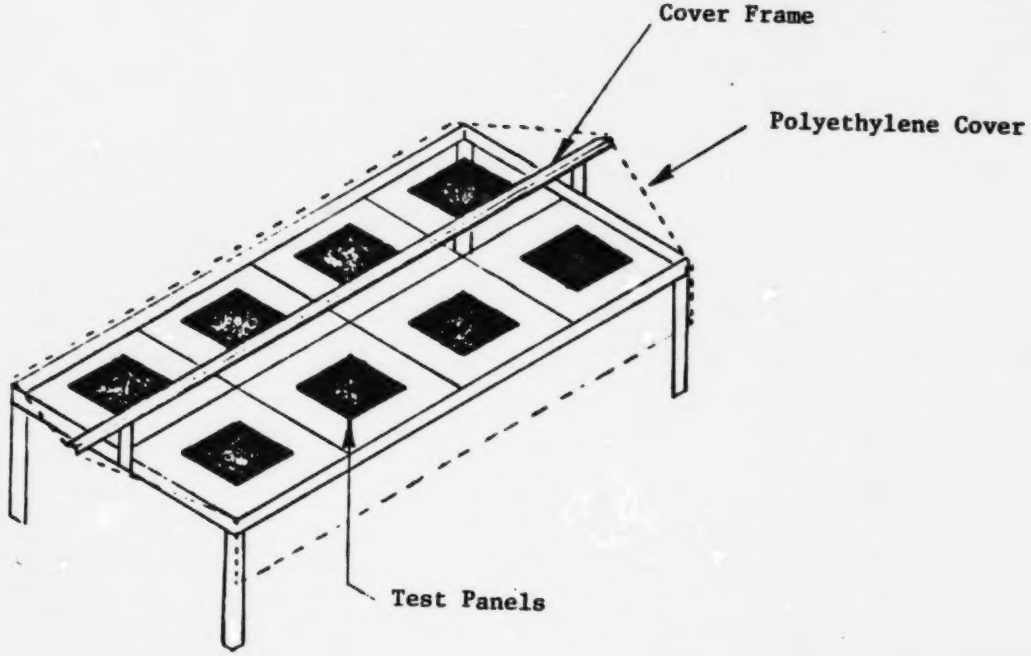
Cover Frame
Polyethylene Cover
Test Panels

Figure 3. Exposure racks with test panels and polyethylene cover.

Each test panel was initially weighed prior to being tested in the wind tunnel. The wind tunnel was operated at several velocities, beginning at the lowest and advancing monotonically. After maintenance of a velocity for 3 minutes, the tunnel was shut down to remove and reweigh the test panel. With the test panel put back, the next velocity was tested. The process was repeated until the maximum test velocity was reached or until the emission rate exceeded 13.04 g/min. The emission rate of 13.04 g/min was selected arbitrarily as a very high emission rate which would indicate that the dust suppressant had failed and the test should be terminated.

RESULTS AND DISCUSSION

In general each test conducted in the wind tunnel was similar in that the dust suppressant nearly completely prevented erosion until a critical velocity was reached. At this critical velocity the dust suppressant failed quickly resulting in a large emission rate. This critical velocity, termed entrainment velocity, was determined by measuring the velocity which produced an entrainment rate of 4.89 g/min selected arbitrarily as indicating failure of the dust suppressant. Figure 3 illustrates the rapid failure of the dust suppressant as the velocity is increased to the entrainment velocity. For the case of Figure 3 the entrainment velocity for 30 days outside is seen to be approximately 17 m/sec.

The results for each of the four dust suppressants evaluated are given in Figures 4 through 7. These plots show entrainment velocity as a function of weather exposure time for each of three concentrations. In general each plot shows that the entrainment velocity increased with increased dust suppressant concentration as expected. What was not expected was that there was no detectable degradation in the performance of any dust suppressant over the period tested.

Several factors should be kept in mind when examining these data. First, as mentioned earlier, the concentrations tested were not intended to duplicate concentrations suitable for field use. The selection of pulverized coal in a shallow test panel is likewise a departure from a practical application. The use of a polyethylene cover compromised the results by limiting the solar radiation and eliminating direct contact with rain. The exposure procedure used deviated from ASTM D 1435 in that the exposure racks were oriented flat instead of at the prescribed 45° facing south. Finally, these were static tests with no activity on the test panels. Nevertheless, these results are believed to be valid for the intended purpose of the study; namely, to evaluate the weathering characteristics of the four dust suppressants tested.

CONCLUSIONS

For the four dust suppressants evaluated it can be concluded that there was no significant degradation in performance over the 90 day test period. In addition, the experimental test procedures used are believed to be valid and would have detected any significant degradation had it occurred. These are welcome findings because they mean that dust suppressant chemical additives do offer an effective means of suppressing fugitive particulate emissions.

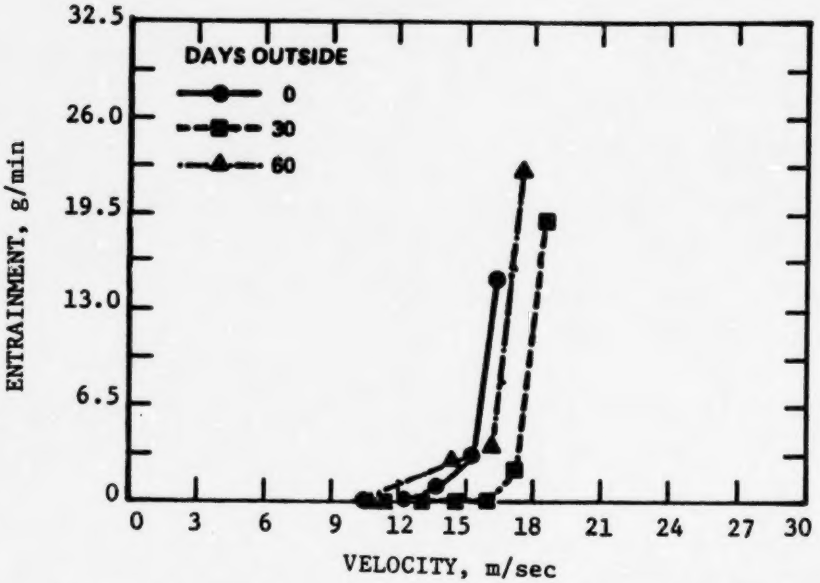

Figure 3. Wind tunnel data: Lignosulfonate (0.005 $1/m^2$)

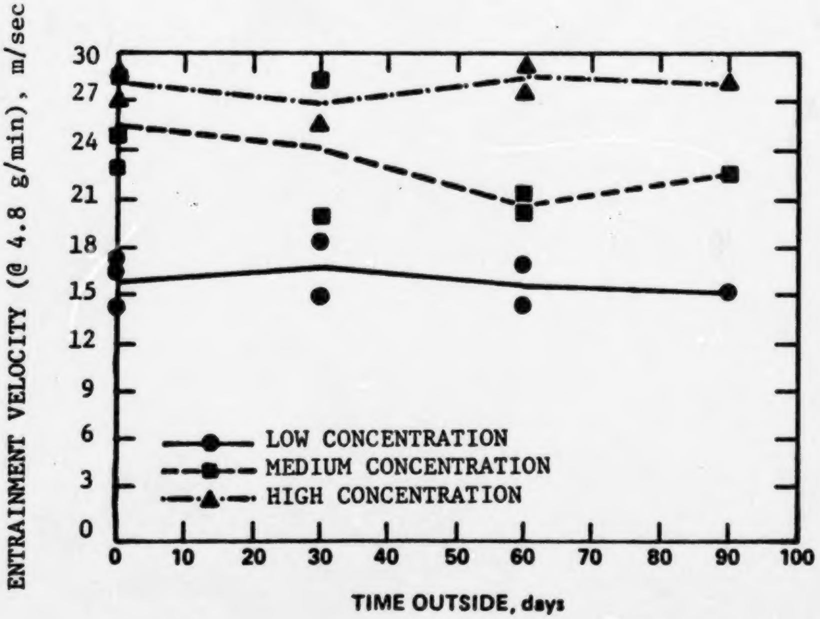

Figure 4. Weathering tests: Coherex.

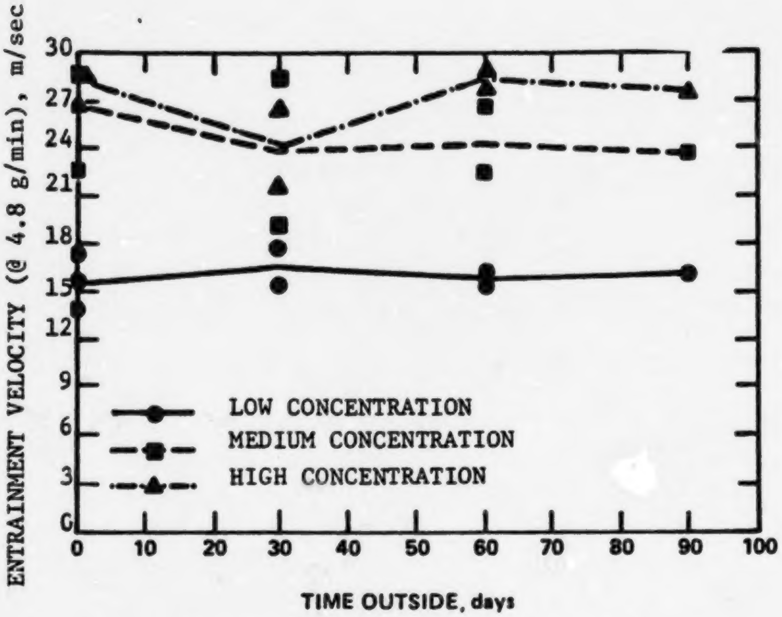

Figure 5. Weathering tests: Lignosulfonate.

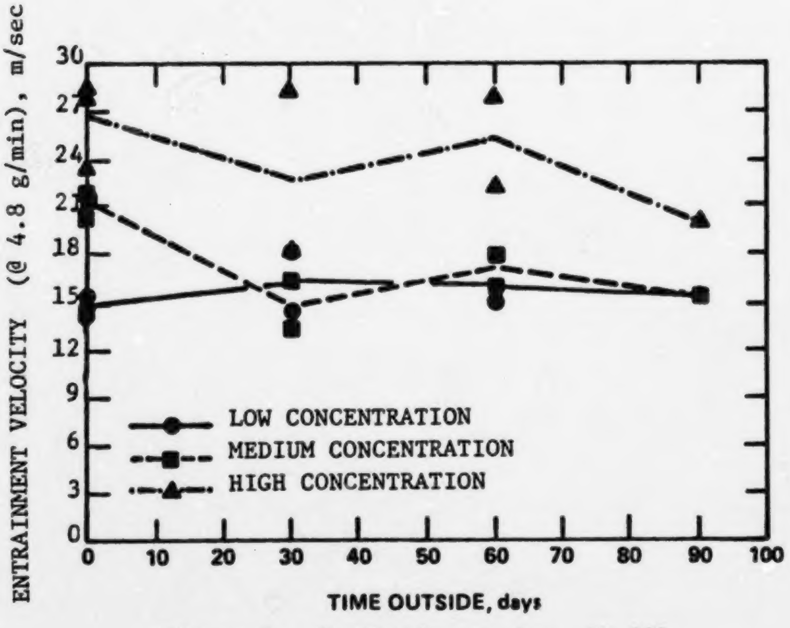

Figure 6. Weathering tests: SP-301.

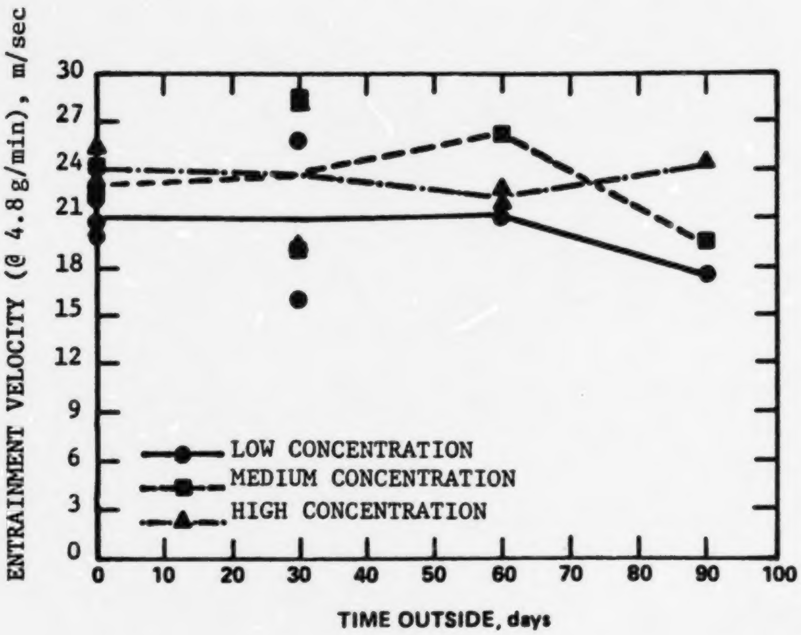

Figure 7. Weathering tests: Polyco 2151

REFERENCES

1. Drehmel, D. C., and Daniel, B. E. Relative Effectiveness of Chemical Additives and Wind Screens for Fugitive Dust Control. In Proceedings: Third Symposium on the Transfer and Utilization of Particulate Control Technology: Vol. IV. Atypical Applications. EPA-600/9-82-005d, July 1982.

2. Larson, A. Evaluation of Road Carpets and Chemical Road Dust Suppressants. Presented at Fifth Symposium on Fugitive Emissions: Measurement and Control, Charleston, S. C., May 1982.

3. Mitton, P.B., and Richards, D. P. A Model for Objective Development of Accelerated Weathering Tests. Journal of Paint Technology, Vol. 43, No. 563, December 1971.

4. Hoffmann, E. Weathering of Paint Films and Development of Accelerated Tests. Journal of Paint Technology, Vol. 43, No. 563, December 1971.

5. Masters, L. W., Wolfe, W. C., Rossiter, W. J., Jr., and Shaver, J. R. State of the Art on Durability Testing of Building Components and Materials. NBS Report No. NBS1R73-132, March 1973.

6. ASTM D 1435, ASTM Book of Standards, Part. 27, 1971.

7. Viner, A. S., Ranade, M. B., Shaughnessy, E. J., Drehmel, D. C., and Daniel, B. E. A Wind Tunnel for Dust Entrainment Studies. In Proceedings: Third Symposium on the Transfer and Utilization of Particulate Control Technology: Vol. IV. Atypical Applications. EPA-600/9-82-005d, July 1982.

TABLE FOR CONVERSION TO ENGLISH UNITS

To Convert	to	Multiply By
m/sec	ft/sec	3.33
l/m^2	gal./acre	1069.73
m^2	acre	4047
mm	in	0.0394
m	ft	3.28
g/min	gr/min	15.34

ON THE USE OF SF_6-TRACER RELEASES FOR THE DETERMINATION OF FUGITIVE EMISSIONS

B. VANDERBORGHT, J. KRETZSCHMAR and T. RYMEN
Nuclear Energy Research Center, B-2400 Mol, Belgium
F. CANDREVA, R. DAMS
Institute for Nuclear Sciences, B-9000 Gent, Belgium

Summary

The principle and applicability of tracer releases for the accurate measurement of fugitive emissions is discussed and illustrated with some practical examples. At the emission source SF_6-tracer gas is released at a well-known constant rate. With proper adaption of the tracer emission device to the fugitive emission source thorough mixing and homogeneous dispersion of tracer and pollutant can be obtained. In this way the tracer to pollutant concentration ratio is the same in the dispersed plume as in the emission and the pollutant emission rate can be calculated by measuring the tracer to pollutant ratio at any place in the plume.

The work described in this paper was not funded by the U.S. Environmental Protection Agency. The contents do not necessarily reflect the views of the Agency and no official endorsement should be inferred.

1. INTRODUCTION

Although dispersion calculation for emissions from high stacks predict a maximum ambient air concentration at a certain distance from the source, the highest concentrations are very often measured very close to the factory. Control of point-source emissions has in certain problem areas not produced the anticipated improvement in ambient air quality. The reason appears to be fugitive emissions at low- or ground-level altitude. Fugitive emissions seem to be especially important for aerosol emissions from metallurgical plants. For the complete understanding of air pollution situations - through emission-inventories, mathematical modelling etc. - it is necessary to be able to quantify the fugitive emissions.

Since the emission area is usually not well defined, and since volume flow rates are usually unknown, the normal emission measurement techniques cannot be applied. The measuring methods actually described in the literature can be classified into "quasistack" sampling or roof monitoring in which the emission area is by some means physically restricted or into "reversed modelling" where emission is calculated from immission measurements and mathematical dispersion models.(1)

In this paper the principle and possibilities of a tracer technique for the quantification of fugitive emissions from a metallurgical plant is described.

A common feature of all mentioned procedures is the discontinuous character preventing routine continuous emission measurements.

2. PRINCIPLE

The principle of the procedure is as follows :

A tracer component is discharged at a constant, well-known rate at the emission site of the pollutant. When the tracer and the pollutant are well mixed in the emission plume and when they are dispersed in the same way, then the concentration ratio of both components will remain constant all over the plume and equal to the emission rate ratio :

or $$\frac{\chi_p}{\chi_t} = \frac{Q_p}{Q_t} \qquad (1)$$

where χ = concentration $[M.L^{-3}]$
Q = emission rate $[M.T^{-1}]$
p = pollutant
t = tracer

Knowing the tracer emission rate and measuring the concentration of the tracer and the pollutant in the plume give the possibility to calculate the unknown pollutant emission rate Q_p. It is obvious that the quality of the results will depend on the validity of equation (1) for which a good homogenization and equal dispersion of tracer and pollutant is necessary. The characteristics of the tracer release (place, time, flow-rate, temperature, shape of nozzle) and the choice of the measuring points for the simultaneous determination of pollutant and tracer concentrations must be optimized as a function of this homogeneity.

When the fugitive emissions out of a factory workplace are to be measured, different sampling strategies are possible. Suppose a building in which two furnaces are the sources of uncontrolled emissions of metal fumes (figure 1). Aerosol is evacuated from the inside atmosphere of the workplace by means of natural draft through rooftop ventilation openings and by means of a ventilator with the hood a few meters above one furnace and the exhaust opening in the wall or the roof of the building. These emissions are easily entrained in the wake on the lee of the building and the source cannot be considered as a point source.

For the determination of these fugitive emissions - by the method of tracer release and measuring tracer and pollutant concentration - three different sampling locations are possible.

1) Tracer and pollutant are sampled outside at distances from a few meters up to a few hundreds meters downwind the building. With this configuration the total emission of the building is measured.
2) Sampling units are placed along the ventilation opening in the rooftop.
3) Isokinetic sampling is performed in the exhaust tube of the ventilator.

In the two latter cases homogenization of tracer and pollutant becomes very critical. By proper adjustment of the tracer release and sampling places the emissions of the different sources are discerned and the emissions through the rooftop and through the ventilator can be calculated separately. In this paper the properties of the three methods will be compared.

3. EXPERIMENTAL

In an antimony (Sb) metallurgical plant the technique has been used to quantify the fugitive emissions emanating from a 18m high 30mx20m long workplace in which a convertor and a refinery furnace were installed (figure 1). One of the experiments, in this workplace, will be described here as an example. Uncontrolled Sb dust emissions originated mainly from the filling and the slag removal from the convertor as well as from the same actions on and the emptying of the refinery furnace. Minor leak emissions on filter installations did also occur. Sb aerosol had a mean aerodynamic diameter of 1 to 2 µm.

Sulfurhexafluoride (SF_6) gas was used as a tracer. SF_6 is an inert, non-toxic gas, stable up to about 500°C, routinely detectable up to 50 $ng.m^{-3}$ and normal background concentrations are below the detection limit. SF_6 was discharged at the convertor (main emission place) at a rate of about 27 $g.min^{-1}$.

SF_6 and Sb were simultaneously sampled at three places in the roof of the workplace (W_1 to W_3 in figure 1), at one place (W_0) in the exhaust tube of the hood above the convertor and 8 places outside at distances between 15 and 180m from the hall (R_1 to R_8 in figure 2).
Up to this distance sedimentation and deposition of Sb aerosol is neglectible, and there is no basic difference between the dispersion of Sb-aerosol and SF_6 gas.
The sampling places outside were chosen in such a way that interferences from other parts of the factory were minimal. Four sampling periods of each 30 minutes were performed. During sampling the Local wind direction at the 30m-level was between 200° en 205° with a windspeed between 7 and 8,5 $m.s^{-1}$ and neutral atmospheric stability. For the sampling points in the roof (W_1 to W_3) the aerosol was sampled on the same filter for the 4 periods as the access to these places was difficult.

Aerosol samples were taken using LIB-type low volume samplers with Whatman 41 filters. Sb was determined by neutron activation and X-ray fluorescence. SF_6 samples were collected by filling plastic bags and were gas chromatographically analysed. For further details on the sampling and analysis procedures see reference (2).

4. Results and discussion

The results of the emission calculation are summarised in table I.

TABLE I : Sb emission from a workplace as determined by the concentration ratio Sb/SF_6 in : ambient air downwind of the building ($R_1 \rightarrow R_7$)
ventilator exhaust tubo (W_0)
rooftop of the building (W_1 - W_3)

sampling period	Sb emission in kg/h based on sampling points			Activities of	
	$R_1 \rightarrow R_7$	r.s.	W_0	Convertor	Refinery furnace
1	1.6 ± 0.4	23 %	2.5	8' filling	17' slag
2	1.1 ± 0.4	33 %	1.3	6' filling 4' slag	short emissions
3	2.6 ± 0.5	19 %	2.7	12' filling	3' slag
4	1.0 ± 0.2	22 %	0.7	9' filling	
Average	1.6	24 %	1.8		

r.s. relative standard deviation in procent on 7 measurements

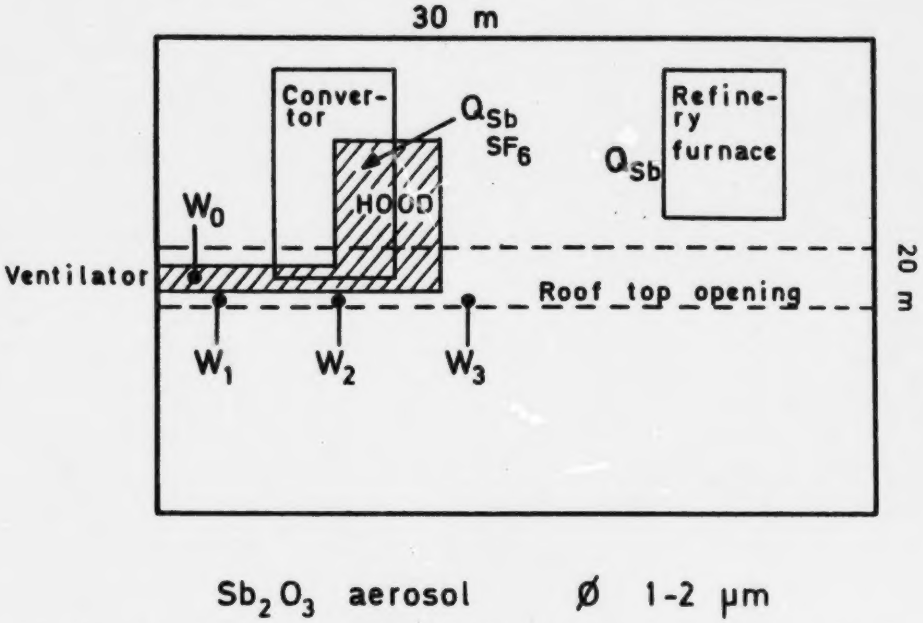
30 m
Conver-
tor
Q_{Sb}
SF_6
HOOD
Refine-
ry
furnace
Q_{Sb}
W_0
Ventilator
Roof top opening
20 m
W_1
W_2
W_3
Sb_2O_3 aerosol Ø 1-2 μm

Fig. 1 - Layout of emission and sampling points in the workplace

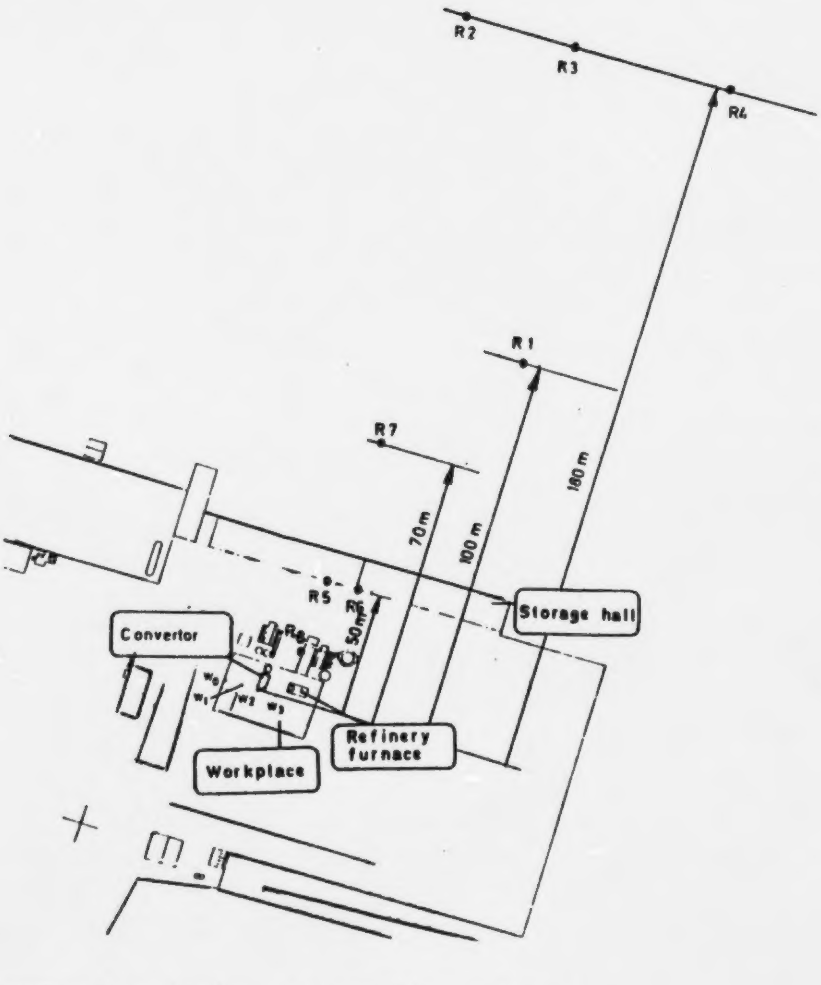
R2
R3
R4
R1
R7
180 m
100 m
70 m
R5
R6
50 m
Storage hall
Convertor
W0
W1
W2
W3
Refinery furnace
Workplace

Figure 2 - Layout of emission and sampling points

sampling place	Sb emission in kg/h averaged over 4 periods
W_0	1.8
W_1	1.4
W_2	1.4
W_3	0.9
average	1.4 ± 0.37

The relative standard deviation on the emission determination for each sampling period through the 7 sampling points ($R_1 \rightarrow R_7$) outside the building and on a distance larger than 30 m ranges between 19 and 33 % with an average of 24 %, and no sampling place gave a systematic deviation from the average. In sampling point R_8, 15 m downwind of the roofcenter, on the other hand the Sb/SF_6 ratio was systematically higher than in the other points. At this short distance, the dispersed plumes from the two Sb sources (convertor and furnace) were not yet well homogenized, resulting in a higher Sb/SF_6 ratio in the plume of the refinery furnace than in the plume of the convertor, where the SF_6 emission was performed. At larger distance the plumes of the two installations seem to be well mixed since the Sb/SF_6 remains from place to place constant between acceptable limits. The considerable aerodynamic turbulence in the wake at the leeside of the building, is responsible for this good result.

The calculated Sb emission for the consecutive sampling periods is compatible with the emission causing activities on the plant apparatus, except that the emission during period 4 is lower than expected in comparison with the three former periods.

The sampling points W_1 to W_3 and the hood of the ventilator, and consequently also point W_0, are placed above the convertor. Visual observation of the emission plumes of the convertor and of the refinery furnace indicates that emission results obtained by these points can in a first approximation be equalized to the emission from the convertor and that the contribution of the refinery furnace to the measurements in those points is neglectible.

With the measurements inside the workplace - respectively in the rooftop (W_1 to W_3) and in the exhaust tube (W_0) - two different methods to calculate the emissions can be used. With the first method the global pollutant emission is obtained, with the second it is possible to determine what fraction goes through the hood, respectively the roof.

a. By using the total SF_6 emission in equation (1) and the SF_6 and Sb concentration respectively in the points W_0, W_1, W_2 and W_3, the total Sb-emission from the convertor is obtained. Averaged over the four sampling periods, the emission results obtained by the points W_0 to W_3 are respectively 1,8 - 1,4 - 1,4 and 0,9 kg Sb/h (table I) and averaged over the four points : 1,38 ± 0,37 kg/h or 1,38 kg/h ± 27 %. If SF_6 and Sb were well homogenized in the plume above the convertor the four results should be the same.
   Considering the relatively long sampling time (4x30'), the 27 % relative standard deviation on the emission calculation indicates that the homogenization of Sb and SF_6 right above the convertor is not completely attained.

b. The measurement of the flow rate in the exhaust tube enables to calculate the mass flow of SF_6 and Sb through the hood and the ventilator (Q^H).
Subtraction from the total SF_6 emission $(Q^T_{SF_6})$ gives the SF_6 emission through the roof $(Q^R_{SF_6})$ by draft ventilation. Substitution of this value in equation (1) gives the Sb emission through the roof (Q^R_{Sb}) instead of the total Sb emission, this of course with the condition of sufficient homogenization of tracer and pollutant. The results of this exercise are summarized in table II.

TABLE II : Sb and SF_6 emission through the ventilator and the roof of the workplace

sampling period	emission in kg/h		
	$Q^H_{SF_6}$ (1)	$Q^R_{SF_6}$ (2)	Q^H_{Sb} (1)
1	0.24	1.48	0.34
2	0.39	1.18	0.32
3	0.41	1.20	0.68
4	0.39	1.23	0.17
average	0.36	1.27	0.38

sampling place	emission in kg/h Q^R_{Sb} (3)
W_1	1.08
W_2	1.07
W_3	0.70
average	0.95

(1) through the volume flow rate measurment in the exhaust tube

(2) $Q^R_{SF_6} = Q^T_{SF_6} - Q^H_{SF_6}$

(3) $Q^R_{Sb} = Q^R_{SF_6} \cdot \left(\frac{\chi_{Sb}}{\chi_{SF_6}}\right)_R$

The sum of the Sb-emission through the roof and through the ventilator should be the same as the total Sb emission from the convertor determined by the previous procedure (sub a). Averaged over the four sampling periods this gives :

$$Q^T_{Sb} = Q^R_{Sb} + Q^H_{Sb} = 0.95 + 0.38 = 1.3 \text{ kg Sb/h}$$

which is only a few procents less than the 1.4 kg/Sb found by the other procedure (table I).
It can easely been shown mathematically that both results should be identical with complete mixing of tracer and pollutant, i.e. when

$$\left(\frac{\chi_{Sb}}{\chi_{SF_6}}\right)_R \equiv \left(\frac{\chi_{Sb}}{\chi_{SF_6}}\right)_H$$

The total Sb emission averaged over the four sampling periods, is slightly higher when determined through places outside the building (Q_{Sb} = 1.6 kg/h) than through the sampling points in the roof and the ventilator (Q_{Sb} = 1.4 kg/h). This was to be expected since the places outside are influenced by the emissions of the complete building while the points inside were focussed on the emissions of the convertor only. Moreover measurements outside can be positively interfered by the background caused by other parts of the factory. Measurements of the Sb concentration upwind the building showed that this was a minor problem.

5. Conclusions and epiloge

Fugitive emissions can be quantified by the method of tracer release and measuring the tracer to pollutant ratio in the dispersed plume. The critical factor of the method is the homogenization of the tracer with the pollutant. This can be optimized by proper adjustment of the tracer emission device, the sampling time and the selection of the sampling places.
With concentration measurements a few tens or hundreds meter away from the source, in the example of the paper this is outside the building, the tracer to pollutant concentration ratio remains constant from place to place within acceptable limits. The total pollutant emission from the building can be determined.
With concentration measurements close to the source, for example in the rooftop and the ventilation of a workplace, sufficient homogeneity is more difficult to obtain. Nevertheless can the emission be determined with reasonable precision, even in presence of another source close to the main source. The efficiency of an exhaust hood can be evaluated.
Within the sampling time, the emission of the pollutant can fluctuate. If during this time the tracer emission and the dispersion conditions remain constant, the time averaged pollutant emission can nevertheless be determined.

The procedure has been used to determine emission factors for fugitive emissions. These data have subsequently been used for the mathematical modelling of the Sb concentration in the environment around the plant (2,3,4). The procedure has also been used to determine the fugitive emissions of a metal refinery installation before and after construction of a system for reduction of the fugitive emission. With this information the reduction of the pollution level in the environment, due to this investment, has been estimated using a bi-gaussian disperion model.

This research was carried out in the "National R & D Programma, Leefmilieu-Lucht" of the DPWB (Ministery of Science Policy).

References

(1) "Wanted : fugitive emissions"
S. Budiansky. Environmental Science and Technology V14, N8 (1980) 904-905.

(2) "Luchtverontreiniging door een metallurgisch bedrijf". Eindrapport Nationaal R-D Programma Leefmilieu-Lucht
Diensten voor de Programmatie van het Wetenschapsbeleid, Brussel, 1981.

(3) "Influence of the meteorological input data on the comparison between calculated and measured aerosol ground level concentrations and depositions"
I. Mertens, J. Kretzschmar and B. Vanderborght
Proceedings of the "12th ITM on air pollution modelling and its application"
NATO/CCMS Palo Alto August 1981

(4) "Depositie rondom een non ferro bedrijf"
B. Vanderborght, I. Mertens, J. Kretzschmar
Extern N4 (1981) in press

AN ATMOSPHERIC TRACER INVESTIGATION OF FUGITIVE EMISSIONS TRANSPORT IN THE COLORADO OIL SHALE REGION

George A. Sehmel

Pacific Northwest Laboratory
Richland, Washington 99352

The work described in this paper was not funded by the U.S. Environmental Protection Agency. The contents do not necessarily reflect the views of the Agency and no official endorsement should be inferred.

This paper is based on work performed under the U.S. Department of Energy Contract DE-AC06-76RLO 1830. This work was done at the Pacific Northwest Laboratory (PNL), operated for the Department of Energy by Battelle Memorial Institute.

ABSTRACT

It is anticipated that spent shale disposal areas could become prime fugitive emissions sources. Atmospheric tracer experiments were conducted to investigate transport and dispersion of fugitive emissions in the complex terrain near a proposed spent shale disposal area. The atmospheric tracer gas SF_6 was released from the Federal oil shale lease Tract C-a in Colorado in July 1981. The SF_6 tracer gas release rate was 26 kg/hr at a tracer release height of 1.7 m.

Airborne SF_6 tracer gas concentrations were sampled at 32 radio-controlled bag-sampling stations (at 15-min sampling times) and along roads with syringe grab-samplers. Sampling sites were 0.6 to 13 km from the tracer-gas release site.

There were four experimental time periods for releasing and sampling tracer gas: two evening and two morning time periods. Results include information on the following: a time-history of pollutant concentration changes upwind and in gulches before, during, and after sunrise; identification of major transport flow paths in the evening and morning; and the behavior of pollutant mixing and channeling in valleys and downwind of valley confluences.

INTRODUCTION

Spatial variations in the airborne transport of pollutant plumes from fugitive emissions from the developing shale oil industry are complex for multiple local flows in the oil shale regions of Piceance Creek Basin of northwestern Colorado. Significant local spatial variations in pollutant plume transport are expected because of the complex terrain. For instance, overall drainage flows affecting downwind airborne pollutant plume concentrations are a combination of multiplicity of drainage flows from gully tributary systems. Each tributary has a drainage plume which may rapidly lose its plume identity when mixing with other drainage flow plumes. The mixing rates of these plumes cannot be adequately predicted. When the tributary is large, i.e., a gulch, cross-gulch mixing of the two converging plume flows may be slow. For instance, as was shown by Sehmel (1981) for August 1980, cross-gulch mixing was usually incomplete at the confluence of the tracer plume from Corral Gulch and the ambient air plume from Box Elder Gulch. A mixing distance was defined, for nocturnal drainage flow, as the distance downwind of the confluence for which the two plumes were uniformly mixed across the gulch. The mixing distance is also compared to gulch widths upwind of the confluence of the two gulches. For the site and times investigated, the mixing distance was from 7 to 20 times the gulch widths, 0.3 and 0.1 km widths upstream from the confluence of the two gulches.

In order to investigate downwind pollutant plume transport from potential fugitive emissions, atmospheric transport investigations were conducted with tracers (Clements et al. 1981, Sehmel 1981, and Whiteman et al. 1981)

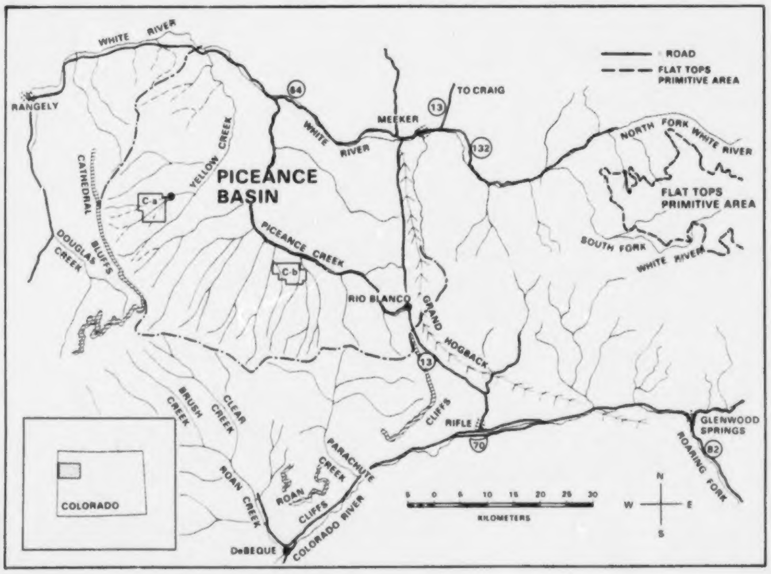
ROAD
FLAT TOPS PRIMITIVE AREA
WHITE RIVER
RANGELY
64
TO CRAIG
13
MEEKER
132
WHITE RIVER
NORTH FORK WHITE RIVER
CATHEDRAL
YELLOW CREEK
PICEANCE BASIN
C-a
FLAT TOPS PRIMITIVE AREA
DOUGLAS CREEK
BLUFFS
PICEANCE CREEK
C-b
SOUTH FORK
WHITE RIVER
RIO BLANCO
GRAND HOGBACK
13
BRUSH CREEK
CLEAR CREEK
CLIFFS
RIFLE
70
GLENWOOD SPRINGS
82
ROARING FORK
PARACHUTE CREEK
ROAN CREEK
ROAN CLIFFS
COLORADO RIVER
COLORADO
5 0 5 10 15 20 25 30
KILOMETERS
N
W
E
S
DeBEQUE

FIGURE 1. Map Showing Tract C-a Location in Piceance Basin

in an area in an adjacent to Federal Lease Tract C-a in Colorado. The site is shown on the map in Figure 1. The site is in the Piceance Creek basin, ~32 km southeast of Rangely, Colorado. Tract C-a is along Corral Gulch which drains into Yellow Creek, a tributary of White River. Previously, both non-depositing SF_6 tracer gas and depositing tracer particles were released from the bottom of the Corral Gulch in August 1980 experiments (Sehmel 1981).

Air pollution control regulations are based partially upon 3-hr maximum concentrations, 24-hr concentrations, and annual average concentrations. In contrast, gas-bag sampling time periods were usually 15 min in this investigation. This short time period, compared to longer time periods for compliance with some air pollution regulations, was selected to investigate the physics of air pollution transport. The rationale for using the 15-min time period was that estimates of air pollution concentrations can be made for longer time periods by integrating tracer concentration data as a function of time, possibly a time period representative of a 3-hr air pollution regulation. In contrast, transport and dispersion information is lost if time-averaged tracer-gas concentrations are experimentally determined only for the longer time periods specified in regulations for maximum air pollution concentrations.

Even shorter sampling durations are important for investigating physics required to develop either site-specific or more generic airborne pollutant transport and air pollution budget models in complex terrain. The sampling time requirement will be dependent upon the multiplicity and complexity of pollutant plume flows and the required evaluated accuracy of predictive models for different distance scales. In this investigation, more spatial and temporal details in identifying major and secondary plume transport flows and interactions were obtained from syringe samples collected nearly instantaneously. An advantage of using syringe samplers was a dense sampling grid at low cost. A disadvantage was that syringe samples were collected in a time sequence, rather than simultaneously throughout the sampling grid. Nevertheless, concentrations investigated with syringe samplers were essential for interpretation of concentrations investigated with the widely spaced time-integrated gas-bag sampling sites and for identifying multiple plume flows and interactions, both drainage and upslope flows.

The objective of the July 1981 experiments reported here were to simulate pollutant transport and dispersion from a proposed spent-shale disposal site during both day and night time conditions. The tracer simulant was SF_6 gas, a non-depositing and non-reactive gas. The July 1981 SF_6 tracer-gas experiments were conducted with the tracer release site at the proposed spent shale disposal site on terrain just north of Corral Gulch. The terrain was a sloping, undulating area between the hilltops along Corral Gulch and Dead Horse Ridge.

EXPERIMENTAL PROCEDURES

Airborne tracer concentrations were investigated using one tracer release site and multiple airborne concentration sampling sites. Details follow which describe tracer release, site locations, gas-bag sampling, syringe sampling, tracer analysis and meteorological data.

Tracer release times ranged from 3 to 9 hours. There were four experimental time periods: two evening and two morning periods. During the evening time periods, tracer release rates were constant from 1500 to 2100 MDT (July 15) and 1800 to 2100 MDT (July 17). During the morning time periods, tracer release rates were constant from 0330 to 0930 (July 19) and 0300 to 1217 MDT (July 21).

Tracer release times included airflow transition times around sunset and sunrise. The evening experiments were conducted first. The results for evening experiments were less successful than those for morning releases. On the first night, the radio control system malfunctioned for automatically collecting gas-bag samples as a function of selected time periods at remote sites. A power lead in the battery supply shorted. On the second night the system was operational, but the experiment was stopped early due to potential safety hazards from lightning in a severe local storm.

Tracer Release

During each experiment, the SF_6 tracer gas was released at a constant rate of 26 kg/hr at a height of 1.7 m. The tracer gas release rate was controlled with rotameters. The reported release rate was calculated from pre- and post-weighting tracer release cylinders. The SF_6 was released through a 1.0 cm inside-diameter tube.

The SF_6 was released from the gas phase in storage cylinders. Buoyance effects on the airborne tracer plume were minimized because tracer-gas cooling is minimized during this release procedure, as compared to the greater cooling during tracer release and SF_6 plume subsidence that occurs if SF_6 is released from the liquid phase in storage tanks.

Site Locations

Tracer release and downwind sampling locations are shown on the map in Figure 2. Important locations are the tracer release site, the tracer-gas sampling sites and the meteorological measurement sites.

Airborne tracer-gas concentrations were investigated by examining gas samples collected in either gas bags or syringes. Gas-bag sampling stations were placed in four radio-controlled signal zones for controlling gas sampling pumps. The zones were chosen to selectively sample major plume flow directions. Sampling pumps in each zone were controlled with tone-specific radio-receivers placed in each zone.

Locations of gas-bag sampling stations 1 through 32 are shown by numbered locations in Figure 2. These thirty-two radio-controlled sampling stations encompassed the release site. Distances from the tracer release site to these sampling stations range from 0.6 to 6 km. Sampling stations were located at sites with road access.

The principal gas-bag sampling zones were zones 2 and 3, which encompass regions of drainage flow from the tracer release site. Air pollution concentrations for upslope flows were also of interest. Consequently, gas-bag sampling stations in all four zones were simultaneously activated (or deactivated) for selected gas-bag sampling time periods.

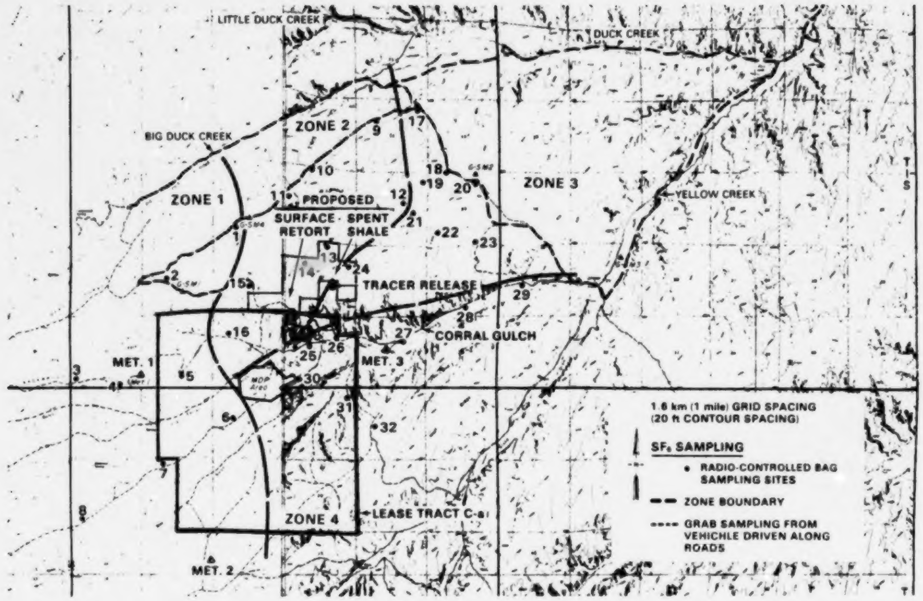
LITTLE DUCK CREEK
DUCK CREEK
BIG DUCK CREEK
ZONE 2
ZONE 1
ZONE 3
ZONE 4
YELLOW CREEK
PROPOSED
SURFACE · SPENT
RETORT SHALE
TRACER RELEASE
CORRAL GULCH
MET. 1
MET. 2
MET. 3
LEASE TRACT C-a
1.6 km (1 mile) GRID SPACING
(20 ft CONTOUR SPACING)
SF₆ SAMPLING
RADIO-CONTROLLED BAG SAMPLING SITES
ZONE BOUNDARY
GRAB SAMPLING FROM VEHICHLE DRIVEN ALONG ROADS

FIGURE 2. Topographic Map Showing Locations of the Tracer Release Site, Sampling Sites 1 thru 32 in Four Radio-Controlled Gas Bag Sampling Zones and Roads Driven During Collection of Grab Samples

Gas-Bag Sampling

Five electrical-control outlets at each gas-bag sampling station were used for activating (or deactivating) air pumps for filling gas sample bags. These 5 L, double-walled, sample bags* were prepared by encasing each sample bag with an outer polyethylene bag as a diffusion barrier to prevent contamination from SF_6 in both ambient and adjacent sample bags. An air pump, or pumps, was attached to each electrical-control outlet, which was activated (or deactivated) by a specific radio-signal tone. The pump sampling times and non-operating times were controlled by operation of a tone-signal radio-repeater, which was in a line-of-sight of antenna for each sampling station.

Each gas-bag sampling station had the following components. An antenna was attached to a bamboo pole, 5.2 m in height, which was taped to a steel fence post. The antenna was attached to a battery-powered radio-signal decoder. The decoder was a radio receiver that responded to one of the four transmitted tone signals. Each tone signal activated (or deactivated) sampling pumps in only one sampling zone; the zones shown in Figure 2. Electrical wires extended upward from the five electrical-control outlets on the decoder. For most gas-bag sampling stations, each electrical-control outlet was attached to only one sampling pump. In this case, sampling tube inlets for all five pumps were located at a sampling height of 1.5 m. In other cases, ten gas-sampling pumps were located at each gas-bag sampling station.

---

* Industry bag, 10 by 15 in., 2.5 mil, flow meter fully inserted, no tubes. B Bar B, Suite 34, 121 West Whittier Blvd. Lahabra, CA 90631.

Two sampling pumps were simultaneously operated at these stations by connecting each pump-signal outlet to two air sampling pumps. Sampling tube inlets were located at heights of 0.3 and 5 m, respectively. Sample outlet tubes from the sampling pumps extended into a double garbage bag within which were five gas sampling bags. One dark garbage bag was inserted into another dark garbage bag to reduce light transmission into gas sampling bags as well as to physically protect the bags.

Syringe Sampling

Relative locations of syringe-sampling sites are shown by dashed lines in Figure 2. The 50 cm^3 syringe* samples were collected at distances of 3 to 13 km from the tracer release site. Most syringe samples were collected along the sides of a triangle formed by roads along Duck Creek, Yellow Creek, and the road adjacent to gas-bag sampling stations 17, 18 and 20, hereafter called road 18. Syringe samples were rapidly collected by driving along roads, stopping, flushing a new syringe with ambient air by reaching out through the driver's window, collecting a syringe sample, stoppering the syringe inlet, marking the time and odometer reading on the syringe, and immediatey driving to the next sampling location.

Tracer Analysis

Collected gas-bag and syringe samples were analyzed in a field laboratory for SF_6 tracer gas concentrations. The laboratory was in the area labeled MDP in Figure 2. This laboratory was always outside the plume of high SF_6 concentration. Neverthless to further minimize the possibility of sample contamination, all samples were analyzed for SF_6 concentrations before tracer was released for the subsequent experiment.

The SF_6 concentrations were determined with an electron-capture gas chromatograph** (GC). The GC was field-calibrated with SF_6 calibration gas contained in cylinders at concentrations from 20 to 2000 pptv (parts per trillion by volume/volume). However, concentrations in some samples were greater than the 2000 pptv upper limit for the calibration gas. In these cases, a gas sample was diluted by using a 50 cm^3 syringe. Dilutions were made by partially expelling high-concentration gas from a syringe and subsequently drawing ambient air into the syringe.

Meteorological Data

Meteorological data were recovered at the tracer release site and at sites labeled MET. 1, MET. 2, and MET. 3 in Figure 2. Data are for 15-min. averages. Meteorological data included wind speed, wind direction and vertical temperature gradients ($T_{60\ m} - T_{10\ m}$). Winds coming from the north are described as a 0° wind direction while winds coming from the west are described as a 270° wind direction. Meteorological data collected at the MET. 1 site included wind speed and direction for both 10- and 60-m heights.

---

* Single-use syringe, Plastipak, BD-5663, Becton-Dickinson, Rutherford, NJ 07070.

** Field-Portable Tracer Gas Monitor, Model 215UP, Systems, Science and Software, JaJolla, CA 92038.

However at other sites, only wind speed and direction were collected at one height. At the MET. 2 and MET. 3 sites, wind speed and direction were measured at 10 m. At the tracer release site, wind direction and speed were measured at 2.1 m.

RESULTS

Meteorological data and airborne SF_6 concentrations are summarized: one figure is used for each experiment. General features of these figures are described here. Subsequently, data for each figure (experiment) are discussed.

The order of presenting results for each experiment is the meteorological data, the SF_6 concentrations determined from radio-controlled gas-bag sampling stations, and SF_6 concentrations determined from syringe grab samples. Concentrations for SF_6 tracer are reported as pptv, i.e., 1 pptv equals 10^{-12} parts by volume. In the figures, airborne SF_6 concentrations are superimposed on topographic maps. Each map is for successive time periods for which radio-controlled gas-bag samples were collected or for which a series of syringe grab-samples were collected or for which a series of syringe grab-samples were collected. For both sample collection types, the time period is in the figure title. In addition, to indicate the collection sequence for syringe samples, selected sampling times are also printed adjacent to selected concentrations.

Sulfur hexafluoride concentrations are shown in different graphical representations. For gas-bag samples, concentrations are printed adjacent to each sampling station location (station locations are indicated by solid circles). In some cases upper and lower concentrations are printed adjacent to a solid circle. In these cases, the concentration represented by the upper printing is for the 15-m height while the lower printing is for the 0.3-m height. In most cases, however, only one concentration is printed adjacent to a solid circle. These concentrations are for a 1.5-m sampling height, i.e., near-respiration height.

Some SF_6 concentrations for gas-bag samples have special meanings. In these cases, either a zero or blank is printed adjacent to the solid circle. A zero indicates that a sample was analyzed, but the concentration was below a detection limit of 1 pptv. If no concentration is printed, this means no samples were collected because either an air pump malfunctioned or the sampling station was not operated.

Concentrations from syringe grab-samples are shown graphically. The graphical representations are oriented with the abscissa approximately parallel to roads used for collecting the respective syringe samples. In most cases, the roads (along Duck Creek, Yellow Creek, and road 18 adjacent to gas-bag sampling station 18) approximate the sides of a triangle formed by roads.

Concentrations shown are plotted at road-sampling locations projected onto the abscissa. Road locations include cross-creek valley sampling traverses for both main roads and two-wheel side trails. Main roads cross valleys at projected locations of about 2.6 and 10 km along Duck Creek and 2.5 and 6.5 km along Yellow Creek. Two-wheel side roads cross valleys at projected locations of about 2.5, 3.7, 5.5 and 7.2 km along Duck Creek and at 7.4 km along Yellow Creek.

Results, July 15

Meteorological data are shown as a function of time in Figure 3 for the first evening tracer experiment. Since the frequency of temperature inversions is relatively high, the occurrence of temperature inversions during each tracer experiment is noted; i.e., $T_{60\ m} - T_{10\ m}$ is positive at MET. 1. A temperature inversion began about 1900 MDT. Other important times noted are tracer release and tracer gas sampling periods. Tracer release was from 1500 to 2100 MDT.

At present, these data are included for completeness since airborne tracer concentration data reduction is incomplete. Analysis of the data collection record will need to be completed before the airborne tracer concentrations can be reported as a function of sampling time. Record analysis is required since this is the experiment in which an electrical short caused transmission of spurious control signals to the radio-controlled gas-bag sampling stations.

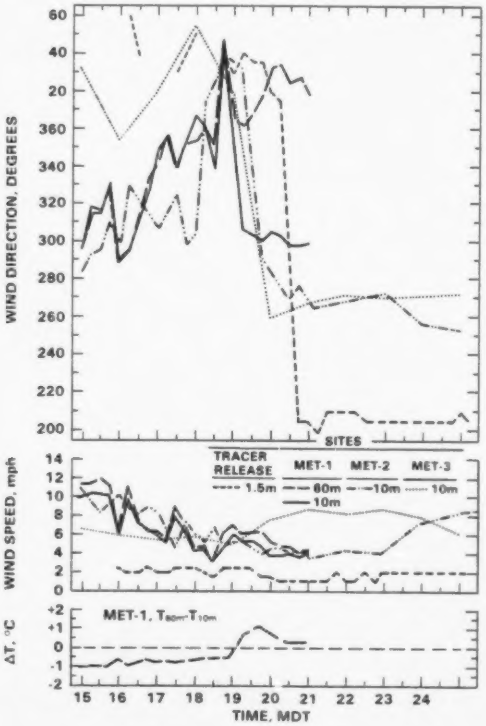

FIGURE 3. Wind Direction, Speed and Temperature Gradients on July 15, 1981

Results, July 17

Meteorological data are shown as a function of time in Figure 4a for the second evening tracer experiment. Temperature inversions below 60 m were intermittent and were only established at about 0945 and 2045 MDT. Other important times are tracer release and the three tracer gas sampling periods. Tracer release was from 1800 to 2100 MDT. Tracer release was stopped due to a local storm. There were three tracer sampling time periods: two gas-bag sampling periods from 1945 to 2000 and 2043 to 2053 MDT and one syringe sampling time period from 1946 to 2235 MDT.

It is significant to note the first gas-bag sampling period was conducted between 1945 and 2000 MDT. As shown in Figure 4a, this was a time period of rapid wind direction change with a variable wind direction at the tracer release site. Surface and upper wind directions were decoupled. Upslope winds at the tracer release site were decoupled from upper wind directions, even at 10 m. The 10- and 60-m wind directions at MET. 1, MET. 2, and MET. 3 were significantly different (about 330 to 0° at 2000 MDT) from the 2.1-m surface wind direction (30 to 165° at 2000 MDT) at the tracer release site.

Decoupled air flow directions are reflected in concentrations shown in Figures 4b and 4c for both gas-bag sampling periods. As shown in Figure 4b, tracer plume transport was to the northwest. Significant airborne tracer

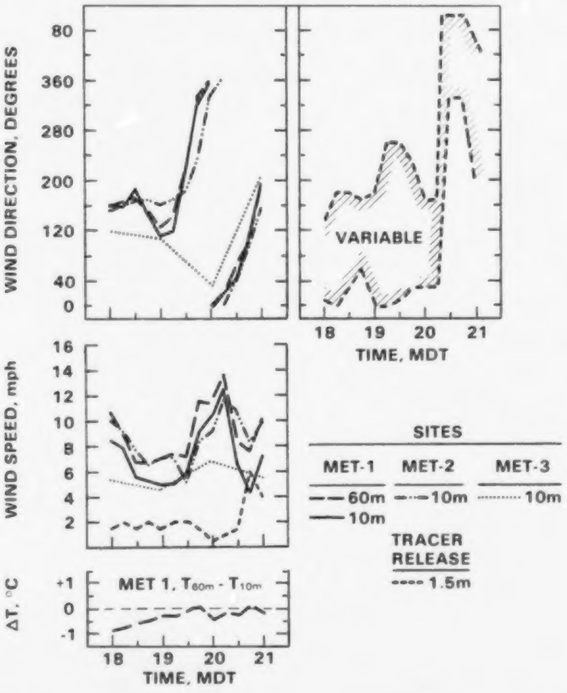

FIGURE 4a. Wind Direction, Speed and Temperature Gradients on July 17, 1981

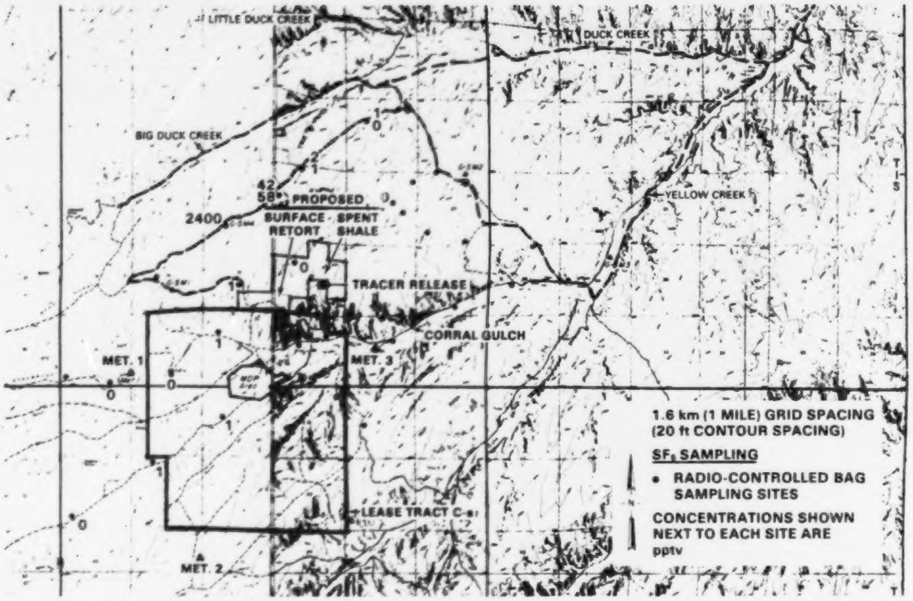
LITTLE DUCK CREEK
DUCK CREEK
BIG DUCK CREEK
YELLOW CREEK
T1S
2400
42
58
0
1
PROPOSED
SURFACE RETORT
SPENT SHALE
TRACER RELEASE
CORRAL GULCH
MET. 1
MET. 3
MET. 2
LEASE TRACT C-a
1.6 km (1 MILE) GRID SPACING
(20 ft CONTOUR SPACING)
SF6 SAMPLING
• RADIO-CONTROLLED BAG SAMPLING SITES
CONCENTRATIONS SHOWN NEXT TO EACH SITE ARE pptv

FIGURE 4b. Airborne Tracer Concentrations from 1945 to 2000 MDT, Collected at the Radio-Controlled Sampling Sites During the Evening of July 17, 1981

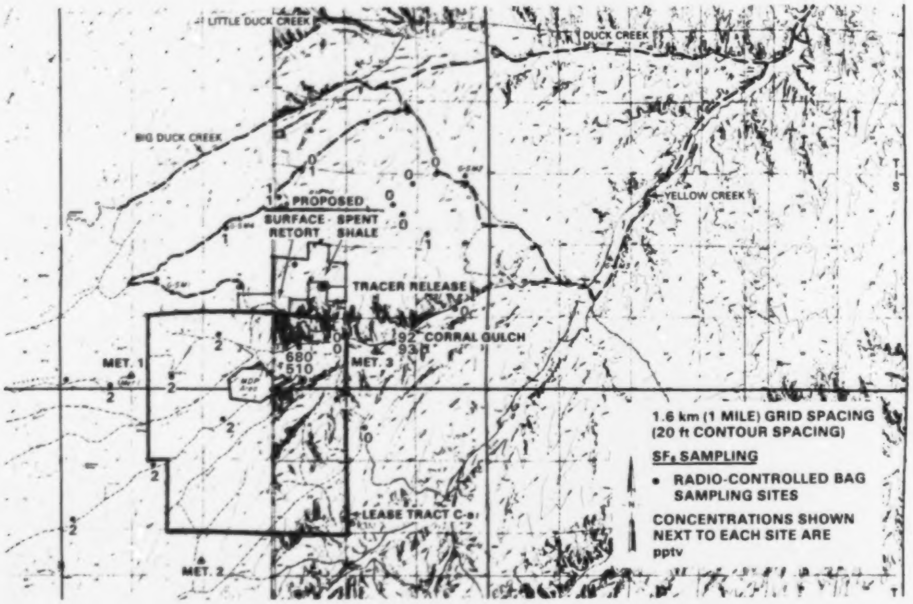
LITTLE DUCK CREEK
DUCK CREEK
BIG DUCK CREEK
YELLOW CREEK
T1S
0
1
2
680
510
192
93
PROPOSED
SURFACE RETORT
SPENT SHALE
TRACER RELEASE
CORRAL GULCH
MET. 1
MET. 3
MET. 2
LEASE TRACT C-a
1.6 km (1 MILE) GRID SPACING
(20 ft CONTOUR SPACING)
SF6 SAMPLING
• RADIO-CONTROLLED BAG SAMPLING SITES
CONCENTRATIONS SHOWN NEXT TO EACH SITE ARE pptv

FIGURE 4c. Airborne Tracer Concentrations from 2043 to 2053 MDT, Collected at the Radio-Controlled Sampling Sites During the Evening of July 17, 1981

concentrations were measured at gas-bag sampling sites 1, 11, and 10 (refer back to Figure 2 for site identification). The maximum concentration was 2400 pptv at site 1.

Indices of both horizontal and vertical diffusion were measured during this experiment. Since tracer concentrations at site 11 were 58 pptv at 0.3 m and 42 pptv at 5 m, concentrations decreased over one order of magnitude in the 1.3 km horizontal distance between site 1 (2400 pptv) and site 11 (58/2400 = 0.02). The tracer plume tended to remain adjacent to the ground during upslope flow. The concentration decrease with height at site 11 was 0.7; i.e., the ratio of 42 pptv at 5 m compared to 58 pptv at 0.3 m.

The direction of the maximum tracer concentration shifted and concentrations decreased in the subsequent sampling time period, from 2043 to 2053 MDT. The tracer plume flowed counter-clockwise from the tracer release site. Tracer concentrations were essentially constant at 2 pptv west of the MDP area.

For this time period, upslope plume flow from the tracer release site spilled into Corral Gulch. Vertical concentration profiles at sites 25 and 27 reflect plume spillage into Corral Gulch. A maximum concentration of 680 pptv was measured at site 25. In contrast to the previously discussed vertical concentration profile decrease for upslope flow at site 11, the relative concentration increase with height at site 25 was a factor of 1.3; i.e., the ratio of 680 pptv at 5 m compared to 510 pptv at 0.3 m. At this site, the tracer plume was overriding drainage flow in Corral Gulch. However at down-gulch site 27, vertical mixing was complete for the two heights investigated.

Plume flow inferences are made since the tracer-plume path was almost certainly between sampling sites 26 and 31. Concentrations were 0 pptv at site 26 and 1 pptv at site 31. Although the tracer plume rotated counter-clockwise, the main plume width was either relatively narrow (the 1.5 km between sites 26 and 31), or the main plume was elevated at sampling sites with 0 or 1 pptv concentrations.

Concentrations from the more spacially frequent syringe samples shown in Figure 4d confirm, in more detail, plume-location and plume-width results from gas-bag samples shown in Figure 4b. Syringe samples were collected along Ridge Road, which is adjacent to sampling sites 1 and 11. The main plume width was narrow; concentrations decreased over two orders of magnitude from the maximum along a plume width of about 0.7 km.

Concentrations from syringe samples reflect tracer plume segments extending across Ridge Road, especially between 4 and 7 km. These relatively high concentration plume segments were of short time duration since corresponding 15 min gas-bag sample concentrations were less, e.g., 1 and 2 pptv at site 10 in Figure 4b.

Tracer plume flow extended into the bottom of Big Duck Creek Valley, a valley immediately north of Ridge Road. Concentrations are shown in Figure 4d; data for a time period between 2145 and 2235 MDT. Samples were collected during heavy rain after tracer release was stopped at 2100 MDT.

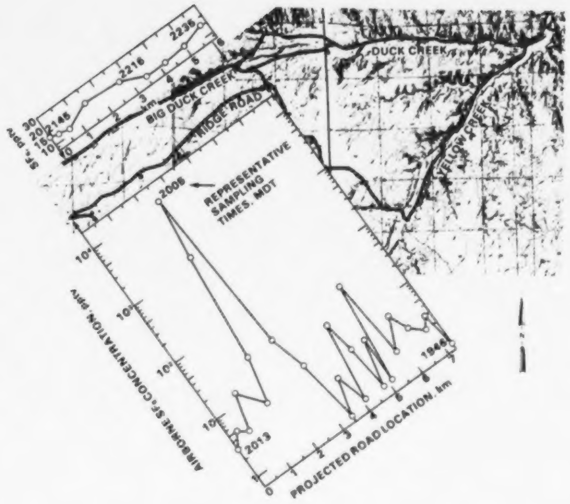
DUCK CREEK
BIG DUCK CREEK
RIDGE ROAD
YELLOW CREEK
REPRESENTATIVE SAMPLING TIMES, MDT
2145
2216
2235
2006
2013
1946
AIRBORNE SF6 CONCENTRATION, ppt
PROJECTED ROAD LOCATION, km

FIGURE 4d. Airborne SF_6 Concentrations Along Roads for Sampling Times from 1946 to 2235 MDT on July 17, 1981

Results, July 19

Meteorological data are shown as a function of time in Figure 5a for the first morning tracer experiment. Establishment of a temperature inversion is unknown since the 60-m height wind and temperature instruments at MET. 1 were not operated. Important times are tracer release and the tracer gas-sampling periods. Tracer release was from 0330 to 0930 MDT. There were seven tracer sampling time periods: five gas-bag sampling periods were 0533 to 0548, 0700 to 0715, 0745 to 0800, 0930 to 0845 and 0937 to 0952 MDT; and two syringe sampling time periods were 0537 to 0652 and 0704 to 0946 MDT.

Concentration data reflect little tracer-plume spread during drainage flows before sunrise, plume spread and dilution after sunrise, and subsequent plume lifting. A coherent plume is shown in Figure 5b with relatively high centerline concentrations, 2200 to 2300 pptv, along sampling sites 18, 19 and 20. As shown in Figure 5c between 0700 to 0715 MDT (an hour after sunrise at 0615 MDT, sunrise was delayed by a cloud), plume spread is reflected in concentrations of 14 and 19 pptv at sampling site 10. Plume spread may reflect increased wind direction variability at the tracer release site. Even with increased plume spread, the concentration remained 2200 pptv at site 18. This high concentration was caused by interactions of a main drainage flow plume with drainage flow containing tracer. (More detailed evidence for plume interaction was obtained in the next experiment on July 21). Further plume spread and also plume lifting are shown 45 min later in Figure 5d. Concentrations at site 18 decreased an order of magnitude to 171 pptv.

Concentrations continued to reflect increased surface heating effects with increasing time. As shown in Figure 5e for 0830 to 0845 MDT, continued

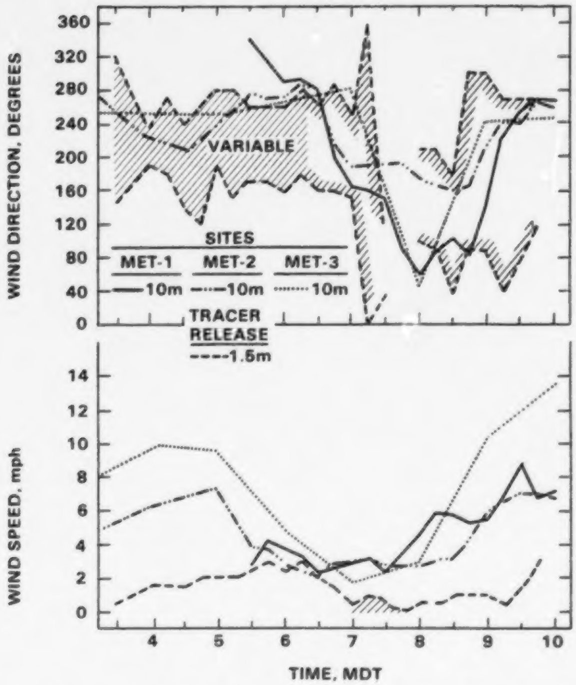

FIGURE 5a. Wind Direction and Speed on July 19, 1981

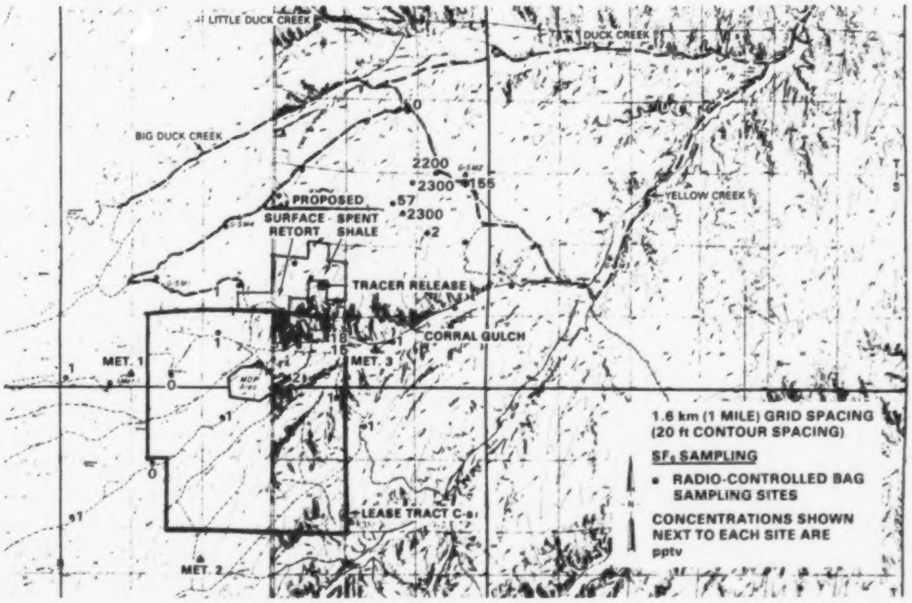
LITTLE DUCK CREEK
DUCK CREEK
BIG DUCK CREEK
YELLOW CREEK
0
2200
2300
155
57
2300
2
PROPOSED
SURFACE RETORT
SPENT SHALE
TRACER RELEASE
CORRAL GULCH
18
16
1
1
MET. 1
MET. 3
1
0
21
1
1
1
0
1
LEASE TRACT C-a
MET. 2
1.6 km (1 MILE) GRID SPACING
(20 ft CONTOUR SPACING)
SF₆ SAMPLING
• RADIO-CONTROLLED BAG SAMPLING SITES
CONCENTRATIONS SHOWN NEXT TO EACH SITE ARE pptv
N

FIGURE 5b. Airborne Tracer Concentrations from 0533 to 0548 MDT, Collected at the Radio-Controlled Sampling Sites During the Morning of July 19, 1981

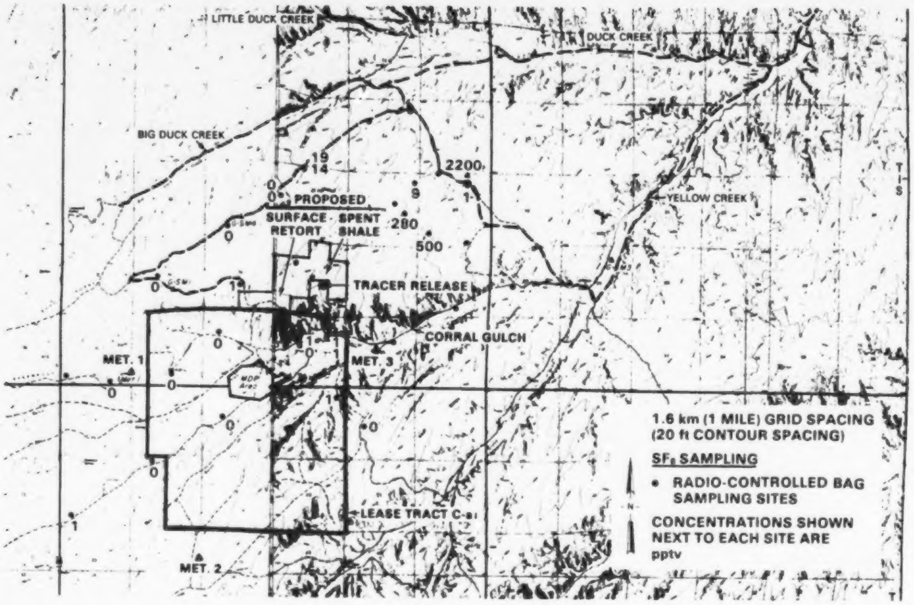
LITTLE DUCK CREEK
DUCK CREEK
BIG DUCK CREEK
19
14
2200
0
0
9
1
PROPOSED
SURFACE RETORT
SPENT SHALE
200
500
0
YELLOW CREEK
T
S
0
1
TRACER RELEASE
CORRAL GULCH
0
1
0
1
MET. 1
MET. 3
0
0
0
1
0
0
0
1.6 km (1 MILE) GRID SPACING
(20 ft CONTOUR SPACING)
SF6 SAMPLING
• RADIO-CONTROLLED BAG SAMPLING SITES
CONCENTRATIONS SHOWN NEXT TO EACH SITE ARE pptv
N
LEASE TRACT C-a
1
MET. 2
T

FIGURE 5c. Airborne Tracer Concentrations from 0700 to 0715 MDT, Collected at the Radio-Controlled Sampling Sites During the Morning of July 19, 1981

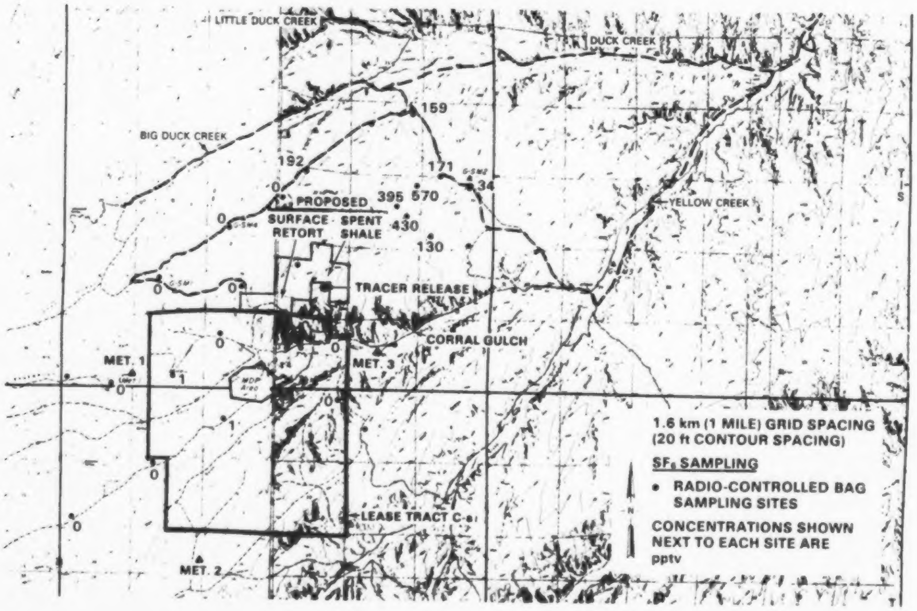
LITTLE DUCK CREEK
DUCK CREEK
BIG DUCK CREEK
159
192
171
34
0
395
570
PROPOSED
SURFACE RETORT
SPENT SHALE
430
130
0
YELLOW CREEK
T
S
0
0
TRACER RELEASE
CORRAL GULCH
0
0
MET. 1
MET. 3
1
0
0
1
0
0
1.6 km (1 MILE) GRID SPACING
(20 ft CONTOUR SPACING)
SF6 SAMPLING
• RADIO-CONTROLLED BAG SAMPLING SITES
CONCENTRATIONS SHOWN NEXT TO EACH SITE ARE pptv
N
LEASE TRACT C-a
0
MET. 2
T

FIGURE 5d. Airborne Tracer Concentrations from 0745 to 0800 MDT, Collected at the Radio-Controlled Sampling Sites During the Morning of July 19, 1981

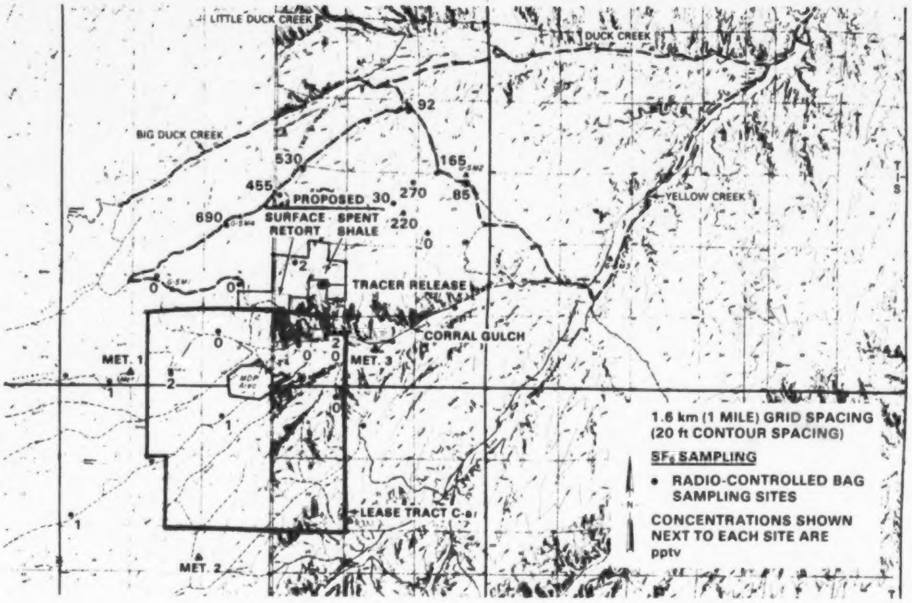
LITTLE DUCK CREEK
DUCK CREEK
BIG DUCK CREEK
YELLOW CREEK
92
530
165
455
PROPOSED
30
270
85
690
SURFACE RETORT
SPENT SHALE
220
0
2
TRACER RELEASE
CORRAL GULCH
MET. 1
MET. 2
MET. 3
LEASE TRACT C-a
1
2
1.6 km (1 MILE) GRID SPACING
(20 ft CONTOUR SPACING)
SF6 SAMPLING
● RADIO-CONTROLLED BAG SAMPLING SITES
CONCENTRATIONS SHOWN NEXT TO EACH SITE ARE pptv
N
T 1 S

FIGURE 5e. Airborne Tracer Concentrations from 0830 to 0845 MDT, Collected at the Radio-Controlled Sampling Sites During the Morning of July 19, 1981

plume spread included site 1. However by 0937 to 0952 MDT, plume lifting resulted in low-surface concentrations shown in Figure 5f.

Concentrations determined from syringe samples confirm that tracer-plume spread was limited during drainage flows before sunrise. As shown in Figure 5g near site 18, syringe-sample concentrations were similar to 15-min gas-bag concentrations shown in Figure 5b. The main-plume width was narrow; concentrations decreased over two orders of magnitude from the maximum along a plume width of about 1.2 km.

Except for concentrations along Ridge Road, syringe data reflect that the tracer plume flowed beyond the terrain investigated with gas-bag samplers. Syringe-sample concentration data in Figure 5g and 5h show the following:

- a time-history of pollutant concentration changes in gulches before, during and after sunrise
- identification of major drainage transport flow paths at greater distances than investigated with gas-bag sampling sites
- pollutant mixing at the confluence of two valleys.

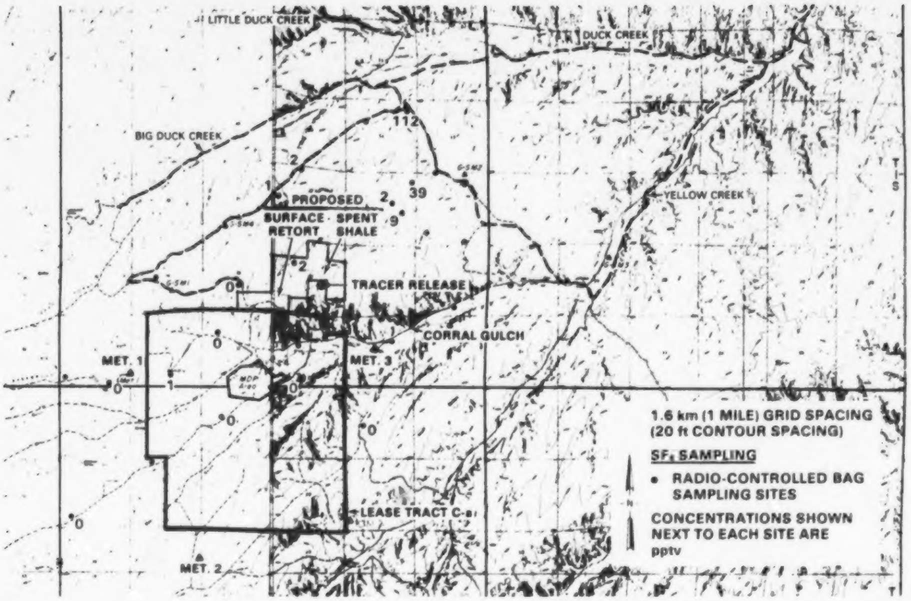
LITTLE DUCK CREEK
DUCK CREEK
BIG DUCK CREEK
112
2
39
1
2
9
PROPOSED
SURFACE · SPENT
RETORT SHALE
2
0
TRACER RELEASE
YELLOW CREEK
CORRAL GULCH
MET. 1
MET. 3
MET. 2
0
1
0
0
0
0
LEASE TRACT C-a
1.6 km (1 MILE) GRID SPACING
(20 ft CONTOUR SPACING)
SF_6 SAMPLING
• RADIO-CONTROLLED BAG SAMPLING SITES
CONCENTRATIONS SHOWN NEXT TO EACH SITE ARE pptv
N

FIGURE 5f. Airborne Tracer Concentrations from 0937 to 0952 MDT, Collected at the Radio-Controlled Sampling Sites During the Morning of July 19, 1981

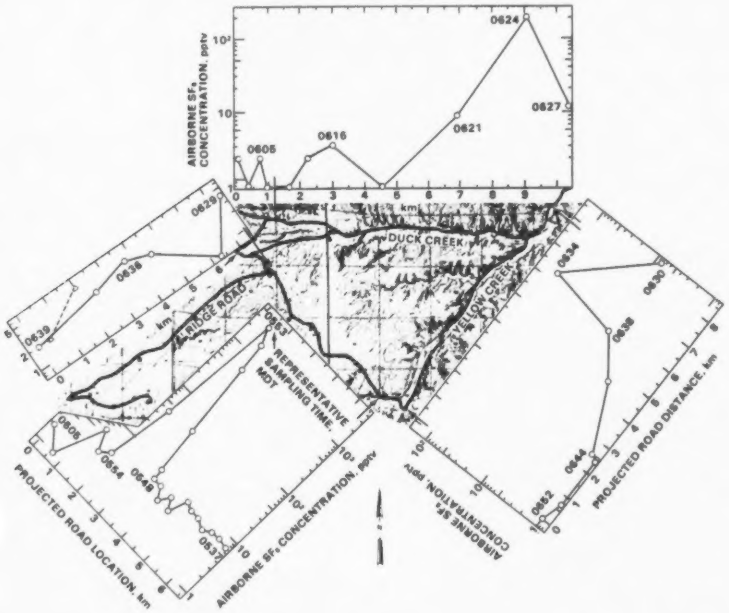

FIGURE 5g. Airborne SF_6 Concentrations Along Roads for Sampling Times from 0537 to 0652 MDT on July 19, 1981

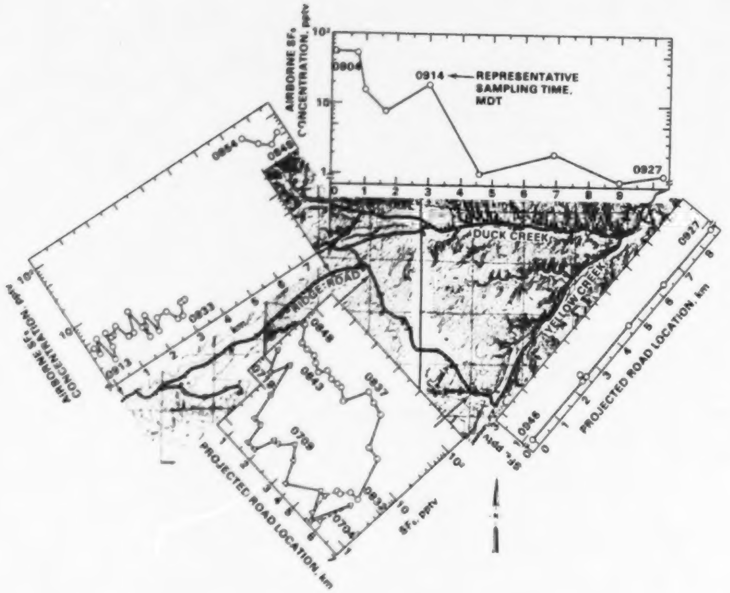
AIRBORNE SF₆ CONCENTRATION, pptv
0804
0914 ← REPRESENTATIVE SAMPLING TIME, MDT
0927
DUCK CREEK
YELLOW CREEK
RIDGE ROAD
0854
0848
0833
0913
0848
0843
0837
0716
0709
0832
0704
0946
PROJECTED ROAD LOCATION, km
SF₆, pptv

FIGURE 5h. Airborne SF_6 Concentrations Along Roads for Sampling Times from 0704 to 0946 MDT on July 19, 1981

In addition, Figure 5g shows that the effects of surface heating immediately after sunrise (0615 MDT) directed a surface plume flow towards Dead Horse Road. Upslope flow was present between 0629 and 0639 MDT; the tracer plume divided along Ridge Road into two identifiable plumes. The high concentration near site 17 at 0629 MDT continued to reflect the tracer following drainage flows. In contrast, concentrations near 3.5 km reflect surface upslope flow from surface heating. Surface wind velocities for upslope flows are significant since tracer was measurable (0639 MDT) even at the road junction between sites 1 and 2. Upslope flows also transported the tracer near to site 15; concentration is indicated by the dashed line.

Concentrations along Duck Creek also reflect plume splitting into major and secondary plumes. The major plume passed across the creek near 9 km while the secondary plume was near 3 km. The secondary plume followed a major tributary into Duck Creek. In contrast, the major plume passed over ridges along Duck Creek. The major plume was uniformly mixed across Duck Creek Valley at the confluence of Duck and Yellow Creeks.

Results, July 21

Meteorological data are shown as a function of time in Figure 6a for the second morning tracer experiment. A temperature inversion dissipated at about 0645 MDT. Important times are tracer release and the tracer gas-sampling periods. Tracer release was from 0300 to 1217 MDT. There were ten tracer sampling periods: seven gas-bag sampling periods from 0500 to 0515, 0700 to 0715, 0745 to 0800, 0830 to 0845, 0937 to 0952, 1100 to 1115; and

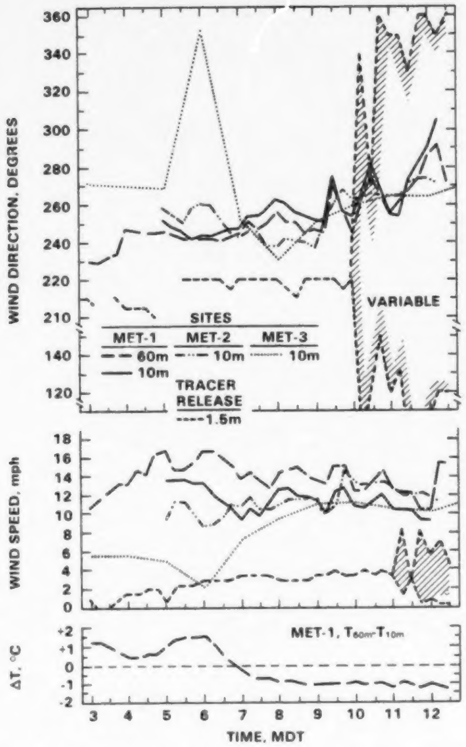

FIGURE 6a. Wind Direction, Speed and Temperature Gradients on July 21, 1981

1200 to 1215 MDT and three syringe sampling time periods from 0500 to 0647, 0548 to 0748, and 0800 to 0938 MDT.

Tracer-plume flow trends were similar to those during the first morning experiment. Concentration data reflect little tracer-plume spread during drainage flows before sunrise, plume spread and dilution after sunrise, and subsequent plume lifting. A coherent plume during 0500 to 0515 MDT is reflected in Figure 6b by large centerline concentrations, 1800 and 20800 pptv, along sampling sites 22 and 20, respectively. Since tracer concentration was an order of magnitude greater at downwind site 20, the tracer-plume axis passed either to the side or over site 20.

A scenario is suggested to explain relative concentrations at sites 19, 18, 20, and 22, concentrations of 130, 210, 20800, and 1800 pptv, respectively in Figure 6b. In the region of sites 19 and 18, there are two significant drainage plumes with concentrations reflecting partial mixing of these two drainage plumes. The smallest of the four listed concentrations, which is 130 pptv at site 19, reflects little mixing of the tracer drainage plume with the main drainage plume. The main drainage plume is directed from site 2 toward regions near site 19 by the deepest local gully, a distance for developing drainage flow depths which is almost twice as long as the distance from the tracer release site. Drainage flow from the tracer

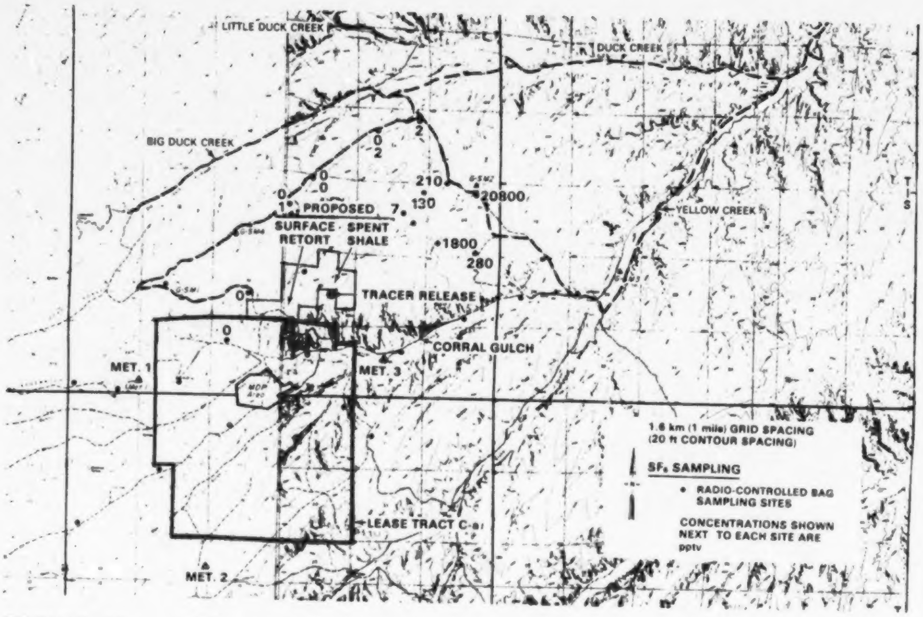
LITTLE DUCK CREEK
DUCK CREEK
BIG DUCK CREEK
0
2
2
0
0
0
1
PROPOSED
7
210
130
20800
SURFACE SPENT
RETORT SHALE
1800
280
YELLOW CREEK
0
TRACER RELEASE
0
CORRAL GULCH
MET. 1
MET. 3
1.6 km (1 mile) GRID SPACING
(20 ft CONTOUR SPACING)
SF₆ SAMPLING
• RADIO-CONTROLLED BAG SAMPLING SITES
CONCENTRATIONS SHOWN NEXT TO EACH SITE ARE pptv
LEASE TRACT C-a
MET. 2

FIGURE 6b. Airborne Tracer Concentrations from 0500 to 0515 MDT, Collected at the Radio-Controlled Sampling Sites During the Morning of July 21, 1981

release site may override the main drainage flow until the two plume mix near site 18, a concentration of 210 pptv. The main plume is deflected northward near site 22, a concentration of 1800 pptv, by drainage flow from the tracer release site. The "undiluted" tracer-plume axis passes near site 20, a concentration of 20800 pptv.

There is subsequent supporting evidence for this two-plume scenario from the succeeding gas-bag sampling period between 0700 and 0715 MDT (an hour after sunrise at 0605 MDT); see Figure 6c. The tracer plume axis was deflected and lifted by interaction with a main drainage flow of less relative strength than earlier because of surface heating. All concentrations were significantly reduced. Nevertheless, concentrations at downwind site 20 remained on an order of magnitude greater than at site 22; i.e., 2070 pptv compared to 235 pptv. Tracer plume spread to the north included sites 10, 9, and 17. The conclusions are that the "undiluted" tracer plume axis was near site 20 and plume interactions resulted in significant tracer concentrations at sites 10, 9, and 17.

Concentrations continued to reflect increased surface heating effects with increasing time. As shown in Figure 6d for 0745 to 0800 MDT and in Figure 6e for 0830 to 0845 MDT, plume spreading and interaction continued. Differential plume heating effects became important. The "major" drainage flow became relatively less significant because of valley side-wall heating. In contrast, the "secondary" drainage plume persisted from the tracer release site. This persistence directed tracer plume flow into the gully between sites 17 and 18. After drainage flows dissipated, plume

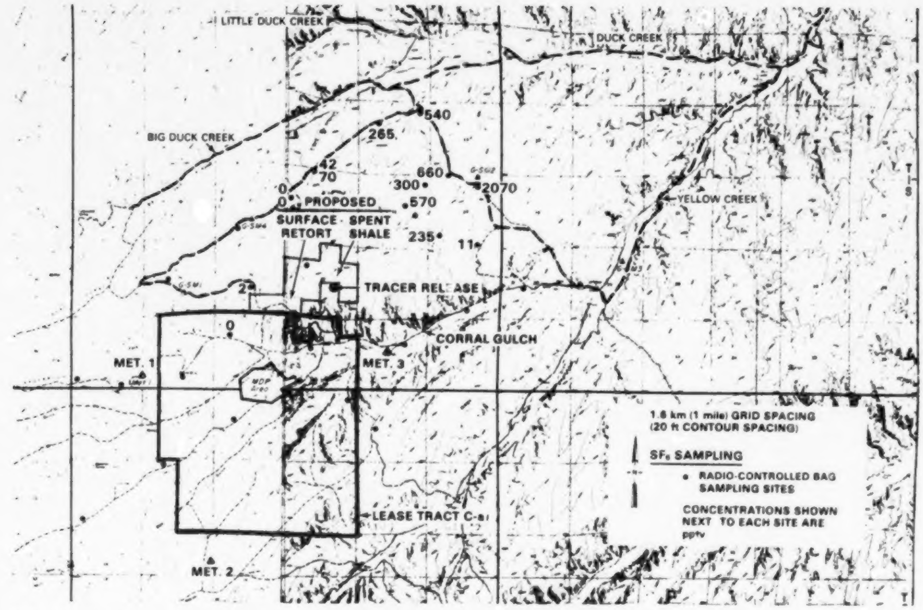
LITTLE DUCK CREEK
DUCK CREEK
BIG DUCK CREEK
540
265
42
70
0
0
660
300
2070
570
235
11
PROPOSED
SURFACE SPENT
RETORT SHALE
YELLOW CREEK
TRACER RELEASE
2
0
CORRAL GULCH
MET. 1
MET. 3
MET. 2
LEASE TRACT C-a
T 1 S
1.6 km (1 mile) GRID SPACING
(20 ft CONTOUR SPACING)
SF₆ SAMPLING
• RADIO-CONTROLLED BAG SAMPLING SITES
CONCENTRATIONS SHOWN NEXT TO EACH SITE ARE pptv

FIGURE 6c. Airborne Tracer Concentrations from 0700 to 0715 MDT, Collected at the Radio-Controlled Sampling Sites During the Morning of July 21, 1981

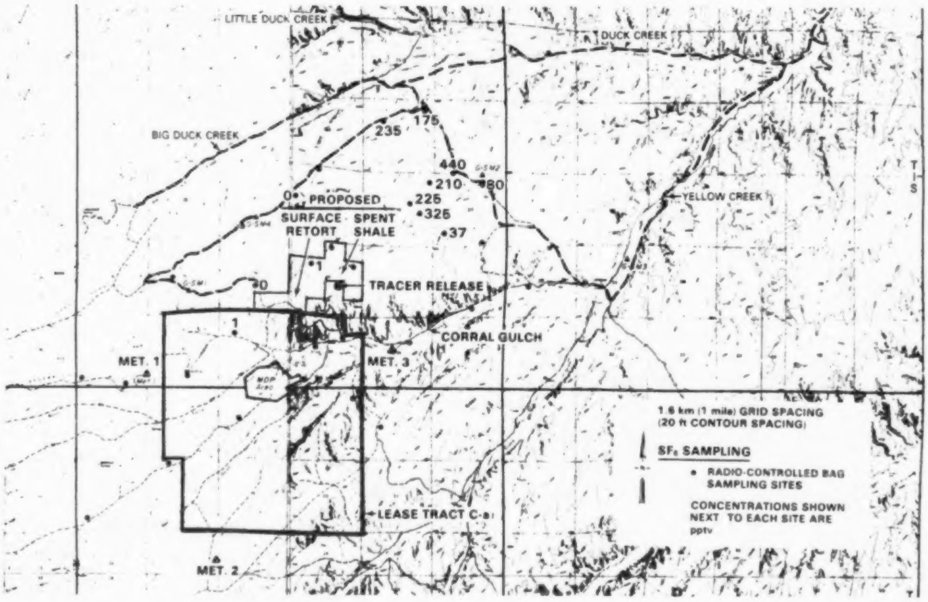
LITTLE DUCK CREEK
DUCK CREEK
BIG DUCK CREEK
175
235
440
210
80
0
225
325
37
PROPOSED
SURFACE SPENT
RETORT SHALE
YELLOW CREEK
1
0
TRACER RELEASE
1
CORRAL GULCH
MET. 1
MET. 3
MET. 2
LEASE TRACT C-a
T 1 S
1.6 km (1 mile) GRID SPACING
(20 ft CONTOUR SPACING)
SF₆ SAMPLING
• RADIO-CONTROLLED BAG SAMPLING SITES
CONCENTRATIONS SHOWN NEXT TO EACH SITE ARE pptv

FIGURE 6d. Airborne Tracer Concentrations from 0745 to 0800 MDT, Collected at the Radio-Controlled Sampling Sites During the Morning of July 21, 1981

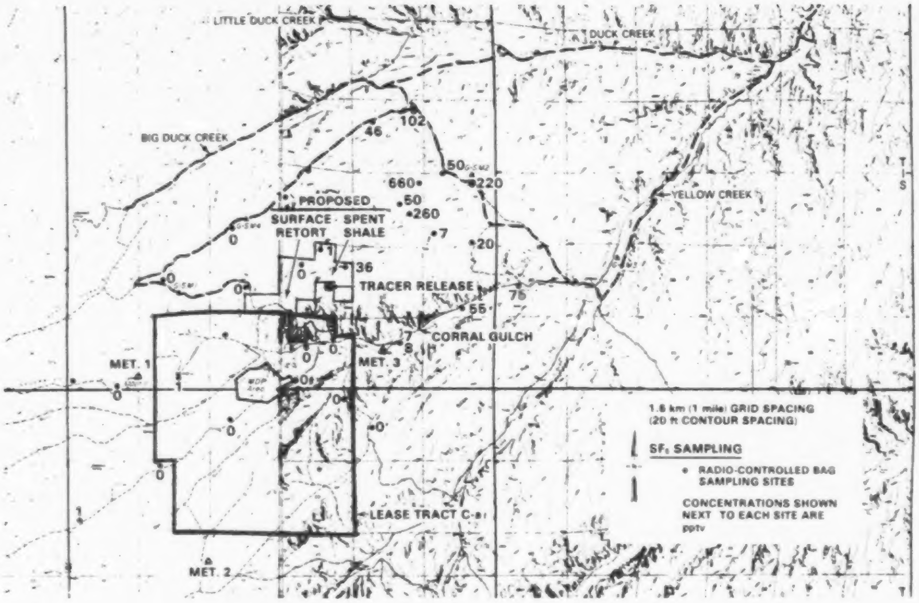
LITTLE DUCK CREEK
DUCK CREEK
BIG DUCK CREEK
YELLOW CREEK
T
S
46
102
50
660
50
260
220
7
20
1
PROPOSED
SURFACE RETORT
SPENT SHALE
0
36
TRACER RELEASE
75
55
CORRAL GULCH
7
8
MET. 1
MET. 3
MET. 2
LEASE TRACT C-a
1.6 km (1 mile) GRID SPACING
(20 ft CONTOUR SPACING)
SF₆ SAMPLING
• RADIO-CONTROLLED BAG SAMPLING SITES
CONCENTRATIONS SHOWN NEXT TO EACH SITE ARE pptv

FIGURE 6e. Airborne Tracer Concentrations from 0830 to 0845 MDT, Collected at the Radio-Controlled Sampling Sites During the Morning of July 21, 1981

lifting occurred. Plume lifting is shown by low concentrations in Figure 6f at times from 0937 to 0952 MDT.

Gas-bag samplers were subsequently collected in zone 1; see zone location in Figure 2 to further investigate pollutant transport during upslope flows. As shown in Figure 6b, downslope winds ceased at about 1000 MDT at the tracer release site, with subsequent variable wind directions. As a result of this variation, upslope surface winds transported the tracer westward towards sampling zone 1. Concentrations for two time periods are shown from 1100 to 1115 MDT in Figure 6g and from 1200 to 1215 MDT in Figure 6h. Concentrations above 1 pptv were not detected in zone 1.

Syringe samples were collected to investigate in detail tracer plume segmentation, effects of tracer plume flow through side tributaries along Yellow Creek, and cross-valley tracer plume flows into Duck Creek. The syringe-sample concentration data in Figures 6i through 6k show the following:

- a time-history of pollutant concentration changes in gulches before, during and after sunrise
- further identification of major drainage transport flow paths at distances greater than those investigated with gas-bag sampling sites
- cross-valley concentration profiles along Duck and Yellow Creeks

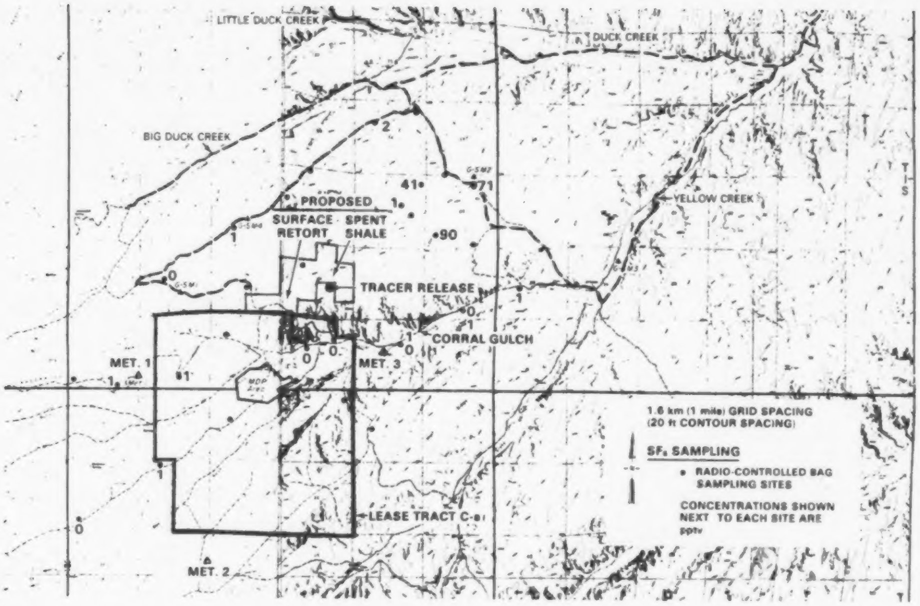
LITTLE DUCK CREEK
DUCK CREEK
BIG DUCK CREEK
YELLOW CREEK
T1S
PROPOSED
SURFACE RETORT
SPENT SHALE
TRACER RELEASE
CORRAL GULCH
MET. 1
MET. 2
MET. 3
LEASE TRACT C-a
2
41
1
71
90
1
0
0
1
0
1.6 km (1 mile) GRID SPACING
(20 ft CONTOUR SPACING)
SF6 SAMPLING
• RADIO-CONTROLLED BAG SAMPLING SITES
CONCENTRATIONS SHOWN NEXT TO EACH SITE ARE pptv

FIGURE 6f. Airborne Tracer Concentrations from 0937 to 0952 MDT, Collected at the Radio-Controlled Sampling Sites During the Morning of July 21, 1981

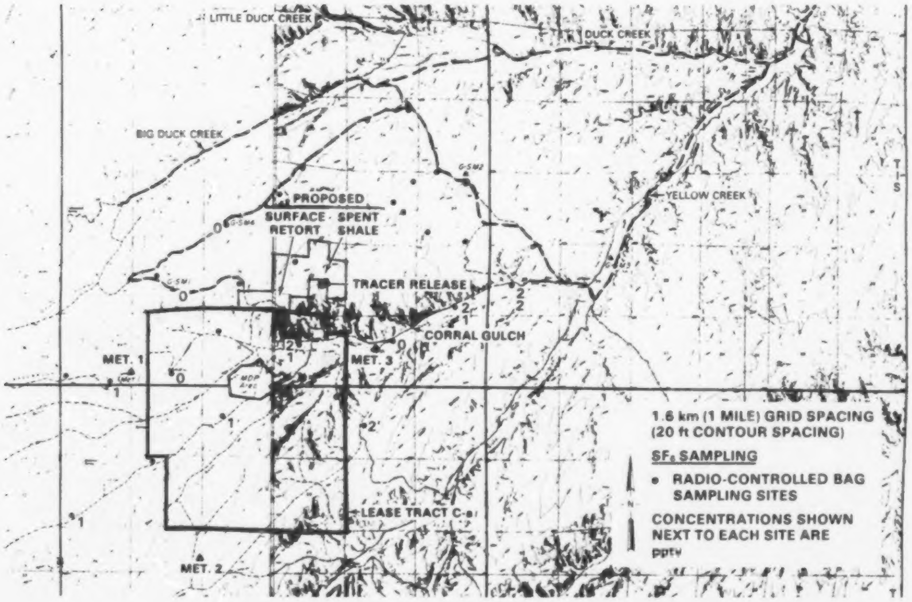
LITTLE DUCK CREEK
DUCK CREEK
BIG DUCK CREEK
YELLOW CREEK
T1S
PROPOSED
SURFACE RETORT
SPENT SHALE
TRACER RELEASE
CORRAL GULCH
MET. 1
MET. 2
MET. 3
LEASE TRACT C-a
0
2
2
2
1
2
0
1
1
2
1
1.6 km (1 MILE) GRID SPACING
(20 ft CONTOUR SPACING)
SF6 SAMPLING
• RADIO-CONTROLLED BAG SAMPLING SITES
CONCENTRATIONS SHOWN NEXT TO EACH SITE ARE pptv

FIGURE 6g. Airborne Tracer Concentrations from 1100 to 1115 MDT, Collected at the Radio-Controlled Sampling Sites During the Morning of July 21, 1981

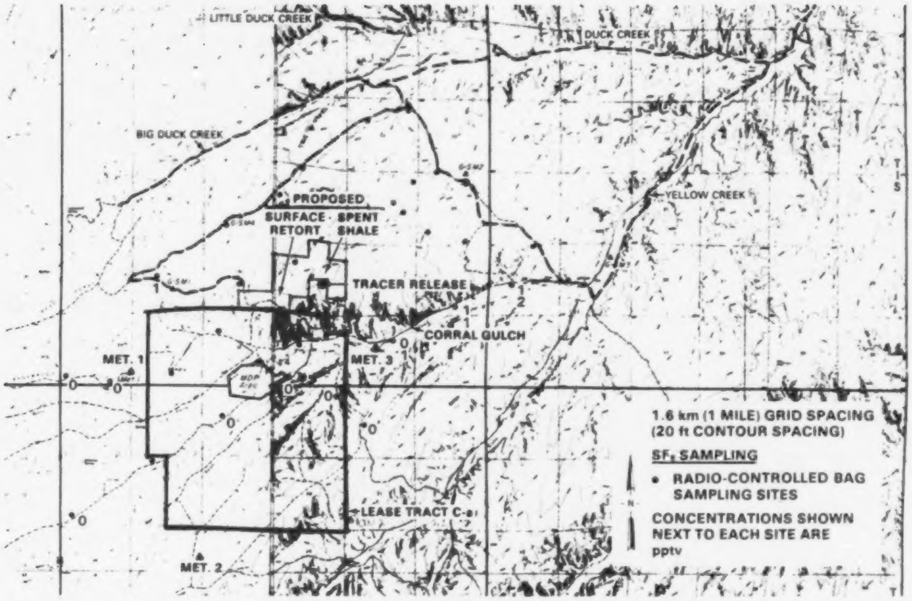
LITTLE DUCK CREEK
DUCK CREEK
BIG DUCK CREEK
PROPOSED
SURFACE RETORT
SPENT SHALE
YELLOW CREEK
TRACER RELEASE
CORRAL GULCH
MET. 1
MET. 3
MET. 2
LEASE TRACT C-a
1.6 km (1 MILE) GRID SPACING
(20 ft CONTOUR SPACING)
SF₆ SAMPLING
• RADIO-CONTROLLED BAG SAMPLING SITES
CONCENTRATIONS SHOWN NEXT TO EACH SITE ARE pptv
N

FIGURE 6h. Airborne Trace Concentrations from 1200 to 1215 MDT, Collected at the Radio-Controlled Sampling Sites During the Morning of July 21, 1981

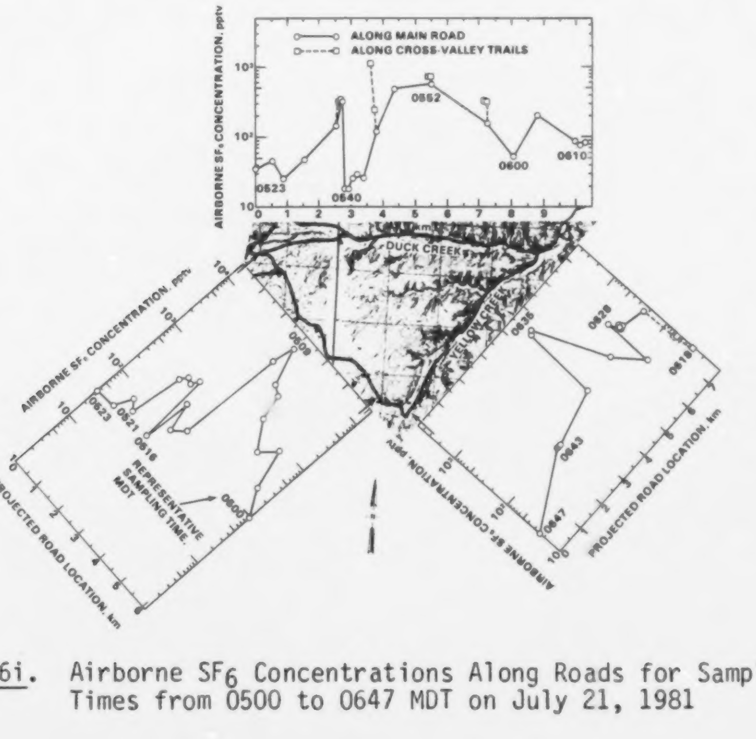

FIGURE 6i. Airborne SF_6 Concentrations Along Roads for Sampling Times from 0500 to 0647 MDT on July 21, 1981

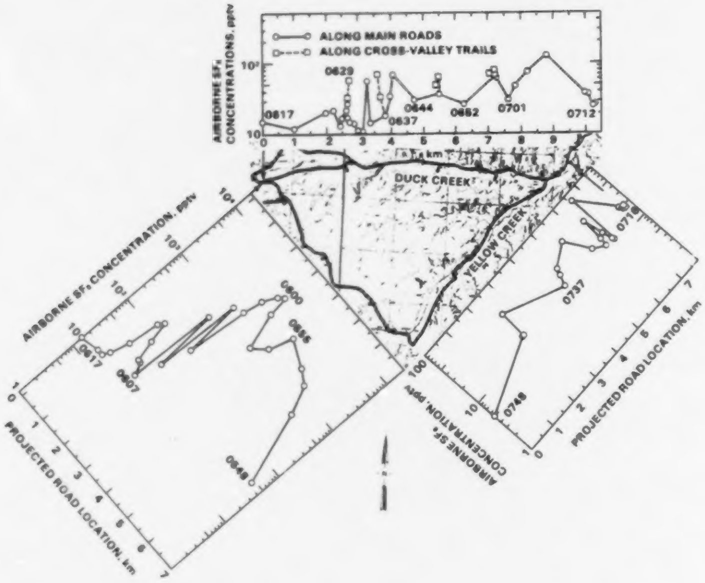

FIGURE 6j. Airborne SF_6 Concentrations Along Roads from Sampling Times from 0548 to 0748 MDT on July 21, 1981

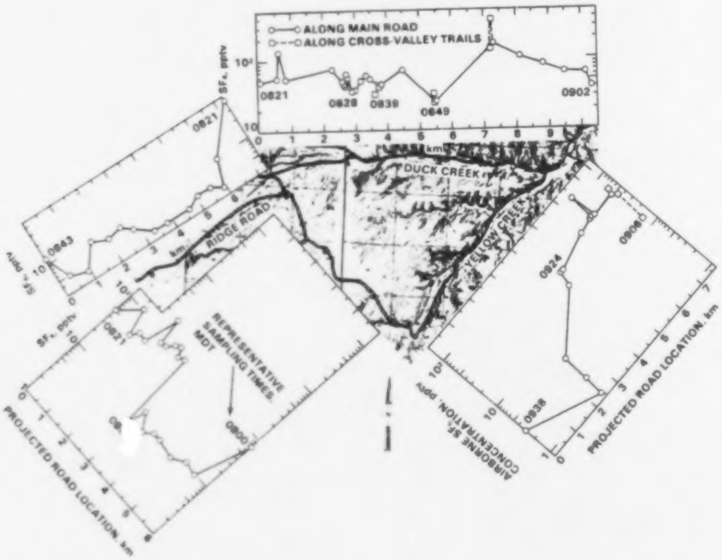

FIGURE 6k. Airborne SF_6 Concentrations Along Roads for Sampling Times from 0800 to 0938 MDT on July 21, 1981

- pollutant flow from side tributaries leading into Yellow Creek and
- pollutant mixing and channeling in valleys at valley confluences, and downwind of valley confluences.

Concentrations determined from syringe samples confirm that tracer-plume spread was limited during drainage flows before sunrise. As shown in Figure 6i near site 18, the maximum syringe-sample concentration is comparable to the maximum 15-min gas-bag concentration of 20800 pptv shown in Figure 6b. The main-plume width was narrow, and concentrations decreased rapidly as a function of cross-wind distance. Relative concentration decrease rates further support the scenario concept: a major drainage flow interacting with a smaller drainage flow containing tracer. Concentrations decreased over two orders of magnitude in a distance of about 0.1 km at a projected road distance of 2.7 km. Hence, the "edge" of the main drainage flow is near 2.7 km. In contrast, the gradual concentration decrease from 3 to 6 km reflects the diverted prinicipal plume flow from the tracer release site.

Tracer plume flow segmented into multiple tracer plume flows as plumes followed along terrain depressions toward Duck and Yellow Creeks. Terrain effects were investigated by collecting some samples either near side-tributaries along main roads or along cross-valley traverses. Cross-valley concentrations were investigated by using side trails from the main roads along Duck and Yellow Creeks.

A more detailed description of main road and side-trail locations is needed to emphasize concentration measurement locations, more detailed than can be read from the figures. Main roads were usually located along either side of each valley. In Duck Creek Valley, the main road was along the valley's northern edge. Side trails extended approximately half-way across the valley towards the tracer release site and terminated at the creek. Beyond the confluence of Duck and Yellow Creeks, the main road continued along the northern edge of the valley to 7 km along Yellow Creek. Beyond 7 km, the main road crossed to the southern side of the valley. Several syringe samples were usually collected along this valley crossing. For the remainder of Yellow Creek Valley used in these experiments, the main road was located along the southern edge of Yellow Creek Valley between 0 and 2.4 km and along the northern edge between 2.4 and 7 km. At 7.5 km, a side trail extended completely across the valley.

Concentrations along Duck Creek shown in Figure 6i reflect tracer plume impingement on a valley side wall at 2.5 km; a major tracer plume with a centerline near 5.5 km, and a secondary plume near 8.8 km. Impingement was along the northern side of a major gulch leading in to Duck Creek, near the juncture with Duck Creek. Impingement occurred prior to the cross-valley traverse: concentrations are indicated by the dashed line. At the traverse, the plume axis was near the center of this major gulch. The traverse was near the confluence with Duck Creek Valley. Beyond the confluence, the tracer plume impacted drainage flow from upper Duck Creek. Consequently, the tracer plume flowed along the southern edge of Duck Creek. At 4 km, concentrations along the center of Duck Creek were an order of magnitude greater than they were along the northern edge of Duck Creek. Nevertheless, plume mixing continued down valley. However, mixing was incomplete since concentrations were always greater near the center of Duck Creek. Also, these greater centerline concentrations probably reflect contributions from segmented tracer plumes flowing over the southern edge of Duck Creek.

The tracer plume segmented in the region between Duck and Yellow Creeks. Segmentation is confirmed by concentrations along Yellow Creek. Along Yellow Creek, the maximum concentration was at 4.5 km, a location adjacent to a side tributary which directed a tracer plume segment into Yellow Creek.

Beyond the confluence of Duck and Yellow Creeks, the tracer plume flowed along the northern valley edge. At 7.5 km along Yellow Creek, concentrations were nearly an order of magnitude less than along the southern edge. It is noted for subsequent referral in Figure 6j that although sunrise was 0605 MDT at the tracer release site, this southern edge was still shaded at 0618 MDT. Concentrations were nearly uniform across the valley further down creek, about 10.2 km along Duck Creek.

Tracer plume segmentation and interaction with ambient air plumes are further confirmed with concentrations shown in Figure 6j. First discussed are concentrations near site 18. Between about 2 and 2.5 km, concentrations cycled about an order of magnitude between succeeding sampling locations. This cycling may have occurred because samples were collected near the undulating interface between the tracer plume and the major drainage plume from near site 2, and the interface width was greater than reflected in Figure 6i. Although plume-interfacing characteristics were changing, a portion of the tracer plume continued to flow as a secondary plume near 1.2 km.

The main concentration trends (cross valley concentration differences and segmented tracer plume flows along side tributaries) continued along Duck and Yellow Creeks. However, significant cross-valley differences also occurred along Yellow Creek. At 2.5 km, concentration near the northern edge was about four times greater than near the southern edge of the valley. At 7.5 km, where the entire valley was not being heated by the sun, there was no longer a cross-valley concentration difference.

Concentrations in Figure 6k are more influenced by surface heating effects since samples were collected two or three hours after sunrise. Surface heating directed a segmented tracer-plume flow between 1 to 3 km along Ridge Road. Near site 18, the tracer plume was also directed between 3 km (the road along site 18) and 6 km along Ridge Road. This last plume direction confirms in more detail the main tracer-plume direction concluded from gas-bag concentrations shown in Figure 6e for times between 0830 and 0845 MDT.

CONCLUSIONS

Fugitive emissions transport and dispersion were simulated in tracer experiments during conditions of relatively low wind speeds; i.e., wind speeds less than the threshold wind speed causing soil suspension. Although spent shale will probably suspend only for greater wind speeds, fugitive emission rates will be nearly independent of wind speed if suspension were mainly caused by mechanical stresses. For instance, constant vehicular traffic on spent shale can produce a relatively constant fugitive emission flux which is independent of wind speed. If this proposed emission scenario occurs, the maximum downwind airborne concentrations will similarly occur during low wind speed conditions. Airborne concentrations will remain relatively large since airborne pollutant concentrations will not be diluted by high wind speeds, u, i.e., downwind airborne concentration decreases are proportional to 1/u.

A multiplicity of plume flows and plume interactions were identified for fugitive emissions transport from the proposed spent shale disposal site. The tracer plume segmented. The greatest concentrations occurred during drainage flows. Plume interactions were between traced plumes and ambient air plumes. Since multiple plume flows and plume interactions were identified, model predictions of downwind transport of fugitive emission plumes on a local scale must include predictions of plume segmentation and interaction.

Predictions on a local scale are essential if maximum "fence-line" concentrations are considered. Two parameters in model predictions are fugitive emission rates, Q, and airborne concentrations, χ. The only controllable parameters in these models are pollutant release heights, release times, and release rate, Q. Predictions of χ/Q ratios both at the fence-line and downwind are used by industry and in regulations. Although further analysis is planned for evaluations of predictive models, the χ/Q ratios can nevertheless be estimated from the reported tracer concentrations; χ with units of pptv, and the constant tracer release rate, Q = 26 kg/hr.

REFERENCES

Clements, W. E., S. Goff, J. A. Archuleta and S. Barr. 1981. Experimental Design and Data of the August 1980 Corral Gulch Nocturnal Wind Experiment, Piceance Basin, Northwestern Colorado. LA-8895, Los Alamos National Laboratory, Los Alamos, New Mexico.

Sehmel, G. A. 1981. "A Dual-Tracer Experiment to Investigate Pollutant Transport, Dispersion, and Particle Dry Deposition at the Rio Blanco Oil Shale Site in Colorado." PNL-SA-9327. In Proceedings of the Second Conference on Mountain Meteorology, November 10-31, 1981, Steamboat Springs, Colorado. Published by the American Meteorology Society, Beacon Hill, Massachusetts, pp. 137-146,

Whiteman, D. C., N. S. Laulainen, G. A. Sehmel and J. M. Thorp. 1981. Meteorological Data Report for Field Studies Conducted in August 1980 in the Oil Shale Region of Northwestern Colorado. PNL-3734, Pacific Northwest Laboratory, Richland, Washington.

Laboratory Testing To Improve Rail Car Sealant Spray and Loading Techniques for the Abatement of Fugitive Coal Dust

Colin J. Williams and William F. Waechter, MHTR Ltd.*

ABSTRACT

The technique of spraying coal rail cars with latex or similar sealants to control fugitive emissions has been used for several years. There are serious deficiencies in the systems used to load coal cars and also in the application techniques of the sealants. This paper reviews these problems and gives practical advice, resulting from laboratory tests and field visits to four coal loading facilities, on how to improve the loading and spraying methods currently used.

A series of laboratory tests has been conducted which subjected over 100 samples of coal to simulated train journeys. These tests, unlike previous tests on sealants, simulated the important parameters of the motion induced vibration of the coal surface and also wind effects on the erosion of the sealed surface. Measurements of the actual vibration levels in a full scale coal rail car were used to design the vibration table and MHTR's boundary layer wind tunnel was used for the wind erosion tests.

The following variables affecting sealant performance were investigated: sloped surfaces; centre humps; settling during transit; concentration of sealant solution; alternative sealants; various application techniques; effect of rainfall; preferential spraying and ambient air temperatures of 15°C and 30°C.

(This is an abstract of a presentation for which a paper is not available.)

(*) Current address: Rowan, Williams, Davies, and Irwin, Ltd., 650 Woodlawn Road, West, Guelph, Ontario, Canada N1K1B8.

Studies of Nontraditional Fugitive Particulate Control Techniques

Brock M. Nicholson, EPA/OAQPS-RTP
Maxine Borcherding, City of Portland (Oregon)
Gary Ekhardt, State of Minnesota
Ray Mohr, State of Colorado

ABSTRACT

Demonstration studies have been conducted with funding assistance from EPA in three U.S. cities to determine the effects of controlling nontraditional sources of fugitive particulate on ambient air quality. These studies involve application of control measures which have not been traditionally required as part of the State Implementation Plans (SIPs) for attaining ambient air standards. It is now generally recognized that many urban areas of the country will be unable to attain the ambient standards solely with application of traditional or stack emissions control. Because of the magnitide of this fugitive problem and the difficulty in defining its character, EPA has allowed states to perform demonstration studies of nontraditional fugitive control techniques as a logical first step in a control strategy for attainment of ambient standards.

The study design, execution, and results to date of these studies are described. Attention is given to the technical and institutional aspects that were followed in an effort to ensure results more reliable than previously obtained in such studies. The SIP development process, as envisioned by EPA in allowing studies, has not resulted in the initiation of a large number of studies. Therefore, it is hoped that the knowledge gained by a few major studies, on the least understood of the nontraditional control measures, will be applicable in many areas throughout the country.

In Denver, the study involves modified winter snow and ice control practices, such as sand cleanup and use of salt as an alternative. In Portland, vacuum sweeping of heavily soiled paved road surfaces in industrial and commercial areas is being studied. In Minneapolis, the study focuses on the control of unpaved roadways at construction sites and the cleanup of mud and dirt carried onto paved roads around construction sites.

(This is an abstract of verbal presentations for which papers are not available.)

This paper has been reviewed in accordance with the U.S. Environmental Protection Agency's peer and administrative review policies and approved for presentation and publication.

A New Charged Fog Generator for Inhalable Particle Control *

by

C. V. Mathai

Arizona Public Service Company
P. O. Box 53999, Station 5680
Phoenix, Arizona 85072-3999

(*) Although this is not the actual presentation made at the May 1982 meeting, it closely resembles that presentation, which was entitled, "Evaluation of the Efficiency of a Charged Fog Generator in Controlling Inhalable Particles at a Steel Plant," by C. V. Mathai and Bradley M. Muller (then of AeroVironment, Inc., Pasadena, CA 91107) and William B. Kuykendal (then of EPA/IERL-RTP, but now of EPA/OAQPS/AQMD). The work was supported by EPA contract 68-02-3145.

A review of the literature shows that control efficiency of inhalable particles using water droplets can be improved significantly if the droplets are electrically charged. A spinning cup fog thrower was developed initially to generate electrically charged water droplets. The poor performance of this device in wind tunnel tests was attributed to the short lifetime of the fine droplets generated, the ineffective ionizer ring method of charging the droplets, and the nonuniform charge distribution observed along different regions of the fog spray pattern.

A new charged fog generator (CFG) was then developed by modifying a commercial rotary atomizer. In this device, the droplets generated are contact-charged to provide a high charge-to-mass ratio of 1.2 μC/g. The droplets have a number concentration median diameter of about 100 μm and a mass median diameter of about 200 μm. The water flow rate is variable (4-70 l/h), and the fog spray pattern can be easily changed from long and narrow to broad and short, with a typical spray coverage of 16-24 m^3. The device uses about 1 kW power (110 VAC) and is portable.

The CFG (at a bentonite ore loading operation) was extensively field-tested to determine the dependence of its inhalable particle control efficiency (PCE) on various instrument settings and field conditions. These tests show that the overall mean PCE is 78% higher than the corresponding value for uncharged fog. Individual PCEs as high as 88% were achieved. The lifetime of the droplets seems to be the dominant factor determining the PCE; and PCE values were higher for higher applied voltages and higher water flow rates. The data suggest that, under optimum instrument settings, PCE of water droplets could be doubled by charging the droplets.

Introduction

Although the total particle mass loading of anthropogenic aerosols is only about 10% of that from natural sources, their effects are significant and largely detrimental. Recent reports indicate that inhalable particles (15 μm and smaller in aerodynamic diameter), in general, and fine particles (2-3 μm and smaller), in particular, may be a human health hazard, and degrade atmospheric visibility. Devices such as electrostatic precipitators and wet and dry scrubbers have performed exceedingly well in controlling pollutants from conventional industrial stack sources. However, effective and economically feasible methods of controlling inhalable particles from non-stack sources in open areas are lacking. Recognizing this situation, the U.S. EPA has been encouraging the development of new methods, such as charged fog technology, to control fugitive emissions.

Removing fine particles from a gas stream in an open area is difficult because of the particles' low mobility and unfavorable inertial properties, as well as uncontrollable external factors (meteorological parameters). The most commonly used dust control (ordinary water sprays) in mining and other material handling areas is only 30%-40% efficient in controlling inhalable particles. Only during the last few years has electrostatics been used to augment particle collection efficiency of water droplets. Numerous studies have shown that most industrial pollutants and naturally occurring dust particles acquire electric charges as they are dispersed into the air. Studies have also shown that the polarity and magnitude of the charges on these particles depend on their size and origin (coal, soil, mineral, etc.). Therefore, the particle collection efficiency (PCE) of water droplets can be significantly enhanced via electrostatic forces of attraction if the droplets are charged to the opposite polarity.

Commercially available charged fog devices for fugitive emission control have certain disadvantages: the need for high pressure air or water to properly atomize the water; the possibility of spray nozzle clogging if the water supply contains high concentrations of dissolved salts and suspended solids; and poor charge-to-mass ratio of the droplets to provide a high degree of fine particle control. Under the sponsorship of the U.S. EPA, AeroVironment, Inc., has developed a new charged fog generator (CFG) which overcomes these difficulties. This research and development project consisted of two phases: Phase I involved examining the theoretical aspects of charged fog technology, developing a bench-scale prototype instrument and evaluating its inhalable PCE in a controlled laboratory experiment, and an economic analysis of the feasibility of the technique to control fugitive emissions; and Phase II involved construction and field-testing of a prototype to evaluate its PCE. This report summarizes both phases.

Theoretical Background

When an aerosol particle approaches a water droplet with a relative velocity, it may collide directly with the droplet (impaction), barely touch the droplet (interception), or miss the droplet entirely. The collection of an aerosol particle by a charged droplet is the result of a number of simultaneous mechanisms of interaction between them; e.g., inertial impaction, direct interception, Brownian diffusion, and electrostatic, diffusiophoretic, and thermophoretic forces. The relative effect of the mechanisms of interaction between the droplet and the particle depends on the size of the particle. For large particles (aerodynamic diameter greater than 2-3 μm), the dominant mechanisms of particle collection by droplets are impaction and interception. For particles smaller than 0.1 μm, Brownian diffusion becomes very important. For particles between these two ranges, electrostatic forces are the dominant interaction mechanisms.

The PCE of uncharged water sprays (where inertial impaction is the major collection mechanism) is given by,

$$E = 1 - \exp\left[-\frac{3}{2}\cdot\frac{Q_L}{Q_G}\cdot\frac{L}{D}\cdot\eta\right] \quad (1)$$

where Q_L and Q_G are the volumetric flow rates of the water (liquid) and air (gas) components of the dust cloud, respectively; L is a characteristic length for the total capture process; D is the mean droplet diameter; and η is the single droplet collection efficiency. Figure 1 is a plot of calculated E versus particle radius for a droplet radius, R, of 106 μm and RH of 75% (curve C). This curve has a minimum (whose magnitude depends on the droplet size) for particles with radius, r, near 1 μm. This minimum is caused by the ineffectiveness of inertial and diffusive interaction mechanisms for particles in that size range. However, if the droplet and the particle are oppositely charged, the minimum in E is eliminated (Curves A and B) as electrostatic forces become the dominant mechanism of particle collection in this size range. This effect is the fundamental principle on which charged fog technology is based. When the droplets and the particles are charged, η is given by,

$$\eta = -4CQ_c\,Q_p/24\,\pi^2\,\varepsilon_o r\,R^2\,\rho U_o, \quad (2)$$

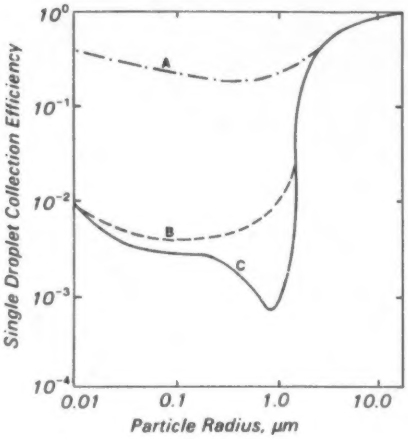

Figure 1. *Calculated single droplet collection efficiency in air of 10°C and 900 mb as a function of particle radius for 106-μm radius droplet at 75% relative humidity for droplet and particle charges of (A) ±20 esu cm^{-2}, (B) ±2 esu cm^{-2}, and (C) zero charge.*

where C is the Cunningham slip correction factor; Q_c and Q_p are the charges on the droplet and particle, respectively; ε_o is the dielectric constant; ρ is the viscosity; and U_o is the free-stream velocity. Thus, for a given particle size distribution, the electrostatic forces are proportional to the magnitude of the charges and inversely proportional to the droplet's size and its free-stream velocity.

Although Figure 1 shows that the addition of electric charges on particles and droplets eliminates the minimum in PCE (near particle radius, r = 1 μm) and yields values of E which are 5 to 10 times higher in certain size ranges than for uncharged sprays, the overall PCE of an operating system may not be that high. Increases in PCEs of about 15% for 1-μm particles to over 45% for 0.3-μm particles (compared to uncharged droplets) have been reported. Values of 50%-80%, with charged droplets under controlled experimental conditions, have also been reported.

When sprayed into the air, the charged droplets will evaporate unless the air is saturated with water vapor. The droplet's lifetime determines the effective contact time between the droplet and particles and thus strongly influences the overall

PCE of the system. The lifetime of a water droplet depends on the temperature and relative humidity of the medium into which it is introduced. To obtain the best PCE, the droplets must be small enough to provide both an adequate spray rate per volume of gas treated and sufficient contact time, yet large enough so as not to evaporate too quickly.

The maximum charge a droplet can carry before it disintegrates is reached when the outward pressure produced by the electric field at the surface of the drop is equal to the inward pressure produced by the surface tension. This limiting charge is called the Rayleigh limit, given by,

$$Q_{Ray} = 8\pi \left[\varepsilon_0 \sigma R^3\right]^{1/2} \qquad (3)$$

where Q_{Ray} is the limiting charge on the droplet (coulombs); ε_0 is the permittivity of the medium in which the droplet is located; σ is the surface tension of the liquid; and R is the droplet radius, in micrometers.

Charged Fog Generator Development

Water droplets may be generated by a spray nozzle or rotating cup. Droplets are generally charged by electrostatic induction, ionized field, or contact charging. Commercially available charged fog devices use water spray nozzles and induction charging.

In this study, a prototype unit, called the spinning cup fog thrower (SCFT), was initially developed in association with the University of Arizona in Tucson. The SCFT consisted of a rotary atomizer, an ionizer, and a vane-axial blower. The rotary atomizer consists of a small hollow-shaft motor and a spinning cup. Water from a low-pressure source is introduced into the hollow shaft and flows toward the other end where the spinning cup is mounted. Entering the rear of the cup, the water stream strikes a rotating "spider" which deflects the water to the sides. A sheet of water then flows toward the lip of the cup where droplets are formed by centrifugal force and the air stream's striking the thin water layer. The droplets were then charged by a stream of positive ions produced by the ionizer containing numerous small discharge needles. It was expected that the ions produced in the region of the ionizer ring would follow the airflow from the vane-axial fan, mix with the droplets, and charge them. The charged droplets were then deflected and projected forward by a stream of air supplied by the vane-axial blower. These droplets had a median diameter of about 20 μm and a charge-to-mass ratio of 1 x 10^{-11}C/g.

To evaluate the PCE of the SCFT, tests were conducted in a wind tunnel at the University of Arizona. These tests showed only about 50% inhalable PCE. This poor performance was attributed to the very short lifetime of the fine droplets generated, the ionizer ring method of droplet charging (which proved ineffective), and the nonuniform charge distribution observed along different regions of the fog pattern. The SCFT was therefore abandoned, and a new charged fog generator (CFG) was developed by modifying a commercial rotary atomizer.

Figure 2 schematically represents the new CFG. Water is introduced through the water tube into the 3600-rpm rotating cup, whose inside is fabricated to a gradual smooth taper. A small deflecting baffle is attached to the open end of the water tube so that the water will be deflected 90° and strike the rear end of the rotating cup. Because of the centrifugal forces, the water becomes a thin film and moves forward into a high velocity airstream from the vane-axial fan. The impact of the high velocity air on the thin water film breaks the water film into fine water droplets.

The water tube, air cone, and rotating cup are made of nonconductive materials. The water tube is attached to the rotating cup, thus rotating with the cup. The other end of the water tube is attached to the water supply through a rotating seal. The water for atomization is stored in an electrically isolated reservoir (120-l capacity), and a small pump is used to pump it to the inlet of the rotating seal. The water flow rate can be varied from about 4 to 70 l/h. The airstream from the fan, controlled by an air butterfly setting, projects the fog forward. By adjusting this setting, the airflow speed can be controlled, thereby controlling the shape of the fog spray pattern to better conform to the shape and size of the source of dust upon which the charged fog is to be applied. The spray pattern covers a volume of 16-24 m^3.

To achieve a high charge-to-mass ratio for the droplets, contact charging by directly connecting a high voltage source to the inflowing water was found to be the most efficient method. However, this method requires that the entire water supply (reservoir) and associated tubing be electrically isolated so that there is no current leakage.

The size distribution of the droplets was determined using a cloud optical array probe and a precipitation optical array probe. These measurements gave a number concentration median diameter of about 100 μm and a mass median droplet diameter of about 200 μm. Collecting the droplets on greased glass slides and observing them under a microscope yielded values consistent with the above results.

The charge-to-mass ratio of the droplets was determined using a special sample train (developed by AeroVironment), consisting of an insulated stainless steel probe tip mounted on a standard glass midget impinger. The probe was connected electrically to copper wool packing inside the midget impinger, which was also connected by a shielded cable to an electrometer. The impinger was immersed in a Dewar flask containing dry ice. An isokinetic sample of droplets was then extracted from the fog spray. As the droplets moved through the impinger they were condensed, transferring their charge to the copper wool packing. The charge transferred to the copper wool was then measured by the electrometer. Knowing the mass of droplets collected and the current produced by them, the charge-to-mass ratio was calculated. This method gave a typical value of 1.2×10^{-6} C/g with an applied voltage of 15 kV, about 25% of the maximum allowed value (Rayleigh limit) for 200-μm droplets.

The charge-to-mass ratio was also estimated using another experimental setup, in which droplets were allowed to transfer their charges to a 125 μm mesh size standard sieve placed in the path of the fog spray and the current generated in the mesh was measured. Knowing the size of the droplets and the number of droplets generated by the CFG per second, the charge-to-mass ratio was estimated. This method gave values consistent with those reported for the gravimetric method.

In summary, the CFG is fairly small, portable, and mounted on a moveable platform. The total power requirement is about 1 kW (110 V AC power supply). It has no nozzle-clogging problem and does not require compressed air. Using a small inverter, the unit can be operated by an automobile battery. This feature may be important because the system has high potential application in locations where commercial electric power is not available. The physical characteristics of the charged droplets from the CFG are such that high inhalable PCE is expected.

Evaluation of the Inhalable PCE of the CFG

The CFG was field tested at the Kaycee Bentonite Corporation's bentonite processing plant in Worland, WY, during the first half of 1981. Bentonite is a water-absorbing material used mainly to seal water leaks in oil wells. Bentonite ore is unloaded from front-end loaders onto the

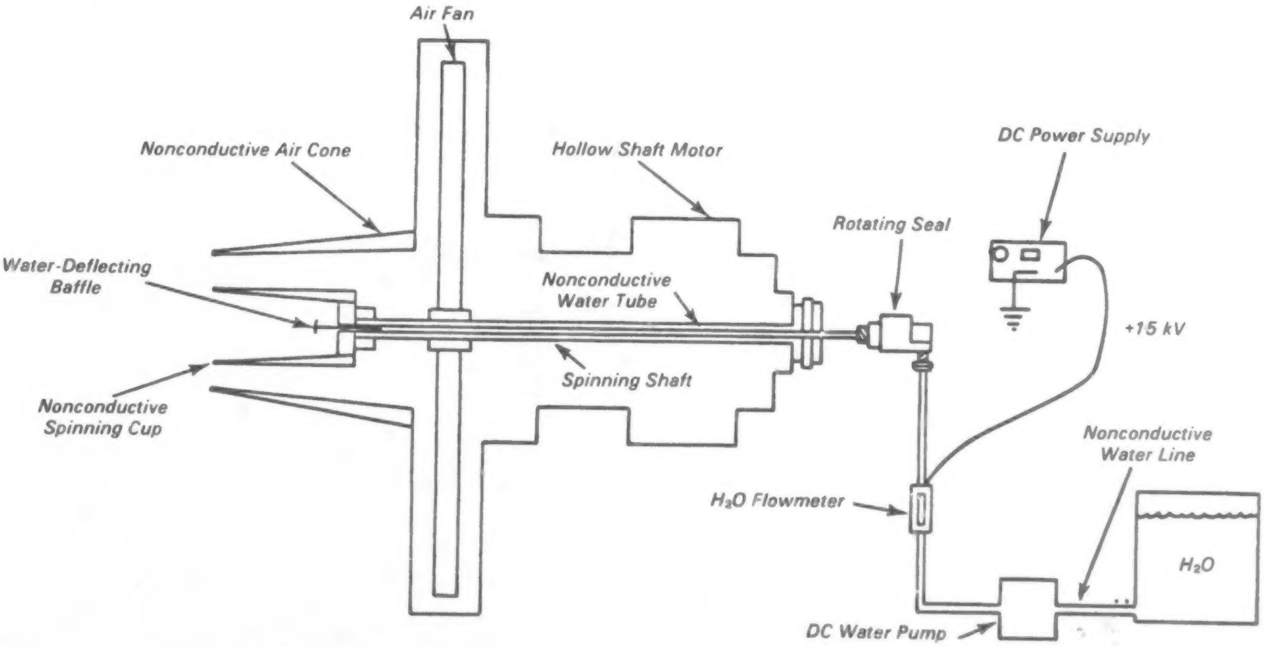

Figure 2. *Schematic of the charged fog generator.*

grill of a hopper which is attached to the west wall of the plant building. From the bottom of the hopper (approximately 4 m below the hopper grill level, inside the plant), the ore is carried by conveyor belts to processing areas. The hopper is completely enclosed except on the side through which the front-end loaders unload. The hopper is 6.7 m wide, about 2 m deep and, from the grill level, about 3 m high. The grill is inclined about 30° to the horizontal.

Bentonite ore from two large piles, approximately 100 m to the northwest and southwest of the hopper, are carried to the hopper by front-end loaders and dropped on the grill. The bucket of the front-end loader is about 2.4 m wide and successive loads are unloaded uniformly over the 6.7 m wide hopper. It takes about 10 front-end loader dumps to fill the hopper to the grill level. These 10 dumps are accomplished in about 25 minutes. The bucket is removed from inside the hopper area in 20-25 seconds. One full hopper of ore will be carried away by the conveyor belt in about an hour.

The land around the plant is fairly flat. A railroad track is east of the plant and a paved road (very little traffic) beyond that. Bottom-dump trucks filled with bentonite ore arrive near the storage piles from the south and, therefore, the dust in the hopper area due to transport of ore to the plant area is negligible compared to the dust generated in the hopper itself. In other words, the hopper can be considered as a fairly isolated source.

The CFG and the particle sampling instruments were mounted on the outside of the south wall of the hopper, about 4 m above ground level. A platform was built to mount these instruments. Ideally, the particle sampler inlet should have been mounted on the east (rear) wall of the hopper, but for practical reasons could not be. The CFG sprayed water droplets across the hopper above the grill. The total volume to be treated by the charged fog was about (6.7 m x 2 m x 3 m) 40 m^3, somewhat larger than the maximum coverage of the CFG fog. Unfortunately, only one prototype CFG was available for these tests. To have had a second unit, mounted on the north wall of the hopper and operated concurrently, would have been ideal.

Particle samples were collected using a Sierra Model 230 CP cyclone preseparator followed by a Sierra two-stage cascade impactor. The cyclone's air inlet protruded 0.3 m into the hopper. The particle sampling system was operated at a flow rate of 0.85 m^3/min (30 cfm), which was calibrated at regular intervals during the entire test program. At this flow rate, the cyclone has a particle cut-point of about 7.3 μm. The impaction plates of the cascade impactor were chosen so that the upper filter would collect particles larger than 1.8 μm. The lower backup filter collects all particles smaller than 1.8 μm. For this report, particles collected on the backup filter are characterized as the fine particle fraction, and those on the upper filter as the coarse fraction. The mass of coarse fraction collected was often an order of magnitude smaller than the fine fraction (possibly indicating a particle bounce problem with particles larger than the cut-point of 1.8 μm reaching the backup filter). Subdividing the samples into more size ranges would have required either much longer sampling time or much higher flow rates to obtain acceptable filter loadings. Neither alternative was desirable.

Field Test Design

Three test scenarios were designed to determine the PCE of the CFG. In the first, no attempt was made to control the dust inside the hopper, except that the CFG's fan ran continuously (this ensured that the mixing of the dust cloud was nearly identical among various runs in order to make direct comparison of tests with and without charged fog). In the second, uncharged fog was applied on the dust cloud. In the third, charged fog was applied. Other governing parameters were varied under each scenario to yield a statistically acceptable set of test data.

The parameters varied were water flow rate, fog pattern (short or long), applied high voltage, wind conditions, and relative humidity. In addition, tests were performed with the polarity of charges on the droplets reversed. This test protocol called for 32 test runs. However, in actual practice, data had to be collected under prevailing field conditions; hence, 96 runs were performed.

Particle samples were collected on preconditioned and preweighed glass fiber filters. Each particle sample was collected during 12-15 front-end loader dumps (roughly 30-40 minutes). Wind speed and direction and relative humidity were also recorded simultaneously. After each sample was collected, the filters were transferred to special envelopes and brought to AeroVironment's laboratory for analysis.

Data Processing

The mass of the fine and coarse fraction and sum of the two were obtained from the final and initial weights of the filters. Using known values of the sample time, number of dumps, and flow rate, particle mass concentration for each dump was calculated.

The amount of dust generated in the hopper fluctuated from dump to dump. To overcome this variation, each sample was collected during 12-15 dumps and the mean value for each dump was calculated. The amount of dust generated also varied from day to day, caused by factors such as changes in ambient conditions and the moisture content of the bentonite ore. The effect of the latter is not too significant since the ore stored in each pile comes from the same mine and a pile is completely processed before a new pile is started. To overcome the day-to-day dust level fluctuations, sample concentrations were normalized for each day with respect to the background value (the fan-only value), and a percentage particle collection (control) efficiency was calculated. Percentage PCE is obtained from:

$$E = \frac{C_o - C}{C_o} \times 100$$

where C_o and C are the particle concentrations corresponding to "fan only" and "fog test" scenarios, respectively.

Values of E are calculated for the fine fraction, the coarse fraction, and the sum of fine and coarse. The report gives these percentage PCEs and the corresponding field condition data, water flow rate, and applied high voltage for the whole field test program.

Comparison Between Charged and Uncharged Fog

Figure 3 shows the mean values of the measured percentage fine PCE and total PCE for charged (striped bars) and uncharged (solid bars) fog. For this comparison, all test runs under all instrument settings and field conditions are included. The mean and standard deviations of the fine PCE are 48.1% and 23.0%, respectively, for the charged fog and 27.8% and 25.3%, respectively, for the uncharged fog. The corresponding values for all the particles (fine and coarse together) are 44.5%, 21.8%, 25.0%, and 24.4%, respectively. These numbers show that, even under average field conditions and instrument settings, inhalable PCE can be almost doubled by electrically charging the water droplets. However, under optimum instrument settings and favorable field conditions, the improvement in inhalable PCE can be expected to be higher. Note that the volume of the dust cloud treated was somewhat larger than the maximum coverage of the CFG.

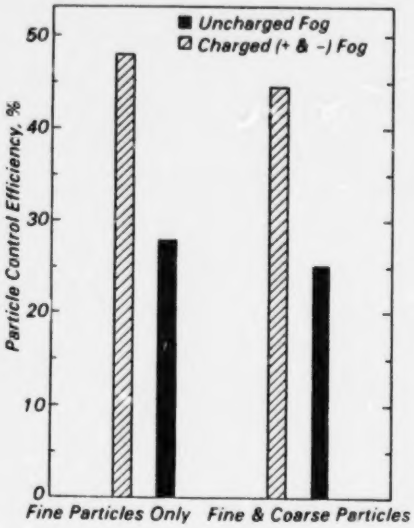

Figure 3. *Mean inhalable PCE of all test runs (for various CFG settings and field conditions) for charged and uncharged fog.*

The size range of particles collected in the coarse mode was fairly narrow, and the mass collected was often an order of magnitude smaller than the fine fraction. Another problem which may have inhibited coarse particle collection is the particle bounce effect, by which some of the larger particles pass the upper impaction plate and settle on the backup filter with the fine particles. Consequently, most of the ensuing discussion concentrates on the sum of fine and coarse fractions of the particles collected. Therefore, this particular experiment could not demonstrate the full effect of charged fog on the coarse particles.

Figure 4 shows total PCE with E plotted as a function of ambient RH for two sets of instrument settings for an applied high voltage of 4 kV (positive charges) and a water flow rate of 60 l/h. The circles represent a broad spray pattern, and squares represent a narrow spray pattern. The method of least squares was used to fit a straight line to the data sets, shown in the figure, yielding a correlation coefficient of 0.93 for the broad spray and -0.19 for the narrow spray. The corresponding slopes are 0.99 and -0.09, respectively. Although the wind conditions were not identical for all data points, the

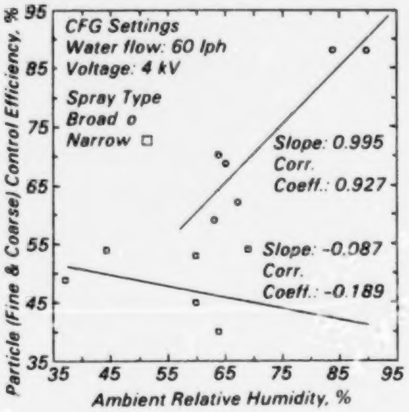

Figure 4. *PCE of the CFG plotted as a function of ambient relative humidity for broad (o) and narrow (□) spray patterns.*

fine PCE increases with increases in ambient relative humidity for a broad spray, but is fairly independent of RH for a narrow spray. The generally lower values of E for the narrow spray can be easily explained: a board spray covers most of the dust cloud in the hopper, while the narrow spray covers a smaller portion, resulting in lower E values.

The difference in the dependence of E on RH for the broad and narrow sprays is also explainable. For a narrow spray, most droplets occupy a volume away from the open side of the hopper. When fog is applied continuously, this area becomes more humid than outside the hopper or near the hopper opening, assuming the wind is not too strong. Thus, there is minimal droplet evaporation and, consequently, fairly steady PCE. However, for a broad spray, the droplets are distributed from the rear wall of the hopper to outside the open side of the hopper. Thus, when the ambient RH is high, fewer droplets will evaporate, leaving more droplets to collect dust particles; on the other hand, when the ambient RH is low, more droplets are lost due to evaporation near the open side of the hopper and outside the hopper.

The effect of the longer droplet lifetime in a higher RH atmosphere increases the PCE. These test observations are thus consistent with the conclusion that the droplets should be small enough to provide high PCE, yet large enough not to evaporate too quickly.

Figure 5 shows PCEs for negatively and positively charged fog for the fine fraction separately, and for both fine and coarse particles combined, with the same water flow rate, the same applied voltage, and nearly identical field conditions. The higher value of E for negatively charged fog suggests that inhalable bentonite particles carry a net excess positive charge.

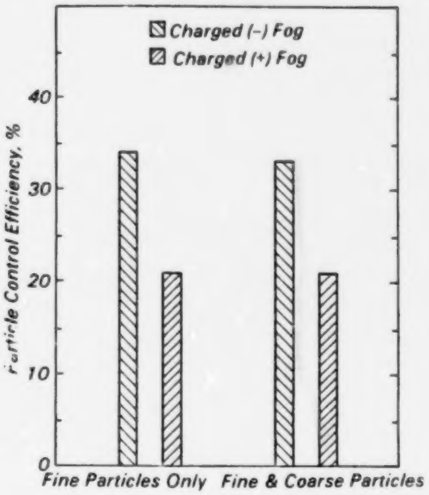

Figure 5. *Comparison of PCE of the CFG for positively and negatively charged fog, with all other parameters nearly identical.*

Figure 6 is a good example of the effect of water flow rate in the CFG on its ability to control particles. The PCE in this case decreased by 42% when the water flow rate was reduced from 60 l/h to 30 l/h, with all other instrument settings and field conditions nearly identical. This effect is expected: increased water flow rate increases the number of charged droplets available for particle collection. Water flow rate was particularly significant in this experiment because the CFG was being applied to control dust in a volume larger than its maximum coverage; therefore, any decrease in the water flow rate further decreased the coverage.

Under a controlled experimental setup one would expect the PCE of charged droplets to decrease if the wind speed in the volume being treated were increased. The increased wind would reduce the time available for the droplet and particle to interact. However, in this experimental situation, because of the location and method of particle sampling, this effect is not evident.

Conclusions

After the initial setbacks with a prototype spinning cup fog thrower, a new charged fog generator was developed. Water droplets are produced in this

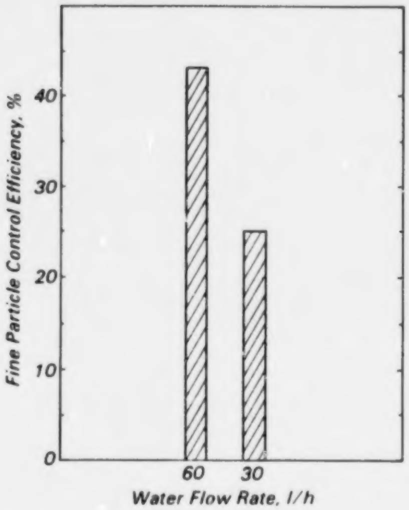

Figure 6. *Comparison of fine PCE of the CFG for two water flow rates, with all other parameters nearly identical.*

device using rotary atomization; therefore, spray nozzle clogging problems are eliminated as well as the need for compressed air. The CFG uses contact charging to yield a high charge-to-mass ratio of 1.2×10^{-6} C/g with an applied voltage of 15 kV. The size distribution of the droplets gives a number concentration diameter of about 100-μm and a mass median diameter of 200-μm.

Extensive field tests of the CFG at a bentonite ore unloading operation show that:

(1) Charged fog is an effective means of controlling fugitive dust emissions. The mean value of the inhalable (fine and coarse fractions combined) PCE of charged fog measured under all instrument settings and field conditions showed a 78% increase when compared with the corresponding value for uncharged fog.

(2) Relative humidity (in this particular experimental setup) plays a significant role in determining the overall PCE. It is believed that the lifetime of the droplet is the dominant factor in determining the PCE. Therefore, the droplets should be large enough not to evaporate too quickly, yet small enough to yield a high PCE.

(3) Under identical or nearly identical field conditions and instrument settings, negatively charged droplets gave higher values of PCE than positively charged fog, suggesting that inhalable bentonite particles carry a net excess positive charge.

(4) Measured inhalable PCEs were higher for higher applied voltages in the 4-10 kV range. At the upper end of this range, the PCE seemed to attain a saturation value.

(5) Measured inhalable PCE was higher when charged droplets could cover more of the dust-laden air in the hopper. In the experimental setup used, higher water flow rates and broad spray patterns resulted generally in higher PCEs, although the key element was the number of particles treated by the droplets.

(6) Because of the type of particle sampling method used and the field setup, the effect of wind speed and direction on PCE can not be quantified with available data.

(7) The optimum CFG instrumental settings are 60 l/h water flow rate, a spray pattern which will cover a maximum volume of dust-laden air (broad or narrow spray depending on the extent of the source), an applied voltage of 8-10 kV, and positive or negative charge depending on the charges of the dust particles. Ideal field conditions are high relative humidity (to ensure long droplet lifetime) and calm or low wind conditions.

Recommendations

In order to utilize the capabilities of charged fog technology in a variety of fields, the following studies would be of value.

(1) Although some qualitative work has been done on the polarity and magnitude of electric charges on airborne particles, a quantitative examination of the polarity and extent of the electrical properties of airborne particles and their dependence on particle sizes and chemical composition, as well as the potential of the CFG to control particles of various origins, would be useful.

(2) The CFG and other commercially available charged foggers use high voltages, and their present designs are such that they could be a safety and fire hazard in an inflammable gaseous atmosphere. Therefore, it would be beneficial to make the devices explosion-proof and to eliminate potential hazards due to human exposure to high voltages.

(3) Use of charged fog to collect airborne submicron- and micron-sized organisms is of interest to the

industrial hygienist. Control of germs and possible decontamination of an area using proper chemical additives in the water spray is also of interest to our defense forces. Preliminary investigation of this application could be coupled with (1), above.

(4) The potential of the CFG to control dust from a mobile source is worth examining. No alternative method of control is available, other than ordinary water sprays, which are not efficient in controlling inhalable particles.

(5) Possible application of charged fog in recovering airborne precious metals should be of great interest to the gold and other precious metal and mineral mining industries.

ESTIMATION OF AMBIENT TSP IMPACTS OF COAL STORAGE AND HANDLING FACILITIES

Robert C. Wells
Enviroplan, Inc.

Dennis C. Doll
Enviroplan, Inc.

John Hattrup
Baltimore Gas & Electric Co.

The work described in this paper was not funded by the U.S. Environmental Protection Agency. The contents do not necessarily reflect the views of the Agency and no official endorsement should be inferred.

ABSTRACT

This paper is directed to those concerned with evaluating the air quality impact of fugitive particulate emissions from coal storage and handling. Site-specific analyses were conducted for the coal handling system planned for Baltimore Gas & Electric's Brandon Shores Power Plant in Anne Arundel County, Maryland. Fugitive particulate emissions were considered significant due to the presence of a designated nonattainment area for TSP near the plant. The analyses employed dispersion modeling with a modified version of the Industrial Source Complex (ISC) Dispersion Model. Emission factors and control efficiencies were taken from available published information. Available emission factors were critically evaluated and specific factors were required to be consistent with available measurements and site-specific conditions. Significant problems developed with the meteorological data base using the standard U.S. EPA preprocessor. Since these problems produce unrealistic prediction under some meteorological conditions, approximations were employed to eliminate the unreasonable predictions from the analysis. Site-specific analyses have aided in defining the appropriate dust control equipment for the coal handling system.

1.0 INTRODUCTION

National Ambient Air Quality Standards (NAAQS) have been established for Total Suspended Particulates (TSP) which define concentrations of suspended particulates associated with health problems and with secondary impact such as property damage. TSP measurements indicate that many areas of the United States do not attain NAAQS for TSP. Further, emissions from "traditional" sources of pollutants (e.g. smoke stacks) often do not account for the observed TSP concentrations. Fugitive particulate emissions, including both natural dust and anthropogenic sources, contribute to measured concentrations. As such, quantification and control of fugitive dust is an important part of achieving and maintaining the NAAQS for TSP.

This paper describes a case study of the application of available estimates of uncontrolled fugitive emissions, control efficiency, and atmospheric dispersion for environmental analysis of a coal-fired power plant. Regulatory criteria are stated in terms of maximum permissible ambient concentrations. Thus, dispersion modeling based on emission estimates is the only suitable technique to adapt available information on fugitive emissions to the specific situation of a proposed facility.

A wide range of control measures is available to suppress or contain fugitive emissions resulting from material storage and handling. Costs associated with different control measures for fugitive emissions vary greatly. In addition, some control measures can affect efficiency and reliability of operations. Therefore, one cannot assume that it is automatically desirable to control fugitive emissions to the maximum degree possible. Ambient impacts of fugitive emissions under various levels of control are important in determining cost-effective measures of attaining ambient air quality goals as defined by the NAAQS.

Additionally, the analyses described here for evaluation of fugitive emissions of a new facility are also useful in identifying emission reduction credits (ERC) for use in emissions trades. Preliminary investigations based on dispersion modeling are useful in defining the most cost-effective controls associated with emission trade-offs, as well as the spatial effects of trades involving both fugitive and stack sources. Current U.S. EPA policy(1) requires that proposed emission trades which control fugitive emissions rather than stacks demonstrate the equivalence of emission reductions using dispersion modeling. These trades will typically require post-approval monitoring to confirm modeling results; however, pre-approval analyses are an important first step in demonstrating the appropriateness of ERC.

The facility evaluated in this study is the Brandon Shores Power Plant being constructed in Anne Arundel County by the Baltimore Gas & Electric Company. Figure 1 details the location of the plant and air quality in the area. The plant was originally designed to burn either oil or coal. Plans initially called for operation with oil and the plant received environmental permits on that basis. During construction, however, it was determined that it would be economically advantageous to burn coal.

Therefore, the plant has been treated for regulatory purposes as an existing facility undergoing coal conversion even though the plant is currently under construction.

The Brandon Shores Power Plant consists of two units each with 620 MW generating capacity. Units I and II are projected to come on-line in 1984 and 1988, respectively. The lay-out of the power plant and on-site coal handling system is detailed in Figure 2.

2.0 STUDY DESIGN CONSIDERATIONS

2.1 REGULATORY APPROACH

There are two basic approaches to regulating fugitive emissions associated with coal handling and storage. First, specific controls can be required as a condition of the appropriate permit. With some restrictions, this approach can apply to federal Prevention of Significant Deterioration (PSD) permits as well as to construction and operating permits issued by a state government. This is common practice in some states. Controls can be either specified by the regulator or proposed by the operator and approved by the regulatory agency.

Second, a facility may be limited to specific maximum ambient impacts. These impacts are defined either as maximum total concentrations including background (e.g., NAAQS) or as maximum incremental concentrations due to the facility (e.g., PSD increments).

The Brandon Shores Power Plant is subject to the latter form of regulation. While a minimum level of control is not dictated by the regulatory agency, the facility must account for ambient concentrations from fugitive emissions. This approach potentially provides for the most cost-effective controls, in that the specific control required will be directly related to the ambient impact of a new facility and to the existing air quality. In practice, the analysis is complicated by limitations of available emission factors and dispersion models.

Three ambient criteria potentially constrain fugitive emissions at Brandon Shores. First, the NAAQS apply in any area of public access. This is generally taken to apply at any point beyond the facility's property line.

Second, in areas that are now attaining the NAAQS (which includes the Brandon Shores Plant site), incremental increases in TSP concentrations due to new sources are limited. As with the NAAQS, these PSD increments apply in all areas of public access. They include impacts from all sources constructed after a specific date. In this case, no other sources are projected to consume PSD increments of TSP in the vicinity of the Brandon Shores facility; therefore, PSD increments apply to concentrations from the Brandon Shores facility alone.

The third case, involving areas that do not attain the NAAQS, is more complicated. The Brandon Shores Plant site is located near a (secondary) nonattainment area for TSP. If the facility does not contribute significantly to ambient concentrations in the nonattainment area, then the facility is permissible. If the facility does contribute significantly to the nonattainment area, it is then subject to two types of control. First, the facility must employ extensive controls to achieve the lowest achievable emission rate (LAER) for particulates. Second, the facility must provide for emission reductions in the nonattainment area to offset the increased emissions at the facility. While it is possible to satisfy these two requirements in some cases, they represent a severe limitation on the siting of new sources. It is often preferable to voluntarily control sources to the point where they exert no significant impact in a nonattainment area.

Criteria for ambient concentrations and incremental impacts are based on both long-term (annual) and short-term (24-hour) averages. Specific concentrations applicable here are presented in Table 1. Criteria for short-term NAAQS and PSD compliance limit the largest second-highest concentration predicted based on approved dispersion modeling procedures. The significance criteria for nonattainment area impact (de minimis increments) are subject to interpretation depending upon the regulatory context and the discretion of the regulatory agency.

The increments were proposed by U.S. EPA to relate to the incremental contribution to a violation of the NAAQS. Hence they should apply only at the time and place of an actual violation of the NAAQS. For long-term averages this includes the entire nonattainment area by definition. For short-term averages, prediction impacts from the proposed facility may or may not coincide with short-term concentrations in excess of the NAAQS.

In this instance, the State of Maryland is free to set its own criteria for significant impact in a nonattainment area. The State has chosen to employ the numerical criteria suggested in federal regulations as applicable to the overall highest concentration predicted from the proposed facility in the designated nonattainment area. This determination ignores the coincidence of the facility's impacts with high background concentrations.

Projection of TSP concentrations in the Baltimore area developed by the State of Maryland for the years 1982 and 1986 indicate that this boundary of the nonattainment area is projected to change drastically in the 1980's (Figure 2).(2) The location of this boundary is an important part of the definition of significant impact. Concentrations at the boundary of the designated nonattainment area ultimately prove to be the limiting concentrations, which determine the level of control required. As such, projecting air quality to the time of plant start-up would significantly alter the conclusions of this analysis.

3.0 METHODOLOGY

Under the regulatory criteria outlined in Section 2, ambient impacts from the operation of coal storage and handling equipment at the Brandon Shores Power Plant and resulting total ambient concentrations must be determined. Projection of ambient impacts for proposed facilities requires the independent estimate of emission rates from the facility and dispersion from the source. In addition, projections of total concentrations resulting from proposed facilities require some consideration of other sources of a pollutant. These three issues are addressed in separate subsections below.

3.1 EMISSION RATE ESTIMATES

Available procedures for estimating emission rates from sources of fugitive particulate emissions require (1) selection of an emission factor which describes uncontrolled emissions from the source, (2) identification of a control efficiency associated with the specified controls, and (3) specification of source extent (area or operating rate).

Emission Factors

Published emission factors quantify emissions from all potential sources of fugitive particulates which are of concern here. The quality of these emission factors varies greatly, however. Quantitative estimates available for some sources are merely assumptions. Other sources have been subjected to empirical field studies and emission factors exist which account for a wide range of potential conditions. In some cases, different field studies employing different methodologies have been conducted to quantify similar sources. It is disturbing to note that field studies conducted with reasonable methodologies arrive at different results.

Appropriate emission factors for a particular facility must be selected from the wide range of available estimates. These emission factors should be based on two criteria. First, the emission factors should be determined from a specific field study or estimation procedure of high quality. Second, the field study or estimation procedure should be as closely related as possible to the specific sources of concern. A third criterion often raised in a regulatory context is conservatism within a range of uncertainty.

An overall quality index has been suggested in past work conducted by U.S. EPA contractors.(3) The proposed rating scale is presented in Table 2. Essentially, the quality index asserts that (1) any data are better than no data; (2) representative data are better than extrapolated data; (3) accurate data are better than inaccurate data; and (4) large quantities of accurate data are better than small quantities of accurate data. The qualitative scale is intuitively reasonable, and will provide a useful measure of the relative quality of different emission factors from different sources. Unfortunately, selection of alternate emission factors is often a choice between extrapolation of high quality data from different processes or the use of lower quality data for more representative processes.

In practice, the authors know of no emission factors for fugitive particulate emissions which deserve an A rating. Some emission factors are available which would be rated B. Most available emission factors would be rated C or D, and a few potentially significant sources must be quantified using E-rated emission factors (assumptions). Generally, D-rated or E-rated data should be disregarded if better information is available. B and C ratings are actually a continuum. Use of any emission factor requires "extrapolation from similar processes." The relative degrees of extrapolation and inherent data accuracy must be balanced in selecting an emission factor.

The regulatory concern for conservatism is often not practical with fugitive emissions estimates. The range of emission factors for some sources can span more than three orders of magnitude. It seems entirely unreasonable to rely on a questionable assumption simply because it is more conservative than the results are a measurement program.

Three sources of published information potentially provide emission factors useful in this study. First, work has been conducted by Midwest Research Institute (MRI) under U.S. EPA contract. Their work began in 1974(4) with additional useful information published in 1978 and 1979.(3,5) Emission factors potentially applicable to coal have been developed based on limited sampling of fugitive emissions from coal handling, and based on extrapolation from more extensive sampling of different materials.

Second, PEDCo Environmental Inc. conducted a limited field study of fugitive particulate emissions from coal mining in the western United States.(6) While coal mines are not identical to power plants, the study represents a moderately large data base specific to coal. An extrapolation of these emission factors may be preferable to use of emission factors developed for other materials and for a specific process.

Climatic conditions must also be accounted for in using emission factors developed for coal mines in the arid west for operations at a power plant in the eastern United States. The effect of climatic conditions on fugitive particulate emissions are poorly understood. However, both empirical studies and theoretical considerations(5,7) suggest that climate is important.

Third, a wide range of emission factors from a variety of sources was summarized in 1977 under U.S. EPA contract.(8) This summary included earlier MRI work, as well as numerous limited field studies, and emission factors which had been used in regulatory determinations in the past. Generally, emission factors cited in this document which are not included in work discussed above would be rated D or E. The compilation provides a useful summary of emission factors which may be considered based on conservatism of regulatory precedent. However, field studies subsequent to its publication generally have found lower emission rates than those previously employed in regulatory determinations.

The uncertainty noted in estimating fugitive particulate emission factors, combined with regulatory concerns of precedent and conservatism, precluded the selection of a single "correct" set of emission factors. First, a set of emission factors was formulated based on adherence to recent regulatory precedent. It was intended that these emission factors provide an upper bound on ambient impacts associated with coal handling equipment at the Brandon Shores Power Plant. A determination that the plant would be environmentally acceptable based on these emission factors would provide strong support for issuance of permits.

A second set of emission factors was formulated based on what seemed to be the most representative factors available. An analysis based on these emission factors provides the best assessment of ambient impacts from fugitive particulate emissions. The substantial margin of conservatism typical of the former set of factors is not the case here, however. Emission factors judged to be best are frequently at the low end of the range of factors quoted.

At the Brandon Shores Power Plant there are three important processes with the potential to produce fugitive particulate emissions. First, continuous transfer equipment removes coal from barges, transfers coal between conveyors, places coal in and out of storage, and supplies bunkers. Second, wind erosion from storage piles on-site is likely to produce emissions. Third, coal must be crushed prior to combustion. In addition, some emissions would be expected from conveyors.

Conservative emission factors for continuous handling equipment were based on a number of emission factors that had been used in a regulatory context. The emission factors for barge unloading and transfer houses are based on commonly used factors with unclear origins.(9,10) Emission factors for load-in and load-out of storage piles were taken from MRI's earlier work with stone quarries.(4) The available emission factor judged the best to quantify emissions from continuous handling operations was developed for fugitive emissions from the iron and steel industry.(5) The emission factor is based on similar activities with different materials. Site-specific correction factors are suggested to minimize the uncertainty associated with extrapolation.

A conservative estimate of wind erosion from coal storage piles was taken from emission factors developed for stone quarries.(4) While the factor is not particularly applicable to coal, it has frequently been used in a regulatory context. The wind erosion emission factor developed for coal mines(6) was judged to be more appropriate for an accurate emission estimate. This factor is based on data directly relevant to coal. The data were collected in an arid region and corrections for climatic differences and storage pile activity were assumed based on past work.(4) The emission factor is stated in terms of a functional relationship with wind speed, which is intuitively reasonable though different from theoretical functional forms.(11,12) This functional relationship is particularly important in avoiding severe overpredictions of ambient impacts from coal storage and handling under low wind speed conditions.

Conservative emission factors for coal crushing were based on U.S. EPA emission factors for stone crushing.(13) Alternative emission factors have been proposed based on limited data specific to coal.(14) While neither factor could be considered ideal, the choice of the more source-specific factor seems preferable to the assumed applicability of stone crushing emission factors based on regulatory precedent.

An available estimate for emissions from conveyors was based on the assumption that 25% of the emissions from "transfer and conveying" or 33% of the emissions from transfers would be due to conveyors.(15) This estimate is based on visual observations and is employed here both for conservative and best estimates.

Emission factors employed in this study are presented in Table 3. Comparison of emission factors is difficult because of different assumptions for the two sets of factors. The conservative emission factors often lump sources together (e.g., all transfers and conveyors), whereas the best emission factors are specific to single sources (e.g., single transfer points). Conservative wind erosion estimates are based on material throughout; best estimates are based on surface area of storage piles and on the wind speed. Table 4 summarizes the alternative emission factors in terms of annual mass emissions. This summary illustrates the assumptions inherent in selection of one factor over another.

Control Estimates

The uncertainties noted above for estimates of uncontrolled fugitive particulate emission rates are compounded in estimating control efficiencies. With the exception of baghouses, where control efficiencies can be readily demonstrated, available control techniques for fugitive particulate emissions are not quantified at all. Available estimates of control efficiency are based entirely on subjective estimates.(3) While use of these subjective estimates is not desirable, there is little choice. The added confusion associated with developing alternative "conservative" and "accurate" estimates of control efficiencies is not warranted. Neither conservatism nor accuracy can be demonstrated, and extensive regulatory precedent does not exist with respect to assumed control efficiencies.

It is important to specify control which will mitigate unacceptable environmental impacts without excessive costs or operational limitation on the facility. An initial set of controls was suggested based on engineering judgement. Selective controls were added as potential problems were identified in dispersion modeling. Table 5 summarizes controls considered for the Brandon Shores Power Plant, together with estimates of control efficiencies employed in dispersion modeling.

3.2 DISPERSION MODELING

In order to accurately represent dispersion of particulate emissions from coal handling, a dispersion model should be able to represent (1) isolated area sources, (2) local turbulence associated with buildings and obstructions, (3) dispersed emissions associated with enclosures and conveyors, and (4) settling and deposition associated with the large particles typically emitted as fugitive dust. Regulatory considerations dictate that the dispersion model also correspond to established U.S. EPA guidelines on dispersion modeling for environmental permitting.(16)

Based on these criteria, the U.S. EPA's ISC Model appears to be a clear choice. The model is flexible enough to account for a variety of source geometries (points, lines, volumes, areas) and specifically accounts for settling and deposition associated with particulates. The ISC Model includes features to account for dispersion due to the mechanical turbulence (downwash) in the wakes of buildings and similar large structures. The downwash algorithm has been extended here to include dispersion associated with area sources which are, in themselves, obstructions to air flow.

The flexibility in specifying source geometry available in ISC was fully utilized in this application. Storage piles were represented as area sources. Sources controlled by baghouses were represented as point sources (without buoyant plume rise) which are subject to building downwash. Sources with controls which do not duct emissions to a specific point were modeled as volume sources, where emissions are assumed to be emitted over the effective cross section of the source.

The particle data needed to determine settling and deposition were based on physical diameters determined from microscopic analysis of hi-vol filters.(6) This corresponds to the implicit definition of TSP as particles subject to hi-vol capture. The continuous particle size distribution observed was divided into three categories: (1) aerosols, (2) slightly settling particles, and (3) rapidly settling particles based on the assumption of stokes settling. Table 6 details the particle size ranges and particle characteristics employed to represent each group.

Receptor Selection

Dispersion modeling requires identification of locations where concentrations are expected to be maximized. Ground level sources will show maximum ground level concentrations near the source. Elevated releases may show maximum ground level concentrations further downwind. Preliminary modeling of the significant sources of fugitive particulates at the Brandon Shores Power Plant yielded the intuitively reasonable result that the release heights of fugitive emissions at Brandon Shores were low enough so that maximum ambient concentrations would be expected at the property line. This corresponds to the nearest source-receptor distance where the NAAQS would apply. Thirty-four receptors were therefore located along the property line. Eight additional receptors were located near the barge unloader at the minimum source-receptor distance recommended for accurate prediction modeling with ISC (100 meters).(17) A total of 42 receptors were located to quantify overall maximum impacts.

Maximum ambient impacts in the designated nonattainment area to the west and north of the plant are anticipated at the nonattainment area boundary. Thirteen receptors were thus located on the boundary. Six receptors were also located at nearby monitoring locations identified in Figure 1. A total of 63 receptors were employed in this analysis.

Meteorological Data

Dispersion modeling employed five years of meteorological data (1964-1968). Surface observations from the Baltimore-Washington International Airport were combined with upper air data from Dulles Airport using the standard U.S. EPA meteorological preprocessor.

Two important anomalies were noted which required corrections. First, extremely low interpolated mixing depths were eliminated because they are not reasonable and because these unreasonable mixing heights affect predictions for low-level releases. Mixing depths from the U.S. EPA meteorological preprocessor were uniformly truncated to a minimum of 75 meters. Second, periods of calm winds recorded in airport data presented both a theoretical problem and a practical problem. In theory, a steady-state Gaussian Dispersion Model does not apply where an established mean flow (wind) does not exist. This problem is typically dealt with by assuming a minimum speed of 1.0 meter per second.

The practical problem is created by the fact that typical airport meteorological instruments cannot measure wind directions accurately at low wind speeds associated with calm conditions. Wind directions are typically assumed to persist over the period of observed calms. This creates the unrealistic situation of multiple hours of persistent wind direction accompanied by low wind speeds.

In any case where prediction of maximum concentrations resulted from this unrealistic representation of calm wind conditions, predictions were reevaluated without the periods of calm winds. The deletion of calm winds provides an important perspective on the limitations of the current state of the art of dispersion modeling.

3.3 BACKGROUND CONCENTRATIONS

Estimating total ambient concentrations associated with a given source requires the inclusion of background concentrations from known and unknown sources which also emit the same pollutants. In the case of particulates, it is impossible to include all other potential sources in dispersion modeling. Ambient concentrations may be dominated by an industrial facility, a highway, a farm, or a wide range of sources. In this situation it is often expedient to make the conservative assumption that high measured background concentrations-- which do not include the proposed facility --added to high predicted concentrations from the proposed facility represent likely maximum total impacts.

Background concentrations representative of the Brandon Shores Plant site were taken from the nearest continuous monitoring station, which is located in the attainment area identified in Figure 1. Measurement data from monitoring stations located in nonattainment areas would obviously show violations of the NAAQS which are assumed not to exist based on the designated attainment status of the Brandon Shores Plant site. In this study, monitoring data for the calendar year 1979 was employed.

Differences in background particulate concentrations should be expected as a function of meteorology. In the case of a pollutant with continuous monitoring data available (e.g., SO_2), background concentrations can be related to specific meteorological conditions. In the case of TSP, which is measured as a daily 24-hour average, this relationship is difficult to define.

The most obvious relationship expected is high ambient concentration associated with a limited range of wind directions. Days of high measured concentrations were examined for persistent meteorological conditions which identify background concentrations as a function of wind direction.

The highest measured concentration (114 ug/m^3) was associated with persistent winds from the south, therefore, this concentration was taken as representative background for receptors to the north of the Brandon Shores Plant site. The second-highest measured concentration (106 ug/m^3) could not be characterized with respect to wind direction. The second-highest measured concentration was thus used to represent background concentrations for all other receptors, as none could be specifically excluded based on meteorological considerations.

4.0 RESULTS

Results of dispersion modeling are evaluated in terms of three regulatory criteria identified above. Prediction modeling generally proceeded from conservative assumptions, which would have unambiguously supported permitting, to better assumptions, which indicate best estimates of projected impacts (but with less conservatism).

Conservative emission factors combined with initial control specifications indicated the potential for exceedence of all three regulatory criteria noted above. While annual average impacts were generally acceptable, appropriate 24-hour impacts were 230 ug/m^3, 124 ug/m^3, and 46 ug/m^3 for the NAAQS, PSD increments, and nonattainment impact, respectively. Examination of source contributions to the predicted concentrations indicated that two sources (inactive storage pile and main yard conveyor) were primarily responsible for the high predicted concentrations. At this point, it was elected to identify more effective controls for these sources based on prediction results.

Additional controls (Phase Two in Table 5) were applied. These controls suggested compliance with the secondary NAAQS; however, applicable PSD increments at the plant boundary and de minimis thresholds for the nonattainment area were both exceeded. Relevant maximum concentrations over five years were predicted to be 43 ug/m^3 and 16 ug/m^3 for PSD increments and nonattainment impact, respectively. It was noted that calm wind conditions contributed significantly to the predicted exceedence of the PSD increment. The predicted PSD increment consumption without calm winds was 40 ug/m^3. Analysis of source contributions to predicted concentrations indicated that the active storage pile area and main yard belt were primarily responsible for predicted high concentrations.

Additional controls were specified for the main yard conveyor (Phase Three of Table 5). Predicted concentrations with additional controls were 40 ug/m^3 and 13 ug/m^3 for PSD and nonattainment impact, respectively.

At this point, it was clear that the conservative assumptions implicit in emission factors employed thus far would not support the permitting of a coal handling facility with conventional fugitive particulate controls. The identical analysis was then conducted using the best estimates of fugitive emission rates identified above.

The control efficiencies for some of the sources were revised for this analysis. These revisions were necessary because, in a few cases, the emission factor itself implicitly accounts for some control. Also, additional information regarding the controls considered for the Brandon Shores Plant became available which necessitated some revision. These revisions are identified in Phase Four of Table 5.

The predicted largest second-highest 24-hour average concentrations at the property line were now 2 ug/m^3. The maximum first highest 24-hour average concentration predicted at the boundary of the nonattainment area was 2 ug/m^3. Both of these concentrations are significantly below the appropriate regulatory criteria. Addition of appropriate background concentrations suggests that ambient air quality standards will also be maintained.

Prediction modeling based on conservative emission factors would have strongly supported environmental permitting. Prediction modeling based on the best estimates does not present as convincing a demonstration of the acceptability of environmental impacts. The analysis does, however, suggest that requirements of extremely stringent controls (e.g., silos for active storage) are not consistent with the best available information concerning fugitive dust emissions.

5.0 DISCUSSION

5.1 RESOLUTION OF PERMITTING FOR THE BRANDON SHORES PLANT

The analysis based on best emission estimates described above demonstrates that the environmental impact from fugitive particulate emissions from coal handling at the Brandon Shores Plant is likely to be well below established regulatory criteria for ambient impacts and low enough to maintain the NAAQS. Analysis based on conservative emission estimates, which are more consistent with regulatory precedent than with scientific evidence, suggests the possibility of significant short term impacts under some conditions. Unfortunately, the conditions associated with maximum impacts are also conditions not treated well by either the conservative emission factors or Gaussian dispersion modeling.

While the possibility of exceedence of applicable regulatory criteria exists, it would seem unreasonable to require extensive (and expensive) controls on the basis of this analysis. The more prudent approach would be to issue environmental permits based on best estimates of environmental impacts. A monitoring program could be established to confirm that environmental impacts are, indeed, acceptable. If problems were identified due to fugitive emissions from coal handling, mitigative measures (e.g. modification of management practices, retrofitting of control equipment, obtaining emission offsets) could be implemented. While there is a risk that more expensive controls would be ultimately required if problems were identified, this risk is more than compensated by the likelihood that environmental impacts will be acceptable.

This course of action was, in fact, pursued at the Brandon Shores Power Plant. The facility received environmental permits with the stipulation that TSP monitors be sited to identify potential maximum impacts from the coal handling facilities.

5.2 LIMITATIONS OF THE METHODOLOGY EMPLOYED

The methodology discussed above did not conclusively predict the environmental impact of fugitive emissions from coal handling. All predictive analyses will be similarly limited by the quality of available emission data and dispersion models.

The requirement of specific controls is a viable alternative. The problem with this approach is that the possibility of minimal impact with little control is not explored and the cost effectiveness of alternative controls for specific problems is not considered.

The regulation of coal handling based on ambient criteria for TSP is difficult. Analytical tools for the analysis must be improved for reasonable and timely permitting based on predicted impacts. Several areas can be readily identified where available analytical tools need improvement. These can be generally classified as problems of estimating emission factors, of control effectiveness, and of dispersion modeling.

Emission Factors

Emission factors specifically for coal handling and storage need to be improved. Demonstrated measurement techniques are probably adequate but the amount of data is not. Material handling emission factors should be based on the full range of typical operating parameters (e.g., drop height). Parameters related to surface moisture and silt content need to be extensively measured in varying climates and/or related to readily available parameters. Some potentially significant sources (e.g., train unloading, crushing) need much more study.

Emission factors for wind erosion need to be related to climate, pile configurations and cumulative erosion. Furthermore, currently available emission factors, which are linearly dependent on wind speed, do not agree with either theoretical relationships or empirical data from wind tunnel testing. At a minimum, more extensive data to quantify the range of variation expected are needed.

Control Effectiveness

Quantification of control effectiveness is extremely important and urgently needed. With the possible exception of baghouses, no controls are quantified. Even baghouses may not be accurately characterized by a simple percentage reduction. Control effectiveness needs to be specified over the range of options available for generic types of control. For example, spray systems should be distinguished on the basis of droplet size (fog vs. spray) and wetting agents.

Dispersion Modeling

Dispersion models employed in regulation development have not been extensively validated for impacts from low-level, non-buoyant releases of particulates near flow obstructions. The area source algorithm (critical to this analysis) has not been validated at all.

Several problems with conventional dispersion modeling are magnified by the situation here. Plume dimensions based on 3-minute average data produce extremes (high and low) of impact at short source-receptor distances when assumed representative of one-hour averages. Near field dispersion from mechanical turbulence near ground level (typical of industrial facilities) is completely neglected except in the context of building downwash. Treatment of extremely low wind speed conditions is neither physically reasonable nor empirically accurate. These problems are of lesser importance for stack-type emissions than for fugitive particulates. It is not surprising that new applications of dispersion models lead to new problems in their application.

In summary, the current state of the art of fugitive dust analysis has provided an adequate quantitative description of fugitive emmisions and resulting ambient impacts from a proposed coal handling facility. An informed regultory decision which accounted for inevitable uncertainties resulted. Much productive work remains, however, which can narrow the range of uncertainty and expedite the consideration of fugitive dust in environmental permitting.

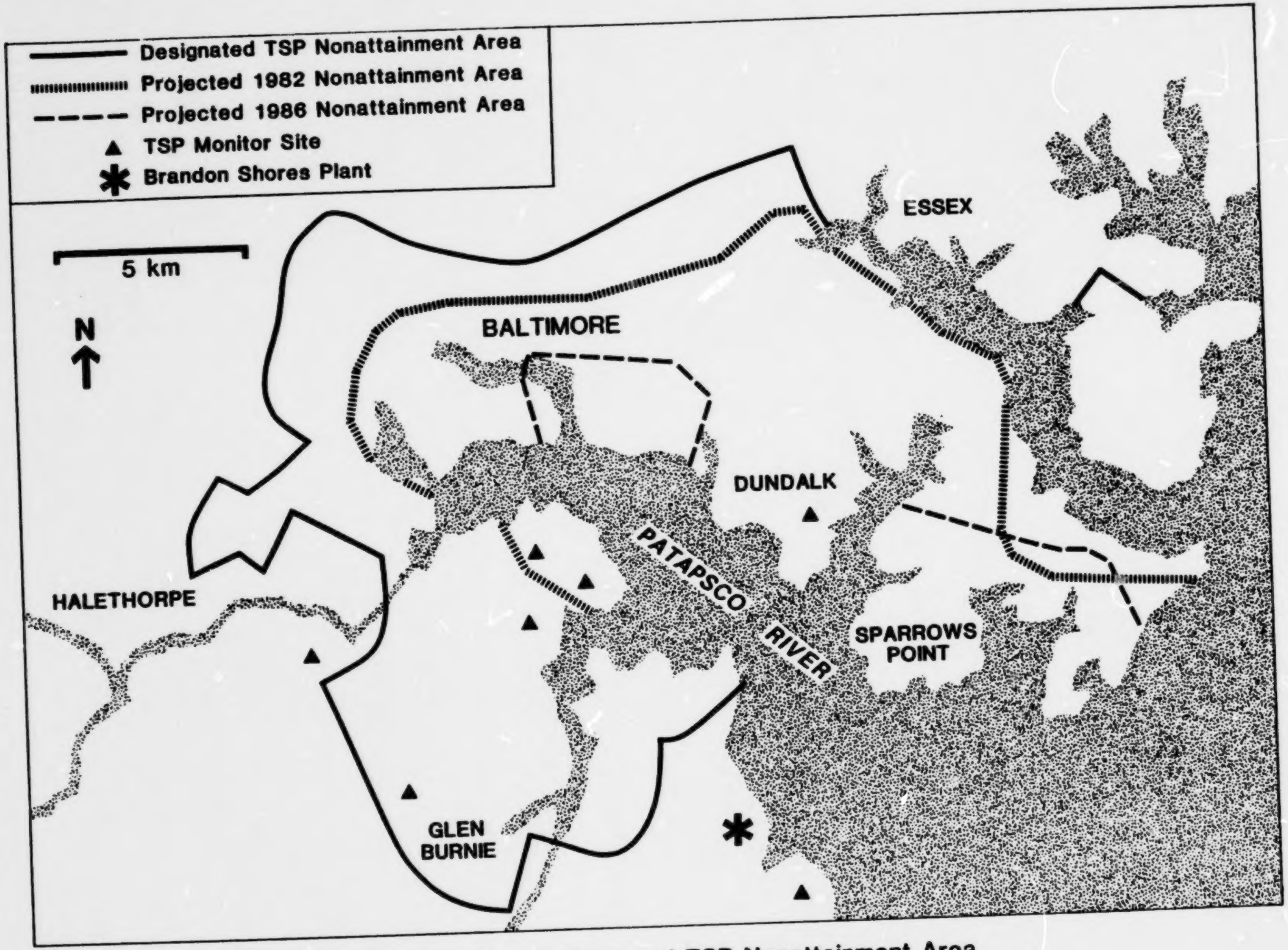
Designated TSP Nonattainment Area
Projected 1982 Nonattainment Area
Projected 1986 Nonattainment Area
▲ TSP Monitor Site
✱ Brandon Shores Plant
5 km
N
ESSEX
BALTIMORE
DUNDALK
PATAPSCO RIVER
SPARROWS POINT
HALETHORPE
GLEN BURNIE

Figure 1: Location of the Brandon Shores Plant and TSP Nonattainment Area

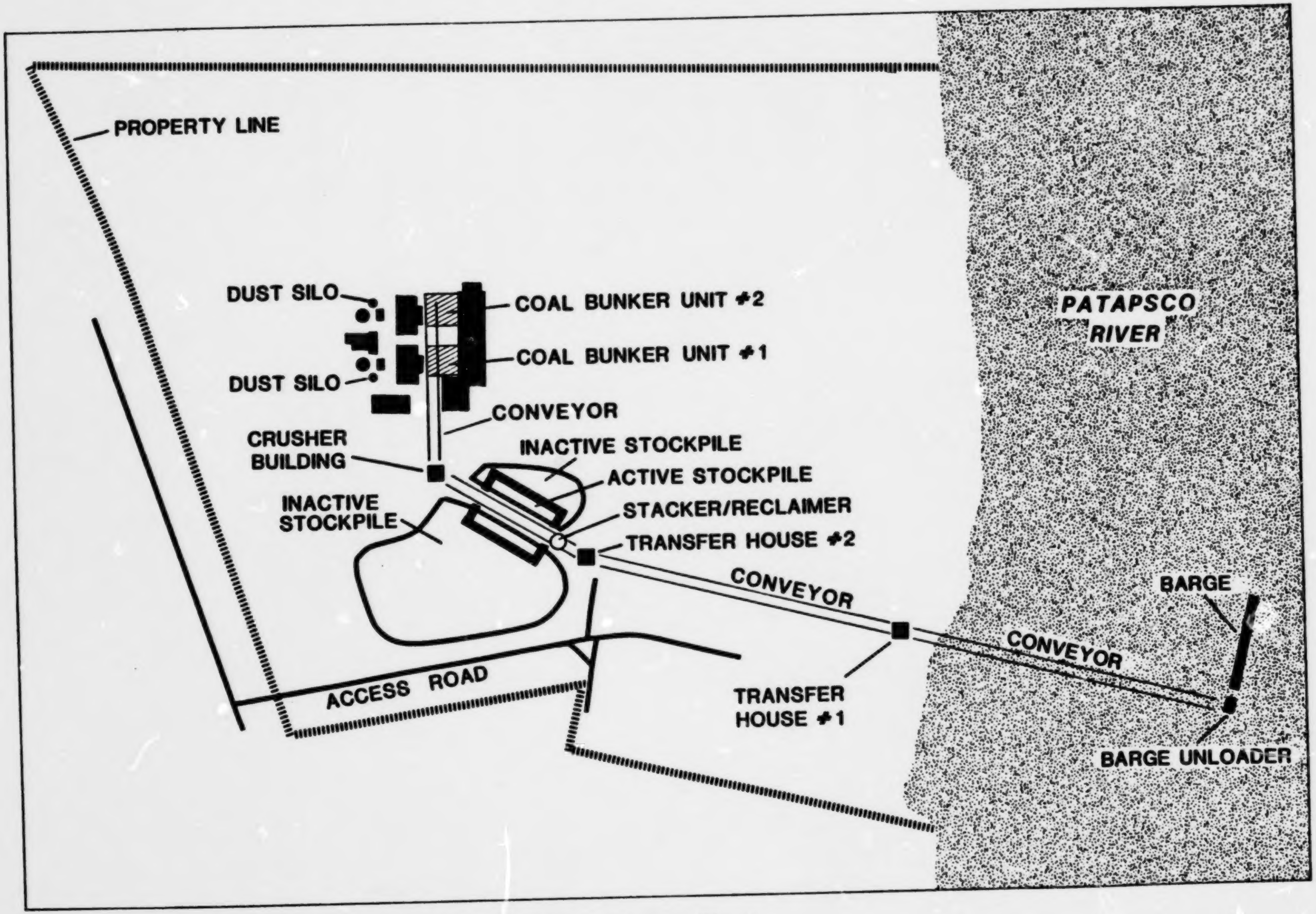
PROPERTY LINE
DUST SILO
COAL BUNKER UNIT #2
COAL BUNKER UNIT #1
DUST SILO
CONVEYOR
CRUSHER BUILDING
INACTIVE STOCKPILE
ACTIVE STOCKPILE
INACTIVE STOCKPILE
STACKER/RECLAIMER
TRANSFER HOUSE #2
CONVEYOR
ACCESS ROAD
TRANSFER HOUSE #1
CONVEYOR
PATAPSCO RIVER
BARGE
BARGE UNLOADER

Figure 2: Coal Handling System at the Brandon Shores Plant

TABLE 1: REGULATORY CRITERIA FOR EVALUATING AMBIENT IMPACT

Criterion	Critical Concentration ($\mu g/m^3$) 24-Hour Basis	 Annual Basis
Clean Areas		
NAAQS (Secondary)	150*	60
PSD Increment	37*	19
Nonattainment Areas		
Impact Threshold	5**	1

* Maximum Second-Highest
** Maximum First-Highest

TABLE 2: CRITERIA FOR FUGITIVE PARTICULATE EMISSION FACTORS

Quality Index	Criteria
A	Based on a statistically representative number of accurate field measurements of a specific process which span expected ranges of parameters
B	Based on a limited number of accurate field measurements of a specific process
C	Based on a limited number of field measurements of a specific process with undetermined accuracy -- or on -- extrapolation of B-rated data from a similar process
D	Estimate based on professional judgment
E	Assumption

TABLE 3: SUMMARY OF EMISSION FACTORS FOR COAL HANDLING AND ASH HANDLING EMISSIONS

Source	Conservative Factor (lb/ton)	Estimated Quality Index	Best Factor (lb/ton)	Estimated Quality Index
Barge Unloader	0.4	D	2.56×10^{-3}(1)	C
Transfers	0.15(2)	D	1.31×10^{-3}(1)	B
Conveyors	0.05(2)	E	4.32×10^{-4}(3)	E
Crusher	0.2	E	0.06	D
Bunkers	0.15	E	3.60×10^{-3}(1)	B
Active Storage Pile Load-In	.028(4)	D	2.18×10^{-4}(1)	B
Active Storage Pile Reclaim	.035(5)	D	2.18×10^{-4}(1)	C
Active Storage Pile Wind Erosion	.320(6)	C	.091u(7) (lb/acre-hr)	B
Inactive Storage Pile Wind Erosion	.320(6)	C	.091u(7) (lb/acre-hr)	B
Fly Ash Unloading	0.30(8)	D	5.08×10^{-4}(2)	C(9)
Fly Ash Storage	0.30(8)	D	.288(1)	C(9)

Notes to Table 3:

(1) Emission factor determined from:

$$(0.0018(S/5)(U/5)(H/10))/(M/2)^2$$

TABLE 3: SUMMARY OF EMISSION FACTORS FOR COAL HANDLING AND ASH HANDLING EMISSIONS

(Continued)

where:

S = Silt content of material in percent (varies)
U = Average wind speed (9.5 mph)
h = Drop height in feet (varies)
M = Surface moisture content in percent (varies)

(2) Based on 0.2 lb/ton for all transfers and conveyors with the assumption that 25% of the total emissions are due to conveyors.

(3) Assumed to be 33% of transfer emissions detemined with the emission factor equation in Note 1. This corresponds to 25% of total emissions from transfer and conveying, as assumed for conservative emission factors.

(4) Emission factor determined from:

$0.04/(PE/100)^2$ (lb/ton)

where

PE = Thornthwaite's precipitation - evaporation index (118 for Baltimore area)

(5) Emission factor determined from:

$0.05/(PE/100)^2$ (lb/ton)

(6) Emission factor determined from:

$(0.11/(PE/100)^2)\ (D/90)$ (lb/ton)

where D = duration of material in storage (365 days)

(7) Emission factor determined from:

$A\ (1.6u)\ (PE_{PEDCo}/PE_{BALTIMORE})^2$ (lb/acre-hr)

where:

A = Activity factor = .33
U = Hourly mean wind speed (m/s)
PE_{PEDCo} = Mean PE index for PEDCo field studies = 49
$PE_{BALTIMORE}$ = Mean PE index for Baltimore area = 118

(8) Personal communication with Mr. William Wagner of U.S. EPA Region IV.

(9) Substantial extrapolation from another material involved.

TABLE 4: ESTIMATES OF ANNUAL EMISSIONS WITH ALTERNATIVE EMISSION FACTORS BASED ON FINAL CONTROL

Source	Conservative Estimate tons/year	Best Estimate tons/year
Barge Unloader	6.0	0.2
Transfers	1.1	0.3
Conveyors	6.4	0.2
Crusher	1.5	0.4
Bunkers	0.9	<.1
Active Storage Pile Load-in	5.4	<.1
Active Storage Pile Reclaim	5.4	<.1
Active Storage Pile Wind Erosion	1.0	0.7(1)
Inactive Storage Pile Wind Erosion	4.3	1.2(1)
Fly Ash Unloading	1.5	<.1
Fly Ash Storage	0.2	.2
Total	33.7	3.6

Notes to Table 4:

(1) Based on an annual average wind speed of 9.5 miles per hour.

TABLE 5: SPECIFICATION OF CONTROLS FOR THE BRANDON SHORES PLANT

Source	Control Method	Efficiency (%)
Phase One		
Barge Unloader	Enclosed with baghouse dust collection system and water sprays	99
Conveyor (Barge Unloader to Transfer House #1)	Enclosed conveyor and gallery	99
Conveyor (Transfer House #1 to Transfer House #2)	Hooded conveyor with wind break return	90
Transfer Houses #1 and #2 and Crusher Building	Totally enclosed with baghouse dust collection	99
Main Yard Conveyor	Uncontrolled	-
Active Storage Pile Load-in	Stacker spray system	75
Active Storage Pile Reclaim	Reclaimer spray system	80
Conveyor (Crusher to Unit No.1 Bunker House)	Enclosed	70
Coal Bunkers	Enclosed with baghouse dust collection	99
Fly Ash Storage	Enclosed in silo with baghouse dust collection	99
Fly Ash Handling	Wet suppression from enclosed rotary unloader	95

TABLE 5: SPECIFICATION OF CONTROLS FOR THE BRANDON SHORES PLANT

(Continued)

Inactive and Active Storage Pile Wind Erosion	Uncontrolled	-
Phase Two		
Inactive Storage Pile Wind Erosion	Crusting Agent	95
Main Yard Conveyor	Water spray	50
Phase Three		
Main Yard Conveyor	Foam suppressant	75
Phase Four		
Barge Unloader	Enclosure with wetting agents	95(1)
Conveyors (except main yard conveyor and the conveyor from Transfer House #1 to Transfer House #2)	Enclosed conveyors and galleries	99.5
Main Yard Conveyor	Foaming agent, wind shields and hooded conveyor/wind break return	90/87.5(2)
Transfer Houses, Coal Bunkers and Crusher	Enclosed with baghouse dust collection	99.5
Active Storage Pile Load-in	Stacker spray system	67(3)

TABLE 5: SPECIFICATION OF CONTROLS FOR THE BRANDON SHORES PLANT

(Continued)

Active Storage Pile Reclaim	Reclaimer spray system	67(3)
Fly Ash Storage	Enclosed in silo with with baghouse dust collection	99.5
Fly Ash Unloading	Wet suppression from enclosed rotary unloader	90(4)
Active Storage Pile Wind Erosion	Wind activated spray system with wetting agents	90

Notes to Table 5:

(1) Based on the average control for the two transfers, conveyor and the scoop which are part of the barge unloader.

(2) First figure refers to load-in. Second figure refers to reclaim. Differences arise because different fractions of the conveying system are enclosed during each operation.

(3) These figures are less than those used for the conservative emission estimates (75% load-in, 80% reclaim) because part of the control mechanism is explicitly accounted for in the "uncontrolled emissions" determined from the best emission estimates.

(4) Control is for enclosure only. Control from uniform moisture addition is accounted for in estimating "uncontrolled emissions".

TABLE 6: REPRESENTATIVE PARTICLE PROPERTIES USED IN DISPERSION MODELING

Mass Fraction (%)	Representative Particle Diameter	Reflection Coefficient	Settling Velocity (m/sec)
16	7.07 um	.97	2.0075×10^{-3}
54	19.31 um	.7375	1.498×10^{-2}
30	40.33 um	.5812	6.533×10^{-2}

REFERENCES

(1) U.S. EPA, Emission Trading Policy Statement, 47 FR 15076, April 7, 1982.

(2) Maryland State Department of Health and Mental Hygiene, Air Quality Program. *Plan for Implementation of the National Ambient Air Quality Standards for Total Suspended Particulate Matter, Photochemical Oxidants and Carbon Monoxide for the Metropolitan Baltimore Intrastate Air Quality Control Region*, December 15, 1978.

(3) Bohn, R., Cuscino, T. and Cowherd, C. "Fugitive Emissions from Integrated Iron and Steel Plants," U.S. EPA Contract #68-02-2120 (Midwest Research Institute), Research Triangle Park, N.C., March 1978, EPA-600/2-78-505.

(4) Cowherd, C., Jr. et al. *Development of Emission Factors for Fugitive Dust Sources*, U.S. EPA, OAQPS, EPA-450/3-74-037, June 1974.

(5) Cowherd, C., Jr. et al. *Iron and Steel Plant Open Source Fugitive Emission Evaluation*, U.S. EPA, IERL, EPA-600/2-79-103, May 1979.

(6) PEDCo-Environmental Inc. *Survey of Fugitive Dust from Coal Mines*, U.S. EPA, Region VIII, Office of Energy Activities, EPA-908/1-78-003, February 1978.

(7) Chepil, W.S. "Influence of Moisture on Erodability of Soil by Wind," *Soil Science Society Proceedings*, pp. 289-292, 195[illegible]

(8) PEDCo-Environmental, Inc. *Technical Guidance for Control of Industrial Process Fugitive Particulate Emissions*, U.S. EPA Contract #68-02-1375, Research Triangle Park, N.C. March 1977, EPA-450/3-77-010.

(9) United Nations. *Air Pollution by Coking Plants*, United Nations Report SECE/COAL/26, 1968.

(10) Johns Hopkins University, Applied Physics Laboratory. *Fugitive Dust Emissions from the Proposed Vienna Unit No. 9*, Prepared for the Maryland Power Plant Siting Program, JHU/PPSE 8-14, February 1981.

(11) Gillette, D. "Tests with a Portable Wind Tunnel for Determining Wind Erosion Threshold Velocities," *Atmospheric Environment*, Vol. 12, No. 12, pp. 2309-2313, December 1978.

(12) Chepil, W.S. "Dynamics of Wind Erosion: II. Initiation of Soil Movement," *Soil Science*, Vol. 60, No. 5, P.397-411, 1945.

(13) U.S. EPA. Compilation of Air Pollutant Emission Factors, Third Edition (including Supplements 1-10), U.S. EPA, OAQPS, February 1980.

(14) Jutze, G.A. et al. Evaluation of Fugitive Dust Emissions from Mining, U.S. EPA, IERL, EPA-600/9-76-001 (Contract Nos. 68-02-1321, Task No. 36), June 1976.

(15) W.P. Reefe. Emission Factors For Mining Operations, Colorado Department of Health, Air Pollution Control Division, Denver, Colorado , Unpublished, March 1978, Cited by Currier, E.L., and B.D. Neal. "Fugitive Emission from Coal-Fired Power Plants," Air Pollution Control Association, Proceedings of the 72nd Annual Meeting (Cincinnati, Ohio, 1979), Publication 79-11.4.

(16) U.S. EPA. Regional Workshops on Air Quality Modeling: A Summary Report, U.S. EPA, OAQPS, April 1981.

(17) Bowers, J.F., et al. Industrial Source Complex (ISC) Dispersion Model User's Guide, U.S. EPA, Source Receptors Analysis Branch, EPA-450/4-79-030, December 1979.

The work described in this paper was not funded by the U.S. Environmental Protection Agency. The contents do not necessarily reflect the views of the Agency and no official endorsement should be inferred.

INHALATION PATHWAY RISK ASSESSMENT OF HAZARDOUS WASTE INCINERATION FACILITIES*

GREGORY A. HOLTON**

THE MAXIMA CORPORATION
OAK RIDGE, TENNESSEE

CURTIS C. TRAVIS
ELIZABETH L. ETNIER
FRANCIS R. O'DONNELL

OAK RIDGE NATIONAL LABORATORY
OAK RIDGE, TENNESSEE

(*) Although this is not the actual presentation made at the May 1982 meeting, it closely resembles that presentation, which was entitled, "A Determination of the Impact of Fugitive VOC Emissions from a Municipal Hazardous Waste Incinerator on the Surrounding Community," G. Holton (Oak Ridge National Laboratory) and L. Staley (EPA/IERL-Cin).

(**) Current address: First Environment, 314 W. Broadway, Lenoir City, TN 37771.

1. INTRODUCTION

One objective of quantitative risk assessment is to arrive at a value or, more realistically, a range of values that describe the possible adverse effects on human health associated with low, chronic exposure to a known or suspected toxic substance. There is increasing impetus to use risk assessment to prioritize research needs in health and environmental areas. Quantitative risk assessment typically consists of two components, the measurement or estimation of the concentrations of pollutants to which a population will be exposed and an estimation of resultant health effects based on available dose-response relationships. These two components are called exposure assessment and health effects assessment, respectively.

Exposure assessment is defined as the determination of the concentration of toxic materials in space and time at the interface of target populations. This description should include identification of all major pathways (air, water, and soil) for movement and transformation of a toxic material in a selected environmental setting. The present assessment focuses only on atmospheric concentrations and exposure via the inhalation pathway.

Health effects assessment consists of relating population exposure to such potential human health impacts as carcinogenicity, mutagenicity, teratogenicity, or neurotoxicity. Unfortunately, adequate data for assessing excess human risk resulting from exposure to most toxicological substances do not exist.

The U. S. Environmental Protection Agency is conducting research to determine air concentrations, public inhalation exposure, and health risk resulting from chemicals emitted during incineration of hazardous wastes. Incineration facilities produce stack and fugitive (non-stack) atmospheric emissions. The magnitude of public exposure to such emissions is dependent on both plant design and operation as well as the physicochemical properties of the waste. Engineering variables include facility design, size, destruction and removal efficiency (DRE), and emission source strength (stack vs fugitive). Physiocochemical waste variables include incinerability, volatility, and toxicity. The present assessment was performed to determine the relative importance of these variables to human inhalation exposure and health risk.

It should be emphasized that both the exposure assessment and health effects assessment methodologies presented in this paper are very generalized, and caution should be exercised in interpreting the results. Site-specific application of our results would require careful evaluation of the extent to which the models and parameter values used in this paper are representative of conditions prevailing at the specific site.

2. INCINERATION FACILITY DESIGN

In the United States, there are at least 219 facilities operating 284 hazardous waste incinerators of varying design and capacity. The liquid injection (LI) design is the most common type of hazardous waste incinerator (51%) employed in the United States. Liquid injection incinerators can be applied to virtually all liquid wastes (liquid, slurries, sludges). Liquid injection systems employ a waste nozzle (burner) which atomizes the waste and mixes it with air to form a suspension that promotes complete combustion. Atomization is achieved mechanically or by pressure atomization systems using high-pressure air or steam.[2]

The rotary kiln (RK) design is employed at 7% of the incineration facilities in the United States.[1] A rotary kiln is a cylindrical refractory-lined shell mounted at a slight incline from the horizontal plane. Rotation of the shell provides for movement of the waste through the kiln as well as for enhanced mixing. Rotary kilns can be applied to both liquid and solid wastes.[2]

Three incinerator sizes (1, 10, 150 x 10^6 Btu/h) were chosen for analysis to provide a profile of existing incinerator capacities. Two facility designs (liquid injection and rotary kiln) for each of the three sizes were selected.

Facility design may be important in determining fugitive emmisions, since such emissions are dependent on the number of pumps, tanks, valves and flanges in operation. Each incineration facility was designed following a review of existing-practice incinerators. For example, the hypothetical 150 x 10^6 Btu/h incinerator used in this study was assumed to possess one receiving tank for each of four categories of waste: clean or dirty high-Btu waste and clean or dirty low-Btu waste (dirty waste is any waste that requires pretreatment to enhance viscosity). Two additional tanks were included to provide extra storage capacity for irregular shipments. The storage area of the facility was designed with sufficient capacity for 14 days continuous operation. The feed area was assumed to have sufficient storage for three days of operation. Other design factors such as piping or numbers of pumps were also considered.

A compilation of important facility design parameters is presented in Table I. Equipment quantities and operating assumptions for the receiving area are identical for both incinerator types, but vary slightly with size. The number of storage tanks in the storage and feed areas remains the same for all sizes of incinerators, but the holding capacity of the tanks increases. The number of pumps, valves, and flanges are identical in the storage and feed areas of the 10 and 150 x 10^6 Btu/h incinerators. Since these areas are the major contributors to fugitive emissions, one should not expect a large change in fugitive emissions as a function of incinerator size.

3. WASTE CHARACTERIZATION AND EMISSION RATES

Operation of a commercial incinerator is characterized by receipt of waste of widely varying composition. Except in settings where an incinerator is dedicated to a particular chemical process waste stream, a detailed qualitative or quantitative makeup of the waste being burned is usually unknown. The EPA has funded several surveys to determine the composition of hazardous waste streams currently being incinerated. A total of 237 different constituents have been identified as present in one or more of the 413 hazardous waste streams reviewed. Table II lists the ten most prevalent constituents of hazardous waste streams currently being incinerated, according to the most recent survey.[3] Unfortunately, data from this survey were not available when this assessment was performed.

To deal with the uncertainties inherent in the characterization of incineration waste streams, it was decided to examine the behavior of representative chemicals from three generic waste classes. To choose these waste classes, data from an earlier survey of industrial wastes[4] were analyzed and grouped by incinerability characteristics. Incinerability in this report is defined as the inherent heating value (Btu/lb) of the waste before fuel oil is added. The three waste groups selected for study, in order of increasing incinerability were: (1) pesticide-related chemicals (3,021 Btu/lb); (2) API separator sludge chemicals (4,049 Btu/lb); and (3) phenol/acetone distillation chemicals (15,850 Btu/lb). Four chemicals from each waste group were selected for analysis. Criteria for choosing specific chemicals were high and low volatility, high and low toxicity, and prevalence of the chemical in U. S. industrial waste streams. The chemicals chosen for the three waste groups were: (1) chloroform, ethylene dichloride, hexachlorabutadiene, and 1,1,2,2-tetrachloroethane; (2) chromium, lead, arsenic, and phenol; and (3) toluene, pyridine, phthalic anhydride, and methyl styrene.

The rate of release (mass per unit time) of specific chemicals in stack emissions is controlled by three facility variables: waste throughput, chemical concentration in the waste stream, and DRE. Waste throughput in an incineration facility is determined by the percent contribution of the waste to the total waste stream after supplementary addition of No. 2 fuel oil to insure combustibility. If the waste has a high enough Btu content (10,000 Btu/lb) to burn without the addition of supplementary fuel (as is the case with phenol/acetone distillation waste), no additional fuel oil was assumed.

To determine the effect of DRE on human exposure and risk estimates, three scenarios were chosen. These scenarios were 99.99, 99.9, and 99.0%. An additional analysis of 95.0% DRE for arsenic, chromium, and lead was performed. Predicted annual incineration rates (MT/y), and annual stack emission rates (g/y) for the 99.99% DRE scenario are given in Table III.

Fugitive emissions consist of tank, pump, in-line valve, open-ended valve, flange, instrument connection, and sampling connection emissions from the receiving, storage, and feed areas of the incinerator. Fugitive emissions were calculated using Monte Carlo procedures reported elsewhere.[5] Expected total fugitive emission rates for each chemical are given in Table III. It should be emphasized that these chemical-specific fugitive emission rates are only first approximations. An exact methodology for estimating volatilization rates of specific chemicals in complex mixtures does not exist.

4. EXPOSURE ASSESSMENT

4.1 SITE DESCRIPTION

The location chosen for this assessment was a hypothetical northern Midwest site (S-1) located in Marathon County, Wisconsin at 44° 55' latitude and 115° 30' longitude. This site is located in a rural area adjacent to several large cities. Thus, even though the total population within 100 km of the site is 0.45×10^6 people, there are no people residing within 875 m of the incinerator site (see Table IV). This location is neither a current nor a planned incineration facility site.

A circular area of 100-km radius around the incinerator facility was assumed for the assessment. Exposure and risk due to long-range transport (greater than 100 km) was not performed in this assessment. Although long-range transport can significantly contribute to total population exposure by incorporating large population centers, the average individual exposure to such transported materials is very low (orders of magnitude less than background in some cases).

4.2 ATMOSPHERIC TRANSPORT MODELS

Annual-average ground-level air concentrations of representative chemical pollutants were estimated using IEM, an automated inhalation exposure methodology.[6] This methodology employs a slightly modified version of the Industrial Source Complex Long Term Model (ISCLTM), a Gaussian plume model developed for EPA.[7]

A circular area of 100-km radius around the incinerator facility was assumed for the assessment. Gaussian plume models are generally applied for distances of 20-50 km around a site. However, this type of dispersion model has been validated out to 150 km over flat terrain at one location,[8] predicting annual-average air concentrations within a factor of three of those measured.

The assessment area was divided into sector segments consisting of 20 concentric circles about the origin and sixteen radial direction vectors. The circles had radii of 0.15, 0.25, 0.50, 0.75, 1.0, 2.0, 3.0, 4.0, 5.0, 7.5, 10, 20, 30, 40, 50, 60, 70, 80, 90, and 100 km. Each radial vector was separated by 22.5° intervals with the first sector being centered on due north (0°), and proceeding clockwise. ISCLTM was then employed to calculate concentration estimates at segment centroids.

The total exposure in a sector segment is calculated by multiplying the annual-average ground level air concentration at the segment centroid by the number of persons located in the segment, as obtained from 1980 Census data tapes using an adaptation of the APORT computer code.[9]

4.3 MODEL INPUT PARAMETERS

IEM input parameters include model plant descriptors, pollutant behavior variables, and region-specific meteorological data. Each of the six hypothetical incineration facilities (two designs in three sizes) was assumed to contain four separate emission sources: a stack and three area sources (the receiving, storage, and feed areas). The stack was located at the center of the circular grid (site origin), and the area sources were represented as square areas centered on the origin. This potentially artificial area source configuration of squares was necessitated by IEM modeling constraints and will not affect pollutant concentration estimates unduly. Each area was centered on the stack to simplify computation and to prevent possible bias of atmospheric dispersion estimates. Stack and area source quantities are summarized in Table I. Inspection of these values shows that stack and receiving parameters are identical for both designs. However, differences in area, width, and generic gas emission rates for the storage (10 and 150 x 10^6 Btu/h sizes) and feed (150 x 10^6 Btu/h size) areas do occur between designs because of size and number of storage tanks. The specific parameters employed are summarized in Table V.

Region-specific meteorological data were obtained from Stability Array (STAR) data tapes[10] and from a compendium of weather statistics[11]. The STAR data were organized into six Pasquill stability categories (A through F) and six wind speed classes with average wind speeds of 0.75, 2.5, 4.3, 6.8, 9.5, and 12.5 m/s. The remaining meteorological parameters were obtained or derived from Ruffner (1978). For the principal site they include an average air temperature of 280.2° K and mixing layer heights of 1819.5, 1213.0, 1213.0, 1024.3, 10000.0, and 10000.0 m for stability categories A through F, respectively. Mixing layer heights were assumed equal for all wind speed classes within each stability category.

Site-specific population data were obtained from 1980 Census data tapes that had been reformatted into coarse and fine rectangular latitude/longitude grids. Approximately 0.45 x 10^6 people reside within a 100-km radius around the generic site.

5. HEALTH EFFECTS ASSESSMENT

A key component of health effects assessment is the determination of human health response to a given exposure. Quantification of the exposure-response relationship can be made in an number of ways, depending on the availability of data and the health impact under consideration. There are many potential health endpoints in humans, including carcinogenicity, mutagenicity, and teratogenicity. Unfortunately, adequate human data for assessing risk to most toxicological endpoints do not exist, although a wealth of animal data are available for selected endpoints.

Toxicity data employed in this assessment are taken from a health effects assessment summary for 300 hazardous organic constituents prepared by EPA's Environmental Criteria Assessment Office (ECAO).[12] Chemicals studied were classified as either carcinogens or non-carcinogens, and separate measures of toxicity were developed for these two classes. Carcinogenic toxicities are etimated in terms of lifetime excess cancer risk factors, while noncarcinogenic toxicity is estimated by acceptable daily intake (ADI), and threshold limit values (TLV).

Health effects data for compounds considered in this assessment are summarized in Table VI. It is apparent that not all health risk estimators are available for each chemical studied. The estimate of excess human lifetime risk to cancer was used for all compounds in the pesticide-related waste. In the absence of cancer risk estimates, the available ADI value was used for all compounds in the API separator sludge waste except for arsenic; the TLV[13] was converted to an ADI for arsenic and for compounds in the phenol/acetone distillation waste for which there is no reported ADI.

6. RESULTS AND CONCLUSIONS

The purpose of this assessment was to determine the relative importance of plant design and waste physicochemical variables on human inhalation exposure and health risk resulting from hazardous waste incineration. A hypothetical waste incineration site in the northern Midwest was chosen for analysis. This site has a population of 0.45 x 10^6 persons, with the closest individuals residing 1500 m from the incineration site.

To account for engineering variables, two facility designs (liquid injector and rotary kiln) of three sizes (1, 10, and 150 x 10^6 Btu/h), each burning three generic wastes, were selected. These are designated LI-1, LI-10, LI-150, and RK-1, RK-10, and RK-150, respectively. Three levels of destruction and removal efficiency (DRE) were considered (99.0, 99.9 and 99.99% DRE). The three waste groups selected for study, in order of increasing incinerability were: (1) pesticide-related chemicals (chloroform, ethylene dichloride, hexachlorobutadiene, and 1,1,2,2-tetrachloroethane); (2) API separator sludge chemicals (arsenic, chromium, lead, and phenol) and (3) phenol/acetone distillation chemicals (toluene, pyridine, phthalic anhydride, and methyl styrene).

Annual-average ground level air concentrations of representative chemical pollutants were estimated using IEM, an automated inhalation exposure methodology.[5] Air concentrations were estimated for both stack and fugitive emissions using region-specific meteorological and climatological data.

Estimates of individual and total population exposure resulting from incineration of hazardous materials were calculated by multiplying ground-level air concentrations by site-specific population data obtained from the 1980 Census. Estimates of risk associated with incineration of hazardous materials were obtained by multiplying the population exposure estimates by health risk estimators supplied by the U. S. Environmental Protection Agency (EPA) Environmental Criteria Assessment Office (ECAO). Chemicals studied were classified as either carcinogens or noncarcinogens, and separate measures of toxicity were used for those two classes. Carcinogenic toxicities are measured in terms of lifetime excess cancer risk, while noncarcinogenic toxicity is measured in terms of acceptable daily intake (ADI). Estimates of life-time excess cancer risk were used for chloroform, ethylene dichloride, hexachlorobutadiene, 1,1,2,2-tetrachloroethane, and arsenic. The ADI value was used for chromium, lead, phenol, toluene, pyridine, phthalic anhydride, and methyl styrene.

Major conclusions to be drawn from this report are:

1. Fugitive emissions may be an important contributor to total polllutant emission rates. The largest contribution occurs when stack emission rates are lowest, that is for small incinerators (1 x 10^6 Btu/h) with DRE's ranging from 99.9 to 99.99%. For large incinerators, fugitive emissions are a relatively unimportant contributor to total emissions at all DRE's studied (Table VII). Caution should be used in interpreting these results as it appears that the fugitive emission predictions in this report may be higher than those actually experienced at incinerator sites.

2. Total population exposure is relatively insensitive to changes in DRE for small incinerators (1 x 10^6 Btu/h), increasing by only a factor of 7 from 99.99 to 99.0%. Total population exposure to volatile compounds is sensitive to incinerator size for low DRE's (99.0%) and is relatively insensitive to incinerator size for high DRE's (99.99%) (see Table VIII).

3. For all chemicals studied, human health risk from incineration was small. For incineration of pesticide-related waste at a site with a population of 0.45 x 10^6, expected number of cancers over 70 years are less than 1.6 x 10^{-3} for a DRE of 99.99% (see Table IX). The excess cancer risk over 70 years to the maximally exposed individual at site S-1 from incineration of pesticide-related waste is less than 1.2 x 10^{-7} for a DRE of 99.99% (see Table X).

4. None of the four selected constituents of the phenol/acetone distillation wastes are known carcinogens. Therefore, using the ADI as a measure of noncarcinogenic risk, estimates of average daily intake as a fraction of the ADI were made. These risk estimates, which account for both stack and fugitive emissions, are highest for pyridine releases from 150 x 10^6 BTU/lb plants, but even these risk values are less than 10^{-7} of the ADI (see Table XI).

5. Risk to exposed individuals (as a fraction of ADI) from incineration of heavy metals is small (see Table XII). Even for the maximally exposed individual, all inhalation exposures to heavy metals result in average daily intakes which are at least 6 orders of magnitude less than the acceptable daily intake.

7. REFERENCES

[1] Keitz, E. L., L. J. Boberschmidt, and C. C. Lee, "A Profile of Existing Hazardous Waste Incineration Facilities," MITRE Corporation, McLean, Virginia (1982 — in preparation).

[2] Bonner, T., B. Desai, J. Fullenkamp, T. Hughes, E. Kennedy, R. McCormick, J. Peters, and D. Zanders, Engineering Handbook for Hazardous Waste Incineration, EPA Contract No. 68-03-2550, Monsanto Research Corporation, Dayton, Ohio (1980).

[3] MITRE Corporation, "Composition of Hazardous Waste Streams Currently Incinerated." Working paper (1983).

[4] U. S. Environmental Protection Agency, Background Document, Resource and Recovery Act, Subtitle C, Identification and Listing of Hazardous Waste, Office of Solid Waste, Washington, D.C. (1980).

[5] Holton, G. A. and C. C. Travis, "A Methodology for Predicting Fugitive Emissions for Incinerator Facilities," Proceedings, 1983 National Meeting of the American Institute of Chemical Engineers, Washington, D.C. (November, 1983).

[6] O'Donnell, F. R., and G. A. Holton, "An Automated Methodology (IEM) for Assessing Inhalation Exposure to Hazardous Waste Incineration Emissions," Incineration and Treatment of Hazardous Waste: Proceedings of the 9th Annual Research Symposium at Fort Mitchell, Kentucky, May 2-4, 1983, U. S. Environmental Protection Agency, Cincinnati, Ohio (in press).

[7] Bowers, J. F., J. R. Bjorklund, and C. S. Cheney, Industrial Source Complex (ISC) Dispersion Model User's Guide, (Volume I), EPA-450/4-79-030, U. S. Environmental Protection Agency, Research Triangle Park, North Carolina (1979).

[8] Buckner, M. R. (ed.), Proceedings of the 1st SRL Model Validation Workshop, Nov. 19-20, 1980, Hilton Head, S. C., Savannah River Laboratory, DP-1597 (1981).

[9] Fields, D. C. and C. A. Little, APORT — A Program for the Area-Based Apportionment of County Variables to Cells of a Polar Grid, ORNL/TM-6418, Oak Ridge National Laboratory, Oak Ridge, Tennessee (1978).

[10] National Oceanic and Atmospheric Administration, Seasonal and Annual Distribution by Pasquill Stability Classes STAR Program, National Climatic Center, U. S. Department of Commerce, Asheville, North Carolina, 1974.

[11] Ruffner, J. A., Climates of the States, Vols. I and II, Gayle Research Company, Book Tower, Detroit, Michigan (1978).

[12] "U. S. Environmental Protection Agency, Environmental Criteria Assessment Office, Health Effects Assessment Summary for 300 Hazardous Organic Constituents in Support of Regulatory Impact Analysis of the Land Disposal Branch (LDB) and Interim Final Incinerator Regulations of the Technical Branch (TB) of the Office of Solid Wastes," OSWER/EPA (1982).

[13] American Conference of Governmental Industrial Hygienists, TLVs - Threshold Limit Values for Chemical Substances and Physical Agents in the Workroom Environment with Intended Changes for 1974, Cincinnati, Ohio (1974).

Table I. Expected equipment quantities and operating assumptions for each incineration facility design

	Rotary kiln			Liquid injector		
	Size, 10^6 Btu/h					
	1	10	150	1	10	150
RECEIVING AREA:						
Capacity, trucks	1	2	2	1	2	2
Capacity, tank cars	0	0	1	0	0	1
Pumps (pairs)	1	3	4	1	3	4
In-line valves	13	39	52	13	39	52
Open-ended valves	2	6	8	2	6	8
Flanges	24	72	96	24	72	96
Instr. connections	4	12	16	4	12	16
Sampling connections	0	2	6	0	2	6
Storage tanks	0	2[a]	6[a]	0	2[a]	6[a]
STORAGE AREA:						
Pumps (pairs)	1	1	1	1	1	1
Pumps (single)	0	2	2	0	2	2
In-line valves	13	39	39	13	39	39
Open-ended valves	2	6	6	2	6	6
Flanges	24	72	72	24	72	72
Instr. connections	4	12	12	4	12	12
Sampling connections	4	4	4	4	4	4
Storage tanks	4[a]	4[b]	4[c]	4[d]	4[e]	4[f]
FEED AREA:						
Pumps (pairs)	1	1	1	1	1	1
In-line valves	13	13	13	13	13	13
Open-ended valves	2	2	2	2	2	2
Flanges	24	24	24	24	24	24
Instr. connections	4	4	4	4	4	4
Sampling connections	1	1	1	2	2	2
Storage tanks	1[g]	1[a]	1[h]	2[i]	2[d]	2[j]

[a] 1.0×10^4 gal capacity.

[b] 2.0×10^4 gal capacity.

[c] 1.5×10^5 gal capacity.

[d] 1.25×10^4 gal capacity.

[e] 2.5×10^4 gal capacity.

[f] 2.0×10^5 gal capacity.

[g] 5.0×10^3 gal capacity.

[h] 1.2×10^5 gal capacity.

[i] 6.0×10^3 gal capacity.

[j] 1.5×10^5 gal capacity.

Table II. Ten most prevalent constituents of hazardous waste streams

Constituent	Amount Incinerated (MT/y)
Methanol	133,168
Acetonitrile	58,646
Toluene	56,620
Ethanol	55,090
Amyl acetate	54,926
Acetone	51,535
Xylene	49,453
Methyl ethyl ketone	42,520
Adipic acid	36,135
Ethyl acetate	32,576

Table III. Consumption, concentration, and emission rates of incinerated chemicals (99.99% DRE)

Pollutant	Amount incin- erated[a] (MT/y)	Fraction of waste stream[b] (%)	Emission rate, g/y											
			Rotary kiln						Liquid injector					
			1		10		150		1		10		150	
			Stack	Fugitive	Stack	Fugitive	Stack	Fugitive	Stack	Fugitive	Stack	Fugitive	Stack	Fugitive
PESTICIDE-RELATED WASTE														
Chloroform	9.13E+4	6.1	1.12E+3	1.52E+4	1.12E+4	4.09E+4	1.68E+5	5.46E+4	1.12E+3	1.60E+4	1.12E+4	4.18E+4	1.68E+5	5.56E+4
Ethylene dichloride	7.85E+4	19.0	3.50E+3	1.73E+4	3.50E+4	4.65E+4	5.23E+5	6.09E+4	3.50E+3	1.82E+4	3.50E+4	4.74E+4	5.23E+5	6.30E+4
Hexachlorobutadiene	6.79E+4	9.2	1.69E+3	1.02E+2	1.69E+4	2.74E+2	2.54E+5	3.59E+2	1.69E+3	1.07E+2	1.69E+4	1.69E+2	2.54E+5	3.73E+2
1,1,2,2-tetrachloroethane	2.10E+4	2.4	4.42E+2	2.03E+2	4.42E+3	5.44E+2	6.62E+4	7.15E+2	4.42E+2	2.14E+2	4.42E+3	5.58E+2	6.62E+4	7.43E+2
API SEPARATOR SLUDGE WASTE														
Chromium[c]	1.10E+2	0.025	1.66E+3	0	1.66E+4	0	2.50E+5	0	1.66E+3	0	1.66E+4	0	2.50E+5	0
Lead[c]	1.08E+1	0.033	2.20E+3	0	2.20E+4	0	3.30E+5	0	2.20E+3	0	2.20E+4	0	3.30E+5	0
Arsenic[c]	2.74E+0	0.006	4.00E+2	0	4.00E+3	0	6.00E+4	0	4.00E+2	0	4.00E+3	0	6.00E+4	0
Phenol	5.40E+0	0.003	6.87E-1	3.63E-2	6.87E+0	9.68E-2	1.03E+2	1.10E-1	6.87E-1	3.81E-2	6.87E+0	9.88E-2	1.03E+2	1.12E-1
PHENOL/ACETONE DISTILLATION WASTE														
Toluene	1.89E+1	0.6	3.91E+3	6.43E+3	3.91E+4	1.76E+4	5.87E+5	3.21E+4	3.91E+3	6.77E+3	3.91E+4	1.80E+4	5.87E+5	3.40E+4
Pyridine	5.02E+1	1.3	2.68E+2	3.45E+2	2.68E+3	9.47E+2	4.01E+4	1.72E+3	2.68E+2	3.64E+2	2.68E+3	9.69E+2	4.01E+4	1.83E+3
Phthalic anhydride	1.22E+1	0.001	2.05E-1	5.34E-3	2.05E+0	1.46E-2	3.09E+1	2.64E-2	2.05E-1	5.60E-3	2.05E+0	1.49E-2	3.09E+1	2.80E-2
Methyl styrene	5.66E+3	1.8	3.72E+3	9.91E+2	3.72E+4	2.72E+3	5.55E+5	4.96E+3	3.72E+3	1.05E+3	3.72E+4	2.79E+3	5.55E+5	5.25E+3

[a] From compilation of waste information (USEPA, 1980a).

[b] Calculated by averaging pesticide-related waste chemical concentrations.

[c] A DRE of 95.0% is assumed for the heavy metals.

Table IV. Cumulative population by distance from the incinerator site

Distance to Ring Center (m)	Population
200	0
375	0
625	0
875	0
1,500	203
2,500	949
3,500	2,378
4,500	4,053
6,250	6,039
8,750	7,437
15,000	76,576
35,000	126,614
55,000	263,097
75,000	349,969
95,000	448,187

Table V. Stack and area source parameters employed in atmospheric dispersion modeling

	Rotary kiln			Liquid injector		
	Size, 10^6 Btu/h			Size, 10^6 Btu/h		
	1	10	150	1	10	150
STACK:						
Height, m	15.24	30.48	30.48	15.24	30.48	30.48
Exit gas temperature, K	355	355	355	355	355	355
Exit gas velocity, m/s	1.10	11.0	41.1	1.10	11.0	41.1
Diameter, m	0.61	0.61	1.22	0.61	0.61	1.22
Generic gas emission rate, g/s	1.0	1.0	1.0	1.0	1.0	1.0
RECEIVING AREA:						
Height, m	6.1	6.1	6.1	6.1	6.1	6.1
Area (square), m^2	74.3	130	390	74.3	130	390
Width of area, m	8.6	11.4	19.8	8.6	11.4	19.8
Generic gas emission rate, g/s	74.3	130	390	74.3	130	390
STORAGE AREA:						
Height, m	6.1	6.1	6.1	6.1	6.1	6.1
Area (square), m^2	325.2	345	2165	325.2	423	2737
Width of area, m	18.0	18.6	46.5	18.0	20.6	52.3
Generic gas emission rate, g/s	325.2	345	2165	325.2	423	2737
FEED AREA:						
Height, m	6.1	6.1	6.1	6.1	6.1	6.1
Area (square), m^2	76.2	130	689	76.2	130	866
Width of area, m	8.73	11.4	26.3	8.73	11.4	29.4
Generic gas emission rate, g/s	76.2	130	689	76.2	130	866

Table VI. Health risk estimators for chemicals in three generic wastes

Pollutant	Health Risk Estimator		
	Excess Risk[a] (mg/kg/d)$^{-1}$	ADI[b] (mg/d)	TLV[c] (mg/m^3)
PESTICIDE-RELATED WASTE			
Chloroform	1.8E-1	8.8E+0	5.0E+1
Ethylene dichloride	3.7E-2	NA[d]	4.0E+1
Hexachlorobutadiene	7.75E-2	1.4E-1	NA
1,1,2,2-tetrachloroethane	2.0E-1	NA	3.5E+1
API SEPARATOR SLUDGE WASTE			
Chromium VI	NA	1.4E-1	5.0E-2
Chromium III	NA	1.3E+2	5.0E-1
Lead	NA	1.0E-1	1.5E-1
Arsenic	1.4E+1	7.0E-2	2.0E-1
Phenol	NA	6.8E+0	1.9E+1
PHENOL/ACETONE DISTILLATION WASTE			
Toluene	NA	1.3E+2	3.75E+2
Pyridine	NA	5.4E+0	1.5E+1
Phthalic anhydride	NA	2.1E+0	6.0E+0
Methyl styrene	NA	1.7E+1	4.80E+2

[a] Excess risk of developing cancer after a lifetime exposure (USEPA, 1982).

[b] Acceptable daily intake (USEPA, 1983).

[c] Threshold limit value is the time-weighted concentration for an 8-h workday and 40-h workweek to be used as a guide in the control of health hazards (ACGIH, 1980).

[d] Not available.

Table VII. Percent contribution of fugitive emissions to total emissions of chloroform at a liquid injection incinerator

% DRE	Contribution (%)		
	LI-1	LI-10	LI-150
99.99	93.5	78.8	24.8
99.90	58.8	27.1	3.2
99.00	12.5	3.6	0.3

Table VIII. The effect of DRE on total population exposure (person-ug/m^3) to chloroform emissions from a liquid injection incinerator

% DRE	LI-1	LI-10	LI-150
99.99	2.5E+0	7.1E+0	2.0E+1
99.90	3.7E+0	1.7E+1	1.2E+2
99.00	1.7E+1[a]	1.1E+2	1.2E+3

[a] Read as 1.7 x 10^1

Table IX. Expected number of excess cancers over 70 years from incineration of pesticide-related waste at a liquid injection incinerator (for a population of 0.45 x 10^6)

% DRE	LI-1	LI-10	LI-150
99.99	1.3E-4	4.0E-4	1.6E-3
99.90	2.6E-4	1.4E-3	1.2E-2
99.00	1.6E-3	1.1E-2	1.2E-1

Table X. Excess cancer risk over 70 years to the maximally exposed individual from incineration of pesticide-related waste at liquid injection incinerators (99.99% DRE)

LI-1	LI-10	LI-150
2.8E-8	7.8E-8	1.2E-7

Table XI. Average daily intake of selected phenol/acetone distillation waste constituents released by hazardous waste incinerators (presented as a fraction of the ADI)

	ADI (mg/d)	Incineration Facility (99.99% DRE)					
		RK-1	RK-10	RK-150	LI-1	LI-10	LI-150
Toluene	134	2.7E-10	1.2E-9	8.4E-9	2.8E-10	1.2E-9	8.5E-9
Pyridine	5.4	3.9E-10	1.8E-9	1.4E-8	4.1E-10	1.9E-9	1.4E-8
Phth. anhyd.	2.1	3.2E-13	2.4E-12	2.5E-11	3.2E-13	2.4E-12	2.5E-11
Methyl styrene	171	9.1E-11	5.8E-10	5.7E-9	9.3E-11	5.8E-10	5.7E-9

Table XII. Average daily intake of heavy metals (as a fraction of ADI) for the maximally exposed individual from incineration at a liquid injection incinerator (95% DRE)

	LI-1	LI-10	LI-150
Chromium[a]	7.4E-8	3.0E-7	7.4E-7
Arsenic	3.8E-8	1.5E-7	3.8E-7
Lead	1.4E-7	5.3E-7	1.4E-6

[a] The ADI value for chromium IV was used.

Impact of Fugitive Emissions on PM-10 Concentrations

Thompson G. Pace, EPA/OAQPS-RTP

ABSTRACT

The National Ambient Air Quality Standard for Particulate Matter is currently being reviewed. Indications are that a revised standard for inhalable particles (IP) will be proposed. This will consider only those particles smaller than 10 μm aerodynamic diameter. Knowledge of the bimodal distribution of particles in ambient air suggests that, while fugitive sources were a major component of TSP, they will be much less significant under an IP standard.

Ambient chemical and size distribution data and assessment of source contributions based on a number of ambient studies will be consolidated into an appraisal of the impact of fugitive emissions on the inhalable particle fraction of Particulate Matter. Empasis will be on size segregated data from dichotomous sampler studies where the coarse mode contribution to ambient IP can be isolated.

(This is an abstract of a verbal presentation for which a paper is not available.)

APPLICATION OF DISPERSION DICTATED MASS BALANCE FOR CALCULATING FUGITIVE DUST EMISSIONS

The work described in this paper was not funded by the U.S. Environmental Protection Agency. The contents do not necessarily reflect the views of the Agency and no official endorsement should be inferred.

CLIFFORD F. COLE, TRC ENVIRONMENTAL CONSULTANTS, INC.
JOHN G. MOLDOVAN, ANACONDA MINERALS COMPANY
PAUL B. KUNASZ, CONSULTANT

ABSTRACT

This paper describes the development and application of a new receptor-source model which provides estimates of emission rates from fugitive dust sources by employing a dispersion dictated mass balance (DDMB) technique. Unlike other chemical or morphological receptor models, the DDMB method considers only one constituent, which in most practical applications will be total suspended particulate matter. One equation is written for each receptor, such that the total concentration of particulate collected at each receptor is set equal to the sum of a contributing source's emission rate times a dispersion factor. The dispersion factor must be calculated from a dispersion model, and in this sense, the DDMB method relies on meteorological data. Given measured particulate concentrations, values of emission rates can be computed by solving a set of simultaneous linear equations.

The DDMB method was applied to compute the emission rates and the contribution of TSP levels of a major mining operation in Butte, Montana. The DDMB results provided an estimate of the mine's "effective emissions" which differed greatly from emissions determined by the traditional emission factor technique. The Butte study is used to demonstrate the DDMB methodology, and findings of the study are discussed.

1.0 BACKGROUND

In airsheds characterized by high particulate concentrations, the quantification of each major source's contribution to ambient air particulate levels is critically important. Only when it is known where particulates come from, and how much an individual source adds to the particulate burden, can controls be applied in a cost-effective way. The large number of areas in the U.S. in which concentrations still exceed particulate ambient air standards, despite expensive control efforts, attests to the difficulty of identifying and quantifying dust sources(1).

Source apportionment--the determination of the mass of particulate matter at a receptor that emanates from various sources--has traditionally been accomplished with source modeling. Emission rates of sources are estimated, and input along with meteorological data into a dispersion model that analytically simulates the transport, diffusion, and deposition of particulate matter. In the vicinity of discrete, well-defined point sources, this modeling method appears to work well. However, in regions where a large portion of the particulate matter is fugitive dust the source modeling method has proven inadequate(2). The failure of traditional modeling to properly account for observed particulate concentrations is due in part to the difficulty in quantifying fugitive dust emission rates. Emission rates from dust sources are hard to measure, and change dramatically with meteorological conditions, type and extent of source activity, and other parameters.

In the last few years receptor modeling has been touted as a remedy to the fugitive dust source apportionment problem(3). Proponents of receptor modeling correctly point out that chemical mass balance (CMB), enrichment factor, time series, and multivariate receptor models eliminate some of the uncertainty associated with source modeling. However, there are two distinct drawbacks that limit most receptor models' use in regions where fugitive dust is suspected of inducing large hi-vol concentrations. First, receptor models are unable to differentiate physically or chemically similar constituents that may be entrained from different sources; and second, receptor models assume that the relative mass fractions of all chemical species are conserved, and that no selective deposition occurs(1). To illustrate that these drawbacks can be severely limiting, consider a TSP nonattainment area where road dust is found to be a significant contributor to concentrations. If the road dust is chemically and physically homogeneous, and if deposition and resuspension of the dust occur, then the receptor model cannot pinpoint which are the offending roadways(2).

This paper discusses a new receptor model method termed Dispersion Dictated Mass Balance (DDMB). The DDMB method utilizes features from both source and receptor modeling technology, thereby overcoming some of the deficiencies in either modeling approach used alone. Because DDMB considers only one constituent, usually total suspended particulate, and because the effects of deposition and reentrainment can be taken into account, the method is especially well suited to fugitive dust source apportionment. The DDMB method is simple and inexpensive to apply, and yields statistically sound results.

2.0 ANALYTICAL METHOD

2.1 GOVERNING EQUATIONS

Like all receptor models, the basis for the DDMB method is a simple model in which the pollutant contribution from a given source at a receptor is set equal to the emission rate of that source times a dispersion factor:

$$\chi_j = (\chi/Q)_j \; Q_j \qquad (1)$$

where χ_j is the concentration at the receptor due to source j

Q_j is the emission rate from source j

$(\chi/Q)_j$ is the dispersion coefficient from source j to the receptor

Equation (1) can be summed over a number of sources, P, so that

$$\chi = \sum_{j=1}^{P} (\chi/Q)_j \; Q_j \qquad (2)$$

The only restrictions imposed by equation (2) are that concentrations are additive, and directly proportional to emission rates. If there are no more than P sources in the vicinity of the receptor that contribute pollutant, then equation (2) will account for all of the pollutant concentration detected. More likely, it will be impossible to identify all of the sources that impact the receptor, but the contribution of unknown sources can be accounted for by an assumed background concentration, B, which is added to the right-hand side of equation (2). Obviously, equation (2) can be written for any number of independent receptors to produce a set of linear equations. Generalizing for n receptors,

$$\chi_n = \sum_{j=1}^{P} (\chi/Q)_{nj} \; Q_j + B \qquad (3)$$

If the χ/Q values and the background concentration are known, if the measured concentrations at each receptor are available, and if the number of receptors equals or exceeds the number of sources, then equation (3) yields a fully determined (or overdetermined) system that can be solved to find source emission rates.

While the above list of necessary data conditions appears restrictive, in fact for many regions these data may already be available or can be readily calculated. Consider an area deemed nonattainment for TSP. Annual average hi-vol concentrations at several locations will undoubtedly be available, and an annual average background TSP concentration can easily be assumed or can be determined from these measured concentrations using a variety of methods(4). The χ/Q values may already be known if adequate modeling studies have been performed in the area. If not, model simulations of TSP concentration at each of the hi-vol receptors must be performed. The X/Q values are determined by dividing modeled concentrations by the source emission rates assumed in the model.

It is important to note that the emission rates of each source or source grouping ultimately determined by the DDMB method depend upon the χ/Q dispersion coefficients that are introduced in equation (3). For this reason every attempt should be made to accurately simulate dispersion in the initial modeling phase. If deposition is thought to be an important phenomenon in the area being studied, then a model which accurately refects deposition should be used. Similarly, meteorological data input to the dispersion model should be screened carefully. If sources are combined, then the resultant χ/Q values depend upon the intial choice of emission rates assumed in the dispersion model, and special care should be taken to estimate these initial emission rates accurately.

2.2 METHODS OF SOLUTION

The set of fully determined or overdetermined DDMB linear equations can be solved with almost any matrix solution software package, although software packages that provide statistical analysis of the data are preferable. For overdetermined systems the standard deviation of the predicted emission rates, and the matrix of correlations between emission rates, are extremely valuable statistics. The standard deviation provides a measure of how "good" a computed fugitive dust emission rate is, and allows one to compute statistical confidence intervals associated with each emission rate. Given the uncertainty in fugitive dust emission factors, confidence intervals should be demanded by every investigator. The correlation matrix between emission rates provides guidance in combining sources, a technique which greatly enhances the DDMB method.

2.3 SOURCE COMBINATION

In order for equation (3) to be solvable the linear system must be fully determined or overdetermined, that is, there must be as many or more hi-vol receptors than sources. One way to achieve this is to combine sources by grouping them together for the purpose of the DDMB computations. For example, two adjacent unpaved parking lots could be considered a single fugitive dust source, thereby reducing the order of the linear system of governing equations by one. Of course, source combination like this reduces the resolution of unknown emission rates, but it may be required to make the matrix fully determined. Even more important, careful source combination can dramatically improve the accuracy of the computed emission rates, as will be demonstrated later in this paper.

In deciding which sources to combine, common sense dictates that sources which have similar impacts on the hi-vol receptors be combined. The hi-vol data cannot discriminate one of these sources from another, so it is not reasonable to ask the DDMB method to make a distinction. Frequently such sources will be located near one another, as in the adjacent parking lot example above. More rigorously, one can determine which sources are linked by examining the correlation between predicted sources' emission rates. When the correlation between two sources approaches -1.0 this indicates that the two emission rates are linked in such a way that if one rate is varied, the other must react oppositely in order to minimize the sum of squares of the residuals. Two strongly negatively correlated sources cannot be resolved by the data at hand, and attempts to do so would yield arbitrary results which would be extremely sensitive to any errors in the data.

3.0 DDMB APPLICATION

The DDMB method was used to determine source apportionment and TSP emission rates from various sources in Butte, Montana for the year 1978. Butte provides an especially attractive study area for the DDMB method because there are a number of fugitive dust sources in and near Butte whose emission rates have proven very difficult to quantify. Conventional fugitive dust inventories have yielded drastically different emission rates for the same sources(5). This is illustrated in Table 1., which shows a summary of emission rate estimates determined by three independent studies.

TABLE 1.

1978 ANNUAL ESTIMATED EMISSION RATE (tons/year)
FROM ANACONDA SOURCES AND BUTTE SOURCES

EMISSION SOURCE	STUDY 1	STUDY 2	STUDY 3
ANACONDA	15,000	5,612	26,142
BUTTE	11,000	3,402	11,564

In the following sections the application of the DDMB method at Butte is illustrated. The major sources in Butte are described, hi-vol and χ/Q input data are tabulated, and the sequential steps in the DDMB process are discussed.

3.1 SOURCE AND RECEPTOR DESCRIPTION

Figure 1. shows the location of major particulate matter sources and hi-vol samplers in Butte. The hi-vol samplers, indicated by stars in Figure 1., provide every-sixth-day measures of total suspended particulate. Of the nine hi-vols displayed in Figure 1., three are operated by the Montana Air Quality Bureau, and the remainder are operated by Anaconda Minerals Company.

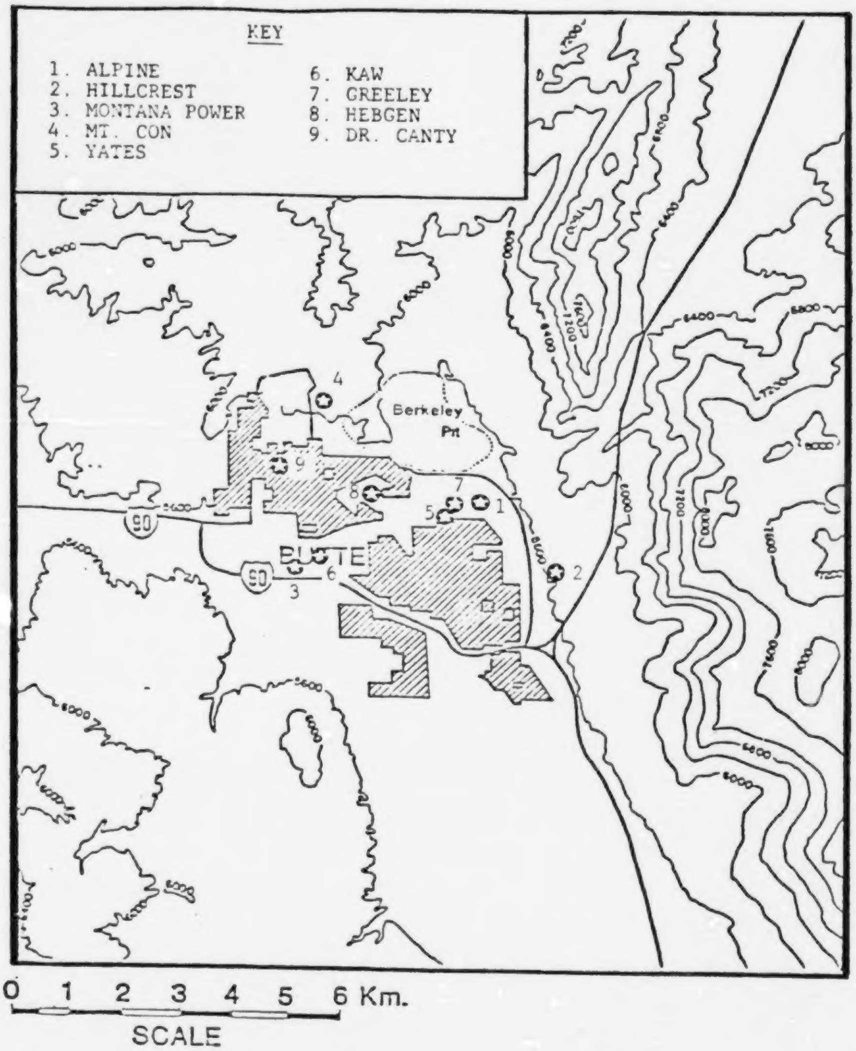
KEY
1. ALPINE
2. HILLCREST
3. MONTANA POWER
4. MT. CON
5. YATES
6. KAW
7. GREELEY
8. HEBGEN
9. DR. CANTY
Berkeley Pit
BUTTE
90
7200
6400
6800
6000
5600
0 1 2 3 4 5 6 Km.
SCALE

FIGURE 1

SOURCE AND HI-VOL
LOCATIONS

Anaconda operations are located from the northeast to the east of the city of Butte, and involve the mining and concentrating of copper ores from the Berkeley Pit. Drilling, blasting, and removal of overburden and copper ore by shovels are dust producing activities that are confined to the 550 meter deep Berkeley Pit. The dumping and storage of ore, as well as crushing and concentrating activities, occur at the southern end of the pit perimeter. Overburden is temporarily stored in primary dumps to the northwest, northeast, and southeast of the pit before being returned in a backfilling operation. Haul roads and access roads link the Berkeley Pit with the crusher, concentrator, and dumps.

The city of Butte, adjacent to the pit, is itself a source of fugitive dust resulting from many different activities. Previous studies have identified paved and unpaved roads, fuel combustion, motor vehicle exhaust, construction, burning, and wind erosion from cleared areas as major particulate sources.

3.2 INPUT DATA

Two separate types of input data are required by the DDMB model: measured TSP concentrations at hi-vol receptors, and the χ/Q values for each source-receptor pair.

The 1978 measured TSP concentrations at nine hi-vols in the Butte area are shown in Table 2. A uniform annual average background concentration of 20.0 $\mu g/m^3$ is assumed to characterize the airshed, so that the contribution of local sources to measured concentrations is determined by subtracting 20.0 from the measured concentrations.

TABLE 2.

1978 BUTTE AMBIENT TSP CONCENTRATIONS

HI-VOL	MEASURED CONCENTRATION ($\mu g/m^3$)	BACKGROUND ($\mu g/m^3$)	MEASURED MINUS BACKGROUND ($\mu g/m^3$)
GREELEY	79	20	59
HILLCREST	37	20	17
YATES	73	20	53
ALPINE	89	20	69
KAW	54	20	34
MT. CON	34	20	14
HEBGEN	70	20	50
DR. CANTY	56	20	36
MONTANA POWER	47	20	27

The χ/Q values used in this study were determined from previously run ISCLT dispersion model simulations of the Butte area. Using 1978

TABLE 3

χ/Q VALUES FOR SOURCE-RECEPTOR COMBINATIONS

	------ TSP EMISSION SOURCES ------						
HI-VOL	INPIT	CRUSHER	STORAGE	HAUL ROADS	BACKFILL	DUMPS	CITY
GREELEY	0.4426	0.7797	0.8525	0.4896	0.1566	0.1351	0.6002
HILLCREST	0.1190	0.1161	0.1195	0.1390	0.0523	0.1574	0.1850
YATES	0.4077	0.8189	0.8092	0.4544	0.1603	0.1283	0.5490
ALPINE	0.5391	0.4287	0.4919	0.6426	0.1204	0.1823	0.6781
KAW	0.1097	0.2464	0.2083	0.0925	0.1583	0.0352	0.6817
MT. CON	0.2098	0.1972	0.2264	0.1412	0.9977	0.0702	0.2560
HEBGEN	0.2636	0.7001	0.5294	0.2132	0.5135	0.0603	0.6457
DR. CANTY	0.0792	0.1415	0.1338	0.0668	0.3044	0.0296	0.5517
MONTANA POWER	0.0738	0.1298	0.1145	0.0585	0.1262	0.0263	0.4408

NOTE: χ/Q values in $sec/m^3 \times 10^6$

meteorological data, the ISCLT model computed the impact of seven distinct sources:

1. Berkeley Pit
2. Crusher dump
3. Active storage
4. Anaconda haul roads and access roads
5. Backfill
6. Primary dumps
7. Butte (unpaved roads, fuel combustion, wind erosion, etc.)

The first six sources are controlled by Anaconda, while the seventh source represents the city of Butte. The source grouping option available in the ISCLT model was used to compute the impact of combined sources where appropriate. The city of Butte, for example, was modeled as 134 discrete area sources.

Values of χ/Q, determined by dividing the model-predicted concentrations by the model-assumed emission rates, appear in Table 3. Each χ/Q value in Table 3. represents a measure of the TSP dispersion coefficient from a source to a hi-vol receptor.

3.3 DDMB SOLUTIONS

Initially, attempts were made to compute TSP emission rates for each of the individual seven major sources in Butte (pit, haul roads, crusher, storage, backfill, dump, and city of Butte). The effective emission rates and confidence intervals resulting from this effort are shown in Table 4.

TABLE 4.

TSP EMISSION RATES AND CONFIDENCE
INTERVALS FOR UNCOMBINED SOURCES

SOURCE	EMISSION RATE (gm/sec)	95% CONFIDENCE INTERVAL (gm/sec)
INPIT	-176	± 1,540
HAUL ROADS	47	± 237
CRUSHER	-35	± 224
STORAGE	196	± 1,230
BACKFILL	11	± 139
DUMP	-6	± 230
TOWN	52	± 41

Clearly, the DDMB method is unable to resolve each of the seven sources, as indicated by the physically unrealistic emission rates, and the very wide confidence intervals which suggest that there is a great deal of uncertainty associated with each predicted emission rate. An explanation for such large error bars is found in the matrix of correlations between emission rates, displayed in Table 5.

TABLE 5.

CORRELATION MATRIX

	CRUSHER	STORAGE	HAUL ROADS	BACKFILL	DUMPS	CITY
INPIT	-.68	.40	-.995	-.978	.11	-.30
CRUSHER		-.92	.71	.66	-.06	-.10
STORAGE			-.45	-.40	-.08	.16
HAUL ROADS				.98	-.17	.27
BACKFILL					-.15	.23
DUMPS						-.13

The correlation between the inpit and haul road sources is very close to -1.0, meaning that these two sources cannot be distinguished by the available data. In essence, the hi-vols "see" these two sources as the same source. This is not surprising since the haul roads are located within and surround the Berkeley Pit. Similarly, the crusher and storage sources are correlated, as are the inpit and backfill sources. These strong negative correlations suggest that emission rate accuracy could be greatly improved by combining sources.

The seven sources were systematically combined and a matrix solution achieved for each combination, partly in an attempt to find the most accurate emission rates, and partly to experiment with the source combination method. Table 6. illustrates the improvement in DDMB performance as the souces are combined. In Case "B" the pit and haul roads are combined as if they constituted a single, indistinguishable source, and the confidence interval associated with the combined source is smaller than for either individual source. Case "C" in Table 6. illustrates the effect of combining the crusher and storage sources, while Case "D" further combines the backfill and primary dump sources. In Case "D" all but one of the physically unrealistic negative emission rates have been eliminated, but confidence intervals still remain large. This condition is not remedied until all of the Anaconda sources are combined (Case "E"). When they are, confidence intervals shrink dramatically, demonstrating the resolution sought between Anaconda and the city of Butte, but at the expense of lack of resolution among the Anaconda sources.

Using the emission rates shown for Case "E" of Table 6., the TSP contribution from the Anaconda sources and from the town can be computed at each hi-vol receptor. The results of these computations appear in Table 7. which lists the concentration contribution in percent for Anaconda sources, for the city of Butte, and for background. The Anaconda contribution is generally lower than that predicted by conventional source modeling techniques, and is in good agreement with recent Anaconda estimates of source contribution(5).

TABLE 6

TSP EMISSION RATES AND CONFIDENCE INTERVALS FOR VARIOUS CASES OF COMBINED SOURCES

SOURCE	CASE "A" NO SOURCES COMBINED	CASE "B" PIT & HAUL ROADS COMBINED	CASE "C" PIT & HAUL ROADS CRUSHER & STORAGE COMBINED	CASE "D" PIT & HAUL ROADS, CRUSHER & STORAGE, BACKFILL & DUMPS COMBINED	CASE "E" ALL ANACONDA SOURCES COMBINED
IN PIT	-176 ± 1540	61.8 ± 64	53.0 ± 63	57.4 ± 37	59.1 ± 22.9
HAUL ROADS	47 ± 237				
CRUSHER	- 35 ± 224	25.2 ± 82	5.5 ± 31	4.7 ± 25	
STORAGE	196 ± 1230	23.1 ± 97			
BACKFILL	11 ± 139	-7.4 ± 14	-7.0 ± 15	-21.1 ± 38	
DUMP	- 6 ± 230	-2.1 ± 110	-3.4 ± 121		
CITY	52 ± 41	50.0 ± 19	52.4 ± 19	52.4 ± 16	48.3 ± 13.7

Note: All emission rates expressed in gm/sec
All confidence intervals at 95% level

TABLE 7.

1978 TSP CONTRIBUTIONS AT SELECTED HI-VOLS

HI-VOL	ANACONDA CONTRIBUTION (%)	BUTTE CONTRIBUTION (%)	BACKGROUND CONTRIBUTION (%)
GREELEY	37.7	36.8	25.4
HILLCREST	20.8	24.6	54.6
YATES	37.4	35.8	26.9
ALPINE	38.7	38.1	23.2
KAW	11.2	55.3	33.5
MT. CON	25.3	28.6	46.1
HEBGEN	24.0	46.4	29.6
DR. CANTY	9.5	51.7	38.8
MONTANA POWER	9.6	44.9	45.6

4.0 DISCUSSION

The DDMB method provides a means of estimating emission rates and source apportionment from a number of simultaneously emitting fugitive dust sources. Analytically the DDMB method finds that combination of source emission rates that yields the best fit (in the "least squares" sense) between measured and modeled concentrations. The method enjoys several advantages over current fugitive dust source apportionment techniques:

- DDMB does not require the detailed laboratory work associated with many receptor models such as CMB, SEM, X-ray diffraction, or optical microscopy.

- DDMB can discriminate among sources that emit chemically and physically identical particulate matter.

- Unlike many spatial receptor models such as trajectory analysis, cluster analysis, and pollution wind roses, DDMB provides quantitative measures of source contribution.

- Depending upon the software package used to solve the linear system of equation, the DDMB method can "police itself" by providing confidence intervals for each computed emission rate.

- The DDMB method is an inexpensive, cost-effective analysis.

Naturally there are disadvantages, too. The number of distinct sources that can be resolved is constrained by the number of hi-vols available. Furthermore, the improvement in confidence intervals achieved by combining sources is made at the expense of the number of sources that can be resolved. It may be that the DDMB method will be most useful when investigators are willing to partition all sources into just a few source categories, as in the example application presented above.

Will the DDMB method always work? Application of the procedures outlined in this paper will always yield emission rate estimates as long as the governing equations are fully determined or overdetermined. But there is no guarantee that the answers will be "correct," or that the confidence intervals will not be so wide as to make the answers meaningless. Based on this study, and other applications of the DDMB method, it seems that there are some criteria that make success of the DDMB method more likely: first, there must be no large systematic errors in the dispersion model used to compute χ/Q values. Random errors in the dispersion model are tolerable, and their effect can be minimized by combining sources. Second, if the measured hi-vol concentrations are appreciably greater than the background concentration, then the unavoidable errors inherent in the hi-vol measurements will have the least impact on computed emission rates. In other words, the DDMB method probably works best in areas where large fugitive dust sources are present. Finally, if particulate sources are spatially separated, and if hi-vol data are available from many different locations, then the method's ability to discriminate sources will be enhanced.

REFERENCES

1. Cooper, J. A. and J. G. Watson, Jr., "Receptor Oriented Methods of Air Particulate Source Apportionment," JAPCA 30: 1,116 (1980).
2. Watson, J. G. and J. C. Chow, "An Overview of Source-Receptor Source Apportionment," presented at APCA meeting, Philadelphia, Pennsylvania, June 21-26, 1981.
3. Core, J. E. and T. G. Pace, "Receptor Models--How Great Thou Art!(?)," presented at APCA meeting, Philadelphia, Pennsylvania, June 21-26, 1981.
4. Yocom, J. E., E. T. Brookman, R. C. Westman, and O. P. Ambardar, "Determining the Contributions of Traditional and Nontraditional Sources of Particulate Matter," JAPCA 31: 17 (1981).
5. Moldovan, G. J. and P. A. Doughty, "The Butte, Montana Particulate Apportionment Analysis," presented at APCA meeting, New Orleans, Louisiana, June 20-25, 1982.

Modeling the Emission of Aerosols in and Around a Metallurgical Plant

B. Vanderborght, I. Mertens, and J.G. Kretzschmar, SCK/CEN,*
Belgium; F. Adams, UIA, Belgium; and R. Dams, INW, Belgium**

ABSTRACT

Dust emissions from a metallurgical plant can cause considerable nuisance and health hazard to the environment. The cost to benefit analysis of pollution abatement investments can only be performed by proper modeling of the emission-immission situation. The problem was thoroughly examined in a case study by daily antimony immission measurements around a metallurgical plant over a period of one year. It soon appeared that low level fugitive emissions and not the high stacks were the major sources of the high immission levels. These sources cannot be monitored continuously so that direct emission data for dispersion model calculations are not available. For every process in the plant an emission factor was obtained by means of a combination of tracer releases, immission measurements, reversed modeling for the fugitive emissions and in stack measurements for chimney emissions. Emission factors, inventory of the plants' production and meteorological observations formed the input data for bi-Gaussian dispersion modeling. In the calculations, the contributions from the fugitive and point source emission can be discerned in the immission. Calculated values fitted the measurements of suspended Sb-aerosols very well. Validation is done by means of scatter diagrams, the comparison of measured and calculated cumulative frequency distributions, time series and pollution roses. Not only the global statistics but also individual measuring periods show very good agreement. Although the global Sb-dust deposition can be well described by wet and dry deposition parameters, and source depletion, some individual measuring sites show systematic deviations from the calculations. It seems that local turbulence conditions were responsible.

(This is an abstract of a presentation for which a paper is not available.)

(*) Nuclear Energy Research Center, B-2400 Mol, Belgium.
(**) Institute for Nuclear Sciences, B-9000 Gent, Belgium.

The work described in this paper was not funded by the U.S. Environmental Protection Agency. The contents do not necessarily reflect the views of the Agency and no official endorsement should be inferred.

NEW YORK STATE INDUSTRIAL COAL PILE DRAINAGE REGULATIONS AND GUIDELINES

By Carol Hornibrook, Senior Project Manager, NYSERDA
2 Rockefeller Plaza, Albany, NY 12223

REGULATIONS

Existing waste water discharge standards applicable for New York Coal Pile Drainage are found in the State Pollution Discharge Elimination System Permit (SPDES). At this time regulations applicable to the industrial sector control only the total dissolved solids at .5 mg/liter/day. This unlike utility coal pile drainage which, in addition to total dissolved solids, requires the regulation of total suspended solids and pH.

GUIDELINES

In 1980 the New York State Department of Environmental Conservation (NYSDEC) published a document entitled "Coal Pile Guidance for SPDES (State Pollution Discharge Elimination System)" which lists a number of requirements for new and existing coal piles. These requirements call for the monitoring of possible toxic pollutants emitted from coal piles and the treatment facilities required to prevent contamination of ground water by leachate and the contamination of surface waters by runoff. Specifically, the New York State guidelines require natural and/or manmade liners under new and some existing coal piles, ground water monitoring systems, storm collection ponds to contain runoff for pH neutralization and heavy metal removal.

At this point I would like to clarify that a 10 year-24 hour storm is a statistical term referring to a certain size storm event (expressed in inches of rain) occurring over a 24 hour period, which has a recurrence interval of 10 years.

The specific limitations for each of the requirements previously mentioned are listed in Table 1. The reader should note that these guidelines are being implemented in the same fashion as regulations and specific discharge limitations are being set in new and renewed SPDES permits.

TABLE 1

COAL PILE GUIDANCE FOR SPDES

To comply with surface and ground water classifications, standards and limitations, (Title 6, Official Compilation of Codes, Rules and Regulations, Part 701 and 703) for the protection of the State's water resources and compliance with promulgated federal best management practices (BMPs) regulations (40 CFR, Part 125) designed for the protection of said resources, the following requirements will apply.

I. New Coal Piles

A. Site Considerations

The control of wastewater containing runoff and leachate from new coal piles shall be as follows:

1) The site shall be designed to prevent runoff from entering the pile.

2) The coal pile shall be placed on an impervious surface. This surface may be a liner or any in-place material which meets Department criteria for impermeability.

3) Liner material shall be selected so as not to deteriorate after contact with coal pile wastewater and shall be protected from puncture from operating equipment. Liner protection and repairability shall be evaluated in the liner design.

4) Wastewater shall be collected and treated.

5) Collection ponds, if used, shall be lined with an imperivous material, and designed to contain the runoff from the ten-year, 24-hour storm.

6) A ground water monitoring system may be required to evaluate and/or monitor the integrity of the facility's impervious lining.

7) Discharge from treatment facilities to surface waters are not to contravene Part 701, (see Table 2) "Classifications and Standards of Quality and Purity" and discharge to the ground are to meet Part 703, (see Table 3) "Ground Water Classifications Quality Standards and Effluent Standards and/or Limitation".

8) Coal pile wastewater may be:

   a) Treated separately;

   b) Recycled for other uses at the facility;

   c) Combined with other waste streams for treatment except for the purposed of dilution.

B. Permit Conditions (SPDES)

1) The permittee shall prepare an engineering report and final plans for construction of facilitites designed to prevent, control, and treat runoff and leachate from coal piles for the purposes of maintaining and protecting water quality standards and compliance with any applicable federal requirements.

2) Organic and inorganic substances will be limited and require treatment, depending on the coal pile characteristics. Most heavy metals may be found in coal pile wastewater. Organic substances which have been detected in coal pile wastewater include chlorobenzene, dichlorethylene, chloroform, pthalates, and methylene chloride. Monitoring and treatment requirements for these compounds will be evaluated on a case and site specific basis because wastewater characteristics are dependent on the characteristics of the coal used and discharge objectives relating to the receiving water.

II. Existing Coal Piles

A. Site Considerations

Existing coal piles will be evaluated on a case-by-case basis utilizing new coal pile considerations. The permittee may be required to undertake a ground and/or surface water monitoring program to determine the extent of possible contamination. As a minimum, ground water monitoring and treatment of contaminated runoff will be required. Ground water monitoring results will be evaluated to determine applicable new coal pile considerations.

B. Permit Conditions (SPDES)

Specific permit conditions may include the following:

1) Permittee to submit a proposed plan of study designed to assess coal pile operations at the applicant's facility, including a study program to evaluate the operation's effect on surface and ground water quality.

   The study program would be subject to Department approval and shall consist of a ground and surface water monitoring program to determine compliance with applicable water quality standards, and monitoring of coal pile runoff and leachate to determine and assess wastewater characteristics.

2) Based upon NYSDEC review of the study program, the permittee may be required to prepare an engineering report and final plans for construction of facilities designed to prevent, control, and treat runoff and leachate from coal piles for the purposes of maintaining and protecting water quality standards and compliance with any applicable federal requirements.

III. Imposition of limitations and monitoring requirements and/or any particular policy guidelines if deemed appropriate for the protection of the environment may precede any of the above considerations for either new or existing coal piles.

Taken from: Bureau of Industrial Program
Division of Water

Dates: April 14, 1980

It becomes immediately evident that compliance with these regulations, from the engineering design study to placement of the liner material and monitoring of its effectiveness, can be fairly costly. NYSERDA sponsored the R&D project presented today with specific intent of better understanding the hydrology of coal piles through extensive data collection and verifying and calibrating a coal pile drainage model, in order to potentially decrease industries cost of compliance with these guidelines.

I hope that the information presented today will prove useful in future efforts to comply with these guidelines and to obtain and renew SPDES permits.

Calibration and Verification of a Coal Pile Drainage Model

John G. Holsapple, New York Power Pool
Gordon T. Brookman, John A. Ripp and
Pamela B. Katz, TRC-Environmental
Consultants, Inc.

Abstract

In 1980 the New York State Department of Environmental Conservation (NYSDEC) published a document entitled "Coal Pile Guidance for SPDES" which lists a number of requirements for new and existing coal piles. These requirements emphasize the monitoring of possible toxic pollutants emitted from coal piles and the treatment facilities required to control leachate contamination of ground water and runoff contamination of surface waters. Specifically, the New York State regulations require natural and/or manmade liners under new and some existing coal piles, ground water monitoring, storm collection ponds to contain runoff from the ten-year 24-hour storm, and treatment facilities for pH and most heavy metals.

Because of these new requirements, New York State utilities must plan for the most efficient coal pile drainage treatment and avoid the unneeded expense of constructing new coal pile runoff storage capacity to collect drainage that does not require treatment.

This paper will present a summary of a research study being performed by TRC-Environmental Consultants for ESEERCO (Empire State Electric Energy Research Corporation) which has the following objectives:

1) The calibration and verification of a mathematical model to simulate coal pile drainage flows and pollutant loadings under historical and design storm conditions. The model will be used to size and design treatment systems to meet NYSDEC specifications. The model will also simulate the changes in coal pile runoff due to changes in coal source and coal characteristics.

2) The development of a data bank on coal pile drainage from two plants which will be useful in characterizing which pollutant parameters appear in significant quantities.

The presentation will include a detailed description of the sampling programs at the two plants and an overview of the mathematical model including its uses and its limitations.

The work described in this paper was not funded by the U.S. Environmental Protection Agency. The contents do not necessarily reflect the views of the Agency and no official endorsement should be inferred.

INTRODUCTION

The United States Environmental Protection Agency (EPA) presently requires that area runoff from coal storage piles at steam electric plants be controlled to prevent the discharge of acidic water and total suspended solids (TSS). Accepted practice dictates that storage/treatment be designed to accommodate all of the runoff from a 10-year, 24-hour storm. Also, TSS must not exceed 50 mg/l and the discharge pH must fall within the range 6.0 to 9.0.

Most state water pollution regulatory agencies have adopted the EPA limitations for permitting purposes. However, some states, including New York, are requiring more stringent controls for coal pile runoff. The New York State Department of Environmental Conservation's (NYSDEC) "Coal Pile Guidance for SPDES" requires natural and/or man-made liners under new and some existing coal piles, as well as groundwater monitoring, and 10-year, 24-hour storm runoff collection ponds and treatment facilities for pH, solids and several trace metals. New York utilities must submit an engineering report with their SPDES permit applications. The report must contain sufficient field data to show what pollutants are being emitted in existing coal pile drainage and the means to predict quantitative and qualitative characteristics for new coal piles. Surprisingly, there is little information on the characteristics of coal pile runoff. There is an incentive and a need, then, in New York State to develop a technique to accurately characterize coal pile drainage.

In June of 1981, TRC Environmental Consultants, Inc. initiated a research project for the Empire State Electric Energy Research Corporation (ESEERCO) involving the calibration and verification of a coal pile drainage model. The project is also partially funded by the New York State Energy Research and Development Authority (NYSERDA). The objectives of this study include 1) field testing and verification of a coal pile drainage model and 2) the development of a large data base on coal pile runoff and coal pile characteristics. The scope of work involves sampling at two sites. Sampling at Site 1 was completed in the fall of 1981 at the Greenidge Station of New York State Electric and Gas Corporation. Site 2 sampling is presently being performed at the Russell Station of Rochester Gas and Electric Corporation.

Upon completion of this project in late summer/early fall of 1982, TRC will provide ESEERCO with a calibrated and verified model to simulate coal pile drainage flows, pollutant loadings under historical and design storm conditions, and a model user's manual. The model will be a useful tool for sizing and designing coal pile drainage treatment systems. It will also be useful for simulating changes in coal pile runoff due to changes in the coal source and in coal characteristics.

This paper presents an overall of the project to date, including the site selection process, a detailed discussion on the sampling program, a description of the model and the calibration and verification process.

SITE SELECTION

In 1981, there were nine major utility plants burning coal in New York State. As part of the site selection process, TRC visited each plant and developed a subjective ranking system, which included the following factors:

- coal pile size
- percentage of sulfur in coal
- coal pile containment
- ease of sampling on pile
- variability of pile shape and size
- climate
- availability of data

The Russell Station (Site 2) was the highest ranked plant for the following reasons:

- The plant has an average size of 96,000 tons, which is near the average size of the piles evaluated;
- The average sulfur content is 2.4 percent, which was one of the highest of all plants evaluated;
- The plant has a partial concrete-lined gutter around the pile which collects most of the runoff;
- Approximately 25 percent of the pile is reserve, which facilitates the installation of in-pile piezometers;
- The pile size and shape remains fairly constant throughout the year.

The Greenidge Station (Site 1) ranked second for the following reasons:

- The plant has an average size of 110,000 tons, which approximates the survey average of 112,000 tons.
- Runoff and leachate are completely contained by an impervious plastic liner under the pile. All runoff and leachate are directed to a single discharge point.
- Approximately 50 percent of the pile is reserve and, therefore, facilitates the placing of in-pile monitoring equipment.
- Size and shape of the pile does not vary significantly during the year.

These two sites were then recommended to ESEERCO as test sites and permission was received from the member utilities to proceed.

FIELD MONITORING PROGRAM

The field monitoring program was designed to provide imput data to calibrate and verify the drainage model and to collect an extensive data base on pile hydrology and chemistry along with site meteorology and runoff quantity and quality. The scope of work for the field program was based on a TRC report to EPA and EEI entitled "Planning Study to Model and Monitor Coal Pile Runoff."[1]

DATA REQUIREMENTS

Figure 1 illustrates the categories of data necessary to the modeling effort and the data base. Site description data includes general information on pile size and shape, proximate analysis of delivered coal, methods of stacking and reclaiming and pertinent existing data on site geohydrology. Meteorological data being collected includes historic information from local U.S. Weather Service stations and continuous monitoring of precipitation, air temperature, relative humidity, solar radiation and pan evaporation during the survey period. Runoff data being measured includes continuous recording of all drainage flows from the coal pile and when flow does exist continuous measurements of pH and conductivity. For each storm event samples are collected on a 30-minute interval at the start of each storm and after 4 hours of runoff on a 60-minute interval for the following analysis:

- Acidity/alkalinity
- Total suspended solids
- Total dissolved solids
- Total organic carbon

---

[1] G. T. Brookman, et al., "Planning Study to Model and Monitor Coal Pile Runoff," EPA-600/7-81-016 (NTIS PB81-152530), February 1981.

- Sulfate
- Hardness
- Total and dissolved forms of 20 metals

Not illustrated in Figure 1 is the geohydrological data being collected at each site to define pile moisture conditions. At the start of each site monitoring, a drilling program is conducted on the pile. During that program, hollow stem auger borings are made with split spoon sampling through the pile at 5-foot intervals. Coal samples are then analyzed for moisture content. Where possible, in-pile piezometers are installed to observe water level fluctuations at the pile base. Simultaneous with the drilling program a resistivity survey is conducted on the pile to map the saturated areas of the pile. Throughout the 10 weeks of runoff monitoring, piezometers are observed for water levels, pH, conductivity and periodically sampled for the runoff parameters. Pile permeability and infiltration rates are also measured throughout each monitoring season to correlate with runoff percentages.

LOGISTICAL CONSIDERATIONS

As mentioned above, 2 sites are being monitored for 10 weeks each. The field program is built around a portable laboratory in which solids and acidity analysis are performed on all runoff samples. Also this laboratory serves as of base of operations for calibrating instruments, preserving and storing samples and cleaning equipment and glassware. An instrument shelter is also located on each site to house recorders for flow, pH and conductivity, along with the automatic sampling equipment. The samplers are programmed to start collecting samples at the start of each storm through an actuator switch which senses an increase in runoff flow. This insures the complete sampling of each storm event. A technical support person is kept on-site during the entire monitoring period to maintain all equipment and perform on-site analysis.

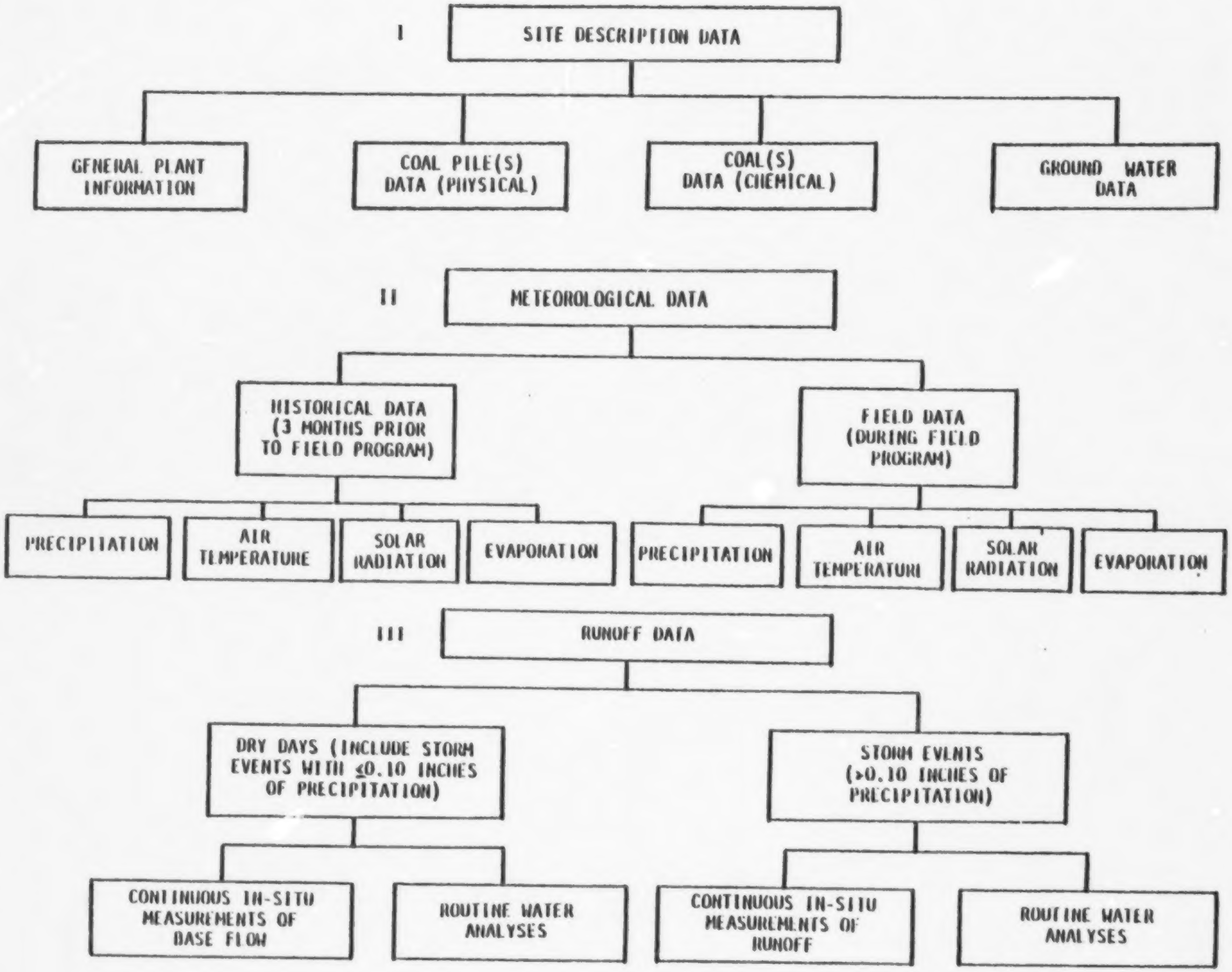
I
SITE DESCRIPTION DATA
GENERAL PLANT INFORMATION
COAL PILE(S) DATA (PHYSICAL)
COAL(S) DATA (CHEMICAL)
GROUND WATER DATA
II
METEOROLOGICAL DATA
HISTORICAL DATA (3 MONTHS PRIOR TO FIELD PROGRAM)
FIELD DATA (DURING FIELD PROGRAM)
PRECIPITATION
AIR TEMPERATURE
SOLAR RADIATION
EVAPORATION
PRECIPITATION
AIR TEMPERATURE
SOLAR RADIATION
EVAPORATION
III
RUNOFF DATA
DRY DAYS (INCLUDE STORM EVENTS WITH ≤0.10 INCHES OF PRECIPITATION)
STORM EVENTS (>0.10 INCHES OF PRECIPITATION)
CONTINUOUS IN-SITU MEASUREMENTS OF BASE FLOW
ROUTINE WATER ANALYSES
CONTINUOUS IN-SITU MEASUREMENTS OF RUNOFF
ROUTINE WATER ANALYSES

FIGURE 1: COAL PILE RUNOFF DATA REQUIREMENTS AT INDIVIDUAL SITES

RESULTS TO DATE

The monitoring program at Site 1 has been completed and a total of 4 runoff events were measured. Storms ranging in size from 0.19 inches to 1.8 inches of rain were measured. A series of hyetograph/hydrographs is plotted for the 4 storms and drainage coefficients were determined. As illustrated in Figures 2 to 6, drainage coefficients never went higher than 39 percent. This indicates that at least 60 percent or more of the rain hitting this pile was absorbed by the coal and lost to either evaporation, pyrite oxidation or base flow seepage. Two observations made during the monitoring at this site lend to the fact that the pile is acting like a large sponge. First, the pile was continuously growing with new coal from 38,000 tons to 120,000 tons and second, the moisture of the pre-fired coal was significantly greater than that of the delivered coal. These measured drainage coefficients are substantially lower than those reported in literature, i.e., 70 to 80 percent.

Most of the chemical analysis data has not been finalized to date, but a number of obvious observations can be made concerning the quality of the runoff. Briefly they include:

1. The pH of both storm runoff and base flow seepage did not vary. All pH's were in the 2.0 to 2.4 range.
2. The conductivity of the runoff was depressed during storm events, as low as 4,000 micromhos per centimeter (umho/cm) and during base flow seepage remained at a higher concentration, 8,000 to 9,000 umho/cm.
3. Conductivities correlated well with dissolved solids.
4. Because of the low pH, most of the metals found in the runoff were in a dissolved form rather than suspended.
5. Analysis of metals data during storm events can indicate the interflow hydrograph.

The completed results of the data collected at Site 1 will be included in the final report to ESEERCO.

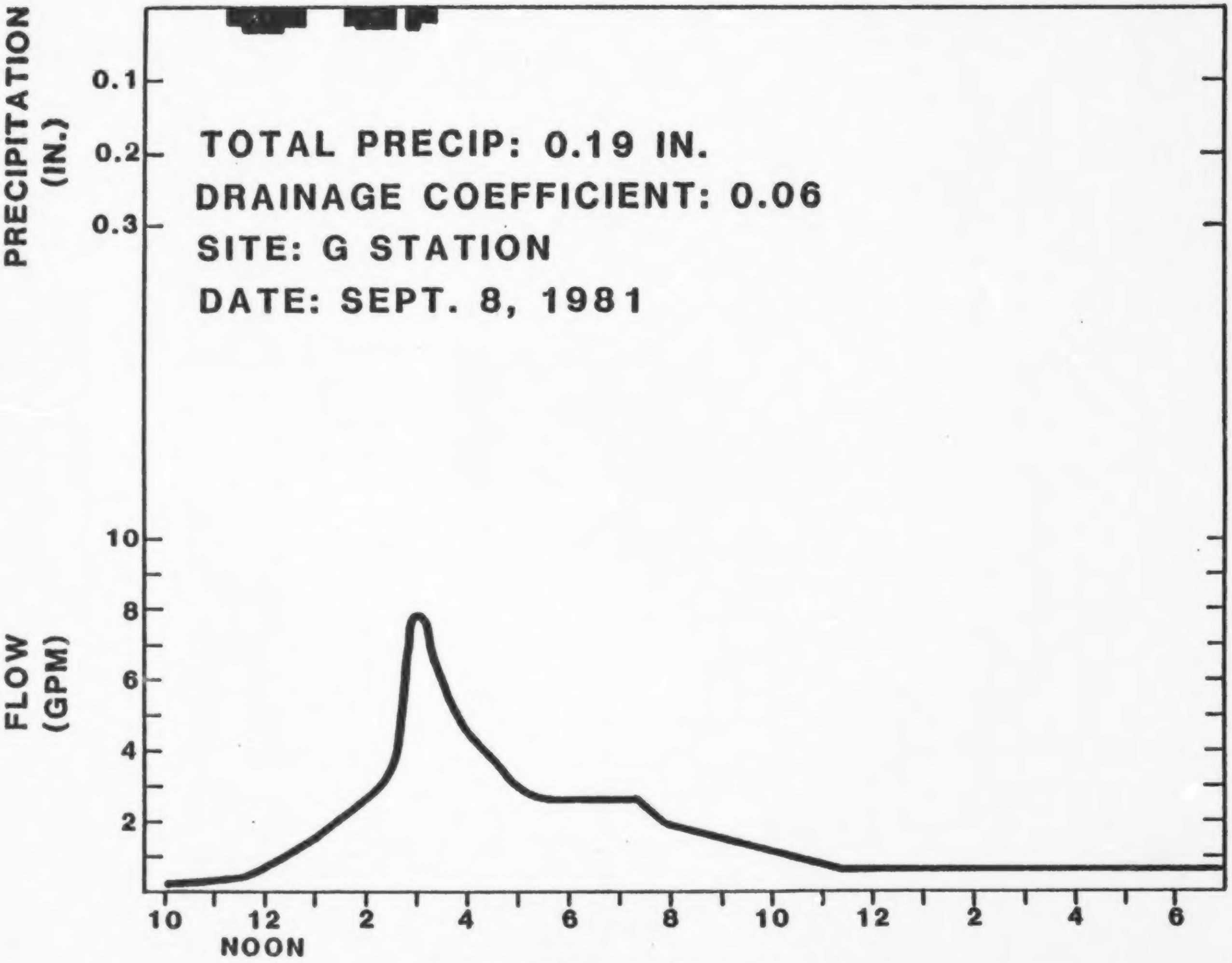

HYETOGRAPH/HYDROGRAPH
STORM EVENT 1

FIGURE 2

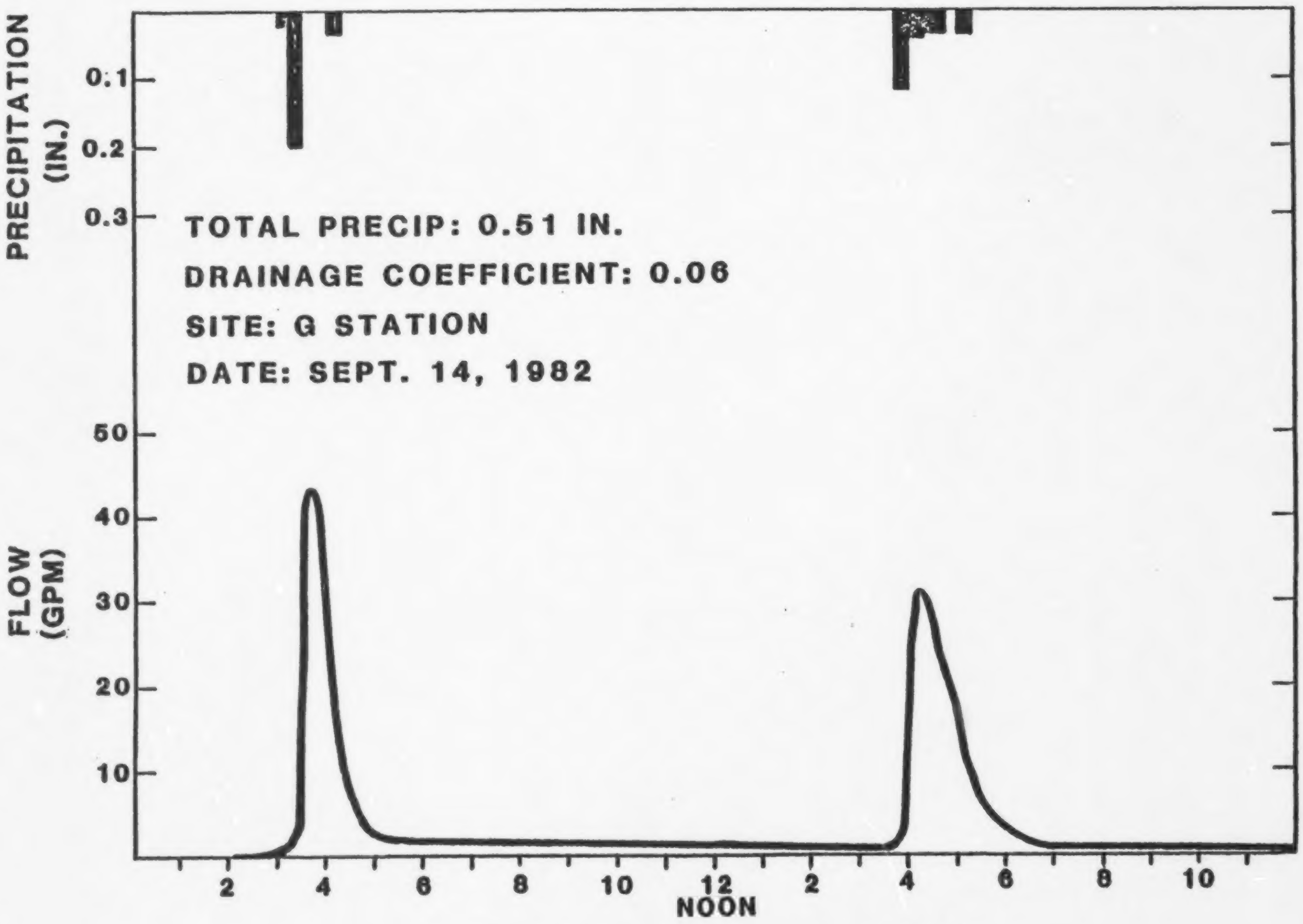

TOTAL PRECIP: 0.51 IN.
DRAINAGE COEFFICIENT: 0.06
SITE: G STATION
DATE: SEPT. 14, 1982

HYETOGRAPH/HYDROGRAPH
STORM EVENT 2

FIGURE 3

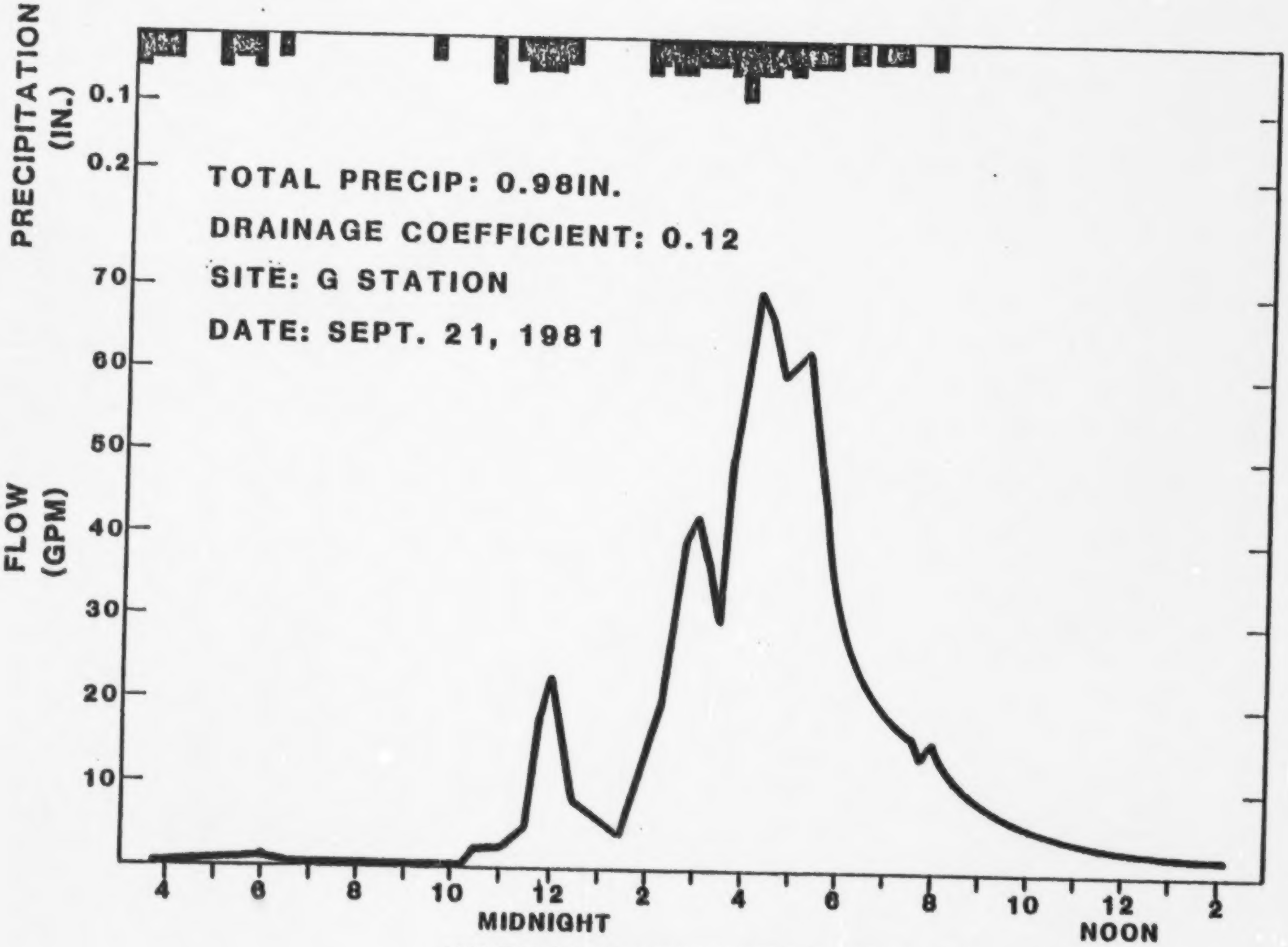

HYETOGRAPH/HYDROGRAPH
STORM EVENT 3

FIGURE 4

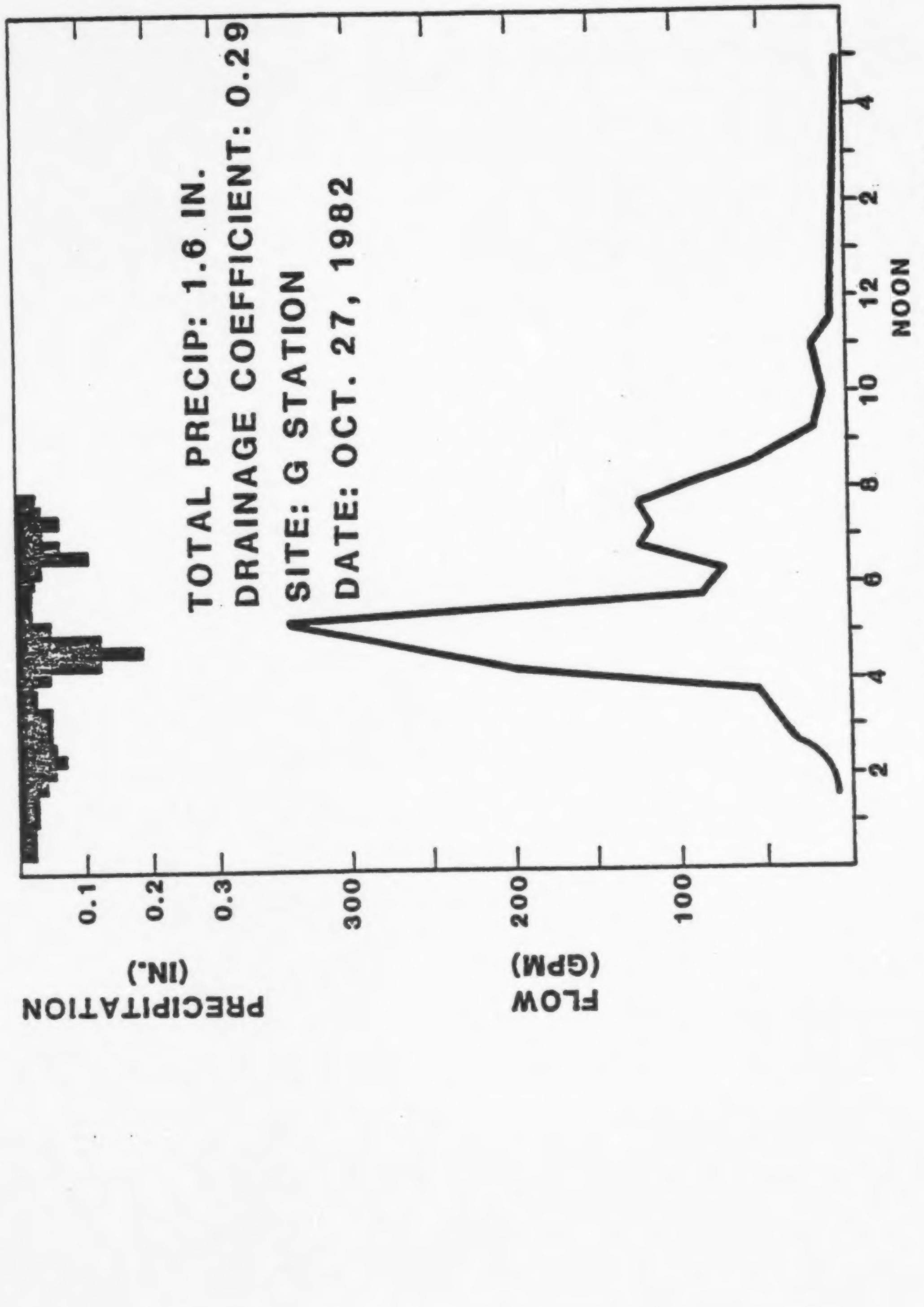

HYETOGRAPH/ HYDROGRAPH
STORM EVENT 4 - 1st PHASE

FIGURE 5

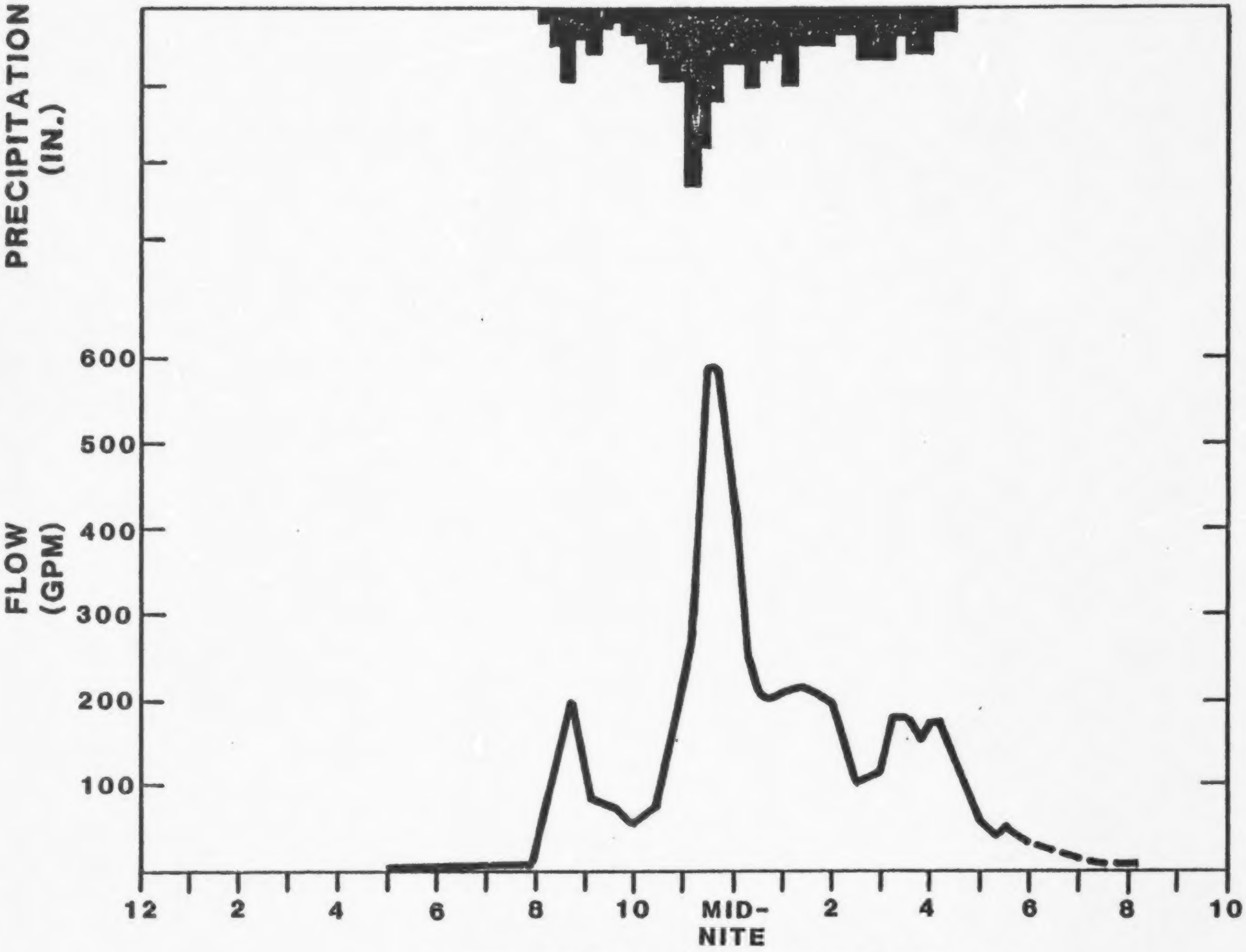

**HYETOGRAPH/HYDROGRAPH
STORM 4 2nd PHASE**

FIGURE 6

MODEL DEVELOPMENT

A 1976 TRC study of nonpoint source pollution at a utility site in Pennsylvania attempted to address sheet washoff from coal storage piles using the SWMM/RECEIV II model. This model was eventually thought deficient in the simulation of coal pile runoff because it did not take into account:

1. Erosion of coal from the pile surface,
2. Percolation of storm-water through the pile,
3. Pyrite oxidation/acid production in the coal pile.

In 1979, a follow-up study was conducted by TRC to determine what physical and chemical phenomena associated with coal pile runoff needed to be addressed so that the model could be used as a prediction tool. A number of phenomena were identified as characteristic of runoff and should, therefore, be included in the model. They are:

1. Precipitation in the form of rain and snow,
2. Surface runoff and infiltration through the pile,
3. Moisture content of the pile,
4. Snowmelt from piles subject to heavy winter accumulations,
5. Groundwater infiltration through the base of the pile,
6. Pyrite oxidation and acid production,
7. Freeze/thaw cycles,
8. Gully erosion along the sides of the pile,
9. Washoff of coal from the pile surface.

A comprehensive search of existing models found that the Ohio State University (OSU) version of the Stanford Watershed Model was a good basis for a coal pile runoff model. With extensive modification of the OSU model, the new model treats the coal storage pile as a small unvegetated watershed with many features similar to larger watersheds. A TRC coal pile runoff model was then developed and consists of two major components: the hydraulic and the qualitative.

BASIC FUNCTION OF HYDRAULIC COMPONENT

A diagram of the hydrologic cycle of a coal pile is shown in Figure 7. The model reads hourly precipitation data in the form of rain or snow input on a meteorological data tape or cards. A continuous water balance simulation in the model uses precipitation, pile moisture content and pile water storage as additions and surface runoff, interflow and base seepage as reductions. The hydraulic component of the model also predicts pile erosion caused by the gullying of the pile slopes during intense storms.

Hydraulic data are presently being measured in New York State at a utility coal pile for the calibration of the hydraulic model.

HIGHLIGHTS OF A WORKING HYDRAULIC MODEL

Once the hydraulic model has been calibrated and verified using data from several coal pile monitoring programs, it will become a working design tool. Input will consists of two data sets: 1) site specific data such as volume and acreage of the coal, average moisture content of the delivered coal and pile compaction data and 2) meteorological data either in the form of historical weather data vailable from the National Climatic Center (NCC) or local on-site measurements taken by the owner of the coal pile. Site-specific data are entered into the model by card deck while the historical weather data are entered on magnetic tape.

The working model lists daily, monthly and annual runoff flows plus the optional output of selected precipitation events with hourly or subhourly data.

Optional output from the hydraulic model are also available. The output are described below.

BASIC OUTPUT	OPTIONAL OUTPUT
1. Table of average daily rainfall.	1. All input data.

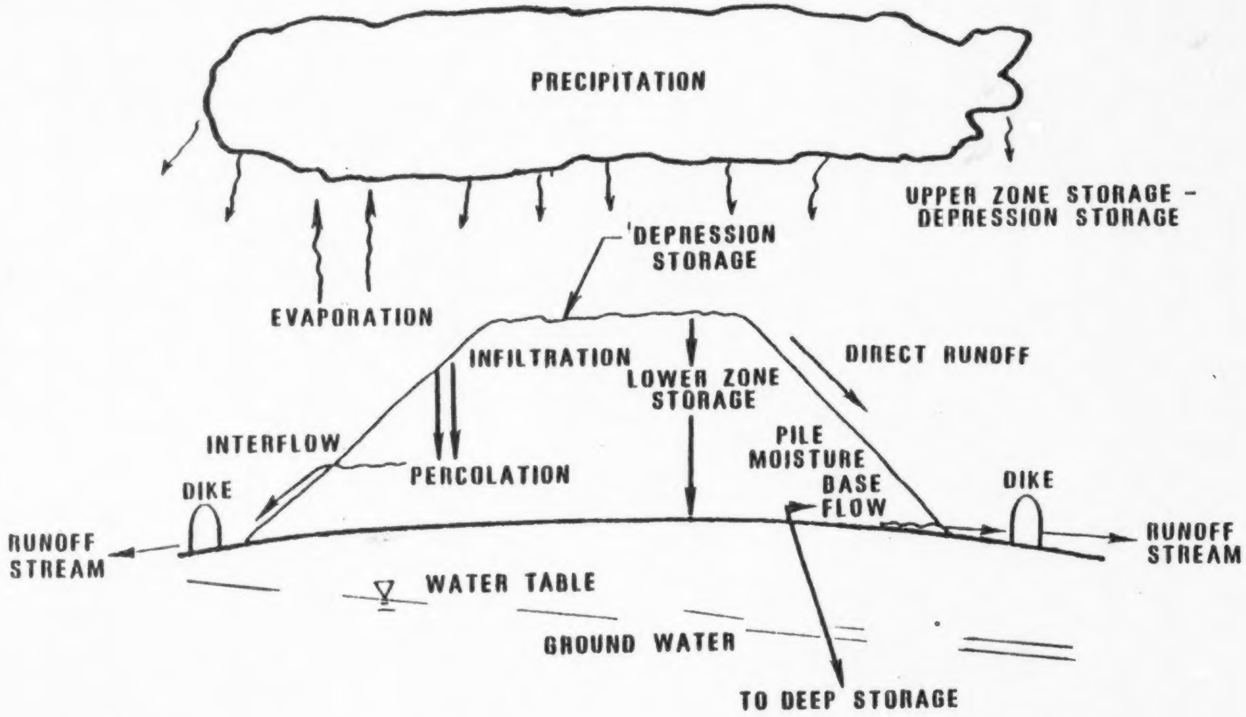
PRECIPITATION
UPPER ZONE STORAGE - DEPRESSION STORAGE
DEPRESSION STORAGE
EVAPORATION
INFILTRATION
LOWER ZONE STORAGE
DIRECT RUNOFF
INTERFLOW
PERCOLATION
PILE MOISTURE
BASE FLOW
DIKE
DIKE
RUNOFF STREAM
RUNOFF STREAM
WATER TABLE
GROUND WATER
TO DEEP STORAGE

HYDROLOGICAL CYCLE OF COAL STORAGE PILE

FIGURE 7

BASIC OUTPUT	OPTIONAL OUTPUT
2. Summation of daily runoff rates for each month.	2. Echo of recorded runoff (when measured) as a comparison with simulated flows.
3. Monthly and annual totals of runoff, seepage and total flow.	3. Daily values of snowpack, snowmelt and snowfall.
4. Monthly and annual total of frozen precipitation.	4. Average daily temperatures.
5. End-of-month values of pile, surface and groundwater moisture.	5. Number of freeze/thaw cycles
6. End-of-month values for snowpack.	6. Simulated gully erosion
7. Annual balance of unaccounted moisture.	7. Plots the hyetograph and hydrograph for selected storms.

BASIC FUNCTION OF THE QUALITATIVE COMPONENT OF THE MODEL

Stored coal exposed to the atmosphere undergoes the physical and chemical process of pyrite oxidation. Products of these reactions are acid, iron and sulfate. The acid further reacts with the coal by dissolving trace metals and elements. During wet weather, these materials are washed off the surface and moved through the interior of the coal pile. Runoff during storm events and seepage from the pile base during wet and dry weather carry these products of the pyrite oxidation to produce a highly acidic wastewater. The qualitative component of the model simulates these reactions; using the water balance produced in the hydraulic model, it will predict the loading of acid, sulfates and trace elements in the runoff.

The model looks at both dry weather reactions and the transport of the products of oxidation during wet weather. For dry weather, the model simulates the total pollutants in the coal and those in a dissolved state available for transport. For wet weather periods, the model simulates the distribution of a component of the dissolved metals, sulfates and acid from the surface of the pile to the interior and directly to surface runoff. In addition, the removal of materials from the interior of the pile by dry weather seepage is simulated. The results of the qualitative model will be a calculation of daily, monthly and totals of acid, metals and sulfates.

HIGHLIGHTS OF A WORKING QUALITATIVE MODEL

Once the qualitative component of the model has been calibrated and verified, it will be available for use. Input to this model are from two sources:

1. A magnetic tape created by the hydraulic model containing data on rainfall, transport routes, flow rates from seepage and runoff and average daily air temperature.
2. Card input describing factors of pyrite oxidation including: percent of pyrite in the coal, density of the coal pile, amount of trace metals in the coal and the solubility of sulfate and iron compounds.

As data from the ongoing field program are evaluated, the oxidation reaction rates will be adjusted. Output of the working qualitative model will be:

1. A calendar for any selected year showing dry versus wet days,
2. A calendar listing daily runoff flow volumes,
3. Daily total loadings of acid, sulfate, iron and trace metals,
4. Optional plots on a detailed storm basis showing the relationships of precipitation, flows and pollutant loadings.

CALIBRATION EFFORT TO DATE

The calibration effort being completed has found that the model can easily simulate the water balance of large storm but usually overpredicts the runoff volume from short intense storms. In addition, gully erosion, which is very sensitive to the intensity of precipitation, is difficult to simulate using precipitation amounts averaged over an hourly period.

SUMMARY

The ultimate purpose of simulating coal pile drainage is for use in the design of systems to treat acid drainage before discharge. Industries storing coal may base treatment system design on short-term monitoring programs; however, that data may not have any relationship to average or worst-case runoff conditions. The runoff model will allow an industry to simulate several runoff conditions and thereby have a better basis for design.

The current coal pile runoff program in New York State has two objects:

1. To provide detailed information on meteorological, coal storage, pile moisture, runoff quality and hydrologic conditions to the developing model so that key coefficients may be adjusted;
2. To provide approximately 10 weeks of continuous data from each of two coal pile monitoring sites as a data bank useful for comparative studies and treatment design.

One important issue to be resolved during this program is whether a runoff condition occurs producing a discharge "clean" enough to bypass treatment. Runoff data collected at two utility sites in Pennsylvania in 1976 indicates that a first flush did indeed occur. However, initial data collected to date showed that runoff acidity and sulfate were very high during all phases of the storm and during dry weather seepage. The analysis of storms of greater volume may help resolve this first flush issue.

The field data collection programs are to be completed in May of 1982 with the runoff model completed in September of 1982.

The work described in this paper was not funded by the U.S. Environmental Protection Agency. The contents do not necessarily reflect the views of the Agency and no official endorsement should be inferred.

Coal Pile Simulation Study

by
Aileen M. Schumacher, P.E.
Senior Associate Engineer

Eric G. Hanson, P.E.
Manager
Industrial Waste Engineering Section

Environmental Science and Engineering, Inc.

ABSTRACT

Runoff and leachate from coal storage piles may contain heavy metals and other pollutants in concentrations that are high enough to be potential hazards to the environment. Consequently, many new coal-fired power plants and other coal-handling facilities may be required to collect and treat contaminated runoff and leachate. This paper presents the methodology used to simulate the characteristics of runoff and leachate from a proposed, full-scale coal storage pile. These studies were undertaken to provide characterization data for input in determination of compliance with applicable effluent criteria. Four coal types, similar in chemical composition including sulfur content, were tested. One of the four coal types resulted in simulated runoff and leachate which consistently violated several criteria. Simulated runoff and leachates from the other three coal types met all effluent criteria.

The testing agreed with previous research, showing that runoff and leachate with low pH values could be expected to have high concentrations of heavy metals. The testing also demonstrated a procedure for use in evaluating alternative coal supplies by assessing their pollution potential.

INTRODUCTION

Various approaches for characterizing coal pile leachate and runoff have been used by other researchers; these approaches have included sprinkling pans of coal with a rainfall simulator (7), recirculating distilled water over an inclined box packed with sample (4), and collecting actual leachate and runoff on site (2). As the methodologies and coals used in different tests varied, so did the results.

One general conclusion of a study (5) concerning the treatability of coal pile leachate and runoff was that heavy metals and other trace elements in leachate were direct functions of acidity. As acidity increased, so did the concentration of heavy metals and trace elements in coal pile leachate and runoff. Verification of this conclusion was an important objective of the study reported herein.

Generally, it would be preferable to collect samples from actual facilities in order to assess the characteristics of runoff and leachate. However, because the coal pile under consideration did not yet exist, it was simulated by the test methodology described in this paper. These efforts were designed to represent actual conditions as closely as possible, including actual dimensions and design density of the full-scale coal pile.

This study was conducted for a facility converting to coal as a primary fuel source. An on-site coal storage pile was therefore required. A coal pile simulation test was conducted to determine the quality of leachate and runoff resultant from rainfall contacting the facility's coal pile. Testing was conducted on four types of coal being considered as fuel sources: Coals 1, 2, 3, and 4. The simulated leachate and runoff were compared to applicable effluent criteria.

TEST METHODOLOGY

A coal pile simulation apparatus was built to the same scale as the proposed coal pile: 10 ft (3 m) in height, 14-ft (4-m) sides sloped 45 degrees to the horizontal. The test apparatus, shown in Fig. 1, consisted of vertical columns and open-top, sloped troughs. Only polyvinyl chloride (PVC) pipe, rubber hoses, fiberglass netting, plastic duct tape, nylon cord, and wood were used to prevent metal contamination, since heavy metals often are the primary concern in coal pile runoff and leachate. Ten-ft (3-m) high vertical columns, constructed of 4-in. (102-mm) diameter PVC pipe and packed with coal at the design density, were intended to simulate rainfall passing through the entire 10-ft (3-m) depth of the coal pile. Fourteen-ft (4-m) long troughs, constructed of 10-in. (254-mm) diameter PVC pipe cut in half and packed with coal at the design density of 55 pounds per cubic foot (lb/cu ft) (881 kg/m^3), were designed to simulate the side slopes of the coal pile. Thus, the troughs simulated runoff, the columns leachate.

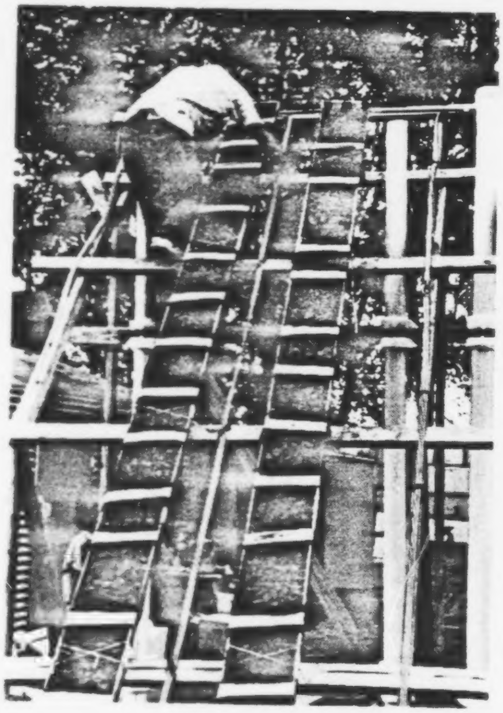

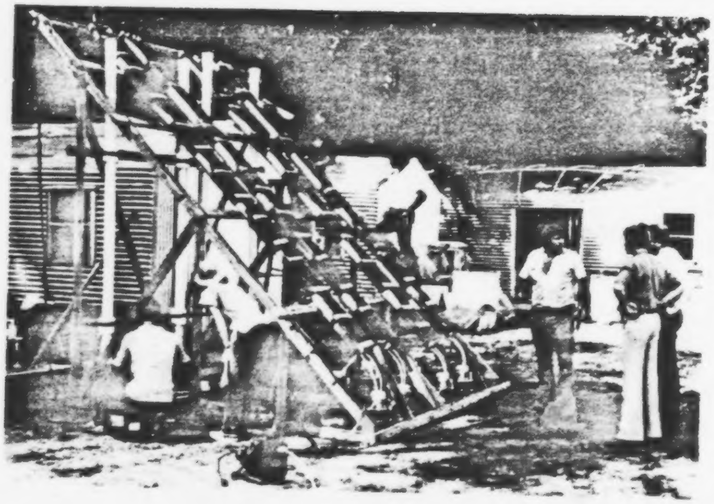

SOURCE: ENVIRONMENTAL SCIENCE AND ENGINEERING, INC.,1980 .

Figure 1 **COAL PILE SIMULATION APPARATUS**	**Coal Pile Simulation Study**

Simulated runoff was drained by two hoses at the end of the trough. The troughs were under-drained at a coal depth of 3 to 3.5 in. (76 to 89 mm) to remove the leachate, as depicted in Fig. 2. If the troughs had not been under-drained, water which infiltrated into the coal pile would have continued contacting the coal as it drained along the bottom of the trough and contributed to the volume of runoff. The under-drains also allowed separation of the volume of water which would infiltrate into a coal pile from the volume of water defined as runoff. These trough leachate samples were collected and analyzed to provide additional data describing runoff characteristics.

Prior to testing, the coal samples were passed through a 2.25-in. (57-mm) sieve to ensure that the tested coal met the size specifications of the actual coal to be stored in the pile. The coal was then packed into both the PVC columns and the PVC troughs at the full-scale design density and secured with fiberglass netting, plastic duct tape, and nylon cord.

Small amounts of certain inorganic salts were added to raw ground water to approximate the characteristics of site-specific rainfall. An average site-specific rainfall event of 0.66 in. (17 mm) was selected as the rainfall volume to be applied for the simulation. The synthetic rainfall was distributed over the PVC troughs via a sprinkling system consisting of plastic lawn sprinkler hoses. The majority of the fiberglass netting securing the coal was removed after initial wetting had occurred and the coal had settled into the trough. Simulated runoff and trough leachate were collected in separate glass containers, as shown in Fig. 3. Several rainfall gauges placed under the apparatus were used to measure the amount of applied synthetic rain water falling on the coal pile apparatus. Sprinkling was continued until the average reading of these gauges was 0.66 in. (17 mm).

To generate simulated leachate from the vertical PVC columns, a measured volume of synthetic rain water was poured on the coal at the top of the columns until leachate appeared at the bottom. All resulting simulated leachate was collected in a glass container. Details of leachate generation are shown in Fig. 4.

Each coal type produced three streams: runoff, trough leachate, and column leachate. Each sample was analyzed for various parameters addressed in applicable effluent criteria. All analyses were performed according to United States Environmental Protection Agency (EPA) Method 60014-79-020 and Standard Methods for Analysis of Water and Wastewater (1).

RESULTS

Table 1 presents the analytical results of the coal pile simulation. The applicable effluent criteria are also presented for comparison.

No consistent difference in concentration was observed between simulated runoff and simulated leachate from the four coal types in the test apparatus. The rainfall event applied to the troughs and the amount of synthetic rain water applied to the columns to obtain leachate resulted in

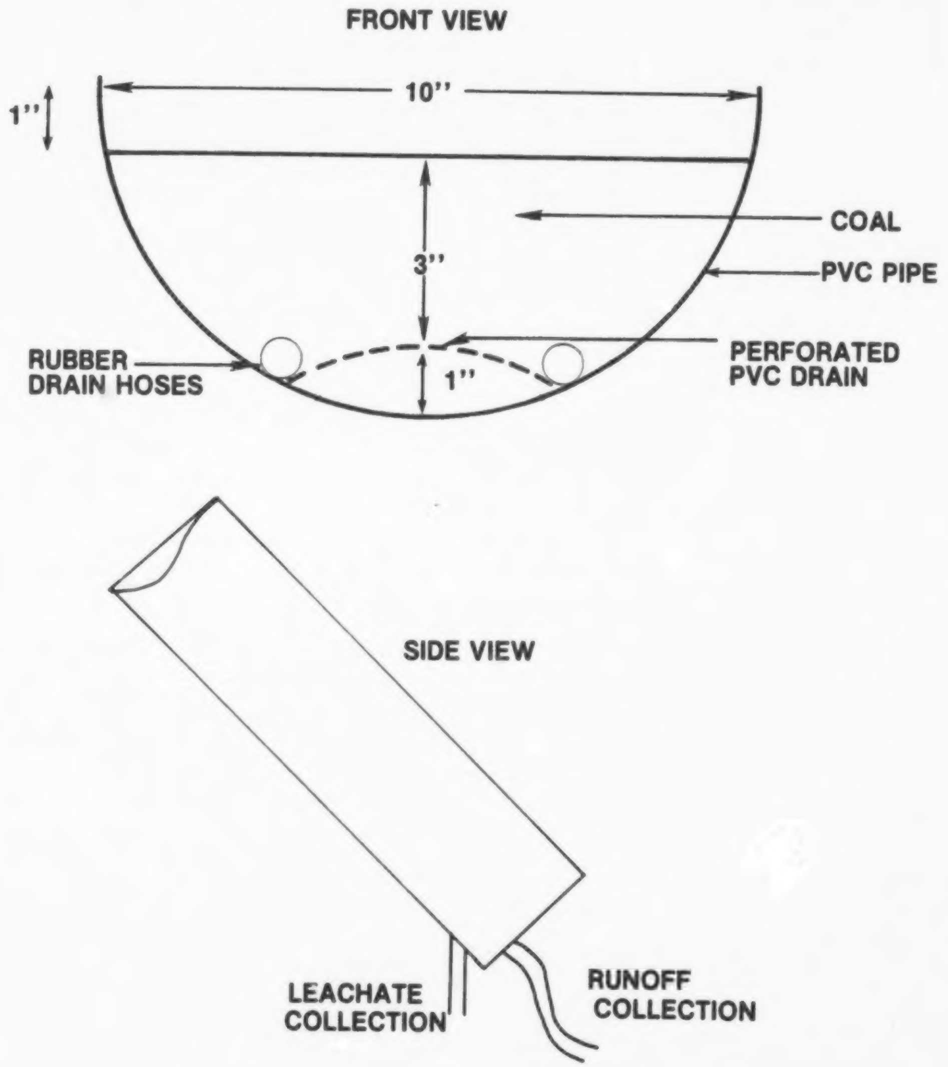
FRONT VIEW
10''
1''
COAL
3''
PVC PIPE
RUBBER DRAIN HOSES
PERFORATED PVC DRAIN
1''
SIDE VIEW
LEACHATE COLLECTION
RUNOFF COLLECTION

SOURCE: ENVIRONMENTAL SCIENCE AND ENGINEERING, INC., 1980.

Figure 2

DETAILS OF TROUGH

Coal Pile Simulation Study

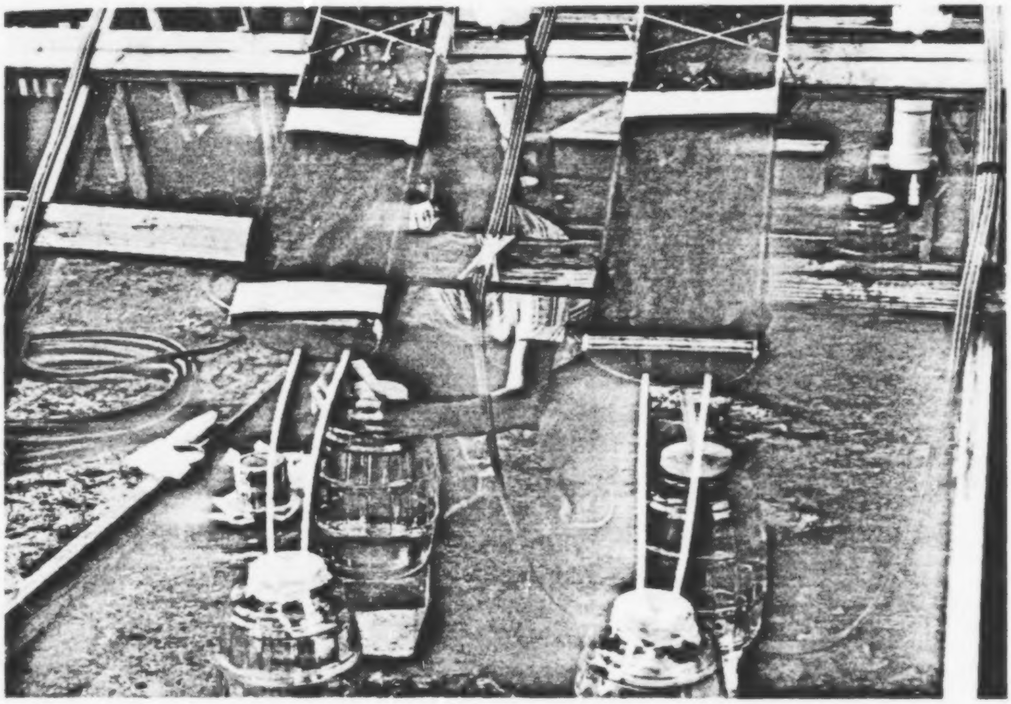

SOURCE: ENVIRONMENTAL SCIENCE AND ENGINEERING, INC., 1980.

Figure 3 TROUGH UNDERDRAINS AND RUNOFF COLLECTION	**Coal Pile Simulation Study**

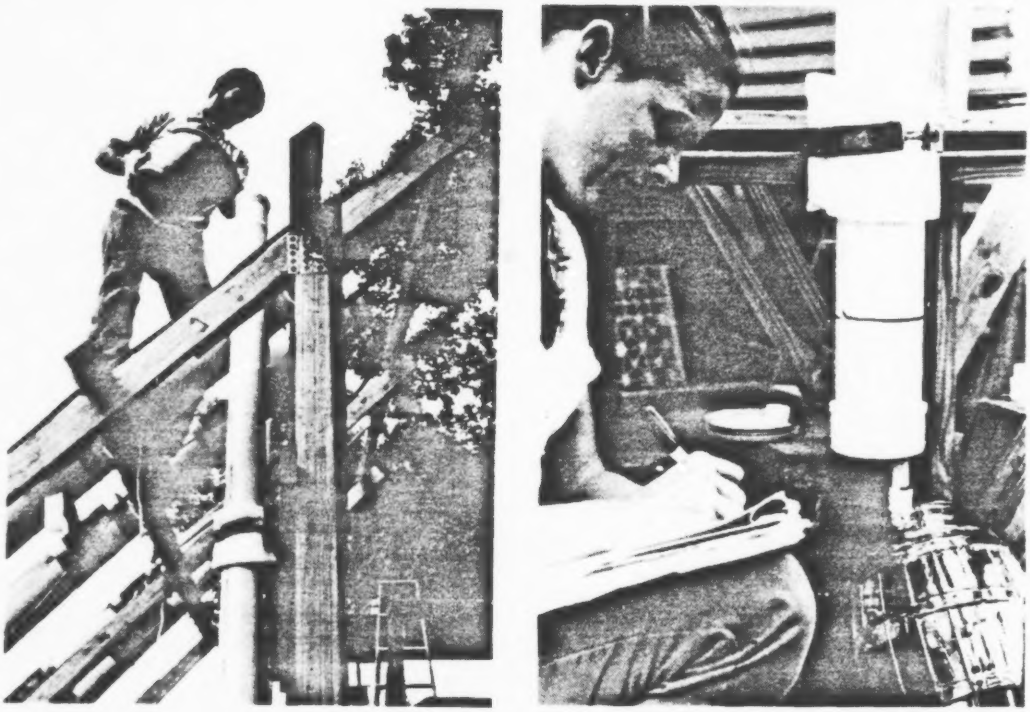

SOURCE: ENVIRONMENTAL SCIENCE AND ENGINEERING, INC., 1980.

Figure 4

COLUMN LEACHATE GENERATION AND COLLECTION

Coal Pile Simulation Study

Table 1. Results of Coal Pile Simulation Test and Applicable Effluent Standards (all values mg/L except pH)

			SAMPLE IDENTIFICATION											
			Coal Type 1			Coal Type 2			Coal Type 3			Coal Type 4		
Parameter (1)	Effluent Standard (2)	Synthetic Rain Water (3)	TR (4)	CL (5)	TL (6)	TR (7)	CL (8)	TL (9)	TR (10)	CL (11)	TL (12)	TR (13)	CL (14)	TL (15)
pH	6.0-8.5	6.6	6.3	6.4	6.5	6.1	6.2	6.5	6.1	6.2	6.5	2.7	2.8	2.8
Arsenic	0.05	N/D	N/D	0.013	0.01	N/D	N/D	N/D	N/D	N/D	N/D	0.221	0.114	0.131
Total Chromium	1.0	N/D	0.003	0.004	0.004	0.004	0.002	0.002	0.002	N/D	0.001	0.068	0.048	0.040
Lead	0.05	0.002	N/D	0.002	0.002	0.012	N/D	0.002	N/D	N/D	0.002	0.132	0.018	0.406
Mercury	N/D	N/D	N/D	N/D	N/D	N/D	N/D	N/D	N/D	N/D	N/D	N/D	N/D	N/D
Chlorides	500.0	81.0	116.0	99.0	124.0	109.0	92.0	106.0	103.0	88.0	114.0	109.0	90.0	96.0
Copper	0.5	N/D	N/D	N/D	N/D	N/D	N/D	N/D	N/D	N/D	N/D	0.687	0.395	0.469
Iron	0.3	N/D	N/D	0.204	0.204	N/D	N/D	N/D	N/D	N/D	N/D	361.0	190.0	214.0
Zinc	1.0	0.188	0.016	0.016	0.024	0.013	0.01	0.016	0.013	0.013	0.013	4.52	6.04	4.93

TR = Trough simulated runoff
CL = Column simulated leachate
TL = Trough simulated leachate
N/D = None detectable

NOTE: 1 mg/L = 1 ppm.

Source: ESE, 1980.

approximately the same solid-to-liquid ratio. This ratio was 5.6:1 for the troughs and 4.5:1 to 5.8:1 for the columns.

Samples of simulated leachate and runoff from Coal 4 in the test apparatus exceeded the criteria for several parameters. Moreover, the simulated leachate and runoff resulting from this coal were highly acidic, with pH values between 2.7 and 2.8.

SUMMARY AND CONCLUSIONS

Coal pile simulation tests were performed on four coal types in order to predict leachate and runoff quality. Samples generated from the testing were compared to applicable effluent criteria. One of the four coal types (Coal Type 4) tested resulted in simulated runoff and leachate which consistently violated several criteria. The other three coal leachates met all effluent criteria.

The testing agreed with previous research, showing that runoff and leachate with low pH values could be expected to have high concentrations of heavy metals. The testing also demonstrated a procedure for use in evaluating alternative coal supplies by assessing their pollution potential.

CONTROL OF ACID PROBLEMS IN DRAINAGE FROM COAL STORAGE PILES

by

Harvey Olem, Tracey L. Bell, and Jeffrey J. Longaker

Office of Natural Resources
Tennessee Valley Authority
Chattanooga, TN 37401

The work described in this paper was not funded by the U.S. Environmental Protection Agency. The contents do not necessarily reflect the views of the Agency and no official endorsement should be inferred.

Abstract

A method has been identified for controlling acid production and subsequent dissolution of toxic pollutants in drainage from coal storage piles. Results of laboratory and field experiments indicate that it may be possible to prevent, rather than treat, acid drainage by applying an environmentally safe detergent formulation periodically to the coal. A mild solution of sodium lauryl sulfate (SLS) was found to effectively block the activity of the bacteria that promote acid formation and chemical leaching. Drainage from coal treated once with 50 mg/L of SLS remained neutral for 60 days, about three times longer than the untreated control sample. Extrapolating results to an industrial-scale application revealed that the cost of the SLS needed for a single application might be as high as $500 per hectare of coal storage area ($200 per acre).

Introduction

As more and more utilities and industries throughout the United States shift from the consumption of oil and natural gas to the more abundant supplies of coal, there should be an increase in onsite storage of the coal. It has been projected that by 1985 the amount of coal in storage in the United States will increase from its current level of 128 million metric tons (1978 estimate) to 227 million metric tons. By the year 2000, the total coal stockpiled could reach 680 million metric tons (1). This projected increase in coal storage has generated renewed interest in the environmental effects of contaminated drainage from coal storage facilities.

The most efficient method currently used for storing large quantities of coal is placement on the ground. Because the coal is exposed to the elements, rainwater falling on the pile can become contaminated by the action of chemolithotrophic bacteria on pyritic materials (usually iron disulfides). This occurs by the same series of reactions that are known to produce acid drainage from coal mines. Consequently, pollution of both surface and ground water is usually the major problem associated with storage of this coal.

Drainage from coal storage areas generally contains high concentrations of metallic ions (aluminum, iron, manganese, mercury, nickel, zinc, etc.), sulfates, and suspended solids. It also usually has an extremely low pH (pH 2 to 3). Currently this drainage is typically collected in a central pond and treated, usually by addition of hydrated lime.

This paper presents results of laboratory experiments which indicate that it may be possible to prevent, rather than treat, acid drainage by applying an environmentally safe detergent formulation periodically to the coal. Laboratory experiments consisted of applying two anionic detergents to columns filled with coal which had been rinsed with water until the pH of drainage was neutral. This was done to simulate freshly mined coal or more nearly, coal that had been processed by coal washing. A third column was filled with coal and did not receive any detergents as a control. Due to the limited number of tests performed to date, the results are considered preliminary.

Background

One of the most common and most troublesome impurities in coal is a metallic sulfide, iron pyrite. When mining exposes pyrite (FeS_2) to water and oxygen, a chain of chemical reactions begins.

$$2FeS_2 + 7O_2 + 2H_2O = 2Fe^{2+} + 4SO_4^{2-} + 4H^+ \quad (1)$$

$$4Fe^{2+} + O_2 + 4H^+ = 4Fe^{3+} + 2H_2O \quad (2)$$

$$Fe^{3+} + 3H_2O = Fe(OH)_3 + 3H^+ \quad (3)$$

$$FeS_2 + 14Fe^{3+} + 8H_2O = 15Fe^{2+} + 2SO_4^{2-} + 16H^+ \quad (4)$$

In reaction 1 pyrite is oxidized to produce ferrous iron (Fe^{2+}), sulfate (SO_4^{2-}), and some acid (H^+). The ferrous iron can then be oxidized with this acid and some oxygen (reaction 2) to form ferric ions (Fe^{3+}). Under certain conditions, the ferric irons will hydrolyze (reaction 3) to form the yellow-orange ferric hydroxide precipitate ($Fe(OH)_3$) that typically appears in acid mine drainage streams. Ferric iron can also react with more pyrite (reaction 4) to form more ferrous iron and acidity. These reactions produce acid at a constant rate.

Acid drainage would develop very slowly if this strictly chemical chain of events were not greatly accelerated by the biochemical action of certain bacteria. First isolated in 1947, Thiobacillus ferrooxidans were then believed to play some role in acid mine drainage formation, but their exact role was not well understood (1). More recently, Singer and Stumm (2) showed that direct oxidation of pyrite by oxygen (reaction 1) was too slow to generate the amount of acidity observed in nature and concluded that the oxidation of ferrous iron to ferric (reaction 2) created a cycle whereby the ferric ions produced in this reaction directly attack pyrite to form considerable amounts of acid (reaction 4). Reaction 2, however, is extremely slow chemically under acid conditions. The half time for spontaneous ferrous iron oxidation in a sterile solution of pH 3.5 has been estimated to be 2,000 days (3). In the presence of T. ferrooxidans, however, this reaction was shown to accelerate by a factor of 10^6, thus producing significant quantities of ferric iron. The subsequent oxidation of pyrite by these ferric ions produces more ferrous ions to allow the cycle to continue, producing more and more acidity until all the reactive pyrite is leached.

Bacterial Inhibition

It is generally considered preferable to prevent the formation of pollutants through at-source control rather than provide continuous treatment of the resulting contaminated water. It is with this objective in mind that bacterial inhibition of acid formation was investigated to prevent the contamination of rainfall-runoff draining through coal piles. Anionic detergents, while normally considered as cleansers rather than bactericides, do possess bactericidal properties. Dugan (4) found that anionic detergents can effectively stop iron oxidation by T. ferrooxidans at concentrations as low as 2 mg/L. Kleinmann (5,6) demonstrated the effectiveness of one one type of detergent, sodium lauryl sulfate, in reducing acid formation in coal refuse piles and surface coal mines at somewhat higher detergent concentrations. The reason for this inhibition is not yet clear, but evidence indicates that the semipermeable properties of the cytoplasmic membrane is altered so that H^+ is allowed to seep into the normally neutral interior of the cell (7). Thus, the bacteria are appropriately attacked by the acid they helped produce.

In this study, two types of anionic detergents were evaluated, sodium lauryl sulfate (SLS) and neutralized benzene sulfonate (NBS). The common use for each detergent is shown in Table 1.

Materials and Methods

Three acrylic plastic columns were set up in the laboratory to simulate a coal pile (Figure 1). The columns were approximately 2 meters high

Table 1. Detergents Tested to Prevent Coal Pile Drainage Contamination

Detergent	Common Use	Percent Active Ingredient in Product Tested
Sodium Lauryl Sulfate	Active ingredient in many hair shampoos	30
Neutralized Benzene Sulfonate	Active ingredient in many laundry detergents	15

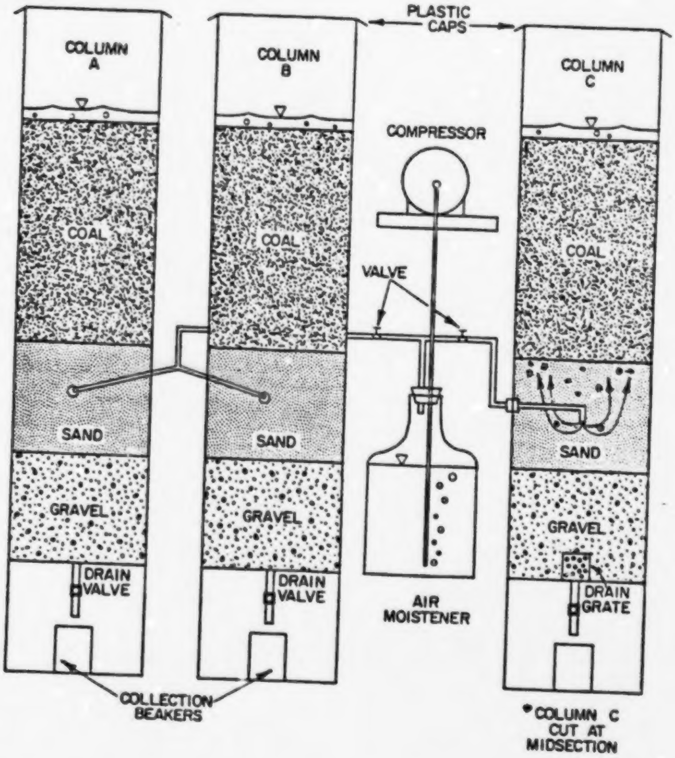
PLASTIC CAPS
COLUMN A
COLUMN B
COLUMN C
COMPRESSOR
COAL
COAL
COAL
VALVE
SAND
SAND
SAND
GRAVEL
GRAVEL
GRAVEL
DRAIN VALVE
DRAIN VALVE
AIR MOISTENER
DRAIN GRATE
COLLECTION BEAKERS
*COLUMN C CUT AT MIDSECTION

Figure 1. Laboratory columns used to simulate coal pile drainage.

and 30 cm in diameter. A 1.5-cm diameter drain valve was located in the bottom of each column to collect leachate. The underdrain system in the columns consisted of a 20-cm depth of thoroughly washed pea gravel under 25 cm of washed sand. To prevent the gravel from clogging the drain, a capped 10-cm diameter, 13-cm long perforated plastic column was glued over each drain hold. Compressed air was passed through water and fed through an "L" shaped glass tube to simulate atmospheric conditions within a coal pile. The tube was located at mid-height in the sand layer. The sand also acted as a diffuser to distribute the air across the coal.

Coal was obtained from the Tennessee Valley Authority (TVA) Cumberland Power Plant located near Nashville, Tennessee. Small samples of the coal were collected from different locations and depths around the coal pile. The samples were then composited. The composite was rinsed with water until the pH of drainage was neutral in order to simulate freshly mined coal or coal that had been processed by coal washing. A portion of the washed coal was analyzed for total sulfur, moisture, volatile matter, ash, fixed carbon, and Btu content.

Approximately 0.057 cubic meters of the coal was divided equally between the three columns. The procedure of the three coal samples was identical except for the different solutions applied.

Each coal sample was initially placed in a 5-gallon bucket and saturated with the necessary solution for one hour. The excess water was poured off and the resultant slurry poured into the appropriate column. In the first column, coal was treated with deionized water only. Coal in another column was treated with a 50 mg/L solution of SLS and deionized water. A 50 mg/L solution of NBS and deionized water was added to coal in the remaining column.

The columns were dosed twice a week with 1,500 mL of deionized water to simulate a 2.5-cm (1-inch) rainfall contacting a coal pile. Leachate was then collected from the drain valves at the bottom of the columns for analysis.

Acidity, pH, conductivity, iron, manganese, and the most probable number (MPN) of iron-oxidizing bacteria were routinely analyzed on the collected samples. Selected trace metals and detergent concentrations were also analyzed periodically during the experiment. The deionized water used in the experiment was routinely analyzed for pH. All chemical analyses were performed according to procedures outlined in "Standard Methods" (8). Enumeration of iron-oxidizing bacteria was estimated by employing the inorganic salts culture medium and the combination multiple tube and microtitre plate procedure described by Olem and Unz (9).

Results and Discussion

Coal Characteristics--Characteristics of the coal used in these experiments are shown in Table 2. The total sulfur content was typical for coal burned at most TVA power plants. Coal with these characteristics has been found to produce strongly acidic drainage exposed to the elements.

Simulated Rainwater--The deionized water used to simulate rainfall had a pH of approximately 5.5. The acidity present in the deionized water was due to contact with atmospheric carbon dioxide.

Leachate Characteristics--The quality of leachate from each coal column three days after initial application of detergents is presented in Table 3. As expected, the drainage was initially pH 7.2 for all three columns. Most other water chemistry characteristics were similar for the drainage from all three columns, although certain parameters varied widely. After remaining nearly neutral for about 20 days, the leachate

Table 2. Analysis of Coal Used in Laboratory Simulation of Coal Pile Drainage

Parameter	Units	Value
Total Moisture	%	3.8
Volatile Matter	% Dry Basis	39.8
Ash	% Dry Basis	9.8
Fixed Carbon	% Dry Basis	50.4
Total Sulfur	% Dry Basis	3.1
Energy Content	Btu/lb Dry Basis	13,162

Table 3. Quality of Leachate from Laboratory Coal Columns Three Days After Initial Application of Detergents

Parameter	Concentration In Leachate (μg/l unless indicated) Control	SLS Treated	NBS Treated
pH (S.U.)	7.2	7.2	7.2
Acidity (mg/l $CaCO_3$)	0.6	0.3	0.3
Conductivity (μmhos/cm)	480	210	600
Fe	1,020	299	1,680
Mn	96	22	100
Pb	4	<1	11
Hg	0.7	0.3	<0.2
As	1	<1	1
Cd	0.2	<0.1	<0.1
Cu	<1	<1	4
Se	1	<1	2
Cr	2	320	1
Ni	<50	<50	<50
Zn	<5	<5	<5

suddenly became ten-thousandfold more acid in the control column, as pH decreased from 7 to about 3 (Figure 2). The pH continued to decline for another 20 days until it leveled off at about pH 2.

Drainage from the test column treated with NBS became slightly more alkaline at first but remained approximately neutral only about five days longer than the control. Then it paralleled the same pattern of rapidly increasing acidity, reaching pH 2 after about 50 days.

Drainage from the coal treated with SLS became even slightly more alkaline for the first 20 days. After a slight decrease in pH, it remained neutral for two and one-half times longer than the control. Even when the pH finally dropped after about 60 days, it hovered for another 25 days between pH 4 and 5. The acidity at this pH was approximately 100 mg/L, compared to 5,000 mg/L for the control column. This difference could be extremely important in terms of the treatment that would be needed to neutralize it.

The coal treated with SLS eventually produced drainage with the same low pH of about 2, but only after 140 days, three and one-half times longer than the 40 days for the untreated control.

Other constituents generally followed the same pattern as the changes in pH. The quality of leachate from each column 56 days after initial detergent application is presented in Table 4. At this point in the experiment, only drainage from the SLS-treated coal was neutral. Acidity in drainage was over 100 times higher in the control and NBS-treated coal. Significantly lower concentrations were also observed in drainage from the SLS-treated coal for conductivity, Fe, Mn, As, Cd, Cu, Cr, Ni, and Zn. Only Pb and Se were higher in drainage from SLS-treated coal compared to the control. However, these concentrations were almost at the detection limits for these constituents.

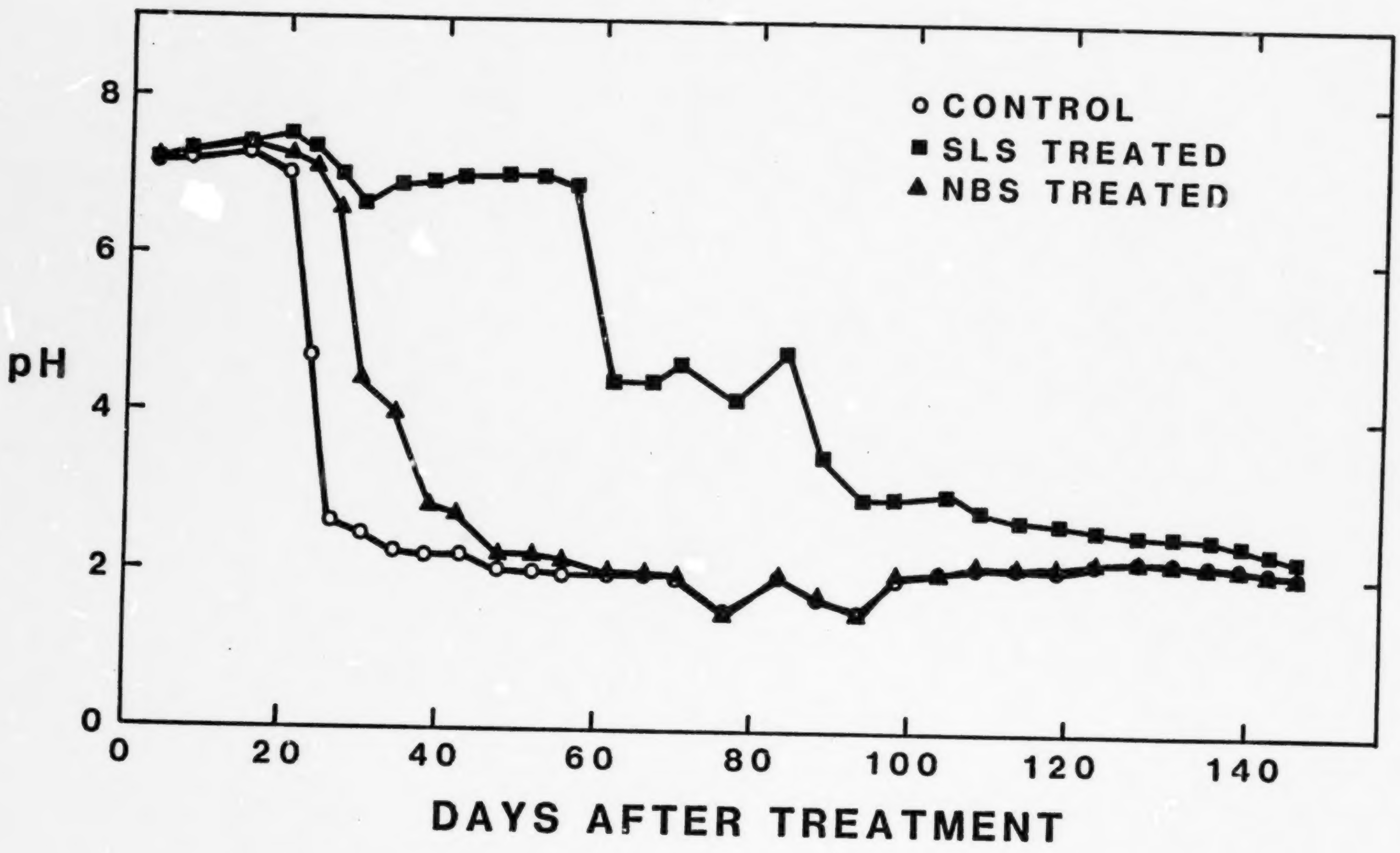

Figure 2. Changes in pH in laboratory-generated coal pile drainage following application of 50 mg/L of sodium lauryl sulfate (SLS) and neutralized benzene sulfonate (NBS).

Table 4. Quality of Leachate from Laboratory Coal Columns
Fifty Six Days After Initial Application of Detergents

Parameter	Concentration In Leachate (μg/l unless indicated) Control	SLS Treated	NBS Treated
pH (S.U.)	2.0	6.9	2.1
Acidity (mg/l $CaCO_3$)	5,000	10	5,500
Conductivity (μmhos/cm)	6,000	1,950	5,500
Fe	1,560,000	365	1,004,000
Mn	48,900	1,780	74,500
Pb	<1	2	7
Hg	0.3	<0.2	<0.2
As	200	1	220
Cd	310	2.3	340
Cu	1,050	7	1,160
Se	<1	4	1
Cr	295	<1	2
Ni	1,500	<50	3,300
Zn	13,700	<5	16,700

Drainage from both treated columns had detergent concentrations below detection limits (<0.1 mg/L measured as methylene blue active substance). This is important because these detergents are toxic to aquatic life. For example, Dailela et al. (10) found the LC_{50} value for a certain species of fish exposed to SLS to be 11.2 mg/L. Apparently, SLS was not washed much out of the coal. Most of it was probably adsorbed onto the coal particles and remained there until its chemical structure was broken down into simple degradation products such as carbon dioxide, water and sodium and sulfate ions.

Kleinmann and Erickson (6) performed a detergent adsorption capacity test on refuse from a coal-cleaning plant and determined that one gram of refuse adsorbed between 50 and 68 μg of SLS. These values were an order of magnitude higher than results for similar tests performed on surface-mined overburden material. The same test was performed on the coal used in the laboratory column experiments. Adsorption capacity was found to be 60 μg SLS/g coal. Because of the lower adsorption capacity of overburden materials, Kleinmann (6) incorporated SLS into rubber pellets which gradually release the detergent into infiltrating rainwater. This method may not be needed for coal storage and coal refuse disposal areas.

The NBS and SLS detergent applications apparently did not kill all the iron-oxidizing bacteria, because small numbers of live, but apparently inactive, bacteria were present even in samples collected after the coal was treated. For example, bacterial numbers in the drainage 28 days after treatment were 160,000 per 100 mL for the control column and 7,900 per 100 mL for the SLS-treated column. Toward the end of the experiment, when drainage from the treated and control columns were acid, bacterial numbers were more similar. One hundred nineteen days after treatment, drainage from the control and SLS-treated columns contained 1,100,000 and 920,000 iron-oxidizing bacteria per 100 mL.

The reasons for the relative effectiveness of SLS treatment compared to NBS are not known. If detergents alter the semipermeable properties of the cytoplasmic membrane and allow H+ to seep into the interior of the cell, as has been reported, then it is possible that a detergent that better attacks protein would be more effective. SLS, being the active ingredient in many hair shampoos, is designed to attack protein-type buildup on hair. On the other hand, NBS is the active ingredient in many laundry detergents and is designed to remove soil particles, not proteinaccous matter. This may be one reason for the relative ineffectiveness of NBS.

Projected Costs--Roughly extrapolating results to an industrial-scale application, the cost of SLS needed for a single application was estimated at about \$500 per hectare of coal storage area (\$200 per acre). This figure assumes a delivered cost of \$1.65 per Kg (\$0.75 per lb) for the SLS used in the experiments and allows for a 50-percent decrease in the efficiency of detergent application in the field. Because of the limited number of experiments performed to date, these costs must be considered preliminary.

Methods of Application--Results of laboratory experiments showed that SLS may be effective in preventing problems of acidity and dissolved metals in coal pile drainage for about two months. If an operating facility stored less than a 2-month supply of coal and always burned the oldest coal first, a single application to each new coal delivery might prevent the development of acid drainage. However, there are probably few plants where these conditions would be met at all times. In the tests performed thus far, it was assumed that it would be necessary to treat all the coal from the top to the bottom of an entire pile each time it is required. There are some indications, however, that bacteria are active mainly in the top layer of coal, where the temperature and availability of air best suit their needs. If that is the case, it might be necessary to treat only the surface of the pile, or it might be possible to extend significantly the time between full-pile treatments by means of supplementary surface layer treatment.

It might even be economical to treat each new coal delivery before it is added to the pile, either as a supplementary treatment or as the only treatment required. At many plants, the surface of the coal pile is routinely sprinkled with water to control dust, and a small amount of SLS might easily be added to the tanks of the sprinkler trucks. A spray system might be installed to treat every truckload or trainload of coal with a small amount of SLS, either as it is dumped or as it moves along conveyors to the pile so that the surface layer of new coal would continually be protected against acid formation. If significant time is expected to elapse between mining and delivery, the coal might even be protected with SLS as soon as it is mined and then treated again when it is delivered.

Additional Research Needs--Since drainage from existing coal piles is often already acid, there is a question as to whether it would be possible to correct an existing problem by application of detergents. A modification of the methods described in these studies would likely be necessary because SLS breaks down rapidly in strong acid solutions. It may be possible to correct an existing problem by treating the coal with SLS in combination with some buffering agent. Further experiments using several buffers such as sodium bicarbinate and phosphate are currently in progress to address this concern.

It is not known whether SLS affects the burning characteristics of coal. This must be determined because laboratory results indicated that SLS was readily adsorbed onto the coal particles. Another potential concern, the added sulfur due to the SLS, should not present a problem. The sulfur content theoretically added to the coal due to the sulfate ions in SLS is insignificant relative to the high-sulfur content of coal.

Conclusions

1. Controlled application of anionic detergents may be useful in preventing acid drainage from coal storage piles.
2. Sodium lauryl sulfate was more effective than NBS in preventing acid production in laboratory-simulated coal piles.
3. Based on laboratory studies, it appears that a single application may last up to 60 days.
4. Extrapolating laboratory results to an industrial-scale application, the cost of SLS needed for a single treatment was calculated to be $500 per hectare of coal storage area ($200 per acre).

Acknowledgements

We thank Robert L. P. Kleinmann and Patricia M. Erickson for performing adsorption tests and Donald J. Rucker for critical review of the manuscript.

Literature Cited

(1) Colmer, A. R.; Hinkle, M. E., Science, 1947, 106, 253.
(2) Singer, P. C.; Stumm, W., Science, 1970, 167, 1121.

(3) Singer, P. C.; Stumm, W., "Oxygenation of Ferrous Iron: The Rate-determining Step in the Formation of Acid Mine Drainage." Federal Water Pollution Control Administration, Report 14010, 1969.

(4) Dugan, R. P., Ohio J. Sci., 1975, 75, 266.

(5) Kleinmann, R.L.P., In "Proceedings, Symposium on Surface Mining Hydrology, Sedimentology, and Reclamation"; Graves, D. H., Ed.; Report No. UKY BU123, University of Kentucky, Lexington, 1980; pp 333-337.

(6) Kleinmann, R.L.P., Erickson, P. M., In "Proceedings, Symposium on Surface Mining Hydrology, Sedimentology, and Reclamation"; Graves, D. H., Ed.; Report No. UKY BU126, University of Kentucky, Lexington, 1981; pp 325-330.

(7) Hugo, W. B., J. Bacteriol., 1967, 30, 17.

(8) "Standard Methods for the Examination of Water and Wastewater." 15th Ed.; American Public Health Association, Washington, D.C., 1980.

(9) Olem, H.; Unz, R. F., Biotechnol. Bioeng., 1977, 19, 1475.

(10) Dailela, R. C., et al., Water, Air and Soil Poll., 1981, 15 1.

ATTENDEES

Antisavage, Joseph P.
Betz Laboratories, Inc.
4636 Somerton Rd
Trevose, PA 19047
215/355-3300 x377

Armstrong, James A.
Denver Research Institute
University of Denver
Denver, CO 80208
303/753-2892

Bohn, Russel
Environmental Services
and Technology
11 E. 69th Ter
Kansas City, MO 64113

Boudreau, Richard M.
Central Illinois Light Co.
300 Liberty St
Peoria, IL 61602
309/672-5471

Bowman, W. Alan
Applied Meteorology, Inc.
Suite 326
9000 Southwest Frwy
Houston, TX 77074
713/777-0106

Bramson, Mark
Syntech Products Corp.
520 E. Woodruff
Toledo, OH 43624
419/241-1215

Brass, Dwight
George A. Rolfes Co.
Box 458
Boone, IA 50036
515/432-3300

Brookman, Edward T.
TRC Environmental
Consultants, Inc.
800 Connecticut Blvd
E. Hartford, CT 06108
203/289-8631

Campbell, Ivor E.
Smelter Control
Research Associates
150 E. Broad St
Columbus, OH 43215

Chalmers, Jerry
S. C. Dept of Health and
Environmental Control
2600 Bull St
Columbia, SC 29201
803/758-5406

Cole, Clifford F.
TRC Environmental
Consultants, Inc.
8775 E. Orchard Rd,
Suite 816
Englewood, CO 80231
303/779-4940

Connolly, Michael
Minnesota Pollution
Control Agency
1935 W. County Rd B-Z
Roseville, MN 55118

Courtney, Peter
Law Engineering
2749 Delk Rd
Marietta, GA 30067

Cowherd, Chatten
Midwest Research Institute
425 Volker Blvd
Kansas City, MO 64110
816/753-7600 x531

Cox, H. B.
U. S. Steel Research
(U. S. Mining, Inc.)
B St
Pittsburgh, PA 15235
412/372-1212 x4291

Craig, Alfred B. (MD-54)
U. S. EPA/AEERL (IERL)
Research Triangle Park, NC 27711
919/541-2824

Attendees (cont.)

Crockett, E. P.
American Petroleum Institute
2101 L St, N. W.
Washington, DC 20036
202/457-7084

Dorsey, James A. (MD-62B)
U. S. EPA/AEERL (IERL)
Research Triangle Park, NC 27711
919/541-2509

Dubrowski, John J.
Exxon Research and Engineering
Florham Park, NJ 07932
201/765-2101

Fletcher, James K.
Kennecott Minerals Co.
PO Box 11248
Salt Lake City, UT 84147
801/322-8262

Gatz, Donald F.
Illinois State Water Survey
PO Box 5050, Station A
Champaign, IL 61820
217/333-2512

Goebel, Gerald R.
DNR and EP/Div of Air
Pollution Control
Ft. Boone Plaza,
18 Reilly Rd
Frankfort, KY 40601
502/564-3382

Hague, William
Julius Koch USA, Inc.
PO Box A-995
New Bedford, MA 02741
617/995-9565

Harris, D. Bruce (MD-54)
U. S. EPA/AEERL (IERL)
Research Triangle Park, NC 27711
919/541-7807

Harrison, Paul R.
Envirosol
1700 N. Fiske
Pasadena, CA 91104
818/797-9581

Hartshorn, Wayne
Sonic Development Corp.
305 Island Rd
Mahwah, NJ 07430
201/825-3030

Holton, Greg (ORNL)
First Environment
314 W. Broadway
Lenoir City, TN 37771

Hyatt, James
Tennessee Valley Authority
940 CSTZ-C
Chattanooga, TN 37401

Hyatt, John G.
Exxon Co., USA
Colony Shale Oil Project
PO Box 440342
Aurora, CO 80044
303/695-2213

Hyde, Raymond G.
Atlantic Research Corp.
5390 Cherokee Ave
Alexandria, VA 22314
703/642-4193

Ives, Jim
Anaconda Minerals Co.
PO Box 5300
Denver, CO 80217
303/575-7504

Kaiser, Robert A.
Ohio Edison Co.
76 S. Main St
Akron, OH 44308
216/384-5770

Kawaters, Woody
TRC Environmental
Consultants, Inc.
800 Connecticut Blvd
E. Hartford, CT 06108

Kretch, Frank
Sonic Development Corp.
305 Island Rd
Mahwah, NJ 07430
201/885-3030

Attendees (cont.)

Kuykendal, William B. (MD-15)
U.S. EPA/OAQPS/AQMD (IERL)
Research Triangle Park, NC 27711
919/541-5372

Larson, Alan G. (TRC)
The Kentwood Moore Co.
5690 Denver Tech Ctr Blvd
Englewood, CO 80111
303/773-3399

Lawrence, Robert
KPN International, Inc.
19 Pebble Rd
Newtown, CT 06470

Letizia, Anthony P.
Envirosphere Co.
2 World Trade Center
New York, NY 10048
212/839-1088

Lewis, Ted P.
Iowa Electric Light and
Power Co.
PO Box 351
Cedar Rapids, IA 52406
319/398-4601

Lubas, Thomas
Port Authority of NY and NJ
1 World Trade Center,
64 Floor E.
New York, NY 10048

Manning, James
US EPA Region 4
345 Courtland St, N.E.
Atlanta, GA 30365
404/347-3286

Martin, Dennis
TRC Environmental
Consultants, Inc.
800 Connecticut Blvd
E. Hartford, CT 06108

Mathai, C.V.
Arizona Public Service Co.
(AeroVironment, Inc.)
PO Box 53999 (Sta. 5680)
Phoenix, AZ 85072-3999
602/371-6467

Milhous, Madison N.
Long Island Lighting Co.
1775 E. Old Country Rd
Hicksville, NY 11801
516/733-4385

Mohr, Ray
Colorado Health Dept
1101 Bellaire St
Denver, CO 80220
303/320-4180

Moldovan, John
Anaconda Minerals Co.
5555 17th St
Denver, CO 80433
303/575-4312

Mulloy, Frederick W.
Phillips Petroleum Co.
7 D 3 Phillips Bldg
Bartlesville, OK 74004

Nicholson, Brock M. (MD-15)
U.S. EPA/OAQPS/AQMD (CPDD)
Research Triangle Park, NC 27711
919/541-5517

Nilsen, Glennyce C.
United Illuminating Co.
80 Temple St
New Haven, CT 06506

Olem, Harvey
Tennessee Valley Authority
245 401 Bldg
Chattanooga, TN 37401
615/751-7338

Pace, Thompson G. (MD-15)
U.S. EPA/OAQPS/AQMD
Research Triangle Park, NC 27711
919/541-5634

Plaks, Norman (MD-61)
U.S. EPA/AEERL (IERL)
Research Triangle Park, NC 27711
919/541-3084

Porter, Richard A.
NAI
1710 Firman Dr
Richardson, TX 75081
214/644-1616

Attendees (cont.)

Rakes, Samuel L. (MD-62)
U.S. EPA/AEERL (IERL)
Research Triangle Park, NC 27711
919/541-2828

Ray, B. Michael
Northrop Environmental Training
PO Box 12313
Research Triangle Park, NC 27709
919/549-0652

Reddy, Tupili S.
Tennessee Air Pollution Control Div
150 - 9th Ave, N.
Nashville, TN 37203
615/741-3651

Ripp, John A.
TRC Environmental
Consultants, Inc.
800 Connecticut Blvd
E. Hartford, CT 06108
203/289-8631

Romaine, Demarest (Dave)
Consolidated Edison Co. of
New York, Inc.
4 Irving Pl
New York, NY 10003
212/460-4600

Rosbury, Keith D.
PEDCo Environmental, Inc.
2420 Pershing Rd
Kansas City, MO 64108

Rovell-Rixx, David C.
National Council for Air and
Stream Improvement, Inc.
PO Box 14483
Gainesville, FL 36204

Sando, Dick
Sonic Development Corp.
305 Island Rd
Mahwah, NJ 07430
201/825-3030

Schumacher, Aileen
Environmental Science and
Engineering
PO Box ESE
Gainesville, FL 32602
904/372-3318

Sehmel, George A.
Pacific Northwest Laboratory
24000 Stevens 1100 Area
Richland, WA 99352
509/375-6161

Shrock, John
Illinois Environmental
Protection Agency
2200 Churchill Rd
Springfield, IL 62706
217/782-1830

Simpson, Charles
SynTech Products Corp.
520 E. Woodruff
Toledo, OH 43624
419/241-1215

Skoney, David
Erie Co. Dept of Environment
and Planning
95 Franklin St
Buffalo, NY 14225
716/846-8556

Smith, M. L.
Andersen Samplers, Inc.
4215 Wendell Dr
Atlanta, GA 30315
404/691-1910

Staley, Laurel J.
U.S. EPA/RREL (IERL)
Cincinnati, OH 45268
513/569-7863

Stark, Phillip E.
Shell Oil Co. - Mining
PO Box 2906
Houston, TX 77001
713/870-4263

Attendees (cont.)

Stone, F. Kenneth
S. C. Dept of Health and
Environmental Control
2600 Bull St
Columbia, SC 29201
803/758-5406

Tucker, A. L.
Jones and Laughlin Steel Co.
3001 Dickey Rd
E. Chicago, IN 46312
219/391-2571

Turetsky, William S.
Allied Chemical Co.
PO Box 1139R
Morristown, NJ 07960
201/455-2690

Wells, Robert C.
Enviroplan, Inc.
59 Main St
West Orange, NJ 07052
201/325-1544

Williams, Colin J.
Rowan, Williams, Davies,
and Irwin, Inc.
(MHTR Ltd)
650 Woodlawn Rd, West
Guelph, Ontario N1K1B8
519/823-1311

Wootten, John M.
Peabody Coal Co.
PO Box 14495
St. Louis, MO 63178

Yocom, John E.
TRC Environmental
Consultants, Inc.
800 Connecticut Blvd
E. Hartford, CT 06108
203/289-8631